Hydrogneation and hydrosilylation reactions catalized by manganese and rhenium complexes

Ruqaya Buhaibeh

▶ **To cite this version:**

Ruqaya Buhaibeh. Hydrogneation and hydrosilylation reactions catalized by manganese and rhenium complexes. Coordination chemistry. Université Paul Sabatier - Toulouse III, 2020. English. NNT : 2020TOU30234 . tel-04544744

HAL Id: tel-04544744
https://theses.hal.science/tel-04544744

Submitted on 13 Apr 2024

HAL is a multi-disciplinary open access archive for the deposit and dissemination of scientific research documents, whether they are published or not. The documents may come from teaching and research institutions in France or abroad, or from public or private research centers.

L'archive ouverte pluridisciplinaire **HAL**, est destinée au dépôt et à la diffusion de documents scientifiques de niveau recherche, publiés ou non, émanant des établissements d'enseignement et de recherche français ou étrangers, des laboratoires publics ou privés.

Université Fédérale
Toulouse Midi-Pyrénées

THÈSE

En vue de l'obtention du

DOCTORAT DE L'UNIVERSITÉ DE TOULOUSE

Délivré par l'Université Toulouse 3 - Paul Sabatier

Présentée et soutenue par

Ruqaya BUHAIBEH

Le 18 décembre 2020

Hydrogenation and Hydrosilylation Reactions Catalyzed by Manganese and Rhenium Complexes

---

Ecole doctorale : **SDM - SCIENCES DE LA MATIERE - Toulouse**

Spécialité : **Chimie Organométallique et de Coordination**

Unité de recherche :
LCC - Laboratoire de Chimie de Coordination

Thèse dirigée par
Yves CANAC et Jean-Baptiste SORTAIS

Jury

Dr. Adrien QUINTARD (Rapporteur), Université d'Aix Marseille
Dr. Lucie NOREL (Rapporteure), Université de Rennes 1
Prof. Vincent RITLENG (Examinateur), Université de Strasbourg
Prof. Eric BENOIST (Examinateur), Université Paul Sabatier Toulouse 3
Dr. Yves CANAC (Directeur de thèse), LCC-CNRS Toulouse
Prof. Jean-Baptiste SORTAIS (Directeur de thèse), Université Paul Sabatier Toulouse 3
Dr. Dmitry VALYAEV (Invité), LCC-CNRS Toulouse

Acknowledgements

Firstly, I would like to express my sincere gratitude and appreciation to my two respected supervisors: Prof. Jean-Baptiste Sortais and Dr. Yves Canac for their continuous support, valuable guidance, warm encouragement, and extensive discussions during the past three years of my Ph.D. study. Yves and J. B., thank you for being nice, kind, patient, and available all the time. Thank you for being tremendously supportive and helpful in all aspects, of both study and personal life. I deeply appreciate everything you have done for me, and I will be always grateful.

I would like to sincerely thank all the committee members: Dr. Adrien Quintard, Dr. Lucie Norel, Prof. Vincent Ritleng, and Prof. Eric Benoist for generously offering their time, their insightful comments and suggestions to evaluate my work.

I am also very appreciative to Dr. Dmitry Valyaev for the tremendous help, for his invaluable advice and for giving me a lot of experimental and theoretical instructions all the time.

I want to express my deepest thank to Dr. Noël Lugan for his useful help and support in my research.

My sincere appreciation goes out to the team members: Dr. Vincent César, Dr. Stéphanie Bastin, Dr. Olivier Baslé, and Cécile Barthes, for their consistent help and support, their valuable advice and discussions during my Ph.D. journey.

I would like to deeply thank my colleagues: Karim Azouzi, Lenka Pallova, Duo Wei, Antoine Bruneau-Voisine, Rachid Taakili, Idir Benaissa, Romane Manguin, Alina Grineva, Katarzyna Gajda, Jompol Thongpaen, for the nice work environment, the fun, and the wonderful moments we have had in the last three years. Special thanks to Mohamed Boundor who helped me a lot in this work during his master internship in the team. My sincere gratitude and thanks go also to my friend Abdelouahd Oukhrib who has always been a major source of support when things get a bit discouraging.

I would like to extend my appreciation to Dr. Oleg A. Filippov for DFT calculations, Dr. Carine Duhayon and Dr. Laure Vendier for their help in X-Ray diffraction analysis, and to thank Dr. Christian Bijani, Antoine Bonnet, and David Paryl for NMR studies.

My sincere thanks also go to all the administrative and technical services in the LCC, for their important help.

I would like to thank my dear friends Sediqa Almasri and Karima Almukri who have always been by my side throughout this Ph.D., thank you for being such amazing friends, words are not enough to express the gratitude that you deserve.

My deep gratitude and sincere thanks to my friends in France: Eman, Allali, Marwan and Nasser, for their tremendous support during my difficult time, and for all the beautiful moments we have shared together.

Finally, I would like to express my heartfelt thanks to my family for always believing in me, encouraging me, and supporting me all the time.

List of Abbreviations

Cat.	Catalyst
M–L	Metal-Ligand
Ra-Ni	(Raney-nickel) Aluminum-nickel catalyst (Al-Ni 50:50 wt. %)
PHMS	Polymethylhydrosiloxane
KHMDS	Potassium bis(trimethylsilyl)amide
$KHBEt_3$	Potassium triethylborohydride
***t*-BuOK**	Potassium tert-butoxide
***t*-AmOH**	2-methylbutan-2-ol
DABCO	1,4-diazabicyclo[2.2.2]octane
DBU	1,8-Diazabicyclo[5.4.0]undec-7-ene
TMEDA	*N,N,N',N'*-tetramethylethylenediamine
OTf	Trifluoromethanesulfonate
THF	Tetrahydrofuran
DCM	Dichloromethane
DCE	Dichloroethane
DMSO	Dimethyl sulfoxide
Cy	Cyclohexyl
DIPP	Diisopropylphenyl
***i*Pr**	2-Propanol
Me	Methyl
Et	Ethyl
Mes	Mesityl
NHC	N-Heterocyclic Carbene
NHSi	N-Heterocyclic Silylene
Ts	Tosyl (*p*-toluenesulfonyl)
Temp.	Temperature
r.t.	Room Temperature
ee	Enantiomeric excess
Conv.	Conversion
Equiv.	Equivalent

TOF	Turnover Frequency
TON	Turnover Number
TS	Transition State
o-	*ortho*
m-	*meta*
p-	*para*
s	singlet
d	doublet
t	triplet
q	quartet
quin	quintet
spet	spetet
m	multiplet
br	broad
NMR	Nuclear Magnetic Resonance Spectroscopy
XRD	X-Ray Diffraction
DFT	Density Functional Theory
GC-MS	Gas Chromatography–Mass Spectrometry
HRMS	High Resolution Mass Spectrometry
LRMS	Low Resolution Mass Spectrometry
ESI	Electrospray Ionization
Anal.	Elemental Analysis
IR	Infra-Red

Content

General Introduction

General Introduction

Catalytic hydrogenation using molecular dihydrogen to reduce unsaturated bond is one of the most efficient, atom-economical, and cleanest methods in synthetic organic chemistry, and thus presenting a great interest for pharmaceutical and industrial sectors[1]. Following the pioneering work of Döbereiner,[2] Sabatier brought in 1912 the first significant contribution in the field, demonstrating that elemental hydrogen could add to an unsaturated bond in the presence of nickel as a catalyst.[3] This breakthrough was followed by many others, in the field of heterogeneous hydrogenation catalysis until the preparation of the first homogeneous rhodium hydrogenation catalyst by Wilkinson.[4] This pioneering work prompted the development of the analogous asymmetric hydrogenation by Knowles[5] and Noyori[6] using chiral phosphine ligands, which allowed them to obtain the Nobel Prize a few years later, like Sabatier in his time.[7] Homogeneous hydrogenation reactions are usually carried out with catalysts based on noble transition metals such as ruthenium, palladium and rhodium[1]. Due to the scarcity and the toxicity of these metals, they have become less attractive compare to earth abundant transition metals such as those of the first raw of the periodic table. In this respect, as the most abundant and thus inexpensive transition metals, iron was the first representative of the first raw to give significant results comparable to those of noble metals in the field of hydrogenation[8]. Manganese is the third most abundant transition metal in the earth's crust, behind iron and titanium, its natural abundance and biocompatibility, make it a very promising element for pharmaceutical production and applications in catalysis.[9–18]

With this objective in mind, we were thus interested in developing well-defined NHC-based manganese complexes and evaluate first their reactivity for the activation of H_2, and then develop efficient catalysts for hydrogenation-type reactions. In line with our interest of designing greener catalytic systems, the use of manganese and rhenium carbonyl complexes in hydrosilylation reactions has also been part of our main objectives.

The first chapter summarizes a selection of the most significant advances in hydrogenation-type reactions catalyzed by well-defined manganese complexes.

The second chapter focuses on the synthesis of various Mn(I) complexes of easily accessible bidentate NHC-phosphine ligands, these complexes were envisaged for the hydrogenation of ketones. This catalytic process highlights a new mode of metal-ligand cooperation involving a non-classical metalla-substituted phosphonium ylide obtained upon C-H deprotonation of a chelating NHC-phosphine ligand in the Mn coordination sphere. The latter can easily activate

H_2, thus providing the first evidence of the involvement of λ^5-phosphorous species in metal-ligand cooperation. Due to the higher rigidity and robustness of pincer complexes, in order to reach more active catalytic systems next to the bidentate series, cationic NHC core Mn(I) pincer complexes based on a PCN and PCP ligands were also prepared and fully characterized. However, they were found to be less active in the hydrogenation of ketones compared to their bidentate analogues.

The third chapter is dedicated to the selective reduction of carboxylic acid and esters to aldehydes, *via* the formation of stable alkyl silyl acetals using the commercially available $Mn_2(CO)_{10}$ and $Re_2(CO)_{10}$ pre-catalysts in the presence of triethylsilane as reducing agent under irradiation at room temperature.

References

[1] J. G. de Vries, and C. J. Elsevier, *The Handbook of Homogeneous Hydrogenation*, WILEY-VCH, Weinhem, **2007**.

[2] G. B. Kauffman, *Platin. Met. Rev.* **1999**, *43*, 122–128.

[3] H. Grünewald, *Angew. Chem.* **1968**, *80*, 52–52.

[4] J. A. Osborn, F. H. Jardine, J. F. Young, G. Wilkinson, *J. Chem. Soc. Inorg. Phys. Theor.* **1966**, 1711–1732.

[5] W. S. Knowles, *Angew. Chem. Int. Ed.* **2002**, *41*, 1998–2007.

[6] R. Noyori, *Angew. Chem. Int. Ed.* **2002**, *41*, 2008–2022.

[7] D. M. Sedgwick, G. B. Hammond, *J. Fluor. Chem.* **2018**, *207*, 45–58.

[8] D. Wei, C. Darcel, *Chem. Rev.* **2019**, *119*, 2550–2610.

[9] R. I. Khusnutdinov, A. R. Bayguzina, U. M. Dzhemilev, *Russ. J. Org. Chem.* **2012**, *48*, 309–348.

[10] D. A. Valyaev, G. Lavigne, N. Lugan, *Coord. Chem. Rev.* **2016**, *308*, 191–235.

[11] R. J. Trovitch, *Acc. Chem. Res.* **2017**, *50*, 2842–2852.

[12] F. Kallmeier, R. Kempe, *Angew. Chem. Int. Ed.* **2018**, *57*, 46–60.

[13] G. A. Filonenko, R. van Putten, E. J. M. Hensen, E. A. Pidko, *Chem. Soc. Rev.* **2018**, *47*, 1459–1483.

[14] N. Gorgas, K. Kirchner, *Acc. Chem. Res.* **2018**, *51*, 1558–1569.

[15] A. Mukherjee, D. Milstein, *ACS Catal.* **2018**, *8*, 11435–11469.

[16] L. Alig, M. Fritz, S. Schneider, *Chem. Rev.* **2019**, *119*, 2681–2751.

[17] K. D. Vogiatzis, M. V. Polynski, J. K. Kirkland, J. Townsend, A. Hashemi, C. Liu, E. A. Pidko, *Chem. Rev.* **2019**, *119*, 2453–2523.

[18] T. Zell, R. Langer, *ChemCatChem* **2018**, *10*, 1930–1940.

Chapter 1: Manganese-Catalyzed Hydrogenation and Hydrogen Transfer Reactions

Chapter 1: Manganese-Catalyzed Hydrogenation and Hydrogen Transfer Reactions

Chapter 1: Manganese-Catalyzed Hydrogenation and Hydrogen Transfer Reactions

1. Introduction

The first applications of manganese in hydrogenation-type reactions of polar bonds were described in 2016 by groups of Beller and Milstein respectively for the hydrogenation of nitriles, ketones and aldehydes[1] and the dehydrogenative coupling of alcohols and amines to form imines.[2] In both cases, the Mn(I) center was stabilized by a rigid and strongly chelating bis(phosphine) amine pincer ligand which allowed in the case of hydrogenation to reduce a large range of unsaturated substrates. Following these promising results, many others related Mn systems exhibiting a pincer-type structure with different N- and P- based donor extremities were elaborated for the hydrogenation of organic substrates containing multiple polar bonds, such as aldehydes, ketones, nitriles, esters, amides, imines, carbonates or CO_2.[3–10] Bidentate systems combining P-, N-, but also C- donor ends were more recently developed leading to spectacular advances in the field. Other Mn containing systems have been more punctually envisaged as molecular complexes based on tetradentate ligands and/or ligands with different donor atoms (O, Si), as well as nanoclusters.[11,12] As an alternative to atom-economic molecular hydrogen, alcohols were shown also to act as a valuable source of hydrogen, rendering thus transfer-hydrogenation a process complementary to classical hydrogenation. Whatever the hydrogenation process, the catalytic efficiency of these metal complexes was largely rationalized with reference to the concept of metal−ligand cooperation, which consists in taking advantage of a strong synergy created between the ligand and the metal to promote H_2 heterolysis followed by H-atom transfer onto unsaturated bonds.[13–15] Most of catalytic Mn systems were thus developed on the basis of two functional architectures verifying the pre-established concept, either through the involvement of an amide/amine interplay (the so-called NH effect) or *via* the aromatization/dearomatization process of a pyridine moiety.

In the present chapter, a selection of the recent advances achieved in the field of hydrogenation reactions catalyzed by well-defined manganese complexes will be discussed. Such metal complexes will be classified according to the ligand structure, and in particular, the denticity and the nature of donor ends.

2. Pincer-type Manganese Complexes

2.1 PNP Ligands

The pioneering reports of Beller et *al*. in the field of Mn-catalyzed hydrogenation have led to the tremendous development of tridentate ligands of PNP-type, these chelating ligands being indeed part of the first catalytic systems to lead to significant results in this area.[1] Beyond the nature of P-substituents, the developed PNP pincer ligands differ also by the hybridization state of the central N-atom. The N-atom can be either of sp^3-type in the form of an amine moiety or of sp^2-type *via* a pyridine or a triazine nucleus (**Scheme 1**).

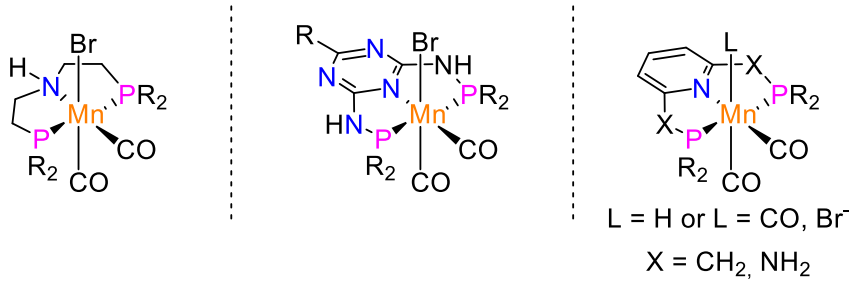

Scheme 1. General representation of Mn(I) pincer-type complexes featuring a PNP ligand.

a- PN-sp³P ligand

Thanks to their expertise in hydrogenation-type reactions using Fe and Ru-based pincer complexes,[16,17] Beller et *al*. became interested in the preparation of well-defined Mn analogues. The first category of Mn pincer complexes envisaged was based on a PN-sp³P structure consisting of a central amine substituted with two lateral phosphines.[18] Two air-stable Mn(I) complexes were thus conveniently prepared upon the reaction of $Mn(CO)_5Br$ complex with corresponding PNP ligands differing by the nature of P-substituents (*i*Pr *vs* Cy).[1] These complexes were tested for the hydrogenation of unsaturated substrates such as aldehydes, ketones and nitriles (**Scheme 2**, *left*). For nitriles, the catalytic system (Cat. 3 mol %, *t*-BuONa 10 mol %, 50 bar H_2, 120 °C, 24 h) was demonstrated to be effective for several representatives, including substituted aromatic, benzylic, aliphatic nitriles, and dinitriles. Electron- donating and withdrawing groups (halogen, Me, MeO, NH_2, CF_3), as well as heterocycles were generally also well tolerated. For ketones, the reduction occurred in the presence of 1 mol % of catalyst, 3 mol % of *t*-BuONa at 100 °C in toluene with 30 bar of H_2. Under these conditions, other reducible groups such as C=C bonds, lactams, and esters were not affected by the reaction. As

an added value, natural products as illustrated with citronellal, perillaldehyde and 5-hydroxymethylfurfural could be converted to corresponding primary alcohols in satisfactory yield. On the mechanism, an outer-sphere mechanism was proposed involving successive amido and hydride Mn species. The amido complex first formed after reaction of the pre-catalyst with a base would react with dihydrogen to afford a hydride complex which would be able by a simultaneous transfer of the hydride from the Mn center (Mn−H) and the proton from the nitrogen (N−H) to reduce the unsaturated bond.

The more challenging hydrogenation of esters was achieved with less hindered pre-catalysts based on the cationic ethyl-substituted PNP backbone which exhibits an unusual *cis*-coordination of the P-atoms (**Scheme 2**, *right*).[19] No activity was indeed observed with more crowded PNP Mn pre-catalysts featuring P-*i*Pr and P-Cy donor ends. This catalytic system (Cat. 2 mol %, *t*-BuOK 10 mol %, 110 °C, dioxane, 24 h, 30 bar H_2) enabled the transformation of aromatic and aliphatic ester derivatives, as well as diesters and lactones in good yields. The corresponding neutral complex showed similar activity under the optimized reaction conditions. Supported by DFT calculations, the efficiency of these catalysts was rationalized through an outer-sphere mechanism involving amido and hydride Mn complexes.

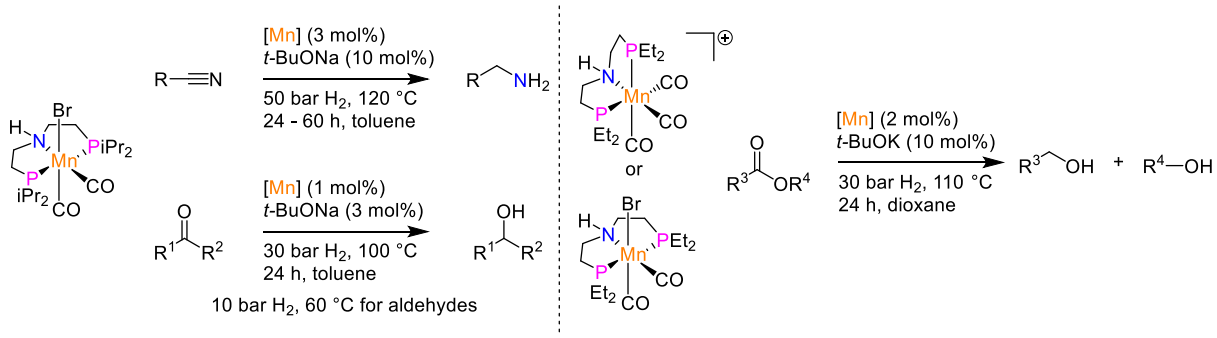

Scheme 2. Mn(I) pincer complexes bearing a PN-sp^{3}P ligand for the hydrogenation of nitriles, aldehydes or ketones (*left*), and esters (*right*).

Air-stable PNP Mn(I) pincer complexes active for aldehyde, ketone and nitrile reductions catalyzed also the sequential one-pot CO_2 hydrogenation to CH_3OH.[20] The transformation involves first the N-formylation of an amine in the presence of CO_2 and H_2 followed by the formamide reduction to methanol and amine products (**Scheme 3**). Thanks to the PN-sp^{3}P pre-catalyst bearing two strongly donating P*i*Pr$_2$ moieties, CH_3OH was produced in good yield from benzylamine or morpholine substrates with a maximum TON of 36 comparable to the values reported earlier with Co-based catalysts.[21]

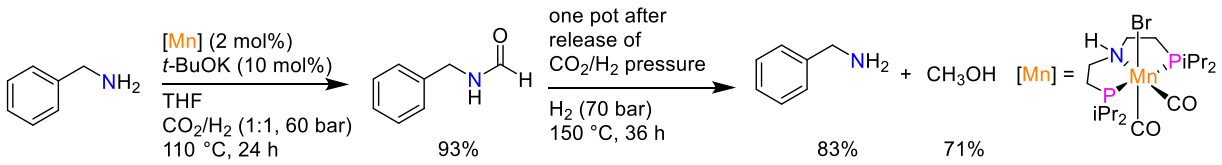

Scheme 3. Mn(I) pincer complex featuring a PN-sp^{3}P ligand for the hydrogenation of CO_2 to CH_3OH.

A Mn(I) complex of such type of PN-sp^{3}P ligand was reported by Leitner et *al*. for the catalytic hydrogenation of cyclic carbonates to diols and methanol.[22] This catalytic system afforded high yields for diols and methanol products under relatively mild conditions (120 °C, 30−60 bar H_2) with respective TONs up to 620 and 400. In the same family of ligands, we can mention the Mn(I) complex bearing an amino-bis(phosphinite) ligand (of PONOP-type) which was shown to be effective for the hydrogenation of ketones.[23]

Mn(I) pincer complexes bearing the chiral PNP ligand bis(2-((2*R*,5*R*)-2,5-dimethyl-phospholanoethyl)amine allowed the enantioselective hydrogenation of ketones (**Scheme 4**, *left*).[24,25] Compared with related pincer complexes based on Ru, Re, and Fe metal centers,[25] the Mn representative showed better performance not only for aromatic substrates but also for aliphatic substrates affording enantioselectivities up to 99% *ee*. For instance, the catalytic conditions required for the hydrogenation of cyclic aliphatic ketones were the following: 1 mol % of catalyst, 5 mol % of *t*-BuOK, 30 bar H_2, 4 h, 40 °C, *t*-amyl alcohol. Based on DFT calculations, the asymmetric induction was rationalized considering the approach of the prochiral ketone perpendicular to the *cis*- N−H and Mn−H groups of the hydride complex with either the *re* or *si* enantioface.

Other variants of P-stereogenic PN(H)P tridentate ligands were reported by Mezzetti et *al*. for the Mn-catalyzed asymmetric hydrogenation of ketones (**Scheme 4**, *right*).[26] Derived from a Mn(I)/Fe(II) comparison, kinetic and DFT studies concluded that a bifunctional mechanism for H^+/H^- transfer occurs here.

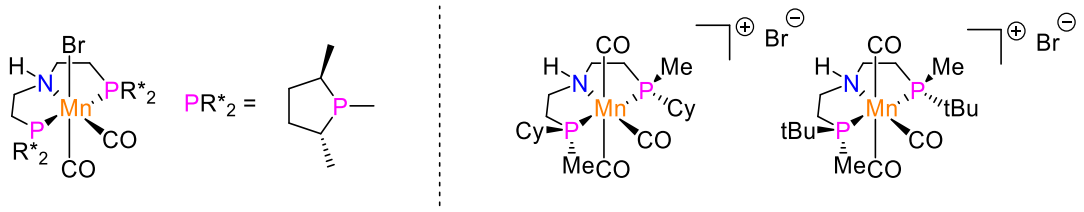

Scheme 4. Mn(I) complexes of chiral PN-sp^{3}P ligands involved in enantioselective hydrogenation.

b- PN-sp²P ligand

Modification of the central nitrogen donor has made it possible to develop effective hydrogenation catalysts. A revealing example was provided by Kempe et *al*. who described the preparation of highly active PN_5P Mn(I) complexes based on a triazine core for the hydrogenation of carbonyl derivatives, pre-catalysts which involve generally milder conditions than systems containing an aliphatic PN-sp^3P skeleton.[27] Related $Mn(CO)_2Br$ and $MnCl_2$ complexes were easily prepared and tested in the hydrogenation of ketones and aldehydes (**Scheme 5**). While no activity was observed with the Mn(II) representative, a broad scope of substrates with high functional group tolerance could be reduced by the PN_5P $Mn(CO)_2Br$ complex. The system was able to reduce acetophenone under the following conditions: Cat. 0.1 mol %, 80 °C, toluene, 4 h, 20 bar H_2. Aryl-alkyl, diaryl, dialkyl, and cycloalkyl ketones, as well as aldehydes were also converted into corresponding alcohols. Thanks to the possibility of using milder conditions, improved selectivity was obtained in particular for unsaturated ketones.

Scheme 5. PN_5P Mn(I) complexes for the hydrogenation of carbonyl derivatives.

Despite lower activity compared to previous systems, Mn(I) complexes exhibiting a PN_3P core catalyzed also the hydrogenation of ketones.[28] The system was based on an air-stable cationic Mn pre-catalyst bearing a tridentate 2,6-(diaminopyridinyl)diphosphine ligand.[29] Under 50 bar of H_2 at 130 °C, various ketones were reduced to the corresponding alcohols with moderate to good yield (**Scheme 6**, *left*). Experimental studies have shown that the active species is likely a Mn−H complex formed *in situ* in the presence of a base and H_2, through a N−H deprotonation-dearomatization process.[30]

A well-defined hydride Mn(I) complex of the same PN_3P ligand was found to be one of the most active catalyst for the hydrogenation of aldehydes (**Scheme 6**, *right*).[31–33] The reaction

which takes place at room temperature under base-free conditions with catalyst loadings between 0.1 and 0.05 mol %, and 50 bar of H_2 allowed the selective hydrogenation of aldehydes in the presence of ketones, and other reducible groups such as C=C bonds, esters or nitriles. The same catalyst enables also the hydrogenation of CO_2 to HCOOH affording TONs up to 10 000 and quantitative yields in the presence of DBU as a base at 80 °C, and 80 bar of H_2.[31–33] Noteworthy in the presence of a Lewis acid (LiOTf) and catalyst loading about 0.002 mol%, TONs up to 30 000 could be reached which stand as the highest activities reported for CO_2 hydrogenation using base-metal catalysts (**Scheme 6**, *right*).

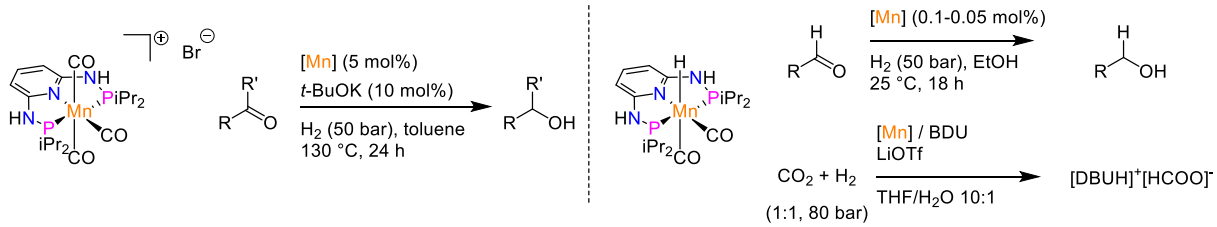

Scheme 6. Mn(I) complexes based on PN_3P ligands for the hydrogenation of ketones (*left*), and aldehydes or CO_2 (*right*).

More recently, Milstein type-Mn PNP catalysts built around a central pyridine were considered for the challenging deoxygenative hydrogenation of amide to amines (**Scheme 7**).[34] The first experiments focused on the feasibility of the reaction using *N*-phenylbenzamide as a model substrate. After optimization, C−O bond cleavage was observed affording in 89 % yield the corresponding secondary amine using the following catalytic conditions (Cat. 5 mol %, *t*-BuOK 6 mol %, $B(C_6F_5)_3$ 1.5 equiv., 150 °C, *m*-xylene, 72 h). The transformation was shown to be highly selective and only traces of C−N bond cleavage products, namely aniline and benzyl alcohol could be detected. This system enabled the efficient and selective reduction of a broad scope of amides, such as benzamides bearing substituents of different electronic nature on the phenyl group (halogen, Me, MeO), *N*-benzyl-, cyclohexyl-, hexyl benzamides, and aliphatic *N*-phenyl amides. The hydrogenation of tertiary amides was also possible, although with a lower yield. According to NMR and mechanistic studies, the authors suggested that an imine could be an intermediate in the hydrogenation of amides, and that Lewis acid may accelerate the hydrogenation of the imine. On this basis, a catalytic cycle involving metal-ligand cooperation through the dearomatization of the pyridine nucleus was proposed (**Scheme 7**, *right*).

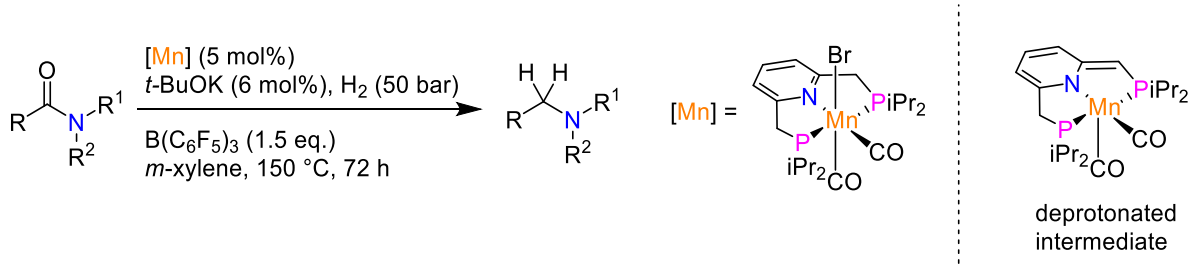

Scheme 7. Mn(I) catalyst featuring a PN-sp^{2}P ligand for the hydrogenation of amides into amines.

The enantioselective transfer hydrogenation of ketones was achieved by a Mn(I) complex containing an unsymmetrical chiral PN-sp^{2}P pincer ligand based on a planar chiral ferrocene and a central chiral aliphatic unit (**Scheme 8**).[35] For a large range of ketones, the reactions proceeded with conversion up to 96% and enantiomeric excess values up to 86% under mild conditions at room temperature in the presence of *t*-BuOK as a base. On the basis of DFT calculations, hydrogen bonding and steric factors were proposed to explain the origin of the (S) selectivity observed.

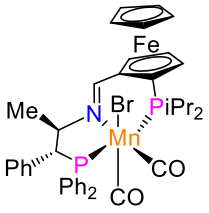

Scheme 8. Mn(I) complex of a chiral PN-sp^{2}P ligand for the enantioselective transfer hydrogenation.

2.2 PNN Ligands

Following the emergence of PNP-type pincer ligands, considerable work has been realized to adjust the ligand structure, in particular by modifying the nature of the coordinating ends in order to study the impact on catalytic properties. In a logical approach, tridentate ligands featuring a PNN skeleton have thus appeared and coordinated with manganese following similar procedures to those developed in the PNP series. PNN Mn pincer complexes can be also classified in two main categories depending of the hybridization state of the central N- atom, the latter being either of *sp*^{3}-type or of *sp*^{2}-type. It should be noted that the advent of these ligands has allowed significant progress in hydrogenation Mn catalysis compared to their PNP counterparts.

a- PN-sp^{3}N ligand

PNN ligands allowed significant advances in the reduction of amides. Indeed, after the successful applications of Ru complexes of such pincer ligand in this area of catalysis,[36,37] Mn analogues were naturally envisaged.[38] For this specific purpose, neutral and cationic Mn(I) complexes containing an imidazolylaminophosphine ligand were prepared in good yield by addition of $Mn(CO)_5Br$ to the corresponding imidazolylaminophosphine precursor (**Scheme 9**). The cationic complex PNN $Mn(CO)_3^+$, Br^- exhibits a distorted octahedral geometry with the PNN moiety adopting a facial coordination mode. Compared to its neutral counterparts, this tripodal-type Mn complex afforded high activity and selectivity in the reduction of secondary and tertiary amides into corresponding alcohols and amines under relatively mild conditions. The selectivity obtained in this case is different to that observed with Mn(I) catalysts based on a PNP ligand.[34] The catalytic system proceeds generally using 2 mol % of catalyst, 5-10 mol % of *t*-BuOK in cyclohexane at 100−120 °C. Several reducible functional groups were tolerated under these conditions such as aryl halides. While the efficiency of the catalyst was demonstrated through the reduction of primary amides and formamides, its selectivity was illustrated by the reduction of amides in the presence of other reducible groups like carbamates or ureas. From mechanistic considerations, experiments in the absence of base confirmed the role of amido complexes as active catalyst species suggesting the existence of an outer-sphere mechanism.

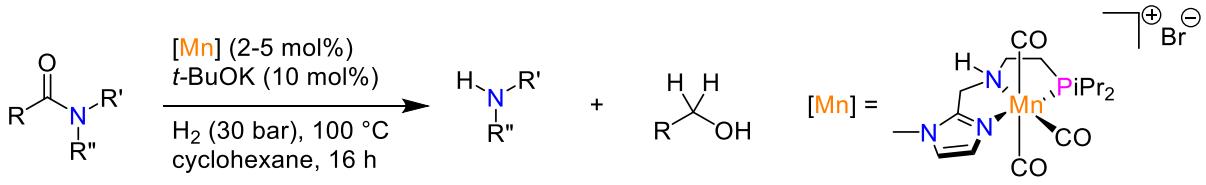

Scheme 9. Mn(I) complex of a PN-sp^{3}N ligand for the hydrogenation of amides.

The imidazole nucleus can be replaced by a pyridine to form PNN Mn(I) complexes able to reduce CO_2-derived carbonates to alcohols.[39] Considering the interest of converting industrially produced cyclic organic carbonates to value-added alcohols, Rueping, El-Sepelgy et *al*. prepared Mn(I) pincer complexes featuring a tridentate pyridine amine phosphine ligand by reacting the corresponding air-stable ligands[40] with $Mn(CO)_5Br$ complex (**Scheme 10**).[39] As a model reaction, the complex featuring a central NH donor with 0.25 mol % catalyst loading showed excellent reactivity for the reduction of ethylene carbonate affording ethylene glycol in quantitative yield and methanol in 92 % yield in 1,4-dioxane at 140 °C under 50 bar of H_2. The

role of the NH function was confirmed by the lower activity obtained with the N−Me analogue complex (1 mol %), where only 14 % of ethylene glycol was formed and no methanol detected. Under optimized conditions, a range of cyclic organic carbonates including five-, six-membered representatives with different alkyl and aryl substituents, as well as polycarbonates were successfully converted to corresponding diols and methanol products with yields between 80−99%. Based on deuterium labeling experiments and DFT calculations, a metal-ligand cooperative catalysis mechanism was evidenced involving the heterocyclic cleavage of three H_2 molecules by metal-ligand cooperation through three successive catalytic cycles. The present system opens promising perspectives for the recycling of wastes.

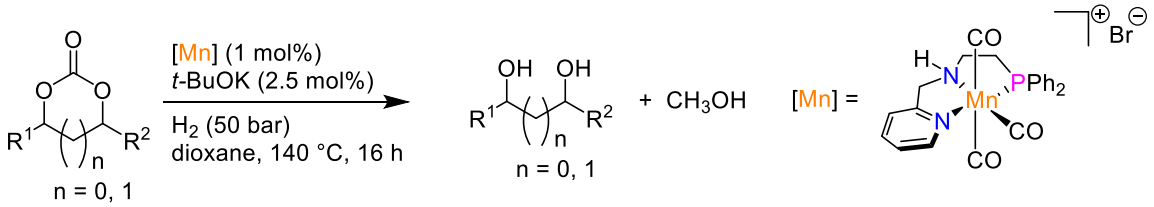

Scheme 10. Mn(I) complex of a PN-sp^{3}N ligand for the hydrogenation of CO_2-derived carbonates.

Asymmetric Mn(I) complexes of such PN-sp^{3}N ligand were considered for enantioselective ketone and ester hydrogenation (**Scheme 11**, *top*).[41] From the enantiopure PNN ligand (S_C,R_P) based on a ferrocenyl backbone, cationic Mn(I) complexes exhibiting planar chirality were prepared stepwise by reaction with $Mn(CO)_5Br$. The bromo- representative was found to be active for the hydrogenation of ketones with high level of enantioselectivity (up to 97% *ee*) superior in some cases than those obtained with non-abundant metal catalysts, as in the case of methyl ketones bearing aromatic rings with *o*-substituents. A range of functionalized ketones could be thus hydrogenated using the following conditions: Cat, 1 mol %, *t*-BuOK 10 mol %, 50 bar H_2, 50 °C, ethanol, 16 h. Additionally to ketones, this system exhibited high activity for the hydrogenation of esters down to 0.1 mol % catalyst loading. Using 1 mol % of catalyst, 10 mol % of *t*-BuOK at 75 °C in *i*PrOH, a variety of esters was reduced with good yield and functional group tolerance, including free amino *p*-phenyl substituted esters. The same catalytic system was successfully applied for the reduction of α-chiral esters (**Scheme 11**, *bottom*).[42] This transformation accomplished with TONs up to 1000 in the presence of potassium carbonate and alcoholic solvents occurred mainly with no loss of enantiomeric purity.

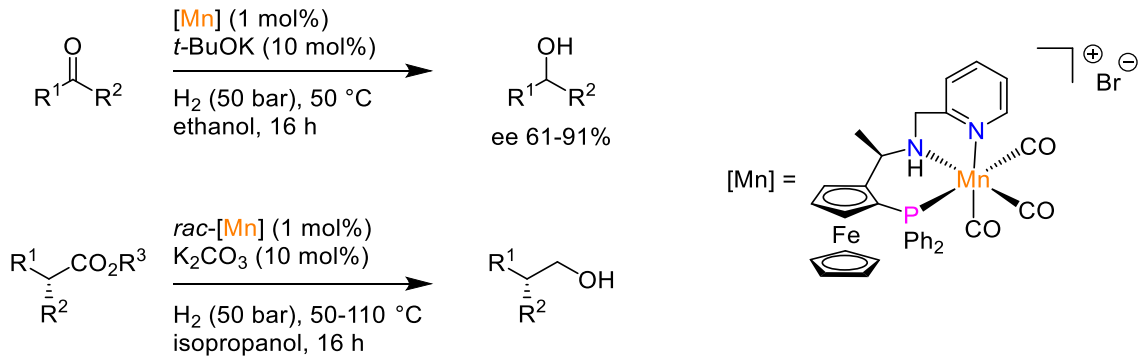

Scheme 11. Mn(I) complex of a chiral PN-sp^{3}N ligand for the enantioselective reduction of ketones and α-chiral esters.

The asymmetric transfer hydrogenation of acetophenone in isopropanol could be achieved with chiral Mn(I) complexes based on tridentate P−NH−NH and tetradentate P−NH−NH−P-type ligands.[43] Despite moderate enantioselectivity, the so-called NH effect described by Noyori[44] was reported to be here a requirement to obtain catalytic activity.

b- PN-sp^{2}N ligand

The combination of P- and N- donor atoms also amounts to modifying the hardness *versus* softness of the coordinating ends, which should make it possible to develop heteroleptic ligands with well-defined electronic properties. In this idea, Milstein et *al*. described the preparation of a PNN-type Mn pincer complex based on a central pyridine and a lateral amine.[45,46] This complex directly obtained by the reaction of a PNN(H) ligand and $Mn(CO)_5Br$ allowed the hydrogenation of a wide range of esters under rather mild conditions (Cat. 1 mol %, KH 2 mol %, 20 bar H_2, toluene, 100 °C) (**Scheme 12**, *left*).[45] Under these conditions, aliphatic and aromatic esters, as well as esters bearing terminal alkenes, CF_3 and CN groups were converted to corresponding alcohols in excellent yields. To get more insight into the mechanism and identify active species, the Mn complex was reacted with a base knowing that the deprotonation can take place either at the benzylic position leading to the dearomatization of the pyridine or at the N−H position. A solid analysis of the deprotonated complex indicated rather the formation of an amido complex able of activating H_2 to form *cis*- and *trans*- dihydride isomers, which slowly isomerize in solution. The same Mn complex was also considered for the hydrogenation of organic carbonates to methanol and alcohols.[46] A large variety of carbonates were thus converted under moderate catalytic conditions (Cat. 2 mol %, KH 4 mol %, 30−50 bar H_2, 110 °C). About the mechanism, the authors proposed the formation of formate and

aldehyde intermediates through metal-ligand cooperation between the Mn center and the N−H coordinating moiety of the ligand.

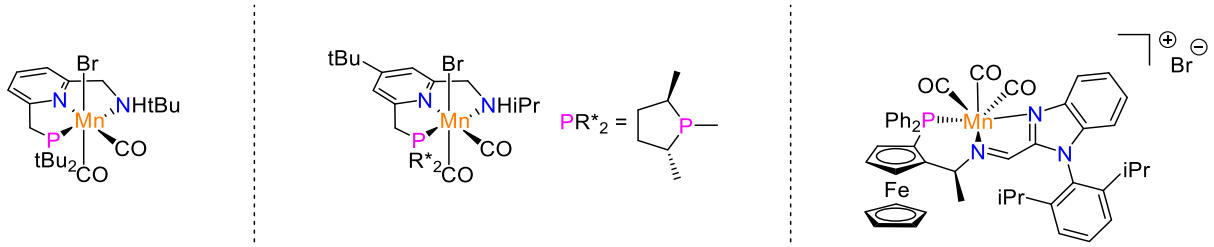

Scheme 12. Mn(I) complexes based on PN-sp^{2}N ligand in the chiral and achiral series.

Introducing a chiral phospholane resulted in the formation of asymmetric PNN pincer Mn(I) complexes combining the features of Milstein's achiral motif PNN[45,46] and those of a stereogenic phosphine as in the Beller's system (**Scheme 12**, *middle*).[24] Upon addition of $Mn(CO)_5Br$ complex, corresponding Mn(I) complexes were obtained as a mixture of two isomers due to the *syn*- and *anti*- orientations of the flexible NH donor relative to the metal-halogen bond.[47] Under 1 mol % catalyst loading, the (*S,S*)- complex afforded full conversion in the hydrogenation of acetophenone with 67% *ee*. Addition of alcohols such as *i*PrOH or $(CF_3)_2CHOH$ resulted in the improvement of both activities and selectivities. The best result was obtained with the (*R,R*)- complex where the catalyst loading was diminished to 0.01 mol % while maintaining quasi-full conversion with 86% *ee* and a TON of 9800. With this system, a wide range of aryl alkyl- and heteroaromatic ketones could be converted to corresponding chiral secondary alcohols in 85−97% *ee*. Benzofused cyclic- and diaryl ketones could be also transformed with high enantioselectivity. Experimental studies confirmed the critical role of the NH moiety in agreement with the existence of an outer-sphere mechanism.

Mn(I) catalysts bearing imidazole-based chiral PN-sp^{2}N tridentate ligands have been prepared allowing the asymmetric hydrogenation of unsymmetrical benzophenones (**Scheme 12**, *right*).[48] This system characterized by a high activity (up to 13 000 TON) and enantioselectivity (up to > 99% *ee*) tolerates a large range of substrates and presents a good tolerance of the functional group. The imine group was invoked to play a key role in the cleavage of H_2 and the activation of the substrate.

The hydrogenation of challenging carbamate and urea substrates was recently reported, thanks to the efficiency of the Mn(I) pincer complex of a PN-sp^{2}N pincer ligand (**Scheme 13**).[49] In both cases, under slight H_2 pressure (20 bar), methanol formation was observed in addition to the amine and alcohol products. This transformation, which represents a sustainable method for

the conversion of CO_2 to methanol, implies a cooperative metal-ligand mode *via* the dearomatization of the pyridine nucleus.

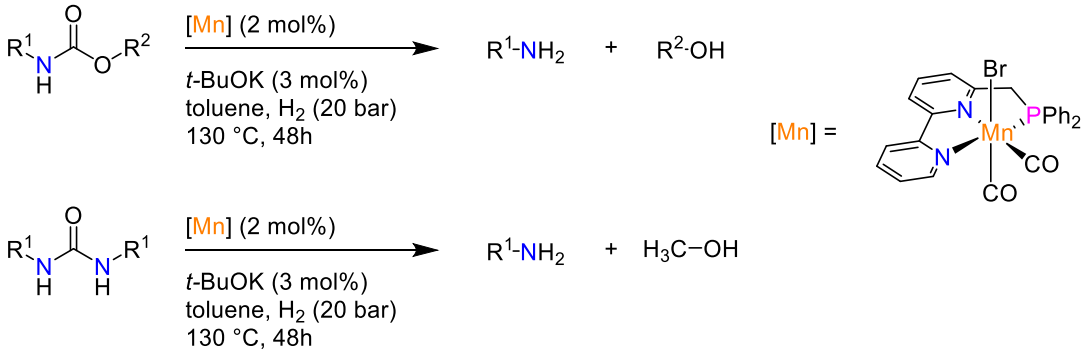

Scheme 13. Mn(I) complex based on a PNsp^{2}N ligand for the hydrogenation of carbamates and ureas.

2.3 NNN Ligands

Transfer hydrogenation is a complementary process to classical hydrogenation, and by varying the nature of donor extremities, the group of Beller discovered that Mn(I) complexes featuring a NNN pincer ligand act as very efficient catalysts for the transfer hydrogenation of ketones (**Scheme 14**).[50] These Mn complexes were easily obtained from commercially available tridentate amine (dipicolylamine) and $Mn(CO)_5Br$ complex. Under optimized conditions (Cat. 1 mol %, *t*-BuOK 2 mol %, 70 °C, *i*PrOH), a broad range of hetero(aromatic) and aliphatic ketones could be reduced with good to excellent yields, especially substrates containing nitrile and ester groups. Cyclic ketones, such as cyclohexanone or 1-ethyl-4-piperidone were also transformed into corresponding alcohols in 90 and 85% yields, respectively. Chemoselectivity was illustrated through the selective reduction of dihydro-β-ionone in 97% yield. The only limitation concerns aldehydes which were found to be unreactive in the developed catalytic conditions. Mechanistic studies indicate that the reaction occurs through a mono-hydride species but that cooperation with the NH moiety is not essential since the N−Me analogue led to similar catalytic results.[51] Even if the mechanism of this process remains unclear to date, an outer-sphere mechanism can be excluded and the catalytic results obtained raise the question of whether the aromatization/dearomatization process through the activation of the benzylic arm that takes place in related PNP pincer complexes applies here. Noteworthy, the same type of NNN ligand was also reported to be efficient for the transfer-dehydrogenation of secondary alcohols.[51]

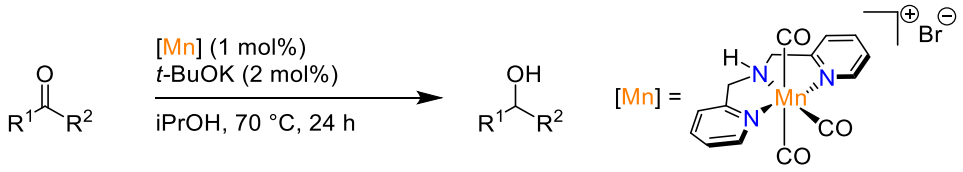

Scheme 14. Mn(I) complex of a NN-sp^{3}N pincer ligand for the transfer hydrogenation of ketones.

2.4 CNP Ligands

In order to improve the stability of manganese catalysts, the group of Pidko described recently the pincer version of the previously reported bidentate CN Mn(I) complex (see **Scheme 23**),[72] by extending the ligand with an additional phosphine donor arm through simple reductive amination. Treatment of the tridentate CNP ligand obtained in 81% yield with $Mn(CO)_5Br$ followed by the addition of KHMDS afforded the corresponding NHC complex in 51% yield (**Scheme 15**, *middle*).[52] This complex was found to be highly efficient for the hydrogenation of ketones, imines, aldehydes and esters. Under the optimal conditions, 50 bar of H_2, 1 mol% of $KHBEt_3$ promoter, and dioxane as a solvent, quantitative hydrogenation of acetophenone to the corresponding alcohol was obtained with very low catalyst loadings (50 ppm) at 60°C with TOF up to (41 000 h^{-1}) and TON up to (200 000). The catalyst tolerates high reaction temperatures (up to 120 °C), which indicates a remarkable improvement in thermal stability over the analogue bidentate CN complex, which does not resist at elevated temperature. Concerning the mechanism involved, similar to most bifunctional hydrogenation catalysts, the formation of Mn hydride pincer complex (**Scheme 15**, *right*) was observed after the reaction of the CNP Mn(I) complex with an excess of *t*BuOK followed by the addition of dihydrogen. However, the reaction is slow and leads to low conversion (24%) at 50 °C over 12 h. As an alternative method, the reaction of the pre-catalyst with 2.5 equiv. of $KBHEt_3$ at room temperature, instantly yielded the Mn hydride species featuring a free phosphine arm (**Scheme 15**, *left*), that was found to be more active than the related pincer, highlighted thus the important role of hemilabile ligands for improving catalytic processes.

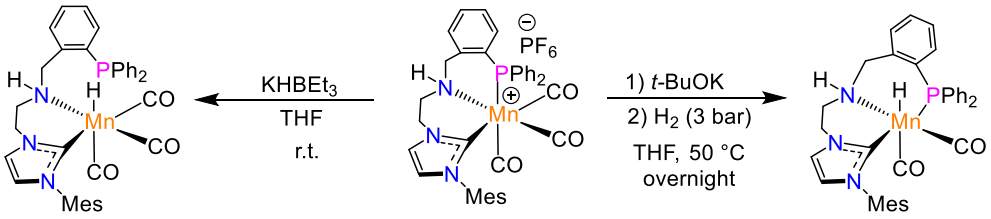

Scheme 15. Mn(I) complex based on a CNP pincer ligand for the hydrogenation of ketones, imines, aldehydes, and esters.

3. Non-Pincer-Type Manganese Complexes

The tridentate coordination mode is not a prerequisite for carrying out hydrogenation-type reactions with manganese complexes. By combining N- and P- donor atoms, different bidentate Mn(I) systems were thus successfully developed as was previously done in the pincer series. The singularity of the bidentate series concerns the presence of the carbon element as coordinating atom. Carbon was introduced here into its sp^2-hybridization state *via* an N-heterocyclic carbene (NHC).

3.1 NN Ligands

Complexes based on NN ligand are the most developed systems in the bidentate series. Three families can be distinguished depending on the hybridization state of the N-donor atoms: *ca*. the N-sp^3,N-sp^3; N-sp^2,N-sp^2; and the N-sp^3,N-sp^2 families.

a- N-sp^3,N-sp^3 ligand

In order to develop simple, sustainable, and practical catalytic systems, Sortais et *al*. reported that nitrogen-based bidentate Mn(I) catalysts featuring a chelating diamine ligand were effective for the transfer hydrogenation of ketones (**Scheme 16**, *left*).[52] A series of simple diamine ligands in the presence of $Mn(CO)_5Br$ as a metal precursor (0.5 mol %), *t*-BuOK as a base (1 mol %) and 2-propanol as a reductant was screened for the reduction of acetophenone. Using ethylene diamine as a ligand, the transfer hydrogenation reaction was shown to proceed in high yield at 80 °C in 3 hours. The generality of the reduction with the *in-situ* prepared Mn(I) ethylene diamine system was then demonstrated through the effective conversion of various *para*-substituted acetophenone substrates into corresponding alcohols. Encouraged by these results, chiral diamines were also engaged as illustrated with the formation of sterically hindered alcohols with enantiomeric excess up to 90% in the presence of the chiral (1*R*,2*R*)-*N,N'*-dimethyl-1,2-diphenylethane-1,2-diamine (**Scheme 16**, *middle*).[52] This approach demonstrated for the first time that simple bidentate, phosphine free ligands can be associated with manganese to promote (enantio)selective reactions in the field of hydrogenation.

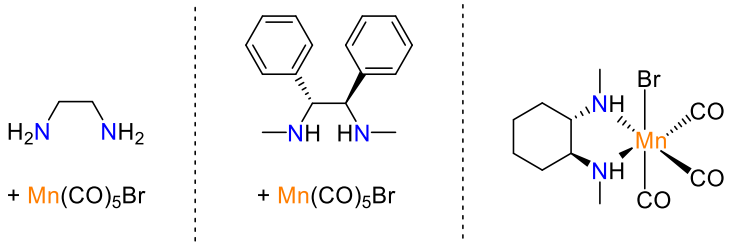

Scheme 16. N-sp^3,N-sp^3 ligands involved in hydrogenation-type reactions.

Based on this preliminary report, Pidko et *al*. described the preparation and the catalytic performance of a series of Mn(I) complexes bearing simple chiral diamine ligands in the asymmetric transfer hydrogenation of acetophenones to the corresponding alcohols with 75−87% *ee* (**Scheme 16**, *right*)[53] From these complexes, experimental and DFT calculations, as well as kinetic studies were performed evidencing the complexity of the different intermediates responsible for the catalytic activity in terms of (enantio)selectivity.

b- N-sp^2,N-sp^2 ligand

Inspired by nature with the role of Fe-hydrogenases based on an *ortho*-OH-substituted pyridine backbone, related Mn(I) catalysts were developed for the hydrogenation of CO_2 (**Scheme 17**). A series of air-stable neutral and cationic Mn(I) complexes bearing readily available substituted 2,2'-bipyridyl ligands were thus prepared and fully characterized.[54] In the series, 6,6'-dihydroxy-2,2'-bipyridyl-based Mn catalysts were shown to present high activity for CO_2 hydrogenation to formate in the presence of DBU base at relatively low temperature leading to TON up to 6250. The hydrogenation of CO_2 to formamide was also achieved in 72 % yield with such complex in the presence of diethylamine as a base with a TON of 588 after 24 h at 80 °C.

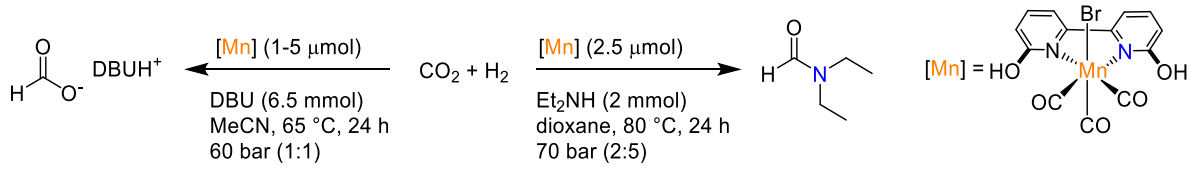

Scheme 17. Mn(I) complex based on a N-sp^2,N-sp^2 ligand for the hydrogenation of CO_2.

In the continuity of this work, the same type of Mn complex based on a bidentate bipyridyl-type ligand was used for the transfer hydrogenation of ketones, aldehydes, and imines.[55] In

addition to reduce a broad scope of ketones and aldehydes with good functional group tolerance, the specificity of the present system lies in the reduction of aromatic N-heterocycles into corresponding saturated cyclic amines. For instance, acridine, quinoxaline, and 1,5-naphthydrine could be reduced with 0.5 mol % catalyst loading, 1.5 mol % of *t*-BuOK at 80 °C in 84, 94, and 92% yields, respectively. Among different substituted bipyridine ligands, the representative bearing two hydroxyl groups appeared to be the best catalyst, surpassing its analogue based on two methoxy groups. Labeling experiments with the help of DFT calculations concluded on the active role of the hydroxyl groups in the hydrogen transfer steps through the formation of mono-hydride species.

Catalytic activity in the transfer hydrogenation of ketones and aldehydes was also observed with 2-hydroxy-substituted NN ligands when a pyridine nucleus is replaced by a quinoline or naphthyridine moiety. The best representative allowed the formation of a series of secondary alcohols in satisfactory yields according to the following catalytic conditions: Cat. 0.5 mol %, *t*-BuOK 20 mol %, 85 °C, 24 h.[56] Noteworthy, the preparation of 1,2-disubstituted benzimidazoles and quinolines *via* acceptorless dehydrogenation condensations was shown to be possible with the latter type of catalysts.

c- N-sp^2,N-sp^3 ligand

In the quest for simple and inexpensive catalytic systems, mixed N-sp^2,N-sp^3 ligands were also envisaged as exemplified with the transfer hydrogenation of carbonyl derivatives catalyzed by Mn(I) complexes bearing 2-(aminomethyl) pyridine ligands (**Scheme 18**, *left*).[57] The Mn(I) complexes of interest were prepared stepwise by reacting aminomethyl pyridine precursors with the $Mn(CO)_5Br$ complex. A large variety of ketones and aldehydes, including α,β-unsaturated aldehydes could be reduced under mild conditions, that is at room temperature with low catalyst loading down to 0.1 mol % and 2-propanol as hydrogen source while having a high tolerance towards functional groups. TONs and TOFs up to 2000 and 3600 h^{-1} respectively, were observed under these catalytic conditions. In the understanding of the catalytic cycle, a dimeric Mn(I) complex resulting from the deprotonation of the NH moiety was isolated as an intermediate species consistent with the generally accepted mechanism of ligand-assisted hydrogen transfer reactions.[58]

The well-defined Mn(I) complex of the bidentate 2-(aminomethyl) pyridine ligand was also used for the transfer hydrogenation of imines.[59] Using 2-propanol as a reductant, in the presence of *t*-BuOK (4 mol %) and the pre-catalyst (2 mol %), a large variety of aldimines (30

examples) was reduced in 3 h at 80 °C with good to excellent yield. Here again, the catalytic conditions were reported to be tolerant with a broad range of functional groups (halogen, methoxy, cyano, ester, amido, acetal, vinyl, alkynyl).

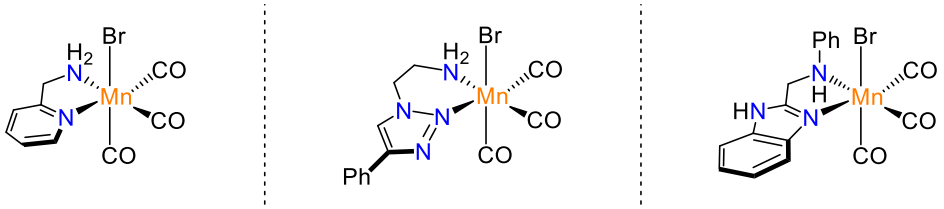

Scheme 18. Mn(I) complexes bearing N-sp^2,N-sp^3 ligands for hydrogenation-type reactions.

On the basis of encouraging results obtained with simple NN ligands, alternative N-donor units were then envisaged. In this logic, several Mn(I)(CO)$_3$Br complexes based on bidentate amino triazole ligands with different substitution pattern were prepared and investigated in the transfer hydrogenation of ketones (**Scheme 18**, *middle*).[60] Under mild conditions, *ca*. at 80 °C for 20 h with 3 mol % of catalyst loading using either *t*-BuOK or NaOH as a base, a wide scope of ketones with large functional group tolerance was reduced to the corresponding alcohols in good to excellent yield. The critical role of the amine function was demonstrated by comparing the catalytic activity of the amino triazole complex with a related complex based on an imino triazole backbone. The superiority of the former evidences the existence of an out-sphere hydrogen transfer with the NH_2 coordinating group acting as a proton source.

Catalytic performances were also observed in the hydrogenation of carbonyl derivatives and imines with Mn(I) complexes featuring cooperative amino benzimidazole ligands (**Scheme 18**, *right*).[61] It was established that both benzimidazole and NH amine donors contribute to the high catalytic activity observed as clearly demonstrated with the higher reactivity of the *N*-((1*H*-benzimidazol-2-yl)methyl) aniline based Mn complex. From this observation, a concerted outer-sphere mechanism was proposed supported by DFT calculations. Concerning its catalytic activity, the present system (Cat. 0.2 mol %, *i*PrONa 20 mol %, 90 °C, 2 h) allowed the efficient reduction of a wide range of ketones, aldehydes, and challenging imines, as well as unsaturated ketones with good chemoselectivity.

3.2 PP Ligands

Bis-phosphine ligands were first considered by Kirchner et *al*. for the manganese catalyzed hydrogenation of nitriles and ketones.[62] The catalytic active Mn(I) complex was obtained in

71% yield by treating the chelating bis-phosphine nPr$_2$PCH$_2$CH$_2$PnPr$_2$ with the Mn(CO)$_5$Br complex (**Scheme 19**, *right*). This catalytic system allowed the effective hydrogenation of a range of (hetero)aromatic and aliphatic nitriles into primary amines. Electron-donating (Me, MeO, H$_2$N), electron-withdrawing groups (Cl, Br), as well as heterocycles were well tolerated in the selected conditions. Chemoselectivity was observed as illustrated with the reduction of the nitrile function in the presence of an ester group or a C=C bond. Also, 4-((trimethylsilyl)ethynyl) benzonitrile was reduced into the corresponding amine in 67% yield without affecting the CC triple bond. Linear aliphatic nitriles and decanedinitrile could be also converted in high yields. The best conditions developed for the hydrogenation of nitriles were the following: Cat. 2 mol %, *t*-BuOK 20 mol %, 100 °C, 18 h. Aromatic and aliphatic ketones were also reduced into the corresponding alcohols in excellent yields (71−96%). The hydrogenation reaction occurred in this case at 50 °C with a catalyst loading of 1 mol % in the presence of 5 mol % of base. On the mechanism, the authors proposed the role of a hydride complex as an active species, arguing that metal-ligand cooperation cannot take place and that an outer-sphere process without involvement of the ligand can probably happen.

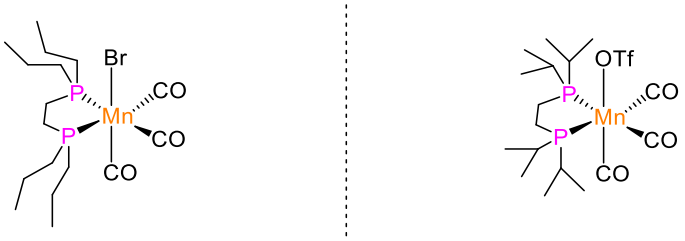

Scheme 19. Mn(I) complexes bearing bidentate PP ligands for hydrogenation reactions.

Almost simultaneously, Garcia et *al*. reported an analogous non-pincer Mn(I) complex for the same catalytic purpose (**Scheme 19**, *right*).[63] The cationic complex *fac*-[(CO)$_3$Mn(iPr$_2$P(CH$_2$)$_2$PiPr$_2$)(OTf)] based on an electron-rich bisphosphine ligand as a catalyst precursor (3 mol %) exhibited catalytic activity toward the hydrogenation of (hetero)aromatic and aliphatic nitriles in the presence of the *t*-BuOK base (10 mol %) affording primary amines in good yields (83−98%) under rather mild conditions (ca. 7−35 bar H$_2$, 90 °C, 15−30 min., 2-BuOH). It is worth noting the efficient hydrogenation of dinitriles, such as terephthalonitrile and adiponitrile into corresponding diamines. As in the case of Kirchner report, unsaturated Mn hydride complexes have been discussed to participate in the determining catalytic steps.

The same authors observed that secondary alcohols such as 2-butanol can substitute for molecular hydrogen in the hydrogenation of nitriles.[64] For such an application, they used the

fac-[$(CO)_3Mn(iPr_2P(CH_2)_2PiPr_2)(Br)$] complex more easily synthesizable than the cationic Mn−OTf analogue. The Mn−Br complex (3 mol %) exhibited catalytic activity in the presence of *t*-BuOK (10 mol %) for the transfer hydrogenation of benzonitrile leading to a mixture of benzylamine and N-*sec*-butylidenebenzylamine. After acidic treatment of the mixture, benzylamine hydrochloride can be formed in 96 % yield. According to this strategy, a series of amine hydrochlorides was readily prepared (39−92 % isolated yields). Aromatic nitriles bearing electron-donating groups (Me, MeO) were more easily converted than those containing electron-withdrawing groups (CF_3). Like in the conventional hydrogenation reaction, unsaturared Mn hydride species were proposed to be involved in the catalytic cycle.

Manganese based catalysts capable of hydrogenating unactivated C=C bonds are still rare. On the basis of this finding, Kirchner et *al*. took advantage of the readily available *fac*-[$(CO)_3Mn(iPr_2P(CH_2)_2PiPr_2)(CH_2CH_2CH_3)$] complex to perform the Mn-catalyzed hydrogenation of alkenes to alkanes (**Scheme 20**).[65] From a mechanistic point of view, the catalytic transformation is initiated by migratory insertion of a CO ligand into the Mn−$CH_2CH_2CH_3$ bond to form an acyl intermediate which affords the catalytically active Mn(I) hydride complex after hydrogenolysis. Except for 4-vinylpyridine (39 % of conversion), this strategy allowed the hydrogenation of mono- and disubstituted alkenes into corresponding alkanes in very satisfactory yields (70−99%). Additionally, the developed conditions (Cat. 2 mol %, 50 bar H_2, 25-60 °C, 18-24 h) are compatible with a high functional group tolerance. The only difference is relative to the temperature, namely that hydrogenation of monosubstituted alkenes and 1,1-disubstituted alkenes take place at 25 °C while 1,2-disubstituted representatives require a higher temperature of about 60 °C. According to DFT calculations and experimental studies, an inner shell mechanism was proposed with catalytic steps involving successively the protonation of the internal C=C bond in the Mn hydride complex followed by H_2 coordination, hydride insertion into the Mn−C bond and final release of the alkane product.

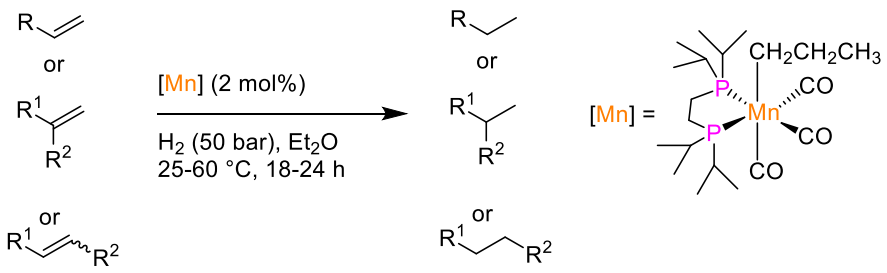

Scheme 20. Mn(I) complex of a bidentate PP ligand for the hydrogenation of alkenes.

3.3 NP Ligands

a- N-sp^3,P-sp^3 ligand

Non-pincer PN Mn(I) complexes based on simple and easily accessible bidentate aminophosphine ligands were first reported by Pidko et *al.* (**Scheme 21**, *left*).[66] They were easily prepared by reacting the $Mn(CO)_5Br$ complex with corresponding PN precursors, and depending on the ratio metal/ligand used, mono- or diligated PN Mn(I) complexes were selectively obtained. In the cationic octahedral bis(PN) $Mn(CO)_2$ complex, the two N-donor groups are located in *cis*-position while the two P-donor groups bind in *trans* position to each other. Both types of Mn(I) complexes were found to be active for ester hydrogenation. However, by using methyl benzoate as a model substrate, the mono-ligated representative exhibited higher activity compared to diligated complexes. Aliphatic and aromatic esters were effectively reduced to very low catalytic levels down to 0.2 mol % in the presence of *t*-BuOK base. Sterically demanding aliphatic esters were almost quantitatively hydrogenated while functional group tolerance (Cl, MeO) was observed with *para*-substituted aromatic substrates. Chemoselectivity of unsaturated esters was only reached for substrates where the C=C bond is located far from the ester group, such as in fatty acid methyl esters. The exact role of the base was experimentally studied and rationalized by DFT calculations, suggesting possible inhibition through the formation of stable Mn−alkoxide species acting as resting states.[67]

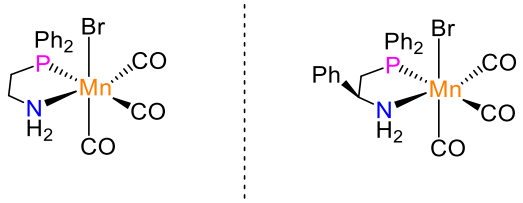

Scheme 21. Mn(I) complexes based on bidentate NP ligands in hydrogenation reactions.

PN ligands based on amino acids were also considered for hydrogenation-type reactions. Mn(I) complexes bearing a *β*-amino phosphine ligand derived from phenylglycine were reported to act as efficient catalysts for the transfer hydrogenation of ketones and chalcones (**Scheme 21**, *right*).[68] The main advantage lies in the high accessibility of *β*-amino phosphines that can be easily produced from cheap amino acid feedstocks. With such bidentate PN Mn(I) complex, transfer hydrogenation of acetophenone in 2-propanol was found to be quantitative at 60 °C with 0.5 mol % catalyst loading and 1 mol % of base. The catalytic conditions tolerated a broad scope of *para*- and *ortho*-substituted acetophenones. Good functional tolerance was generally

achieved under mild conditions excepted for phenolic acetophenones, which appeared to be non-reactive. The challenging *p*-nitroacetophenone was reduced in 71% yield after refluxing 3 days. Thanks to the unique properties of *β*-amino phosphine ligands, chalcone derivatives were selectivity reduced to the saturated ketones, further reduction to the corresponding alcohols being observed only under drastic conditions. The isomerization of allylic alcohols was also described with *β*-aminophosphine-supported Mn(I) catalysts.

b- N-sp^2,P-sp^3 ligand

Mn(I) complexes featuring bidentate 2-aminopyridinyl phosphine ligands were reported to be highly active in the hydrogenation of carbonyl derivatives (**Scheme 22**).[69] Different Mn(I) complexes were readily prepared in excellent yield upon treatment of $Mn(CO)_5Br$ with corresponding PN ligands derived from the reaction between a chlorophosphine R_2PCl (R = Ph, *i*Pr) and 2-aminopyridine, 2-picoline, or 2-methylquinoline. All complexes exhibit a typical octahedral geometry for the Mn center, the PN ligand being coordinated in a k^2*P,N*- fashion with the three CO ligands adopting a facial arrangement. The catalytic activity of these heteroleptic complexes was evaluated for the hydrogenation of a wide range of carbonyl derivatives, such as *para*-substituted aromatic ketones, aliphatic ketones, unsaturated ketones, and *para*-substituted benzaldehydes. The reaction proceeds generally with low catalyst loading (0.5 mol %) under mild conditions (50 °C) with yields up to 96 %. High functional group tolerance was also observed compared to the most active catalytic systems. Based on these results, the authors point out that bidentate complexes can compete with pincer systems, knowing that these complexes bearing 2-aminopyridinyl phosphine are more effective than related PNP-type pincers,[28] reducing the catalyst loading by a factor of ten, and lowering the temperature from 130 °C to 50 °C with the same activity and chemoselectivity. Noteworthy such Mn pyridinyl phosphines complexes were also used for the alkylation of amines *via* reductive amination of aldehydes using molecular dihydrogen as a reductant.[70] After the initial condensation step, the reduction of imines formed *in situ* was achieved under mild conditions with 2 mol % catalyst loading, 5 mol % of *t*-BuOK at 50 °C in ethanol under 50 bar of hydrogen. High yields were obtained for a large range of aldehydes and amines (**Scheme 22**).

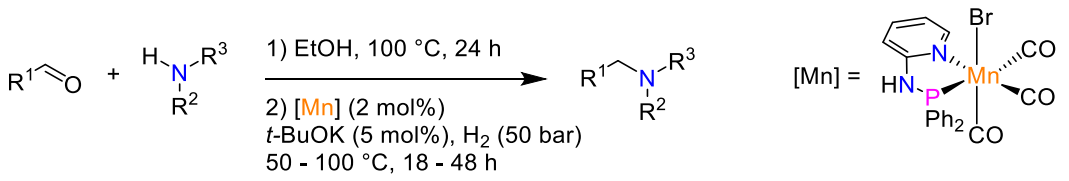

Scheme 22. Mn(I) complex featuring a PN ligand for the reductive amination of aldehydes.

3.4 CN Ligand

Considering the unique steric and electronic properties of NHC ligands, and the recent developments in the field of NHC Mn(I) catalysis, bidentate ligands incorporating electron-rich NHC donors were naturally envisaged for hydrogenation reactions. Pidko et *al*. reported the preparation of Mn(I) complexes bearing strongly donating bidentate NHC-amine ligands (**Scheme 23**).[71] The pre-ligands were prepared by reacting 1-mesityl-1*H*-imidazole with 2-bromoethylamine hydrobromide salts. The Mn(I) complexes were then obtained in satisfactory yield through the reaction of *in-situ* generated free NHCs with Mn(CO)Br. While the complex featuring the N(Me)H donor was found to be highly active for the transfer hydrogenation of ketones with *i*PrOH, the $N(Me)_2$ analogue appeared to be inactive under the same conditions. The Mn(I) NHC-N(Me)H complex exhibited unprecedented catalytic activity affording quasi-quantitative reduction of acetophenone with very low metal concentration down to 75 ppm (0.0075 mol %). A wide range of aromatic ketones could be reduced, except for very hindered representatives, such as 2,4,6-trimethylacetophenone. Aliphatic cyclic and linear ketones were also converted to corresponding alcohols but generally with lower efficiency. Chemoselectivity was observed for the reduction of unsaturated ketones, as illustrated in the case of benzylideneacetone with the formation of the corresponding unsaturated alcohol in 82% yield. Functional group tolerance was demonstrated with the efficient reduction of *para*-substituted acetophenones bearing halide atoms, phenyl and esters groups. Lower conversions were however observed for substrates containing hydroxyl, cyano and nitro substituents. Mechanistic studies evidenced that metal-ligand cooperativity operates through a bifunctional protonation/deprotonation mechanism, thanks to the presence of the N(Me)H donor group. The authors concluded that the present catalytic Mn system can compete with more conventional catalysts based on Ru or Ir noble metals.

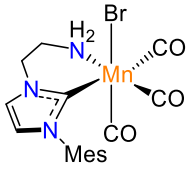

Scheme 23. Mn(I) complex based on a bidentate CN ligand for the hydrogenation of ketones.

4. Other Manganese Complexes

Bidentate and pincer-type manganese complexes based on C, N, P- donor atoms are not the only possible systems for catalyzed hydrogenation-type reactions. Mono- and tetradentate manganese complexes built from different atoms such as oxygen and silicon exist.

4.1 Monodentate Ligand

N-heterocyclic silylenes (NHSi) are not only exotic species but can act as strong donor ligands towards transition metals as behave their famous NHC analogues. Driess et *al*. reported thus the preparation of monodentate NHSi, bidentate bis(NHSi) ferrocene, and pincer-type bis(NHSi) pyridine Mn(II) complexes from the reaction between $MnCl_2$ and related ligands (**Scheme 24**).[72] Whatever the denticity of the ligand, all complexes exhibit a distorted tetrahedral environment for the Mn(II) center. In the pincer series, the central pyridine moiety is reluctant to coordinate the metal because of the stronger σ-donor character of the two NHSi extremities. All NHSi Mn(II) complexes were successfully engaged in the transfer semi-hydrogenation of alkynes using ammonia-borane as a hydrogen source. From 1-phenyl-substituted alkynes, using 1 mol % of catalyst, all systems led to high conversions and *E*-selectivity, the pincer-type Mn complex being the most efficient catalyst showing excellent *E*-stereoselectivity up to 98%. Despite a certain tolerance to functional groups, the presence of CN, NH_2, NO_2 and OH substituents at the phenyl group of 1-phenyl substituted alkynes was found to inhibit the reaction, probably due to a coordination of the active species. On the mechanism, Mn hydride active species were proposed to be involved in the catalytic cycle supported by IR measurements which evidence the presence of the corresponding Mn−H frequency at 1900 cm^{-1}. These results offer new perspectives in Mn-catalyzed hydrogenation reactions by the use of other types of ligands.

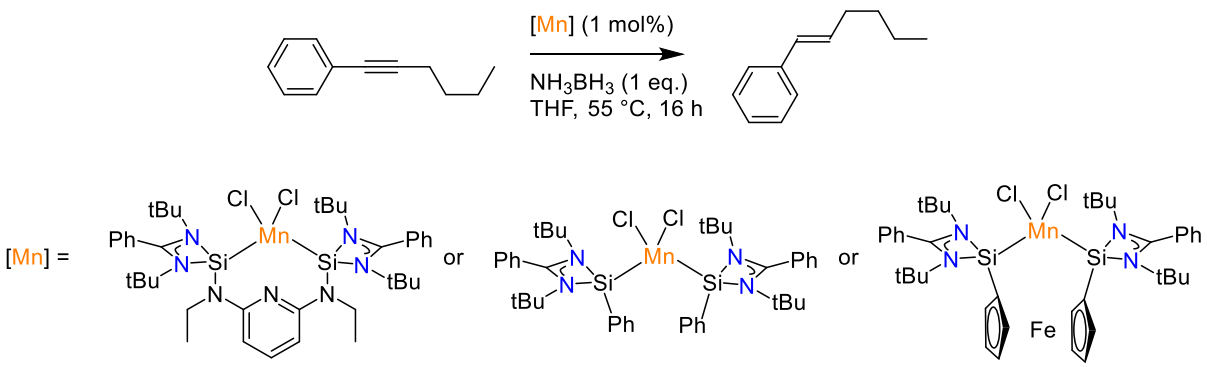

Scheme 24. Mn(II) complexes featuring Si-based ligands for the semi-hydrogenation of alkynes.

4.2 Tetradentate Ligand

In the presence of $Mn(CO)_5Br$, the ONNO-type (*S*,*S*)-Jacobsen ligand was reported by Beller et *al*. to catalyze the asymmetric transfer hydrogenation of acetophenone with 36% *ee* (**Scheme 25**, *left*).[73] Following this observation, other tetradentate ligands combining N- and O- donor atoms, especially those based on inexpensive C_2-symmetric bisoxalamides, were evaluated for such application.[73] The ligands were easily prepared by amidation of dimethyl oxalate with different amino alcohols. The *in situ* generated Mn(I) pre-catalyst derived from *N,N'*-bis(2-hydroxyethyl) oxamide ligand exhibited high activity for the reduction of aliphatic ketones with *ee* up to 93% (**Scheme 25**, *middle*). Under optimized conditions ([$MnBr(CO)_5$] 6 mol %, ligand 2 mol %, *t*-BuOK 20 mol %, *i*PrOH, 80 °C, 20 h), a variety of cyclic aliphatic prochiral ketones could be reduced with satisfactory yields and selectivities opening the door to a new class of ligands.

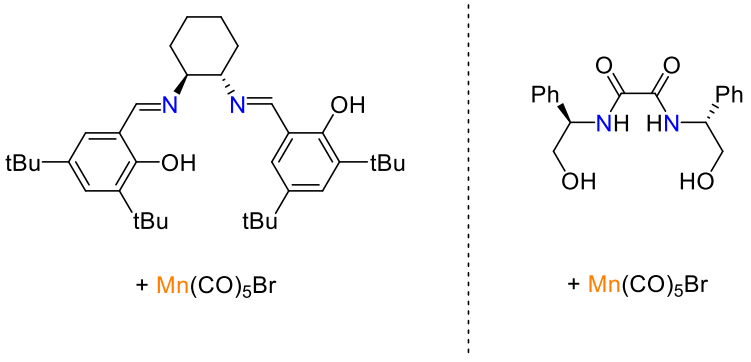

Scheme 25. Polydentate systems combining N- and O- donor atoms for the hydrogenation of ketones.

5. Conclusion

In a very short period of time, the use of base metals and especially that of manganese for catalytic purposes has grown considerably due to its availability but also to its unique properties. Hydrogenation-type reactions represent one of the most extensively developed fields of manganese catalysis, and the recent accomplishments confirm that manganese can provide a valuable alternative to noble metals. The design of a large diversity of chelating ligands, mainly in the bi- and tridentate series combining different coordinating extremities based on N-, P-, and C- donor atoms, largely explain this huge and rapid development. In addition to electronic (donation *versus* acceptation) and steric properties (rigidity *versus* flexibility) intrinsic to each ligand, the metal-ligand cooperativity has undoubtedly played a determinant role in the successful applications of manganese complexes in hydrogenation catalysis. The metal is here not the only actor but it is its role associated with that of the ligand, which is at the origin of the catalytic transformation. In order to maximize the catalytic potential of such metal complexes in terms of activity and selectivity, a better understanding of the structure-activity relation-ship will be however needed, and in particular how the metal reactivity is influenced by the ligand structure. If the access to simple and cheap catalytic systems is clearly of great interest for industrial purposes, further improvement of these systems will require the development of alternative ligands. It is very likely that carbon-based ligands will soon become very popular in this field of manganese catalysis. The selective reduction of less polar bonds is one of the many challenges that could be overcome with this latter type of ligand.

6. References

[1] S. Elangovan, C. Topf, S. Fischer, H. Jiao, A. Spannenberg, W. Baumann, R. Ludwig, K. Junge, M. Beller, *J. Am. Chem. Soc.* **2016**, *138*, 8809–8814.

[2] A. Mukherjee, A. Nerush, G. Leitus, L. J. W. Shimon, Y. Ben David, N. A. Espinosa Jalapa, D. Milstein, *J. Am. Chem. Soc.* **2016**, *138*, 4298–4301.

[3] M. Garbe, K. Junge, M. Beller, *Eur. J. Org. Chem.* **2017**, *2017*, 4344–4362.

[4] B. Maji, M. K. Barman, *Synthesis* **2017**, *49*, 3377–3393.

[5] L. Maser, L. Vondung, R. Langer, *Polyhedron* **2018**, *143*, 28–42.

[6] N. Gorgas, K. Kirchner, in *Pincer Compd.* (Ed.: D. Morales-Morales), Elsevier, **2018**, pp. 19–45.

[7] N. V. Kulkarni, W. D. Jones, in *Pincer Compd.* (Ed.: D. Morales-Morales), Elsevier, **2018**, pp. 491–518.

[8] J. I. van der Vlugt, in *Pincer Compd.* (Ed.: D. Morales-Morales), Elsevier, **2018**, pp. 599–621.

[9] H. Valdés, M. A. García-Eleno, D. Canseco-Gonzalez, D. Morales-Morales, *ChemCatChem* **2018**, *10*, 3136–3172.

[10] Z. Wei, H. Jiao, in *Adv. Inorg. Chem.* (Eds.: R. van Eldik, R. Puchta), Academic Press, **2019**, pp. 323–384.

[11] U. Chakraborty, E. Reyes-Rodriguez, S. Demeshko, F. Meyer, A. Jacobi von Wangelin, *Angew. Chem. Int. Ed.* **2018**, *57*, 4970–4975.

[12] U. Chakraborty, S. Demeshko, F. Meyer, A. Jacobi von Wangelin, *Angew. Chem. Int. Ed.* **2019**, *58*, 3466–3470.

[13] H. Grützmacher, *Angew. Chem. Int. Ed.* **2008**, *47*, 1814–1818.

[14] J. I. van der Vlugt, *Eur. J. Inorg. Chem.* **2012**, *2012*, 363–375.

[15] J. R. Khusnutdinova, D. Milstein, *Angew. Chem. Int. Ed.* **2015**, *54*, 12236–12273.

[16] E. Alberico, P. Sponholz, C. Cordes, M. Nielsen, H.-J. Drexler, W. Baumann, H. Junge, M. Beller, *Angew. Chem. Int. Ed.* **2013**, *52*, 14162–14166.

[17] M. Nielsen, E. Alberico, W. Baumann, H.-J. Drexler, H. Junge, S. Gladiali, M. Beller, *Nature* **2013**, *495*, 85–89.

[18] W. Kuriyama, T. Matsumoto, O. Ogata, Y. Ino, K. Aoki, S. Tanaka, K. Ishida, T. Kobayashi, N. Sayo, T. Saito, *Org. Process Res. Dev.* **2012**, *16*, 166–171.

[19] S. Elangovan, M. Garbe, H. Jiao, A. Spannenberg, K. Junge, M. Beller, *Angew. Chem.* **2016**, *128*, 15590–15594.

[20] S. Kar, A. Goeppert, J. Kothandaraman, G. K. S. Prakash, *ACS Catal.* **2017**, *7*, 6347–6351.

[21] J. Schneidewind, R. Adam, W. Baumann, R. Jackstell, M. Beller, *Angew. Chem. Int. Ed.* **2017**, *56*, 1890–1893.

[22] A. Kaithal, M. Hölscher, W. Leitner, *Angew. Chem. Int. Ed.* **2018**, *57*, 13449–13453.

[23] H. Li, D. Wei, A. Bruneau-Voisine, M. Ducamp, M. Henrion, T. Roisnel, V. Dorcet, C. Darcel, J.-F. Carpentier, J.-F. Soulé, J.-B. Sortais, *Organometallics* **2018**, *37*, 1271–1279.

[24] M. Garbe, K. Junge, S. Walker, Z. Wei, H. Jiao, A. Spannenberg, S. Bachmann, M. Scalone, M. Beller, *Angew. Chem. Int. Ed.* **2017**, *56*, 11237–11241.

[25] M. Garbe, Z. Wei, B. Tannert, A. Spannenberg, H. Jiao, S. Bachmann, M. Scalone, K. Junge, M. Beller, *Adv. Synth. Catal.* **2019**, *361*, 1913–1920.

[26] A. Passera, A. Mezzetti, *Adv. Synth. Catal.* **2019**, *361*, 4691–4706.

[27] F. Kallmeier, T. Irrgang, T. Dietel, R. Kempe, *Angew. Chem. Int. Ed.* **2016**, *55*, 11806–11809.

[28] A. Bruneau-Voisine, D. Wang, T. Roisnel, C. Darcel, J.-B. Sortais, *Catal. Commun.* **2017**, *92*, 1–4.

[29] W. Schirmer, U. Flörke, H.-J. Haupt, *Z. Für Anorg. Allg. Chem.* **1987**, *545*, 83–97.

[30] A. Bruneau-Voisine, D. Wang, V. Dorcet, T. Roisnel, C. Darcel, J.-B. Sortais, *J. Catal.* **2017**, *347*, 57–62.

[31] F. Bertini, M. Glatz, N. Gorgas, B. Stöger, M. Peruzzini, L. F. Veiros, K. Kirchner, L. Gonsalvi, *Chem. Sci.* **2017**, *8*, 5024–5029.

[32] M. Glatz, B. Stöger, D. Himmelbauer, L. F. Veiros, K. Kirchner, *ACS Catal.* **2018**, *8*, 4009–4016.

[33] M. Mastalir, M. Glatz, N. Gorgas, B. Stöger, E. Pittenauer, G. Allmaier, L. F. Veiros, K. Kirchner, *Chem. – Eur. J.* **2016**, *22*, 12316–12320.

[34] Y.-Q. Zou, S. Chakraborty, A. Nerush, D. Oren, Y. Diskin-Posner, Y. Ben-David, D. Milstein, *ACS Catal.* **2018**, *8*, 8014–8019.

[35] A. Zirakzadeh, S. R. M. M. de Aguiar, B. Stöger, M. Widhalm, K. Kirchner, *ChemCatChem* **2017**, *9*, 1744–1748.

[36] J. R. Cabrero-Antonino, E. Alberico, H.-J. Drexler, W. Baumann, K. Junge, H. Junge, M. Beller, *ACS Catal.* **2016**, *6*, 47–54.

[37] R. Adam, E. Alberico, W. Baumann, H.-J. Drexler, R. Jackstell, H. Junge, M. Beller, *Chem. – Eur. J.* **2016**, *22*, 4991–5002.

[38] V. Papa, J. R. Cabrero-Antonino, E. Alberico, A. Spanneberg, K. Junge, H. Junge, M. Beller, *Chem. Sci.* **2017**, *8*, 3576–3585.

[39] V. Zubar, Y. Lebedev, L. M. Azofra, L. Cavallo, O. El-Sepelgy, M. Rueping, *Angew. Chem. Int. Ed.* **2018**, *57*, 13439–13443.

[40] D. Spasyuk, S. Smith, D. G. Gusev, *Angew. Chem. Int. Ed.* **2012**, *51*, 2772–2775.

[41] M. B. Widegren, G. J. Harkness, A. M. Z. Slawin, D. B. Cordes, M. L. Clarke, *Angew. Chem. Int. Ed.* **2017**, *56*, 5825–5828.

[42] M. B. Widegren, M. L. Clarke, *Org. Lett.* **2018**, *20*, 2654–2658.

[43] K. Z. Demmans, M. E. Olson, R. H. Morris, *Organometallics* **2018**, *37*, 4608–4618.

[44] H. Doucet, T. Ohkuma, K. Murata, T. Yokozawa, M. Kozawa, E. Katayama, A. F. England, T. Ikariya, R. Noyori, *Angew. Chem. Int. Ed.* **1998**, *37*, 1703–1707.

[45] N. A. Espinosa-Jalapa, A. Nerush, L. J. W. Shimon, G. Leitus, L. Avram, Y. Ben-David, D. Milstein, *Chem. – Eur. J.* **2017**, *23*, 5934–5938.

[46] A. Kumar, T. Janes, N. A. Espinosa-Jalapa, D. Milstein, *Angew. Chem. Int. Ed.* **2018**, *57*, 12076–12080.

[47] L. Zhang, Y. Tang, Z. Han, K. Ding, *Angew. Chem. Int. Ed.* **2019**, *58*, 4973–4977.

[48] F. Ling, H. Hou, J. Chen, S. Nian, X. Yi, Z. Wang, D. Song, W. Zhong, *Org. Lett.* **2019**, *21*, 3937–3941.

[49] U. K. Das, A. Kumar, Y. Ben-David, M. A. Iron, D. Milstein, *J. Am. Chem. Soc.* **2019**, *141*, 12962–12966.

[50] M. Perez, S. Elangovan, A. Spannenberg, K. Junge, M. Beller, *ChemSusChem* **2017**, *10*, 83–86.

[51] S. Budweg, K. Junge, M. Beller, *Chem. Commun.* **2019**, *55*, 14143–14146.

[52] D. Wang, A. Bruneau-Voisine, J.-B. Sortais, *Catal. Commun.* **2018**, *105*, 31–36.

[53] R. van Putten, G. A. Filonenko, A. Gonzalez de Castro, C. Liu, M. Weber, C. Müller, L. Lefort, E. Pidko, *Organometallics* **2019**, *38*, 3187–3196.

[54] A. Dubey, L. Nencini, R. R. Fayzullin, C. Nervi, J. R. Khusnutdinova, *ACS Catal.* **2017**, *7*, 3864–3868.

[55] A. Dubey, S. M. W. Rahaman, R. R. Fayzullin, J. R. Khusnutdinova, *ChemCatChem* **2019**, *11*, 3844–3852.

[56] C. Zhang, B. Hu, D. Chen, H. Xia, *Organometallics* **2019**, *38*, 3218–3226.

[57] A. Bruneau-Voisine, D. Wang, V. Dorcet, T. Roisnel, C. Darcel, J.-B. Sortais, *Org. Lett.* **2017**, *19*, 3656–3659.

[58] B. Zhao, Z. Han, K. Ding, *Angew. Chem. Int. Ed.* **2013**, *52*, 4744–4788.

[59] D. Wei, A. Bruneau-Voisine, M. Dubois, S. Bastin, J.-B. Sortais, *ChemCatChem* **2019**, *11*, 5256–5259.

[60] O. Martínez-Ferraté, C. Werlé, G. Franciò, W. Leitner, *ChemCatChem* **2018**, *10*, 4514–4518.

[61] K. Ganguli, S. Shee, D. Panja, S. Kundu, *Dalton Trans.* **2019**, *48*, 7358–7366.

[62] S. Weber, B. Stöger, K. Kirchner, *Org. Lett.* **2018**, *20*, 7212–7215.

[63] J. A. Garduño, J. J. García, *ACS Catal.* **2019**, *9*, 392–401.

[64] J. A. Garduño, M. Flores-Alamo, J. J. García, *ChemCatChem* **2019**, *11*, 5330–5338.

[65] S. Weber, B. Stöger, L. F. Veiros, K. Kirchner, *ACS Catal.* **2019**, *9*, 9715–9720.

[66] R. van Putten, E. A. Uslamin, M. Garbe, C. Liu, A. Gonzalez-de-Castro, M. Lutz, K. Junge, E. J. M. Hensen, M. Beller, L. Lefort, E. A. Pidko, *Angew. Chem. Int. Ed.* **2017**, *56*, 7531–7534.

[67] C. Liu, R. van Putten, P. O. Kulyaev, G. A. Filonenko, E. A. Pidko, *J. Catal.* **2018**, *363*, 136–143.

[68] V. Vigneswaran, S. N. MacMillan, D. C. Lacy, *Organometallics* **2019**, *38*, 4387–4391.

[69] D. Wei, A. Bruneau-Voisine, T. Chauvin, V. Dorcet, T. Roisnel, D. A. Valyaev, N. Lugan, J.-B. Sortais, *Adv. Synth. Catal.* **2018**, *360*, 676–681.

[70] D. Wei, A. Bruneau-Voisine, D. A. Valyaev, N. Lugan, J.-B. Sortais, *Chem. Commun.* **2018**, *54*, 4302–4305.

[71] R. van Putten, J. Benschop, V. J. de Munck, M. Weber, C. Müller, G. A. Filonenko, E. A. Pidko, *ChemCatChem* **2019**, *11*, 5232–5235.

[72] Y.-P. Zhou, Z. Mo, M.-P. Luecke, M. Driess, *Chem. – Eur. J.* **2018**, *24*, 4780–4784.

[73] J. Schneekönig, K. Junge, M. Beller, *Synlett* **2019**, *30*, 503–507.

Chapter 2: Synthesis and Catalytic Applications of Bi- and Tridentate NHC-Phosphine Manganese Complexes

Chapter 2: Synthesis and Catalytic Applications of Bi- and Tridentate NHC-Phosphine Manganese Complexes

Chapter 2: Synthesis and Catalytic Applications of Bi- and Tridentate NHC-Phosphine Manganese Complexes

1. Introduction

1.1 Metal ligand cooperativity

In the past 20 years, organometallic systems where the metal center is stabilized by a cooperative ligand have emerged as powerful tools for the design of efficient metal catalysts. In these systems, the ligand and the metal are both involved in the formation of a product without any change of the metal oxidation state, by contrast to the typical oxidative addition /reductive elimination pathways (**Scheme 1**).[1]

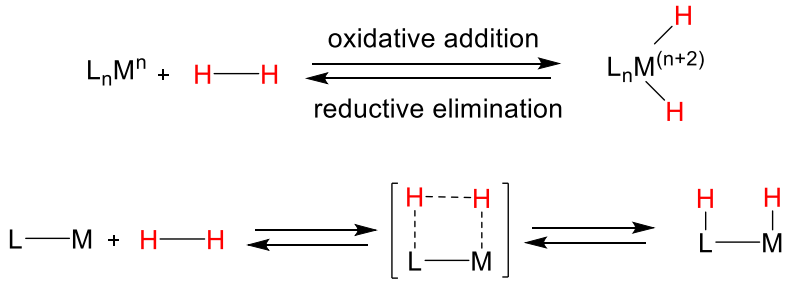

Scheme 1. Oxidative addition/reductive elimination (*up*) and bond activation through metal-ligand cooperation (*down*).

Following the discovery of Shvo-type catalysts,[2,3] a wide variety of transition metal complexes bearing non-innocent ligands was exploited for E–H bond activation (E = H, C, S, Si, N, O, B),[1] recently supplemented by related reactivity of frustrated Lewis pairs[4] and main-group ambiphiles.[5,6] Among all these transformations, the activation of dihydrogen is of utmost importance because of its essential role in catalytic transfer-hydrogenation[7–9] and hydrogen borrowing[10,11] processes relevant in the fine chemicals industry.

1.1.1 Metal–Ligand Cooperation through M–L Bonds

Many examples of H_2 bond activation through M–L bonds involving various donor atoms (N, O, P, S, B, C) were described over the years.[1,12] Three relevant examples where the donor atom can be nitrogen, oxygen or phosphorous will be more particularly discussed in the present section (**Scheme 2**).

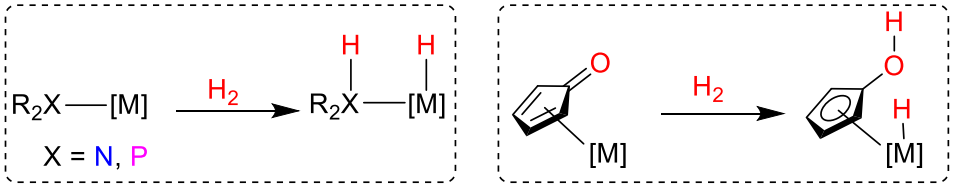

Scheme 2. H_2 activation by non-innocent ligands *via* metal-ligand cooperation.

➢ *M–NH cooperativity*

One of the most important and widely used systems to activate H_2 is the cooperation of NH moieties of ligands with the metal center, such cooperation leading indeed to considerably improved catalytic activities and selectivities with the corresponding organometallic catalysts.[13] The most impressive example of M–NH cooperativity is the Ru(phosphine)$_2$–diamine system developed by Noyori and co-workers in 1995,[14] which exhibited very high activity for the hydrogenation of ketones. Noyori discovered in particular that the addition of an amine additive containing at least one NH group such as ethylenediamine has a dramatic effect on the reactivity of the Ru catalyst. TOF of 6700 h^{-1} was indeed achieved for the hydrogenation of ketones using [$RuCl_2(PPh_3)_3$] complex with 1 equiv. of ethylenediamine in the presence of 20 equiv. of KOH in 2-propanol as a solvent and under 3 atm of H_2, while performing the reaction under the same conditions but without the diamine additive, the turnover frequency was dropped to 5 h^{-1}. Under identical conditions, amine additives without NH moieties, such as *N,N,N',N'*-tetramethylethylenediamine (TMEDA) were found to be ineffective confirming that the presence of NH moieties is necessary to increase the catalyst activity. The asymmetric version of this Ru system was also widely studied,[13,15] showing unprecedented high activities (TOF > 200 000 h^{-1}, TON > 2 × 10^6) and excellent enantioselectivity (*ee* > 98%) for the hydrogenation of ketones (**Scheme 3**).

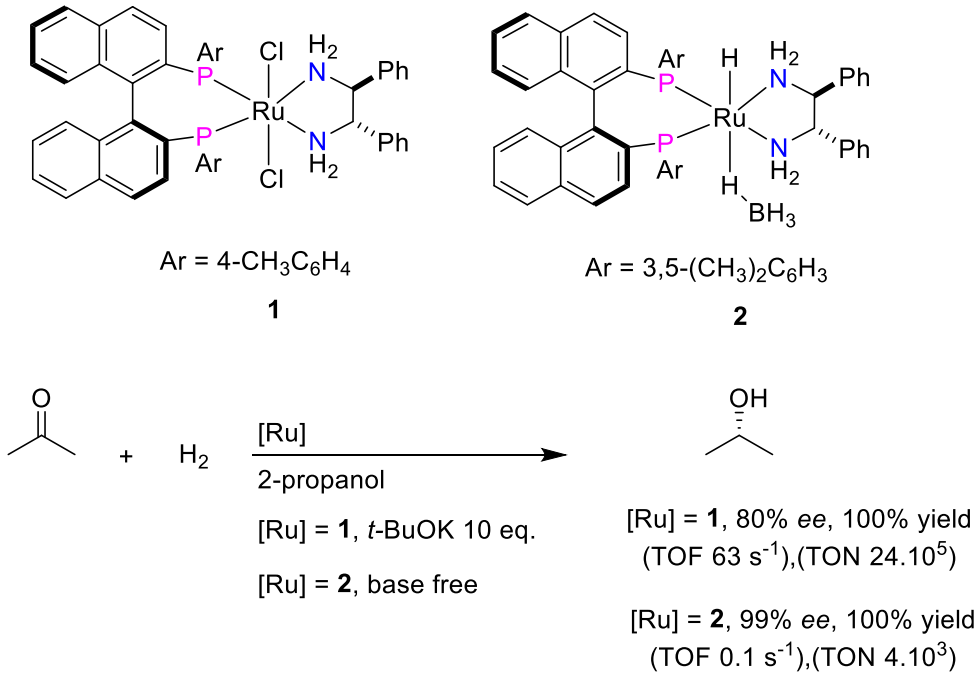

Scheme 3. Highly active chiral Ru–NH complexes for asymmetric hydrogenation of ketones.[13,15]

Mechanistic studies were investigated to explain the important effect of the NH moiety on the catalyst activity. An outer-sphere mechanism was thus proposed for the hydrogenation of ketones (**Scheme 4**).[16,17] More precisely, it was postulated that the deprotonation of the complex [$RuCl_2$(phosphine)$_2$(1,2-diamine)] **3** under H_2 atmosphere led to the formation of the active species 16 e^- amido Ru complex **4** followed by a coordination step of H_2 to the vacant site of the Ru center *via* a σ-bond to give complex **5**, which then undergoes a heterolytic cleavage across the Ru(II)–amido bond to form a Ru(II) amino hydride complex **6**. In the latter, the proton from the amine ligand and the hydride from the metal are simultaneously transferred to the C=O group of the carbonyl substrate through a six-membered transition state **TS1** to produce finally the corresponding alcohol and regenerate the 16e^- amido Ru complex **4**.

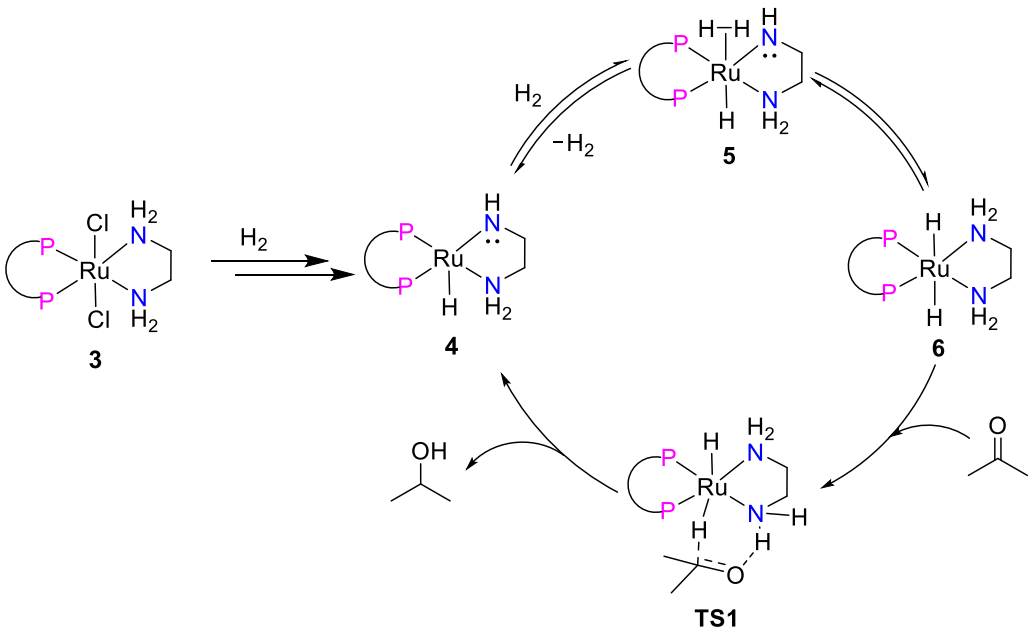

Scheme 4. Proposed mechanism for Ru–NH based-complexes in the catalyzed hydrogenation of ketones.[16,17]

- *M–L-OH cooperativity*

Compared to metal amide/amine complexes, cooperative activation with metal alkoxide/alcohol catalysts is less common.[18–23] The most known example of this type of metal-ligand cooperation concerns the hydroxy-cyclopentadienyl ligand coordinated to ruthenium discovered by Shvo.[24] The dinuclear Ru complex **7** is indeed one of the earliest developed complex in the field of metal-ligand bifunctional catalysts and it was found to be an effective pre-catalyst for many transformations including hydrogenation-type reactions of various substrates such as alkenes, alkynes, carbonyl, and imine derivatives.[25] The key role of its high catalytic activity is in fact related to the possible dissociation of the dimeric complex **7** during the catalytic process into its monomer **8** and in the η^4-cyclopentadienone ruthenium species **9** (**Scheme 5**).

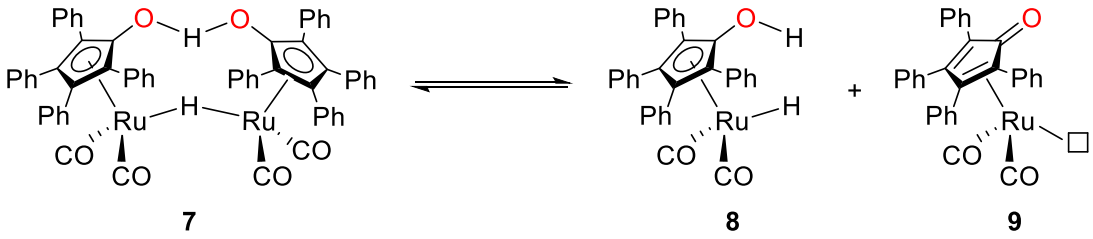

Scheme 5. Shvo's catalyst **7** in equilibrium with its active monomers **8** and **9**.[25]

Experimental and theoretical studies[26–28] supported an outer-sphere mechanism *via* a six-membered transition state for carbonyl hydrogenation. The active reducing complex **8** simultaneously transfers the hydride from the Ru(II) center and the proton from the proximal O–H group of the ligand to the carbonyl group of the substrate to form the desired product and generate Ru complex **9** (**Scheme 6**).

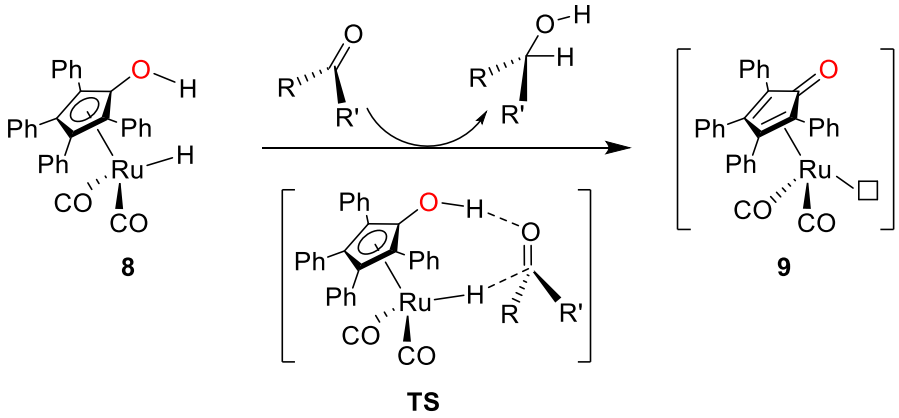

Scheme 6. Proposed mechanism for carbonyl hydrogenation by Shvo catalyst.[26]

➢ *M–PH cooperativity*

Similar transformations implying phosphorous analogues remain scarce,[29–34] the first example of H_2 activation across a M–P bond being recently reported by the group of Thomas.[29] The coordination of the tridentate PPP- ligand **10** to the metallic precursor $CoCl_2$ in THF at room temperature yielded the corresponding Co(II) complex **11** which can be reduced using KC_8 in the presence of PMe_3 to give the pincer Co(0) complex **12**. In the latter process, both phosphorus and cobalt centers were effectively reduced. The reaction of complex **12** with 1 atm of H_2 produced then the hydride complex **13** corresponding thus to the first example of hydrogen activation involving cooperativity between a first-row metal and a phosphorus atom (**Scheme 7**).

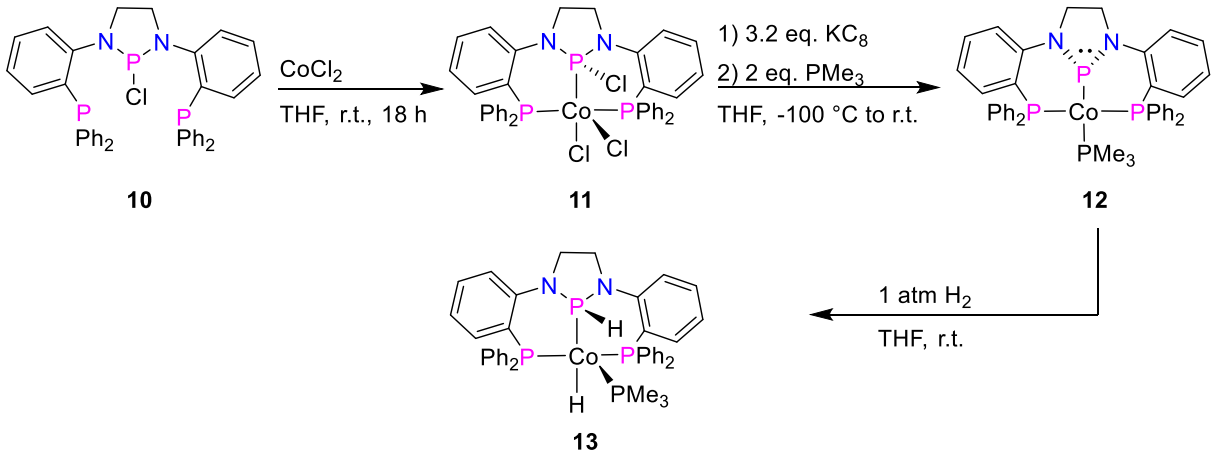

Scheme 7. Synthesis of pincer Co complexes **11** and **12**, and activation of H_2 bond by complex **12** to form the hydride complex **13**.[29]

1.1.2 Metal–Ligand Cooperation through Aromatization/De-aromatization of pyridine.

The association of N- and P- donor moieties for catalytic applications was more developed, in particular in the pincer series through the work reported by Milstein *et al.* In this specific case, the species resulting from the deprotonation of the methylene bridge in phosphine-pyridine complexes are capable to activate H_2 across the metal center and the ligand arm through a mechanism in which the re-aromatization of the pyridine nucleus ring plays a key role (**Scheme 8**).[35,36]

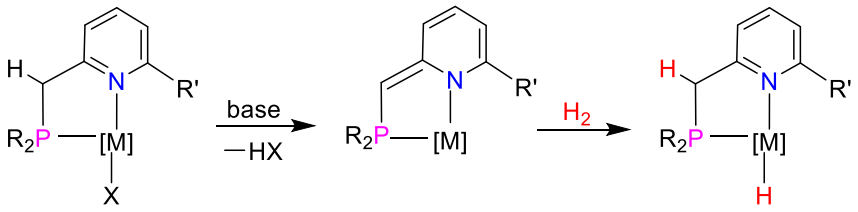

Scheme 8. Aromatization/de-aromatization process in Milstein pincer complexes.

A large variety of PNP- and PNN- pyridine-based ruthenium pincer complexes was developed catalyzing a range of C–O, and C–N dehydrogenative coupling processes. For example, the de-aromatized PNN- Ru complex **14** was found to be a very efficient catalyst for the dehydrogenation of equivalent amounts of alcohols and amines to amides and dihydrogen using only 0.1% catalyst loading (TON up to 1000) (**Scheme 9**).[37]

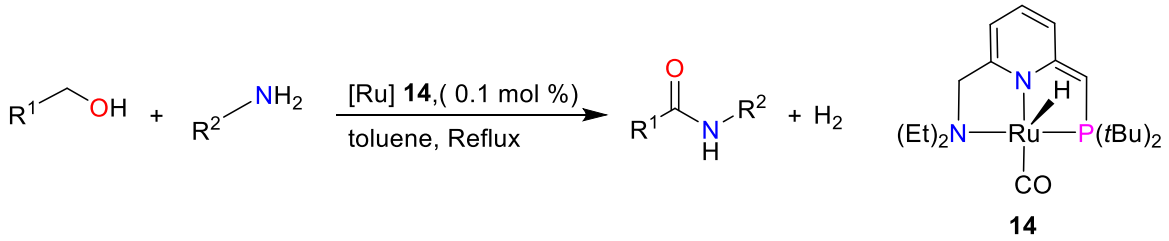

Scheme 9. PNN- Ru complex **14** for the catalyzed dehydrogenative coupling of alcohols and amines into amides.[37]

The proposed catalytic cycle involves dehydrogenation of the primary alcohol to corresponding aldehyde using Ru complex **14**. In a second time, the reaction between the aldehyde and the amine yielded a hemi-aminal derivative which reacts with complex **14** to give the aromatic intermediate **15** followed by a *β*-H elimination step to form the desired amide product and generate the Ru dihydride complex **16**. Elimination of dihydrogen from the dihydride complex **16** regenerates finally catalyst **14**, completing thus the catalytic cycle (**Scheme 10**).

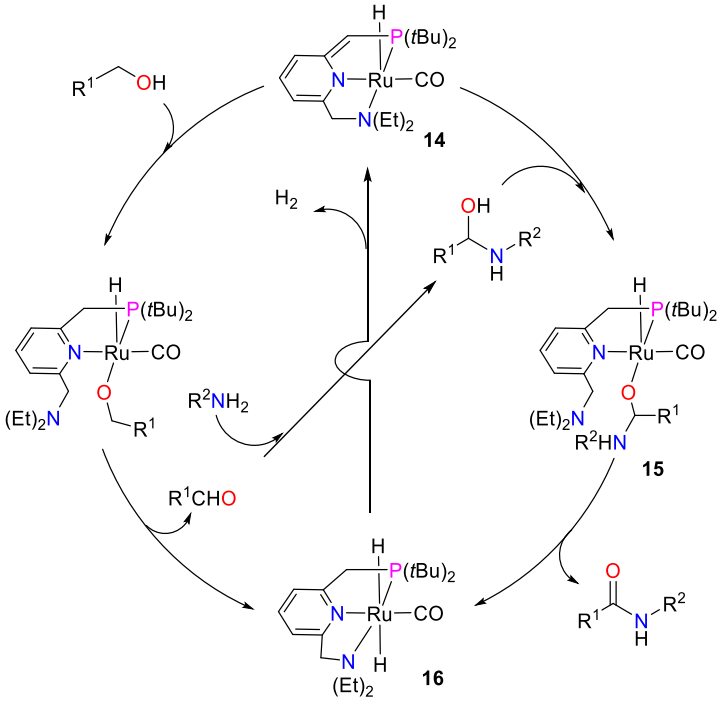

Scheme 10. Mechanism proposed for the dehydrogenative acylation of amines with alcohols using PNN- Ru pincer complex **14** as catalyst.[37]

Several analogous metal complexes have been developed by structural modulation of the ligand and the metal center. Earth-abundant metals[36] including manganese showed also excellent performances as privileged cooperating ligands in de/hydrogenation catalysis (see Chapter 1).

On the basis of these different studies and on the expertise of the group in carbene and phosphorous chemistry, we were interested in the development of new NHC-phosphine ligands characterized by unique steric and electronic properties. Upon deprotonation, these chelating ligands could possibly act as cooperative ligands through the involvement of carbon and phosphorus donor atoms in the metallic complexes where they are involved. The final objective was then to study their coordinating properties, mainly with respect to manganese(I) centers and test their stoichiometric and catalytic reactivity for the activation of dihydrogen with possible applications in the field of hydrogenation catalysis (**Scheme 11**).

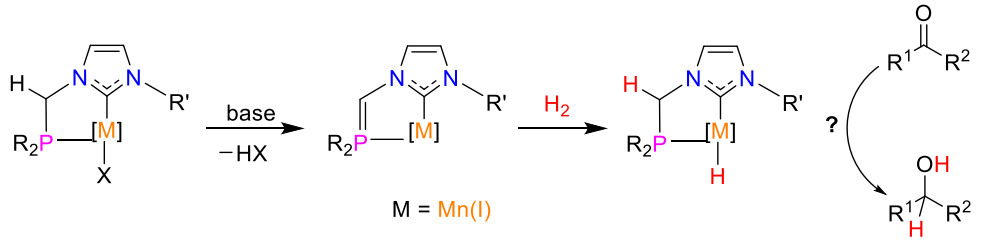

Scheme 11. H_2 activation by non-innocent ligands of NHC-phosphine type *via* metal-ligand cooperation.

1.2 Brief presentation of NHC-Phosphine ligands

Phosphorus-containing NHC derivatives can be classified into four main families: 1) Imidazoliophosphines vs. NHC-phosphenium salts,[38] 2) 4-phosphino and 4,5-diphosphino-substituted imidazolium salts,[39–44] 3) N-phosphorylated-imidazolium salts,[45–49] and 4) N-tethered phosphino-imidazolium salts (**Scheme 12**).[50]

For our part, we will focus exclusively on N-tethered phosphino-imidazolium salts (with n = 1, 2). The state of art on the synthesis of these derivatives will be discussed in the next part.

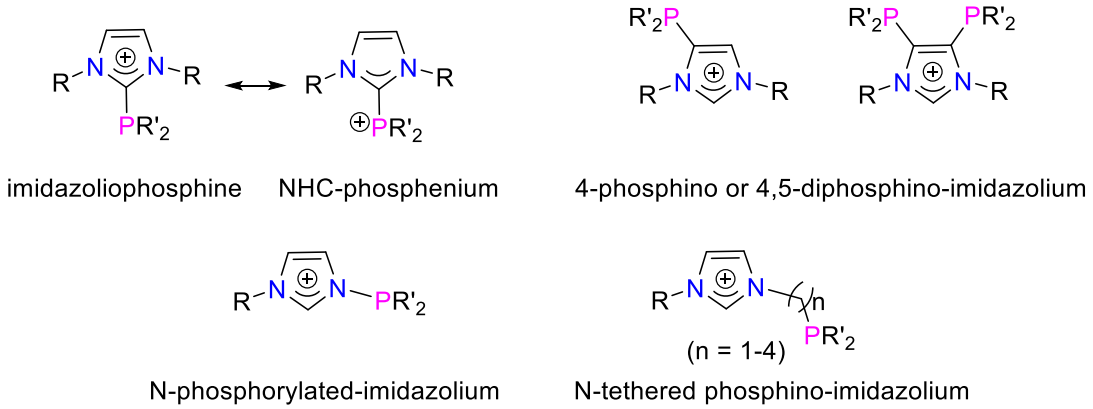

Scheme 12. Phosphorus-based NHC derivatives.[50]

1.2.1 Synthesis of N-tethered phosphino-imidazolium salts

Two general approaches have been developed for the synthesis of N-tethered phosphino-imidazolium salts. The first method (**A**) involves the quaternization of a N-substituted imidazole with a dihalogenated derivative followed by a nucleophilic substitution reaction using secondary phosphines in the presence of a base. The second method (**B**) consists of a quaternization process of a N-substituted imidazole with a phosphorylalkyl halide derivative followed by a reduction step of the P(V) pending arm to form the desired N-phosphino-imidazolium salt (**Scheme 13**).

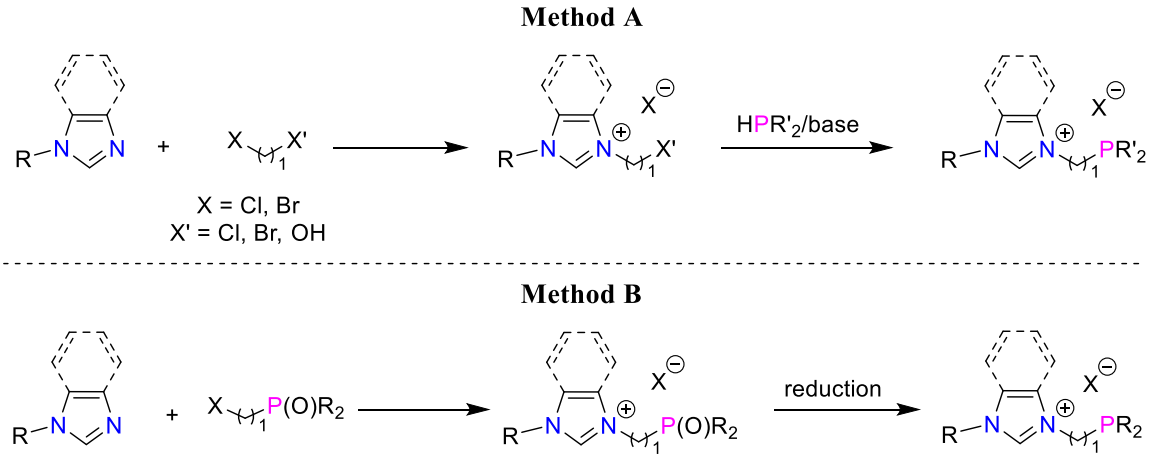

Scheme 13. General methods for the synthesis of N-tethered phosphino-imidazolium salts.

1.2.2 Synthesis of bidentate NHC-Phosphine ligands

Method A

Several examples of bidentate NHC-phosphine pre-ligands have been prepared using this synthetic route. For example, treating 1-(mesityl)imidazole[51] or 1-(methyl)imidazole[52] with an excess of 1,2-dibromo-ethane yielded the corresponding N-substituted imidazolium salts. Then in a second step, addition of potassium diphenylphosphide prepared in situ by mixing diphenylphosphine and *t*-BuOK in DMSO on these bromo(alkyl) imidazolium salts afforded the related N-phosphino imidazolium salts **17** and **18** isolated in 91% and 74% yields, respectively (**Scheme 14**).

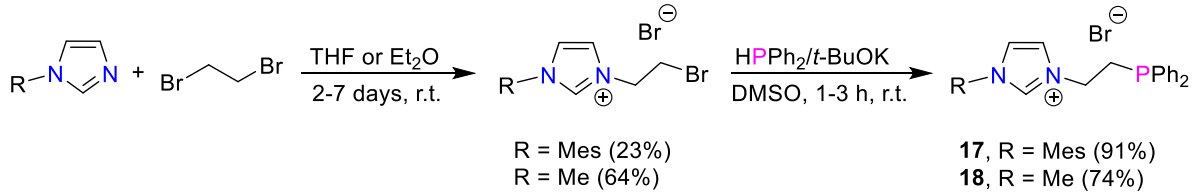

Scheme 14. Two-step synthesis of N-phosphino-imidazolium salts **17** and **18** from corresponding imidazole precursors.[51,52]

To improve the yield of formation of imidazolium salt **17**, an alternative procedure was developed based on the quaternization of the N-substituted imidazole precursor by a hydroxy(alkyl) halide derivative. The bromination of the corresponding N-substituted hydroxy(alkyl) imidazolium salt with PBr_3 followed by subsequent nucleophilic substitution with $KPPh_2$ produced the desired imidazolium salt **17** in 67% overall yield. The same procedure was also applied to the imidazole bearing a diisopropylphenyl substituent (DIPP) affording the related salt **19** in 52% overall yield (**Scheme 15**).[53,54]

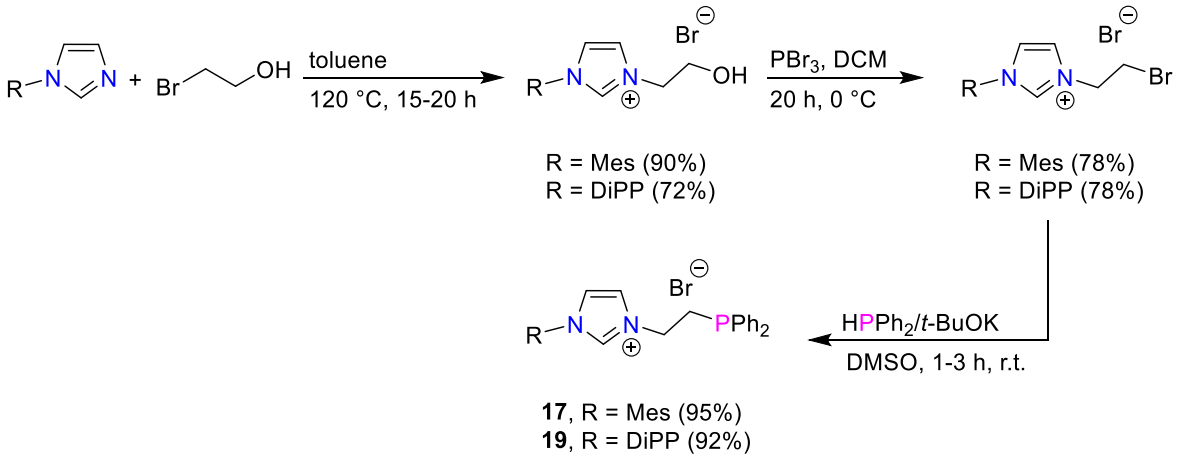

Scheme 15. Synthesis of N-phosphino imidazolium salts **17**-**19** by an alternative method.[53,54]

This method was also shown to be compatible for the formation of N-substituted benzimidazolium salts.[55] Treatment of N-alkyl benzimidazole precursors with 1-bromo-2-chloroethane for one week at room temperature afforded thus the corresponding 2-chloroethyl-functionalized benzimidazolium salts in good yields (*ca.* 83-93%). Nucleophilic substitution with $KPPh_2$ then yielded the targeted phosphine-functionalized benzimidazolium salts **20**-**22** in 86-91% isolated yields (**Scheme 16**).

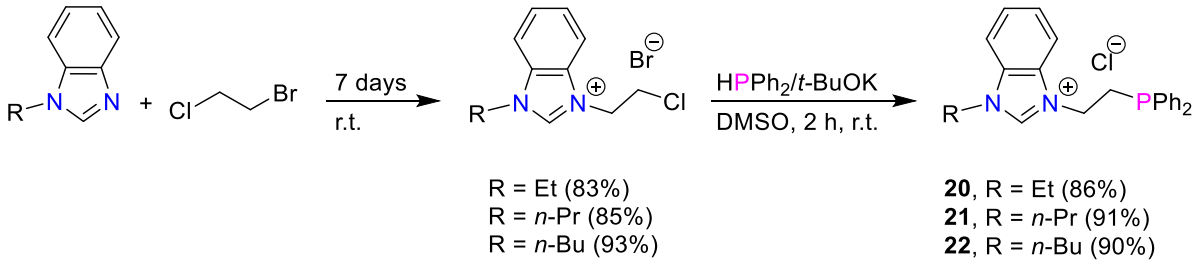

Scheme 16. Synthesis of N-phosphino-benzimidazolium salts **20**-**22**.[55]

The synthesis of methylene-bridged NHC-phosphine systems could be also realized using this approach. A representative example was described by Hoffman *et al*[56] based on the quaternization step of N-substituted imidazoles with ICH_2Cl. The substitution with *t*-Bu_2PLi of the latter under various conditions gave then the desired products but in low yields (*ca*. 20%). However, performing the reactions with *t*-Bu_2PBH_3Li generated in situ from corresponding phosphino-borane adduct and *n*-butyllithium led to the formation of the borane protected imidazolium salts in better yields. Treatment with DABCO in 1,4-dioxane at 100 °C was finally reported to remove the BH_3 protecting group producing the target imidazolium salts **23** and **24** in 65% and 87% yields, respectively (**Scheme 17**).

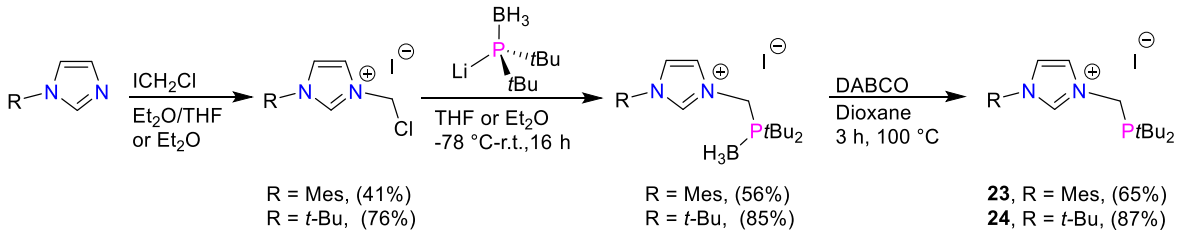

Scheme 17. Synthesis of (t-Bu)$_2$phosphinomethyl-substituted imidazolium salts **23** and **24**.[56]

Method B

Quaternization process between N-substituted imidazoles and bromo(ethyl) diphenylphosphine oxide afforded under heating the corresponding phosphine oxide imidazolium salts in good yields. These salts were then effectively reduced by using $HSiCl_3$ at 120 °C in C_6H_5Cl for 3 h leading to the N-phosphino tethered imidazolium salts **17** and **19** in 75% yields (**Scheme 18**).[57]

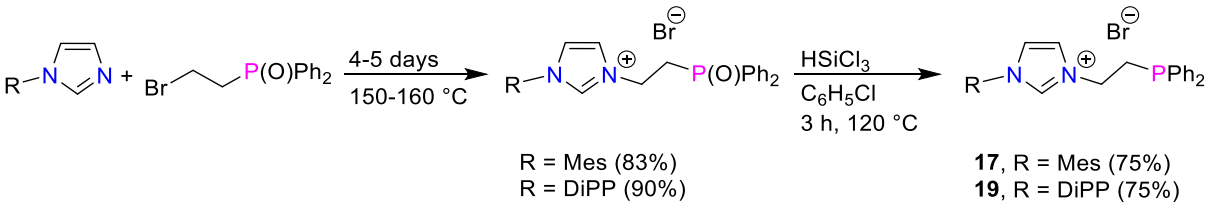

Scheme 18. Synthesis of N-phosphino-imidazolium salts **17** and **19**.[57]

The order of introducing arms on the N-positions of the imidazole core can be realized in a reversed way. For instance, in the following example, potassium salt of 1*H*-imidazole was first reacted with a phosphoryl(alkyl) halide at room temperature in toluene resulting in the formation of the N-phosphine oxide imidazole in 96% yield. In a second step, N-quaternization with iodomethane in chloroform at room temperature produced the corresponding P-oxidized imidazolium salt in 70% yield. The reduction of the phosphoryl group by the system $MeSiCl_2H$/ethanol afforded finally the desired product **25** in 89% yield (**Scheme 19**).[58]

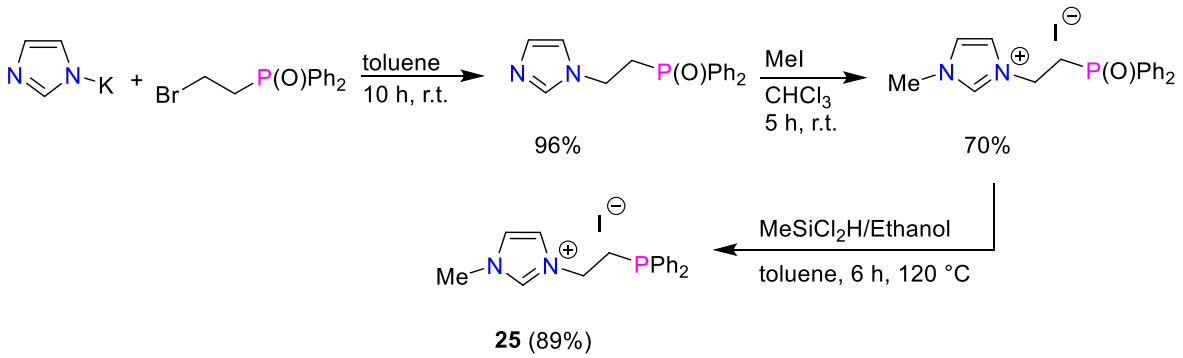

Scheme 19. Synthesis of N-tethered phosphino-imidazolium salt **25**.[58]

Various NHC-phosphine pre-ligands featuring a simple CH_2 linker between the phosphine and the imidazolium moieties were also prepared according to the second method, based on a quaternization reaction between appropriate N-substituted imidazole and phosphine oxide precursors of type $R'_2P(O)CH_2X$ (R'= *t*-Bu, Ph; X = Br[59], OTs[60]) and followed by a reduction with $HSiCl_3$. As a result, the corresponding N-phosphino-imidazolium salts **26**-**28** were thus isolated in moderate to good yields (65-78%) (**Scheme 20**).

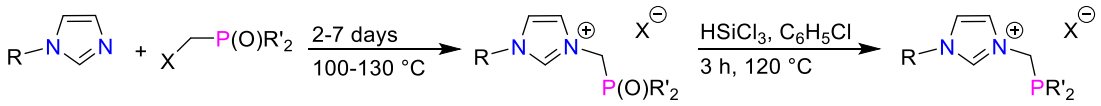

26, R = R' = *t*-Bu, X = OTs (72%)
27, R = Mes, R' = *t*-Bu, X = OTs (65%)
28, R = Mes, R' = Ph, X = Br (78%)

Scheme 20. Synthesis of N-phosphino-imidazolium salts **26-28** featuring a methylene linker.[59,60]

Other methods

In 2015, our group described an elegant method to prepare NHC-based ligands using methylene phosphonium ions in the coordination sphere of manganese.[61] This strategy was based on the nucleophilic addition of a N-substituted imidazole at the carbon center of the methylene phosphonium complex affording the phosphine Mn complex **29**. Facile demetallation under visible light irradiation gave finally the NHC-phosphine pre-ligand **30** (**Scheme 21**). This original method was then applied to the preparation of a wide range of bidentate NHC-phosphine pre-ligands.[62]

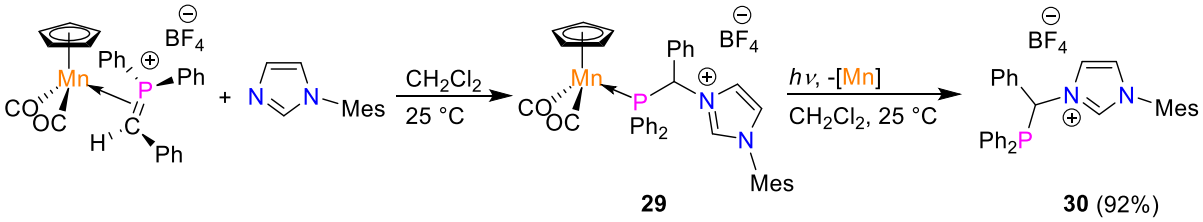

Scheme 21. Access to NHC-based pre-ligands following the methylene phosphonium strategy developed in the group.[61]

1.2.3 Synthesis of tridentate NHC-Phosphine ligands

The two main strategies (**A** and **B**) as well as the method involving methylene phosphonium ions described in the bidentate series were also used for the preparation of tridentate NHC-phosphine ligands.

Method A

Lee *et al.* synthesized the NHC core pincer ligand **31** exhibiting two pending phosphine donor extremities by the N-fonctionalization of 1*H*-imidazole with an alkyl dihalide in the presence of a base followed by N-quaternization of the resulting N-substituted imidazole with 1,2-dichloroethane. The corresponding 1,3-bis(2-chloroethyl)-3*H*-imidazolium chloride salt isolated in a 77% yield was then converted to the 1,3-bis(2-diphenylphosphanylethyl)-3*H*-

imidazolium chloride **31** by a substitution reaction using diphenylphosphine as nucleophile in the presence of *t*-BuOK in DMSO (**Scheme 22**). [63]

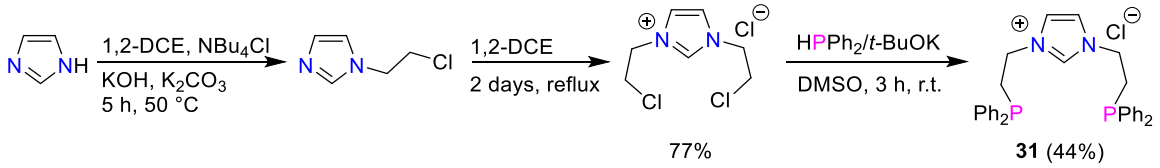

Scheme 22. Synthesis of 1,3-bis(2-diphenylphosphanylethyl)-3*H*-imidazolium chloride **31** from 1*H*-imidazole.[63]

Similar approach was used by Hahn *et al.* to prepare the analogous benzimidazolium salt **32** from 5,6-dimethylbenzimidazole (**Scheme 23**).[55] In contrast to the previous imidazolium salt **31**, the introduction of the second 2-chloroethyl arm using 1,2-dichloroethane failed due to the lack of reactivity of 1,2-dichloroethane. To overcome this limitation, the N-substituted imidazole was treated with more reactive 1-bromo-2-chloroethane for one week at room temperature affording thus the targeted imidazolium salt in 82% yield. The substitution step in the presence of the diphenylphosphine/*t*-BuOK system allowed finally the formation of the desired tridentate benzimidazolium salt **32** in 77% yield.

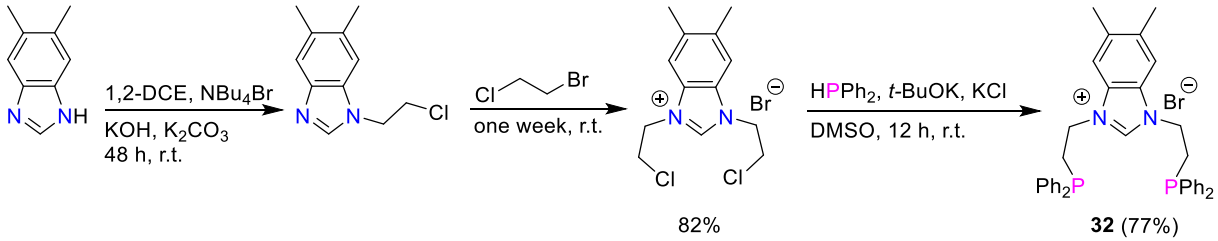

Scheme 23. Synthesis of the NHC core pincer pre-ligand **32** from 5,6-dimethylbenzimidazole.[55]

In a variant of this method, a chiral tridentate ligand where an NHC is combined with two phosphaferrocenyl units was reported by Ganter *et al.*[64] The latter was prepared in two steps from 3,4-dimethylphosphaferrocene-2-carbaldehyde by reductive amination and subsequent methylation of the amine followed by the treatment of the ammonium salt formed with 1*H*-imidazole under reflux for 12 h. These specific conditions led ultimately to the formation of the tridentate pre-ligand **33** in 81% yield (**Scheme 24**).

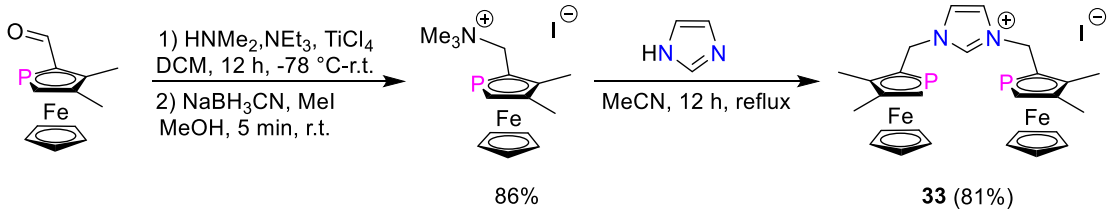

Scheme 24. Synthesis of the tridentate NHC phosphine pincer ligand **33** exhibiting two ferrocenyl side arms.[64]

Another tridentate PCP- pincer ligand based on two ferrocenylphosphine donor arms was synthesized from commercially available *N,N*-dimethyl-1-ferrocenylethylamine, which undergoes diasteroselective *ortho*-functionalization with R_2PCl followed by the substitution of the dimethylamino group by an acetate. The resulting phosphine was then treated with 1*H*-imidazole for 3 days followed by ion exchange in the presence of NaI to afford the desired products **34**-**36** in moderate to good yields (**Scheme 25**).[65–69]

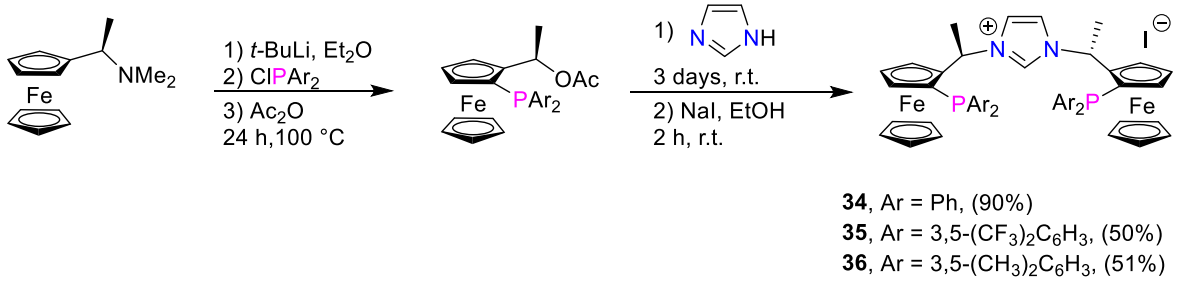

Scheme 25. Synthesis of the tridentate NHC core pincer ligands **34**-**36** from *N,N*-dimethyl-1-ferrocenylethylamine.[65–69]

Similar synthetic route was used to prepare the pincer pre-ligand **37**,[70] starting from benzaldehyde which undergoes condensation with dimethylamine followed by a reduction step with $NaBH_4$ to give the N,N-dimethylbenzylamine intermediate. *Ortho*-lithiation reaction was then carried out to introduce the diphenylphosphine unit, followed by the substitution of the amine group by a chlorine atom using ethyl(chloro)formate. In a last step, the tridentate imidazolium salt **37** was obtained in 32 % yield by treating 2-chloromethylphenyldiphenylphosphine with 1*H*-imidazole in the presence of K_2CO_3 in ethanol under reflux for 2 days (**Scheme 26**).

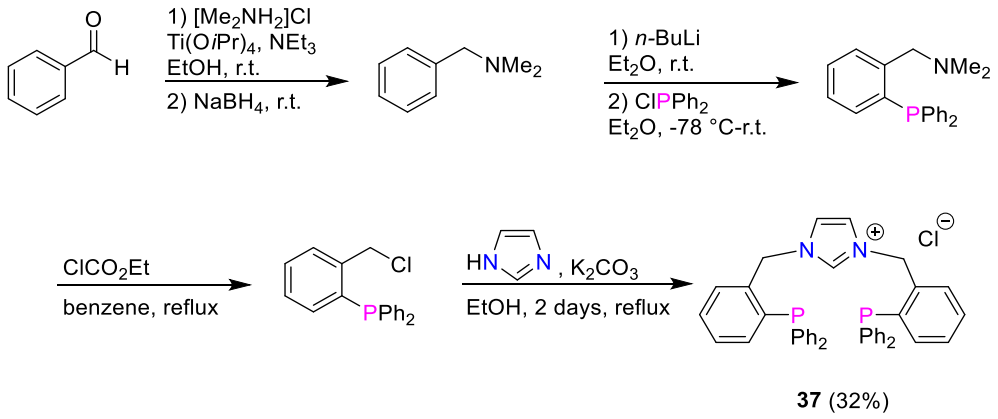

Scheme 26. Synthesis of the NHC core pincer pre-ligand 37 from benzaldehyde.[70]

Method B

Rieger *et al*. reported the synthesis of the cationic phosphine-functionalized methylene-bridged tridentate benzimidazolin-2-ylidene ligand precursor **38** from readily available 1*H*-benzimidazole through a sequential strategy consisting of introducing step by step the two side arms.[71] Both arms were thus introduced through sequential nucleophilic substitution, the second one leading to the benzimidazolium salt. The reduction of phosphine oxide moieties was found to be not selective using $HSiCl_3$ as a reducing agent leading only to hydrogenation of the imidazolium moiety without P−O bond reduction. The $Ti(OiPr)_4$/PHMS system was thus required to afford the reduction of the phosphine oxide extremities affording corresponding benzimidazoline intermediate which was finally transformed into the targeted benzimidazolium salt **38** by hydride abstraction using $[Ph_3C][PF_6]$ in THF (**Scheme 27**).

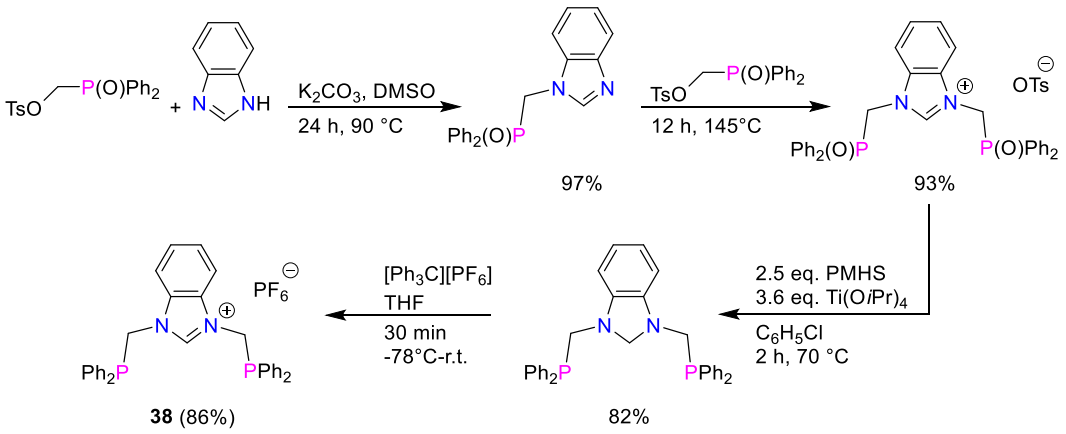

Scheme 27. Synthesis of the NHC core pre-ligand **38** through sequential introduction of the two side arms.[71]

Other methods

As mentioned previously, our group has recently developed a new method to prepare bidentate NHC-phosphine ligands based on the nucleophilic addition of N-substituted imidazoles on methylene phosphonium cations.[61] Interestingly, this strategy allowed also the preparation of tridentate imidazolium salts. For instance, the addition of one equivalent of 1*H*-imidazole to a methylene phosphonium Mn complex resulted in the formation of the binuclear imidazolium core Mn complex **39** as an equimolar mixture of *rac*- and *meso*- isomers, which gave the corresponding tridentate imidazolium salt **40** featuring two phosphine arms after irradiation under visible light in 80% yield.[61] Later on, this method was successfully applied to the preparation of other tridentate NHC-phosphine pre-ligands.[72]

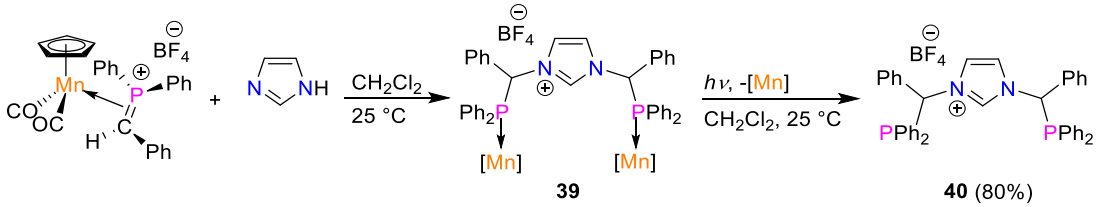

Scheme 28. Synthesis of the pincer-type NHC, bis(phosphine) pre-ligand **40** using the methylene phosphonium strategy.[61]

The two common routes widely cited previously are not suitable for synthesizing chelating imidazolium-type salts based on a saturated heterocycle. For this purpose, an alternative route was described by Fryzuk *et al*. for the preparation of a saturated NHC-based PCP pre-ligand exhibiting *o*-phenylene linkers. The synthesis of the latter starts from phenylisocyanate which was transformed into the corresponding primary amine bearing a diisopropylphosphino group followed by protection of the two P- centers and nucleophilic substitution with 1,2-dibromoethane. The bis(phosphinesulfide) imidazolinium salt obtained was then cyclized with triethylformate and reduced with an excess of Ra-Ni in MeOH to form the expected bis(phosphine) imidazolinium salt **41** in 70% yield (**Scheme 29**).[73]

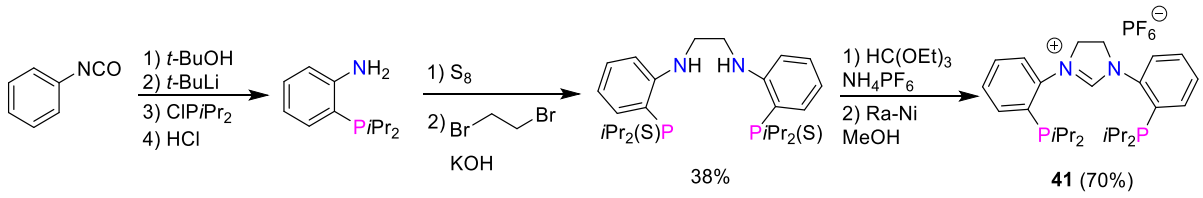

Scheme 29. Synthesis of the tridentate imidazolinium salt **41** featuring a saturated backbone.[73]

2. Results and discussion

Contributions in this part: Synthesis, Optimization, Scope, and Mechanistic studies: Ruqaya Buhaibeh, DFT calculations: Dr. Oleg Filippov.

R. Buhaibeh, O. A. Filippov, A. Bruneau-Voisine, J. Willot, C. Duhayon, D. Valyaev, N. Lugan, Y. Canac, J. B. Sortais, *Angew. Chem. Int. Ed.* **2019**, *58*, 6727-6731.

R. Buhaibeh, C. Duhayon, D. A. Valyaev, J.-B. Sortais, Y. Canac, *Organometallics* **2021**, DOI 10.1021/acs.organomet.0c00717.

2.1 Synthesis of Bidentate NHC-Phosphine Complexes

2.1.1 Synthesis of NHC-phosphine complex C1

Compassing our recent investigations on the application of manganese complexes supported by bidentate ligands in hydrogenation-type catalysis,[74–78] we turned our attention to the use of ligand systems now associating phosphine and NHC donor moieties. Our first target phosphine-imidazolium precursor [Ph_2PCH_2Im]OTs (**L1**) was obtained by the modification of literature procedure previously used for the synthesis of [Ph_2PCH_2Im]Br.[59] The reaction of 1.2 equiv. of 1-mesityl-imidazole with $Ph_2P(O)CH_2OTs$ at 130 °C overnight gave the N-substituted phosphine oxide imidazolium salt **L1(O)** in 86% yield, which was then reduced by an excess of $HSiCl_3$ (20 equiv.) at 80 °C in chlorobenzene to afford the desired N-phosphino-imidazolium **L1** in 93% isolated yield (**Scheme 30**).

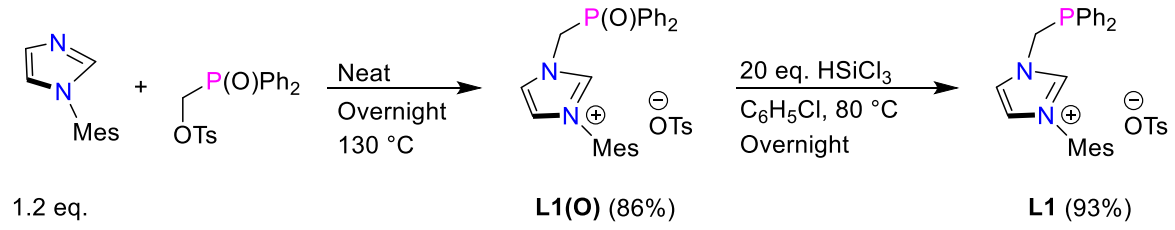

Scheme 30. Synthesis of the N-phosphino-imidazolium salt **L1** from 1-mesityl-imidazole.

We then studied the complexation of the pre-ligand **L1** with respect to a Mn(I) center. The sequential addition of KHMDS and [$Mn(CO)_5Br$] precursor to a solution of **L1** in toluene at room temperature, followed by heating the resulting mixture at 60 °C for 30 min. led to the selective formation of complex *fac*-[$MnBr(CO)_3(\kappa^2P,\hat{C}\text{-}Ph_2PCH_2NHC)$] (**C1**) in 86% yield (**Scheme 31**).

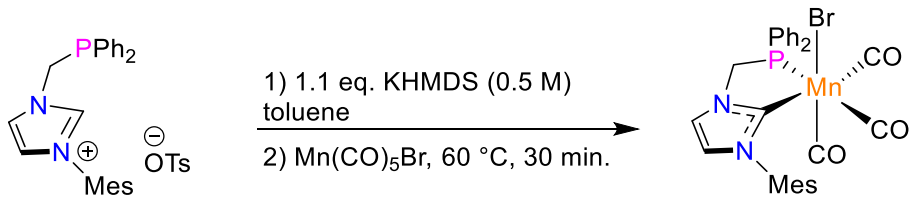

L1 **C1** (86%)

Scheme 31. Synthesis of NHC-phosphine Mn complex **C1** from pre-ligand **L1**.

According to IR and NMR spectroscopy, the air stable Mn complex **C1** was formed as a single isomer (IR: ν_{CO} 2020 (vs), 1948 (s), 1908 (s) cm^{-1}; NMR: δ_P 71.3 ppm (s), δ_{N2C} 197.7 ppm (d, $^2J_{PC}$ = 17.5 Hz)). An X-ray diffraction study of complex **C1** was realized, indicating the octahedral geometry of the Mn center and the facial arrangement of the three carbonyl co-ligands (**Figure 1**).

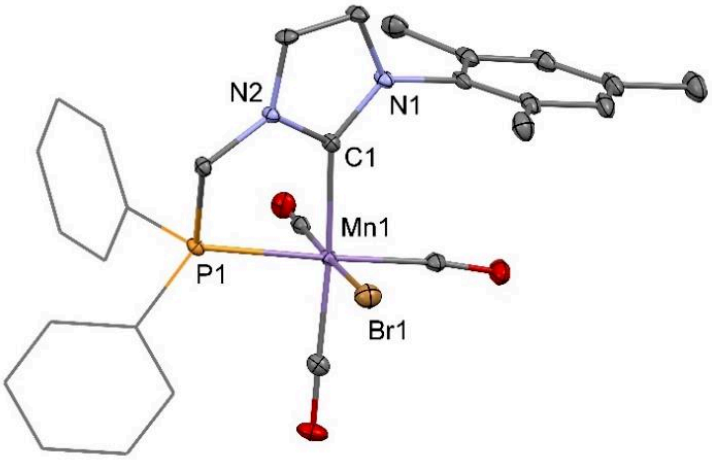

Figure 1. Molecular geometry of complex *fac*-**C1** (30% probability ellipsoids, aryl groups represented as a wireframe for clarity, solvate THF molecule for complex *fac*-**C1** not shown). Selected bond lengths (Å) and angles (°): Mn1–C1 2.032(2), Mn1–P1 2.3030(7), Mn1–Br1 2.4125(6), C1−Mn1−P1 80.11(7), C1−Mn1−Br1 83.78(6), P1−Mn1−Br1 89.18(2).

2.1.2 Reactivity of NHC-phosphine complex C1

- *Towards H_2 activation*

To explore the chemical behavior of Mn complex **C1** towards dihydrogen, the latter was first reacted with KHMDS in toluene at 0 °C under 1 atm. of H_2. Under these conditions, **C1** was smoothly converted into the corresponding hydride Mn complex **C1.a** in a few minutes upon warming up to room temperature (**Scheme 32**). After washing with degassed water, complex

C1.a was finally isolated in 78% yield, standing up as the first example of a Mn hydride complex bearing a NHC ligand.

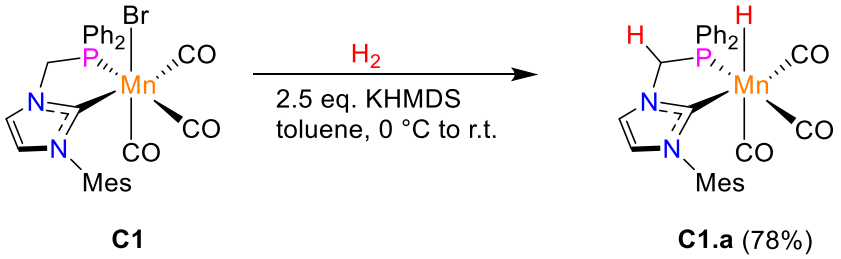

C1 **C1.a** (78%)

Scheme 32. H_2 activation by complex **C1** to generate the hydride Mn complex **C1.a**.

The ^{1}H NMR spectrum of **C1.a** displays a doublet at δ_H –7.25 ppm with a $^{2}J_{PH}$ constant of 53.8 Hz agreeing with the *cis* arrangement of hydride and phosphine moieties (**Figure 2**). The ^{31}P NMR signal of **C1.a** (δ_P 94.2 ppm) was found shifted downfield compared to the bromide precursor **C1** (δ_P 71.3 ppm). A similar trend was observed for the carbenic resonance in the ^{13}C NMR spectrum (**C1.a**: δ_C 205.4 ppm (d, $^{2}J_{PC}$ = 14.3 Hz); **C1**: δ_C 197.7 ppm (d, $^{2}J_{PC}$ = 17.5 Hz)).

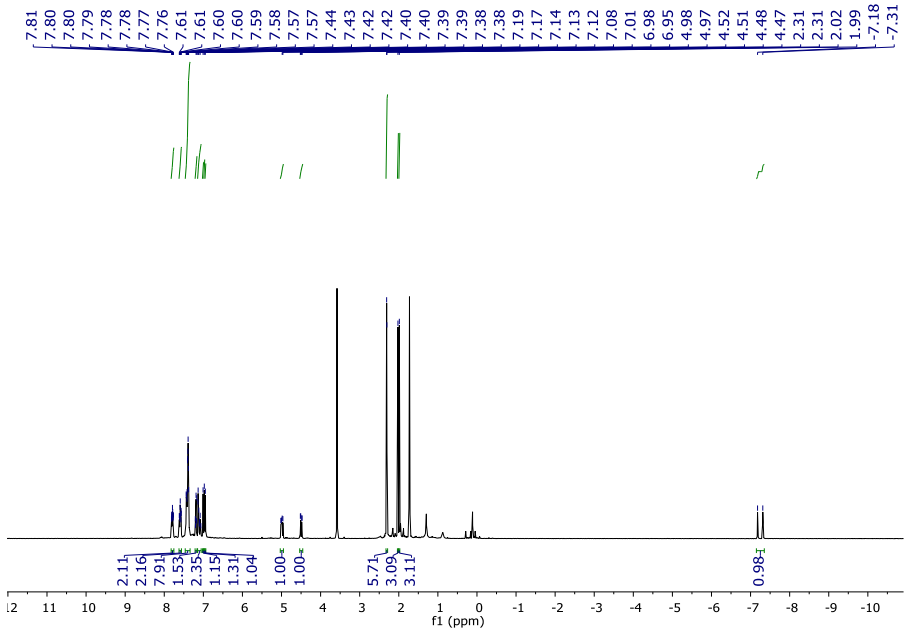

Figure 2. ^{1}H NMR spectrum of the hydride Mn complex **C1.a** (400.1 MHz, Tol, 25 °C).

As observed in the bromide precursor **C1**, the facial arrangement of the three carbonyls co-ligands of complex **C1.a** was univocally confirmed by an X-ray diffraction study (**Figure 3**).

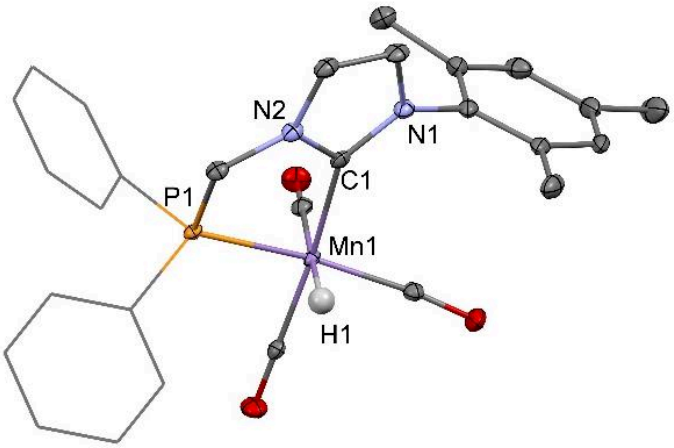

Figure 3. Molecular geometry of complex *fac*-**C1.a** (30% probability ellipsoids, aryl groups represented as a wireframe for clarity). Selected bond lengths (Å) and angles (°): Mn1–C1 2.034(3), Mn1–P1 2.2371(9), Mn1–H1 1.63(4), C1−Mn1−P1 79.95(9), C1−Mn1−H1 81.0(14), P1−Mn1−H1 78.5(14).

Noteworthy, performing the previous reaction under D_2 atmosphere led to the formation of two isomers (50% syn and 50% anti) with a full incorporation of deuterium at the hydride (Mn-D) and CH_2 positions (CH-D) (**Scheme 33**). The formation of two isomers can be *a priori* the result of a base-catalyzed epimerization of the bridging carbon atom or a rotation of the entire [$Mn(CO)_3D$)] moiety as evidenced recently with the chelating bis(diphenylphosphino)methane ligand.[79]

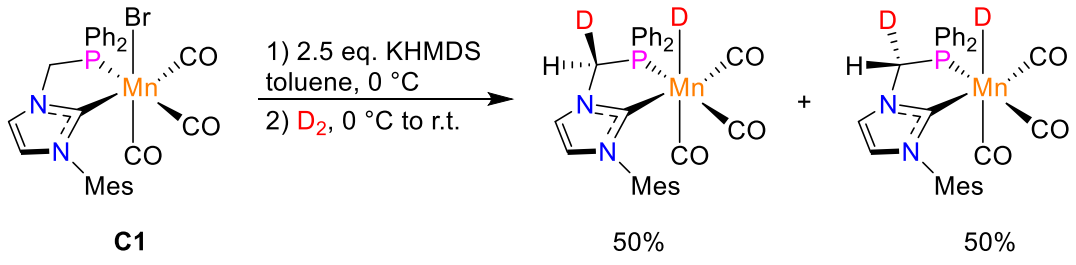

Scheme 33. D_2 activation by NHC-phosphine Mn complex **C1**.

➢ *Towards electrophiles such as MeI and CO_2*

In order to further characterize the acidic site in the complex **C1**, *i.e.* the one that undergoes the deprotonation reaction, different trapping experiments were then carried out. For this purpose, complex **C1** was first treated with KHMDS followed by the addition of a classical alkylating agent such as MeI (5 equiv.). The corresponding complex **C1.b** showing methylation of the

carbon atom linking the phosphine and NHC moieties was isolated in a moderate yield (*ca.* 40%) as a mixture of two diastereomers (ratio 6:1) differing by the position of the methyl group with respect to the coordinated iodine atom (**Scheme 34**).

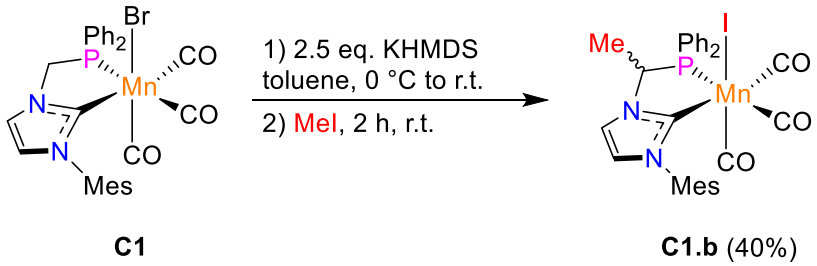

C1 **C1.b** (40%)

Scheme 34. Synthesis of NHC-phosphine complex **C1.b** from complex **C1**.

Both isomers of complex **C1.b** (major isomer: δ_P 74.5 ppm (s); δ_C 195.9 ppm (d, $^2J_{PC}$ = 16.6 Hz, C_{N2C}); minor isomer: δ_P 81.2 ppm (s); δ_C 195.6 ppm (d, $^2J_{PC}$ = 17.5 Hz, C_{N2C}) display similar spectroscopic features compared to the bromide precursor **C1**. An X-ray diffraction analysis of complex **C1.b** evidenced the presence of the *anti*-isomer in the solid state with a similar geometry around the metallic center compared to previous Mn complexes **C1** and **C1.a** (**Figure 4**).

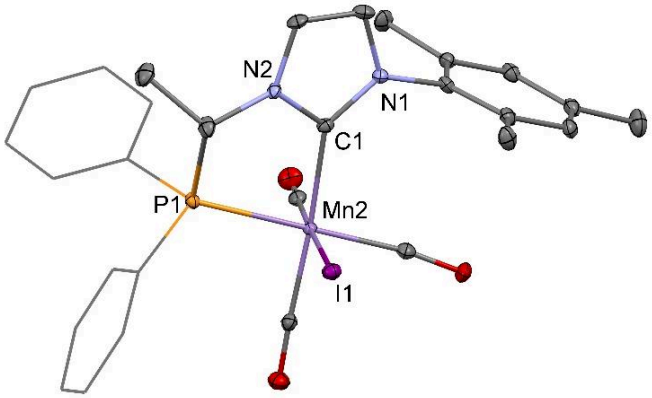

Figure 4. Molecular geometry of complex **C1.b** (30% probability ellipsoids, aryl groups represented as a wireframe for clarity). Selected bond lengths (Å) and angles (°): Mn2–C1 2.024(3), Mn2–P1 2.2949(9), Mn2–I1 2.7561(5), C1−Mn2−P1 80.31(9), C1−Mn2−I1 85.55(9), P1−Mn2−I1 86.38(3).

In a second time, the deprotonated species was exposed to a stream of CO_2 (1 atm.) and the reaction was stirred at room temperature for 2 h until IR analysis evidenced the formation of complex **C1.c** as sole product (ν_{CO} 2024 (s), 1949 (s), 1910 (s) cm^{-1}, $\nu_{C=O}$ 1653 (m, br.) cm^{-1}). The ^{31}P and ^{13}C NMR signals at (δ_P 92.8 ppm (s); δ_C 198.6 ppm (d, $^2J_{PC}$ = 16.6 Hz, C_{N2C}) were

found shifted downfield compared to the bromide precursor **C1**. Crystallization of the crude product in THF/hexane mixture afforded the desired complex **C1.c** in 89% yield (**Scheme 35**).

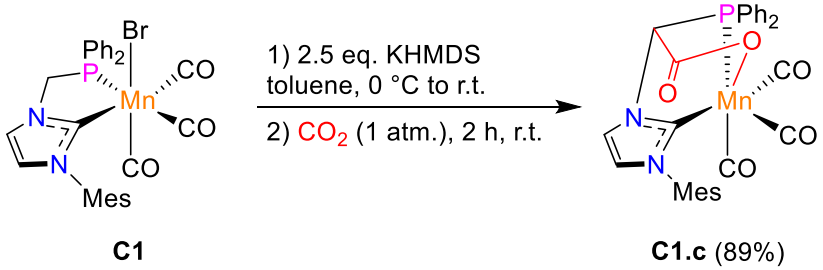

C1 **C1.c** (89%)

Scheme 35. Synthesis of NHC-phosphine Mn complex **C1.c** from complex **C1**.

The solid-state structure of **C1.c** highlights the existence of a tripodal NHC-phosphine-carboxylate scaffold with a facial arrangement of the carbonyl ligands (**Figure 5**).

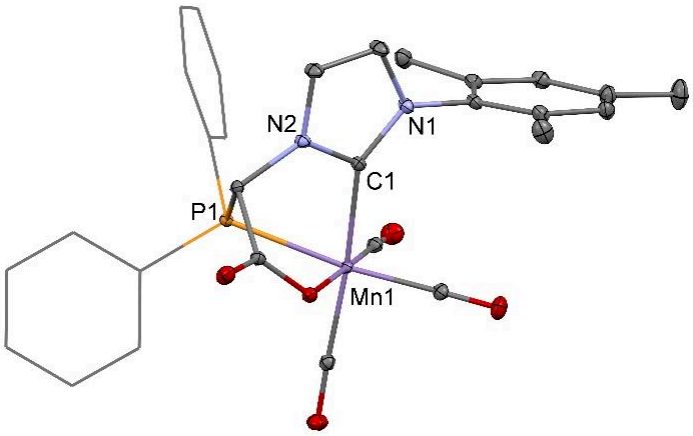

Figure 5. Molecular geometry of complex **C1.c** (30% probability ellipsoids, aryl groups represented as a wireframe for clarity). Selected bond lengths (Å) and angles (°): Mn1–C1 2.0365(9), Mn1–P1 2.3340(3), C1−Mn1−P1 76.90(2).

These results clearly indicated that the deprotonation of complex **C1** occurs at the methylene bridge forming a sufficiently nucleophilic carbon species to react with electrophiles such as MeI or CO_2.

2.1.3 Mechanistic studies

- *Characterization of the deprotonated form (complex C1.d)*

After proving the involvement of a deprotonated intermediate **C1.d** of general formulae [$Mn(CO)_3(Ph_2PCHNHC)$] for the formation of Mn complexes **C1.a**, **C1.b**, and **C1.c** from

precursor **C1**, arose the question of its structure. Despite its relative instability (half-life time of *ca*. 30 min. at room temperature, decomposition time of *ca*. 16 h at –30 °C), optimization of reaction parameters allowed to prepare suitable samples of complex **C1.d** for complete spectroscopic characterization (**Scheme 36**). The IR spectrum of **C1.d** in toluene exhibits two ν_{CO} bands at 1993 (s) and 1901 (vs) cm^{-1} consistent with the presence of three CO ligands in a facial arrangement. The $^{31}P\{^{1}H\}$ NMR spectrum recorded in a [D_8] toluene solution at –30 °C revealed the complete conversion of **C1** (δ_P 71.7 ppm) into **C1.d**, the latter being characterized by a shielded chemical shift at δ_P 51.6 ppm (s). The deprotonation site was finally revealed by the concomitant presence of doublets at δ_H 3.55 ($^{2}J_{PH}$ = 8.6 Hz, 1H) and at δ_C 22.7 ppm ($^{1}J_{PC}$ = 18.2 Hz) in the ^{1}H and $^{13}C\{^{1}H\}$ NMR spectra respectively, consistent with the presence of a CH group in the α-position of phosphorus atom and confirming that the deprotonation does take place at the methylene bridge. Noticeably, while the $^{13}C\{^{1}H\}$ NMR spectrum displays three distinct resonances for CO ligands (δ_C 228.9, 227.2, and 223.6 ppm) at standard chemical shifts, the carbenic carbon atom appears to be strongly shielded (δ_C 178.0 ppm, d, $^{2}J_{PC}$ = 14.2 Hz) by *ca*. 20-25 ppm compared to the antecedent Mn complexes **C1**, **C1.a**, **C1.b**, and **C1.c**.

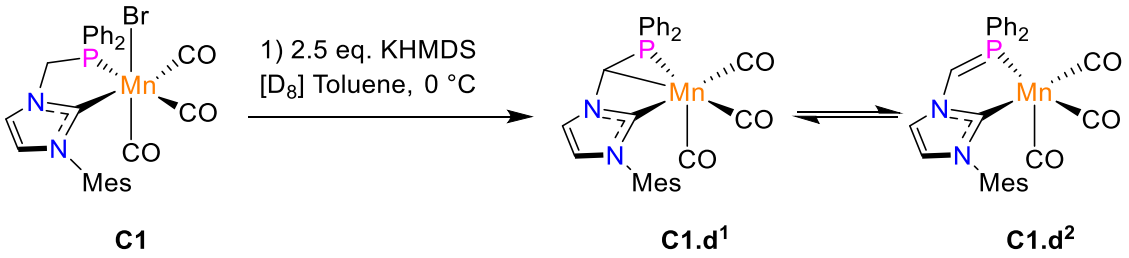

C1 **C1.d¹** **C1.d²**

Scheme 36. Deprotonation of complex **C1** to characterize the intermediate complex **C1.d**.

➢ *DFT studies*

Despite all our efforts, single crystals of deprotonated complex **C1.d** could not be obtained. Its structure was therefore further investigated by theoretical calculations. DFT study at the BP86/def2-TZVP level revealed five minima on the PES. The global minimum corresponds to the strongly distorted octahedral 18-e complex *fac*-[$Mn(CO)_3(\kappa^3P,C,\hat{C}$-$Ph_2PCHNHC)$] (**C1.d¹**, **Figure 6** (*left*)) featuring a facially coordinated, 5-e donor, NHC-phosphinomethanide ligand.[80–85] Calculated metrical parameters within the phospha(mangana)cyclopropane moiety are comparable to those experimentally found in the related [$(\kappa^2P,C$-$Ph_2PCH_2)Mn(CO)_4$] complex.[86] The other minima correspond to the four possible isomers – two *fac* and two *mer* – of square pyramidal 16-e [$Mn(CO)_3(\kappa^2P,\hat{C}$-$Ph_2P$=CHNHC)] complex **C1.d²** showing an unusual bidentate NHC-phosphonium ylide ligand. The most thermodynamically stable isomer

of NHC-ylide complexes *fac*-**C1.d²**, yet being destabilized by +7.5 kcal.mol^{-1} relative to **C1.d¹**, is depicted in **Figure 6** (*right*). The calculated P–C bond length in complex *fac*-**C1.d²** (1.741 Å) is consistent with an ylidic P–C bond, in agreement with experimental values found in a related iron-substituted phosphonium ylide complex (1.766(11) Å)[87] and in metal complexes (M = Rh, Pd) bearing more conventional NHC-phosphonium ylide ligands (1.750(7)-1.794(8) Å).[88–91]

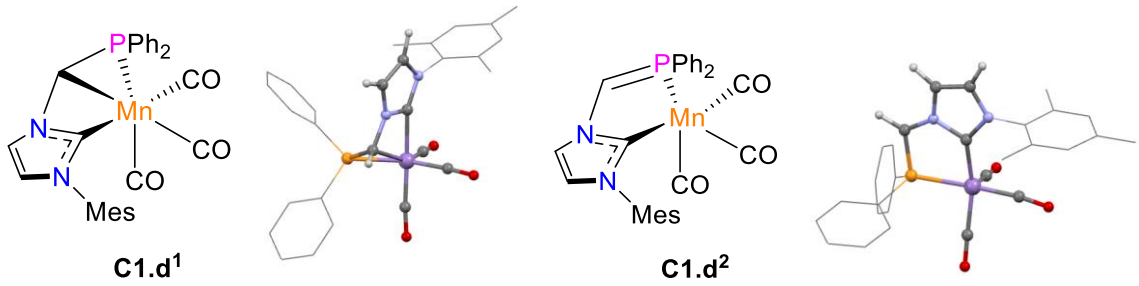

Figure 6. Structures and DFT optimized geometries of complexes **C1.d¹** and *fac*-**C1.d²** (BP86/def2-TZVP, toluene SMD model).

Very significantly, the relatively constrained coordination of the NHC-phosphinomethanide ligand in **C1.d¹** results in a strong distortion of yaw angle θ[92] for the NHC ligation (**C1.d¹**: θ 29.5° *vs.* **C1** and **C1.a-C1.c**, **C1.d²**: 6.2-7.2°). Considering that the shielding of the ^{13}C NMR chemical shift of carbenic carbon atoms in metal complexes increases as the value of θ,[93] the carbenic resonance recorded at δ_C 178.0 ppm for **C1.d** in solution appears to be totally consistent with the most thermodynamically stable structure **C1.d¹**. In addition, computed ^{13}C NMR chemical shift for the carbenic atom in complex **C1.d¹** (δ_C 181.5 ppm) matches well with the corresponding experimental value (δ_C 178.0 ppm), a value significantly different from that computed for complex *fac*- **C1.d²** (δ_C 215.1 ppm). Based on ^{13}C NMR data and DFT calculations, the deprotonation product of **C1** must thus be assigned to the NHC-phosphinomethanide complex *fac*-[Mn(CO)$_3$(κ^3*P,C,Ĉ*-Ph$_2$PCHNHC)] (**C1.d¹**).

The mechanism of H_2 activation by **C1.d¹** was then investigated by DFT calculations. Among the different activation pathways considered, the process showing the lowest energy profile is depicted in (**Scheme 37**). Complex **C1.d¹** is first converted into the 16-e NHC-ylide species *fac*- **C1.d²** with an energy barrier of 15.7 kcal.mol^{-1} (**TS1**) which then coordinate H_2 to form the dihydrogen complex **C1.e** *via* a **TS2** of 11.3 kcal.mol^{-1}.[94–96] Noteworthy, the ylidic P–C

bond (1.726 Å) in complex **C1.e** became even shorter compared to *fac*- **C1.d²** reflecting stronger double bond character. Finally, complex **C1.e** undergoes a facile heterolytic cleavage of the H–H bond through the low-lying transition state **TS3** with an energy barrier of only 3.2 kcal.mol^{-1} affording finally the experimentally observed manganese hydride complex **C1.a** (ΔG = –21.9 kcal.mol^{-1}).

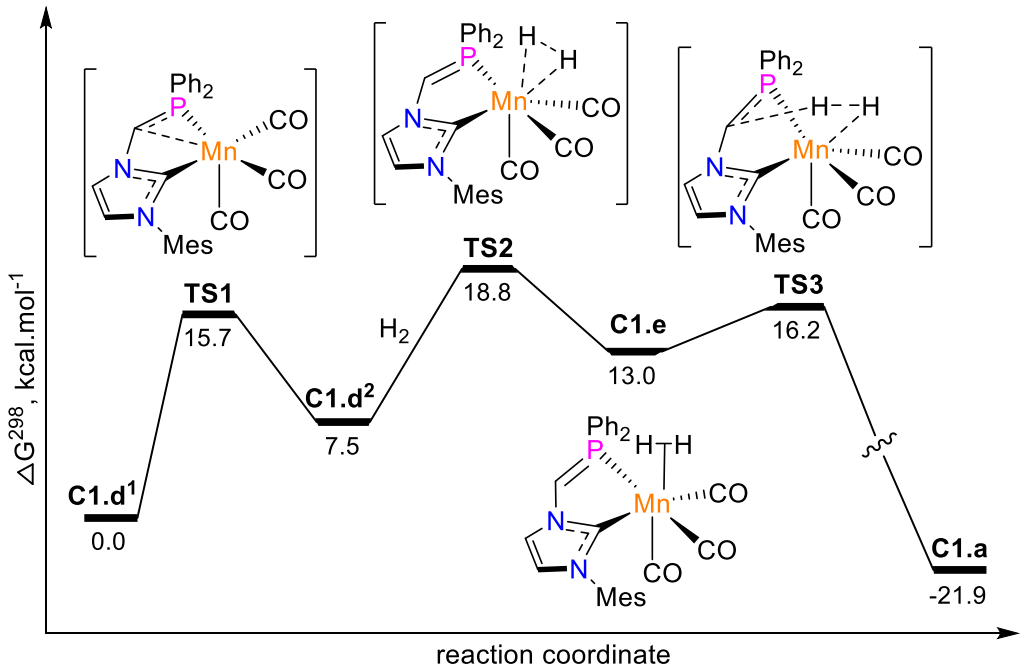

Scheme 37. The preferred mechanism of dihydrogen activation with complex **C1.d** (BP86/def2-TZVP, toluene SMD model, Gibbs free energies are given in kcal.mol^{-1} and referred to **C1.d¹**).

2.1.4 Hydrogenation of Ketones

- *Optimization of the reaction conditions*

Having established that complex **C1** could effectively activate H_2 in basic conditions, we next focused our attention on the hydrogenation of carbonyl derivatives as benchmark reaction.[74,97–100] Gratifyingly, at 60 °C, in toluene, in the presence of 1.0 mol% of **C1** and 2.0 mol% of KHMDS (**Table 1**), acetophenone was fully reduced to 1-phenylethanol (entry 1). The temperature has a real influence on the catalytic reaction reactivity, carrying out the reaction at 30 °C led to 0 conversion of acetophenone **a1** (entry 2). The catalyst loading of **C1** could be decreased to 0.1 mol% at 60 °C to give alcohol **b1** in 87% yield (entry 4). Continuing reducing the catalytic charge to 0.05% the conversion dropped to 8% (entry 5). Under the same conditions when we increase the temperature to 100 °C, 95% conversion of **a1** was observed

(entry 6). Performing the reaction in *t*-AmOH as a greener solvent, 1.0 mol % of *t*-BuOK and 0.1 mol% of **C1** at 60 °C, led to a full conversion of **a1** (entry 8). A maximum TON of 6200 (0.01 mol%, entry 10) was achieved, showing that this catalyst is competitive with the best Mn-based systems for this reaction.[98,99] Isolated hydride complex **C1.a** was also tested (entries 11-12). No reaction took place in the presence of the sole complex **C1.a**, while catalytic activity could be restored in the presence of base, showing its critical role in the catalytic cycle.[101–104]

Table 1. Optimization of the reaction parameters for hydrogenation of acetophenone catalyzed by NHC-phosphine Mn complexes **C1** and **C1.a**[a]

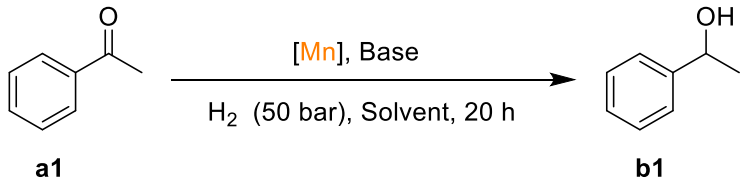

Entry	Cat. (%)	Base (%)	Solvent	Temp. (°C)	Conv.[b]
1	**C1** (1.0)	KHMDS (2)	toluene	60	>98
2	**C1** (1.0)	KHMDS (2)	toluene	30	0
3	**C1** (0.5)	KHMDS (1)	toluene	60	90
4	**C1** (0.1)	KHMDS (1)	toluene	60	87
5	**C1** (0.05)	KHMDS (1)	toluene	60	8
6	**C1** (0.05)	KHMDS (1)	toluene	100	95
7	**C1** (0.01)	KHMDS (1)	toluene	100	52
8	**C1** (0.1)	*t*-BuOK (1)	*t*-AmOH	60	>98
9	**C1** (0.05)	*t*-BuOK (1)	*t*-AmOH	100	>98
10	**C1** (0.01)	*t*-BuOK (1)	*t*-AmOH	100	62
11	**C1.a** (5.0)	–	toluene	60	0
12	**C1.a** (5.0)	KHMDS (2)	toluene	60	>98

[a] Typical procedure: an autoclave was charged with catalyst, solvent (4 mL), acetophenone (4 mmol) and base in this order and then rapidly pressurized with H_2 (50 bar) and heated under stirring for 20 h at the indicated temperature.

[b] Conversions determined by GC and ^{1}H NMR spectroscopy.

Additional solvents and bases were tested in this catalytic transformation (**Table 2**), under the optimal conditions (0.1 mol% of **C1** and 1 mol% base at 60 °C). Using THF as solvent and *t*-BuOK as base, acetophenone was reduced to the corresponding alcohol in 90% yield (entry 1), while with *i*-PrOH the conversion dropped to 41% (entry 2). No conversion of **a1** was observed when the reaction was performed in primary alcohol solvents such as EtOH and MeOH (entries 3 and 4). Potassium and sodium hydroxide bases in *t*-AmOH afforded the desired alcohol in good yields >98 and 92% respectively, (entries 5 and 6). Finally, no reaction took place in the presence of Cs_2CO_3 as a base (entry 7).

Table 2. Additional solvent and base screening for acetophenone hydrogenation catalyzed with Mn complex **C1**

Entry	Base	Solvent	Conv. %[a]
1	*t*-BuOK	THF	90
2	*t*-BuOK	*i*-PrOH	41
3	*t*-BuOK	EtOH	0
4	*t*-BuOK	MeOH	0
5	KOH	*t*-AmOH	>98
6	NaOH	*t*-AmOH	92
7	Cs_2CO_3	*t*-AmOH	0

[a] Conversions determined by GC and ^{1}H NMR spectroscopy.

- *Scope of the reaction*

Having the optimal conditions in hand, we then enlarged the synthetic scope of this catalytic transformation (**Scheme 38**) and found that a large variety of aryl(alkyl)ketones could be readily reduced. With 0.5% of catalyst loading, sterically hindered ketones, 1-phenyl-3-methyl-1-butanone **a2** and 2,2,2-trimethylacetophenone **a3** were reduced to the corresponding alcohols

in 89 and 85% isolated yields, respectively. *o*-, *m*-, *p*-Methyl substituted methyl 2-acetophenone **a4**, **a5**, and **a6** were reduced in excellent isolated yields (93-97%), including the bulky substrate mesityl ethanone **a7** which gave the desired product **b7** in 72% isolated yield. *p*-Methoxy acetophenone **a8** was converted to the corresponding alcohol **b8** in 98% isolated yield. Interestingly, the reaction is tolerant to aryl groups substituted with halogen atoms (F, Cl, Br, I) and CF_3 moiety (**a9**-**a14**), the corresponding products **b9**-**b14** being obtained in good yields (79->98%). 2-Naphthylethanol **b15**, 1-indanol **b16**, and 1,3-diphenylpropanol **b17** were isolated in moderate yields (52-71%). Notably, the cyclopropyl ring remains untouched during the catalytic reaction and the corresponding alcohol **b18** was obtained in 37% isolated yield. Aliphatic 2-decanone **a19** was hydrogenated in the efficient manner albeit at 100 °C. The heterocyclic substrates bearing potentially coordinating groups can also be reduced (**a20**-**a22**) but with lower efficiency. At this stage, limitations were only observed with nitro-aryl ketones, 1,3-β-diketones and conjugated enones.

Scheme 38. Scope of hydrogenation of ketones catalyzed by Mn complex **C1**[a]

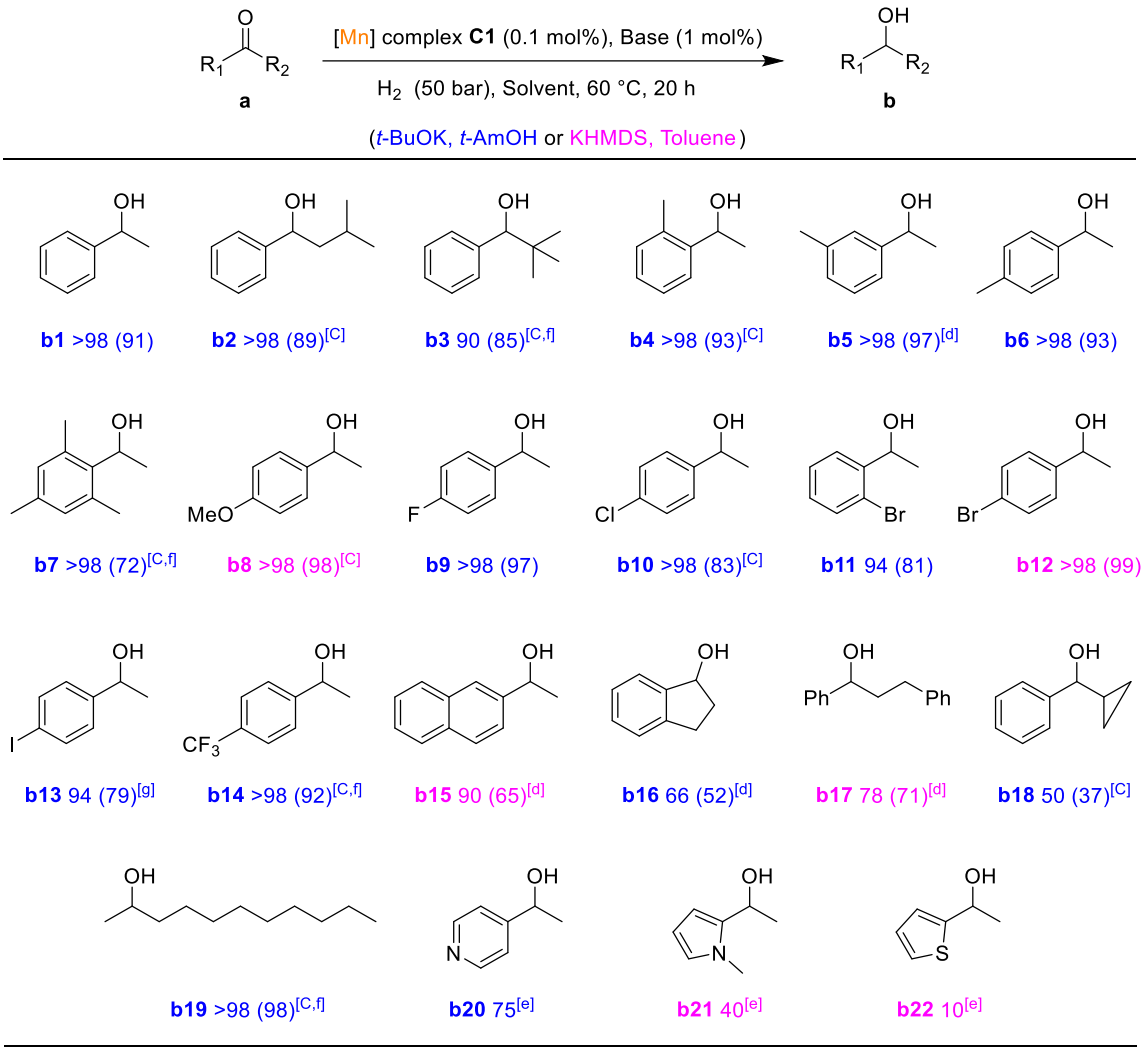

[a] General procedure: pre-catalyst **C1** (0.1 mol%), ketone (2.0 mmol), base (1.0 mol%; **A**: *t*-BuOK, **B**: KHMDS), solvent (2 mL, **A**: *t*-AmOH, **B**: toluene), H_2 (50 bar), 60 °C, 20 h.

[b] Conversion determined by ^{1}H NMR, isolated yield in parenthesis

[c] 2% of base, 0.5% catalyst

[d] 2% of base, 0.2% catalyst

[e] 1% catalyst, 5% of base, 100 °C, 72h

[f] 100 °C

[g] 5% of KOH

Following these encouraging results, we were interested in modifying the substituents at the N- and P- positions and changing the carbon chain between the two coordinating moieties in the NHC-phosphine pre-ligands, in order to study the effect of the substituents on the reactivity of corresponding Mn(I) complexes and especially on the catalytic properties (**Scheme 39**).

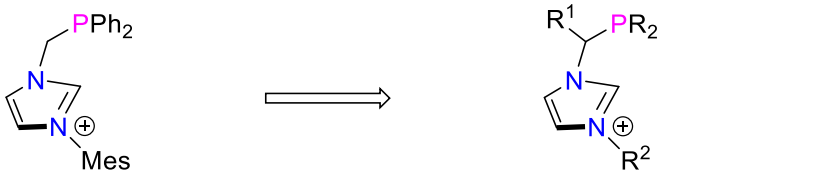

L1

L2, R = Ph, R^1 = H, R^2 = Me
L3, R = Ph, R^1 = H, R^2 = iPr
L4, R = iPr, R^1 = H, R^2 = Mes
L5, R = Ph, R^1 = Ph, R^2 = Mes

Scheme 39. Representation of NHC-phosphine pre-ligand **L1** and related targeted NHC-phosphine pre-ligands **L2**-**L5** by modifying the substituents at the N-, P- and carbon bridge positions.

2.1.5 Synthesis of NHC-phosphine pre-ligands

- *Modification of nitrogen substituents*

NHC-phosphine imidazolium precursors **L2** et **L3** were prepared according to the same strategy previously used for the synthesis of pre-ligand **L1**, starting from the N-quaternization reaction of 1-methyl- or 1-isopropyl imidazole by $Ph_2P(O)CH_2OTs$ at 130 °C. The corresponding N-phosphine oxide imidazolium salts **L2(O)** and **L3(O)** were thus isolated in 83 and 88% yields, respectively. Reduction of the phosphine oxide moiety with an excess of $HSiCl_3$ at 80 °C in chlorobenzene afforded finally the targeted N-phosphino-imidazolium salts **L2** and **L3** in 90 and 92% yields, respectively (**Scheme 40**).

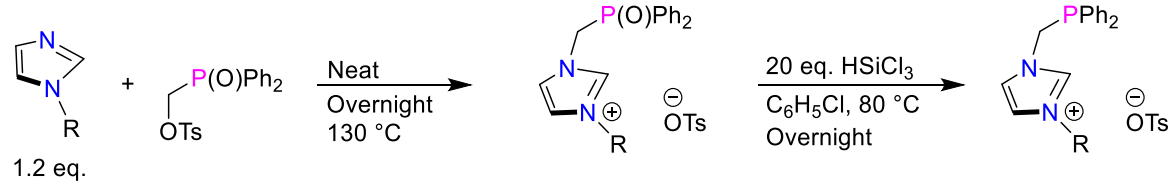

1.2 eq.
R = Me, iPr

L2(O), R = Me (83%)
L3(O), R = iPr (88%)

L2, R = Me (90%)
L3, R = iPr (92%)

Scheme 40. Synthesis of N-phosphino-imidazolium salts **L2** and **L3** from imidazole precursors.

- *Modification of phosphorus substituents*

The modification on the phenyl substituents on the phosphorus atom by isopropyl substituents was carried out in four steps, starting from $(i\text{Pr})_2P(O)CH_2OTs$ which was obtained according to the literature procedure previously described for the related $(t\text{-Bu})_2P(O)CH_2OTs$.[105] In a

first step, treatment of diisopropyl(chloro)phosphine with formaldehyde under acidic conditions at 100 °C for 18 h led to the alcohol derivative $(iPr)_2P(O)CH_2OH$ in 24% yield. Substitution reaction with *p*-toluenesulfonyl chloride in the presence of Et_3N resulted then in the formation of the corresponding tosylate adduct **L[a]4(O)** in 56% yield (**Scheme 41**, *up*). Quaternization reaction of 1-mesityl-imidazole with $(iPr)_2P(O)CH_2OTs$ gave the N- phosphine oxide imidazolium salt **L4(O)** in quasi quantitative yield, which upon reduction by the same method used for the previous pre-ligands **L1-L3** ($HSiCl_3$, chlorobenzene, 80°C) afforded finally the desired imidazolium salt **L4** in 82% yield (**Scheme 41**, *down*).

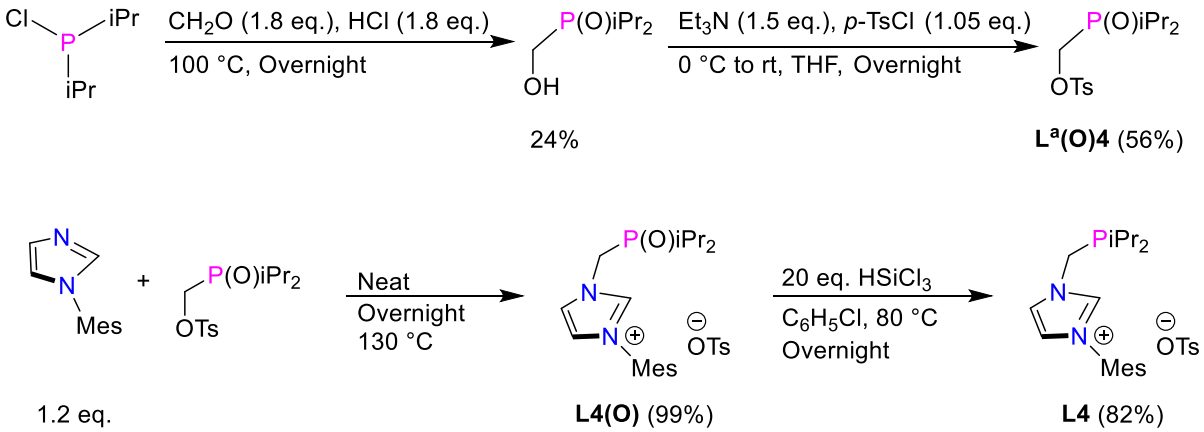

Scheme 41. Synthesis of the N-phosphino-imidazolium salt **L4** from diisopropyl(chloro)phosphine.

➢ *Modification of the Carbon chain*

The pre-ligand **L5** can be prepared according to the method recently described in our group, namely the methylene phosphonium strategy (**Scheme 21**).[106] However, this synthetic route which involves 8 steps motivated us to develop an alternative method. Thus, we succeeded to prepare **L5** using an approach similar to that used for the synthesis of pre-ligands **L1**-**L4**. For this purpose, the tosylate derivative $Ph_2P(O)CHPhOTs$ **L[a]5(O)** was prepared in 61% yield by reacting the alcohol precursor $Ph_2P(O)CHPhOH$[107] with 1 equiv. of *n*-BuLi at -40 °C in THF for 15 min., followed by the addition of 1 equiv. of *p*-toluenesulfonyl chloride and stirring the reaction mixture at room temperature for 18 h (**Scheme 42**, *up*). Quaternization of 1-mesityl-imidazole with $Ph_2P(O)CHPhOTs$ **L[a]5(O)** in toluene at 190 °C for 18 h afforded then the N-phosphine oxide imidazolium salt **L5(O)** in 75% yield, which was finally reduced by $HSiCl_3$ in chlorobenzene at 80 °C to give the desired salt **L5** in 67% yield (**Scheme 42**, *down*).

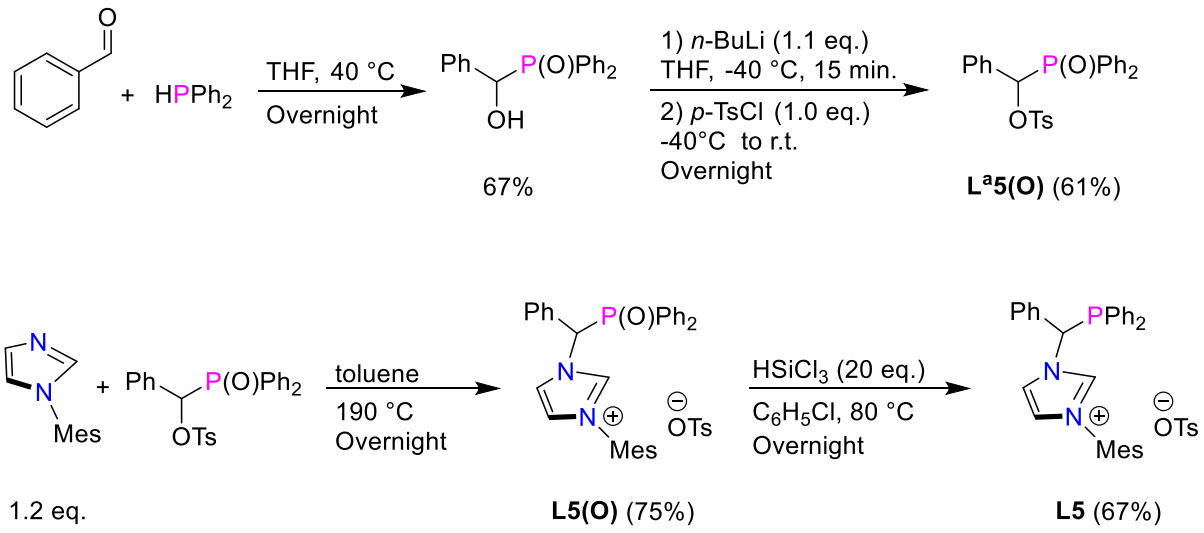

Scheme 42. Synthesis of the N-phosphino-imidazolium salt **L5** bearing a phenyl group at the methylene bridge from benzaldehyde.

➢ *NMR characterization of NHC-based pre-ligands L2(O)-L5(O) and L2-L5*

Multi-nuclear NMR analysis confirmed the formation of these pre-ligands based on their characteristic ^{31}P, ^{1}H and ^{13}C NMR resonances (**Table 3**). The ^{31}P NMR spectrum for N-substituted diphenyl phosphine oxide imidazolium salts **L2(O)**, **L3(O)** and **L5(O)** displayed singlets at in the typical range for such P(V)-based derivatives. The corresponding reduced pre-ligands **L2**, **L3** and **L5** were characterized by shielded ^{31}P NMR chemical shifts at δ_P – (5.2−12.2) ppm, in line with the presence of P(III) donor extremities. For the N-substituted alkyl phosphine oxide **L4(O)** and its reduced form **L4**, the ^{31}P NMR signals appearing respectively at δ_P 53.4 and 11.5 ppm, were found shifted downfield compared to their P-phenylated analogues. For all imidazolium salts, ^{1}H and ^{13}C NMR spectroscopy exhibited characteristic low field signals of the CH imidazolium fragment at δ_H 9.42−10.17 ppm and δ_{CH} 135.9−139.3 ppm.

Table 3. Selected ^{31}P, ^{1}H and ^{13}C NMR chemical shifts in $CDCl_3$ (ppm) for imidazolium salts **L2(O) – L5(O)** and **L2 – L5**.

	L2(O)	**L2**	**L3(O)**	**L3**	**L4(O)**	**L4**	**L5(O)**	**L5**
δ_P	27.0	−12.2	27.3	−12.1	53.4	11.5	30.2	−5.2
δ_{CH}	10.01	9.89	9.80	9.42	9.75	10.17	9.99	10.09
δ_{CH}	139.1	137.7	136.9	135.9	138.6	139.3	138.0	138.3

2.1.6 Synthesis of NHC-based Mn(I)complexes

The coordination step of pre-ligands **L2**-**L5** was achieved using the same approach developed in the case of complex **C1** (**Scheme 31**). Thus, complexes **C3**-**C5** were prepared by reacting 1.1 equiv. of KHMDS with the corresponding precursors **L3**-**L5** in toluene at room temperature, while the deprotonation of pre-ligand **L2** was carried out in THF at -40 °C. The addition of 1 equivalent of [$Mn(CO)_5Br$] precursor to the generated free carbenes and heating the reaction mixture at 50 °C afforded related Mn(I) complexes **C2**-**C5** in moderate to good yields (60-82%) (**Scheme 43**).

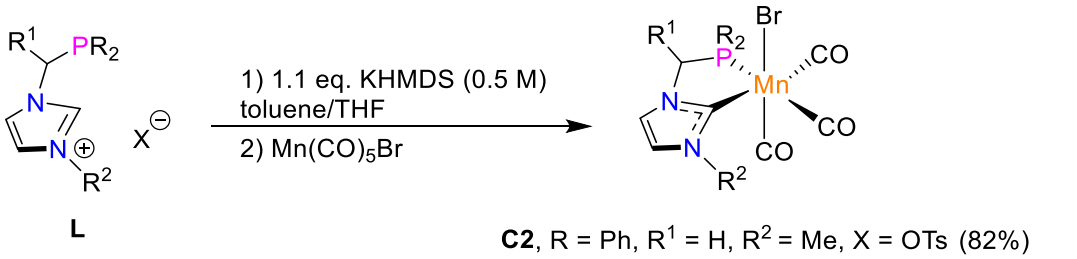

Scheme 43. Synthesis of NHC-phosphine Mn(I) complexes **C2**-**C5** from corresponding imidazolium salts **L2**-**L5**.[a] Yield taken from reference 62.

The selective coordination of pre-ligands **L2**-**L5** was confirmed by NMR and IR spectroscopy. ^{31}P NMR spectra of complexes **C2**-**C4** displayed a single signal at lower field (δ_P 70.6−91.0 ppm) compared to the pre-ligands **L2**, **L3**, and **L4** (δ_P –12.2, –12.1, and 11.5 ppm), respectively. ^{31}P NMR spectrum of complex **C5** showed two singlets at δ_P 93.9 and 82.5 ppm indicating the presence of two isomers differing by the position of the phenyl group with respect to the coordinated bromine atom (**Figure 7**). In all cases, ^{1}H NMR spectroscopy showed the disappearance of the characteristic signal of the imidazolium salts and $^{13}C\{^{1}H\}$ NMR spectra exhibited typical downfield signals for the carbenic carbons at δ_{N2C} 194.9−198.9 ppm, as a doublet with J_{PC} constants of 16.3-21.3 Hz. As expected, and in accordance with the information obtained from NMR analysis, the IR spectrum of all NHC Mn complexes **C2-C5** exhibited three ν_{CO} bands consistent with the presence of three CO co-ligands in a facial arrangement (**Table 4**).

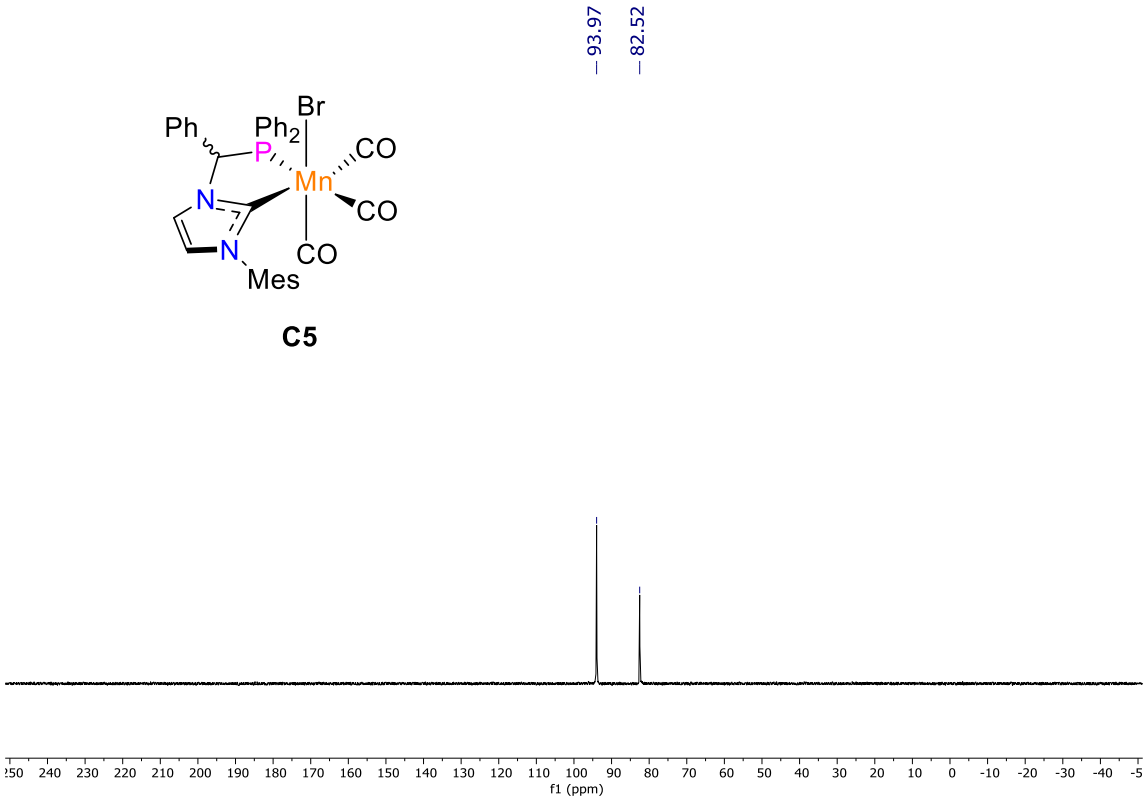

Figure 7. $^{31}P\{^{1}H\}$ NMR spectrum of Mn complex **C5** (162.0 MHz, $CDCl_3$, 25 °C).

Table 4. Selected ^{31}P and ^{13}C NMR chemical shifts in CD_2Cl_2 (ppm) with J_{CP} coupling constants (Hz), and IR ν_{CO} frequencies in THF (cm^{-1}) for bidentate NHC-based Mn(I) complexes **C2**-**C5**.

	C2	**C3**	**C4**	**C5**
δ_P	72.1 (s)	70.6 (s)	91.0 (s)	93.8 (s), 81.6 (s)
δ_{N2C}	196.4 (d) J_{CP} = 16.9	194.9 (d) J_{CP} = 16.9	197.9 (d) J_{CP} = 16.3	197.4 (d) – 198.9 (d) J_{CP} = 21.3, 18.2
δ_{CO}	223.1 (d) 221.3 (d) 220.0 (d)	223.6 (d) 221.3 (d) 220.3 (d)	225.1 (d) 220.4 (d) 217.2 (d)	225.1 (d) – 222.5 (d) 219.7 (d) – 219.7 (d) 217.4 (d) – 216.5 (d)
ν_{CO}	2013 1937 1906	2017 1940 1915	2018 1943 1899	2020 1953 1909

➢ *Solid-State Structural Studies*

The molecular solid-state structures of NHC-phosphine Mn complexes **C2**, **C3**, and **C4** were confirmed by single crystal X-ray diffraction studies (**Figure 8**). In all cases, the Mn(I) center lies in an octahedral environment with a *cis*-arrangement on the NHC and phosphine donor moieties (C1−Mn1−P1 78.72−80.16°). As expected, the three carbonyl ligands adopt a facial arrangement in all representatives. Noteworthy, the geometry of Mn complexes **C2**, **C3**, and **C4** is similar to that found in complex **C5** recently characterized in our group.[62] The C1−Mn1 bond distances are similar for complexes **C2**, **C4**, and **C5** (2.045(3), 2.042(4), and 2.043(5) Å) and a little bit longer for complex **C3** (2.060(2) Å). By contrast, no significant change was noticed regarding the P1−Mn1 bond lengths in all complexes (**Table 5**).

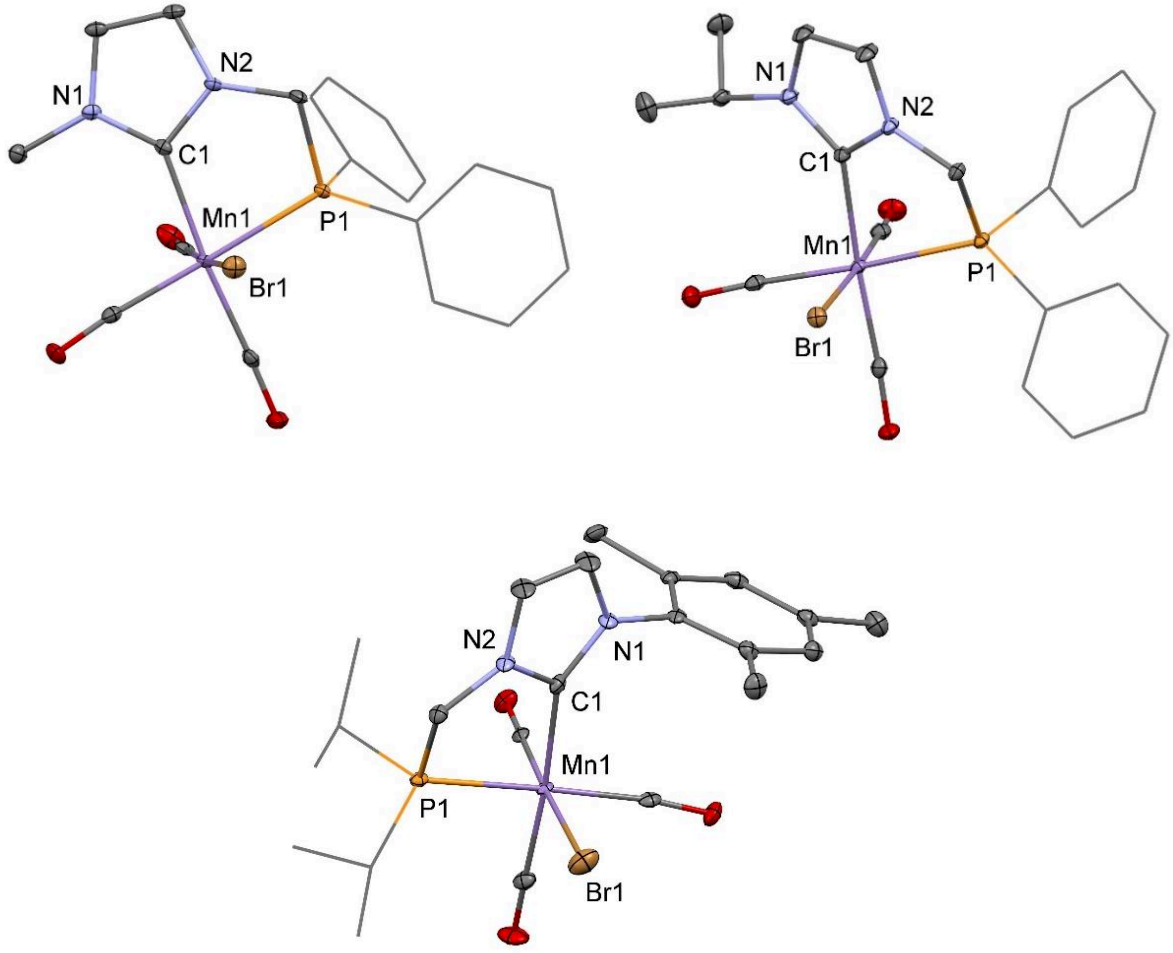

Figure 8. Perspective views of bidentate NHC Mn(I) complexes **C2**, **C3**, and **C4** with thermal ellipsoids drawn at the 30% probability level. The H atoms are omitted for clarity.

Table 5. Selected bond lengths (Å) and bond angles (°) for bidentate Mn complexes **C2-C5**

Complex	C2	C3	C4	C5[a]
C1−Mn1	2.045(3)	2.060(2)	2.042(4)	2.043(5)
P1−Mn1	2.2939(9)	2.3097(6)	2.3085(11)	2.306(3)
Mn1−Br1	2.5230(6)	2.5354(4)	2.5149(7)	2.559(3)
C1−Mn1−P1	79.72(9)	78.72(6)	80.16(12)	78.65(13)

[a] X-ray diffraction analysis described in the reference 62.

2.1.7 Synthesis and spectroscopic characterization of NHC-phosphine Mn hydride complexes

To synthesize hydride Mn complexes **C2.a**-**C5.a**, two complementary methods were considered. The hydride complex **C5.a** was obtained according to the previous approach used for the synthesis of hydride complex **C1.a**, from deprotonation of the corresponding bromide complex **C5** using 2.5 equiv. of KHMDS under H_2 atmosphere. Interestingly, a simple and convenient approach was developed to prepare such type of Mn complexes. The hydride complexes **C2.a**–**C4.a** were indeed obtained by reacting directly their corresponding bromide precursors **C2**-**C4** with 2 equiv. of $NaBH_4$ in ethanol and heating the reaction mixture at 80 °C for 2 h. Similar reactivity was initially reported in iron chemistry.[108,109] To the best of our knowledge, this is the first example of a hydride complex obtained in the manganese series using these specific conditions. Whatever the method, all hydride Mn complexes were isolated in good yields (71-80%).

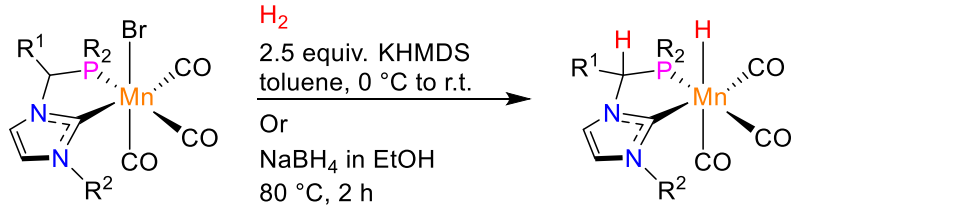

Scheme 44. Synthesis of Mn hydride complexes **C2.a**-**C5.a** from their corresponding bromide precursors **C2**-**C5**.

The identity of all hydride Mn complexes was mainly established on the basis of their characteristic ^{31}P, ^{1}H and ^{13}C NMR resonances (**Table 6**). The ^{1}H NMR spectrum of complexes **C2.a-C4.a** displayed shielded doublets at δ_H –(7.00−7.47 ppm), with $^{2}J_{PH}$ constants of 49.8−66.0 Hz. The ^{31}P NMR signals were found to be deshielded at δ_P 97.3−114.2 ppm compared to their bromide precursors **C2**-**C4** (δ_P 70.6−91.0 ppm). As in the case of **C5**, ^{1}H and ^{31}P NMR spectra of hydride complex **C5.a** confirmed the presence of two isomers by showing two doublets at δ_H –(6.49−6.73 ppm), with $^{2}J_{PH}$ constants of 52.3−51.7 Hz, and two singlets at low field at δ_P 119.2−115.5 ppm (**C5**: δ_P 93.8 (s), 81.6 (s) ppm). Similar information was obtained by ^{13}C NMR spectroscopy, the characteristic doublet signals for the carbenic carbon atoms at δ_{N2C} 203.7−205.7 ppm, with $^{2}J_{PC}$ = 14.2–16.6 Hz, being shifted downfield by (≈ 7.4 ppm) in comparison to their bromide precursors **C2**-**C4** (δ_{N2C} 194.9−197.9 ppm). The IR spectrum exhibited two intense ν_{CO} bands for complexes **C2.a**-**C3.a** (**C2.a**: 1987 (s) and 1905 (vs) cm^{-1}; **C3.a**: 1986 (s) and 1903 (vs) cm^{-1}), and three ν_{CO} bands at 1984 (s), 1903 (s), and 1882 (s) cm^{-1} for complex **C4.a** consistent with the presence of three CO ligands in a facial arrangement.

Table 6. Selected ^{31}P and ^{13}C NMR chemical shifts in Toluene (ppm) with J_{CP} coupling constants (Hz), and IR ν_{CO} frequencies in EtOH (cm^{-1}) for hydride Mn(I) complexes **C2.a**-**C5.a**

	C2.a	**C3.a**	**C4.a**[a]	**C5.a**[b,c]
δ_H	–7.00	–7.10	–7.47	–6.49, –6.73
	J_{PH} = 64.8	J_{PH} = 66.0	J_{PH} = 49.8	J_{PH} = 52.3, 51.7
δ_P	98.3 (s)	97.3 (s)	114.2 (s)	119.2 (s), 115.5 (s)
δ_{N2C}	203.7 (d)	202.0 (d)	205.7 (d)	205.8 (d)
	J_{CP} = 16.4	J_{CP} = 16.6	J_{CP} = 14.2	J_{CP} = 17.3
δ_{CO}	227.8 (br)	227.6 (br)	227.1 (d)	225.6 (d)
	226.0 (br)	226.2 (d)	225.1 (br)	225.0 (d)
	223.1 (br)	223.3 (br)	224.3 (br)	221.9 (br)
ν_{CO}	1987	1986	1984	1991
	1905	1903	1903	1914
	-	-	1882	1896

[a] NMR data was recorded in THF.

[b] IR ν_{CO} frequencies were measured in a toluene solution.

[c] Only the major isomer was detected in ^{13}C NMR

2.1.8 Catalytic Investigations

As demonstrated previously, the NHC-phosphine Mn(I) complex **C1** proved to be one of the most efficient Mn pre-catalyst in the hydrogenation of ketones. The purpose of changing the substituents at the N, P positions and on the carbon chain was to study the influence of these modifications on catalytic activity. Based on the previous results obtained with complex **C1** for the hydrogenation of acetophenone, the same optimal conditions (0.1 mol% of catalyst loading, 1 mol% of *t*-BuOK in *t*-AmOH (**A**), or 1 mol% of KHMDS in toluene (**B**) at 60 °C, 50 bar H_2, 20 h, **Table 7**) were first considered with Mn complexes **C1.b** and **C2-C5**. As in the case of complex **C1**, the system (**A**) was found to be more efficient than system (**B**), as illustrated in entries 6, 10, and 22. Under optimal conditions using system (**A**), with complexes **C3**, **C4**, and **C5**, the acetophenone **a1** was fully reduced with conversions of about 94-100% (entries 5, 9, and 13). However, complex **C2** gave a lower conversion of **a1**, the corresponding alcohol being produced in only 73% yield (entry 1). Decreasing the catalytic charge to 0.05 mol% did not affect the reactivity of complexes **C4**, **C5**, and **C1.b**, the acetophenone being converted to 1-phenylethanol in quantitative yields (entries 11, 15, and 21). In contrast, using 0.05 mol% of complexes **C2** and **C3** dropped the conversions of acetophenone to 22 and 64%, respectively (entries 3 and 7). As observed in the case of complex **C1**, the temperature has a significant influence on the catalytic activity. Using the same catalyst loading 0.05 mol% of **C2** and **C3** at 100 °C increased indeed the conversions to 74 and 96%, respectively (entries 4 and 8). For complexes **C4** and **C5**, the catalytic loading could be decreased to 0.01 mol% at 60 °C giving the desired alcohol in 57 and 88% yields, respectively (entries 12 and 16). Interestingly, complex **C5** was able to reduce the acetophenone in 76% yield using only 0.005 mol% of catalyst loading at 100 °C (entry 19). These results indicate clearly that the nature of the NHC-phosphine ligand has a significant influence on the catalytic activity of corresponding Mn complexes. The superiority of complex **C5** bearing a phenyl substituent on the carbon bridge can be *a priori* related to the increased acidity of the corresponding CH position, in accordance with previous experimental and theoretical evidences showing that the deprotonation takes place at the carbon bridge.

Table 7. Catalytic hydrogenation of acetophenone with bidentate NHC-phosphine Mn(I) complexes **C1.b** and **C2-C5**[a]

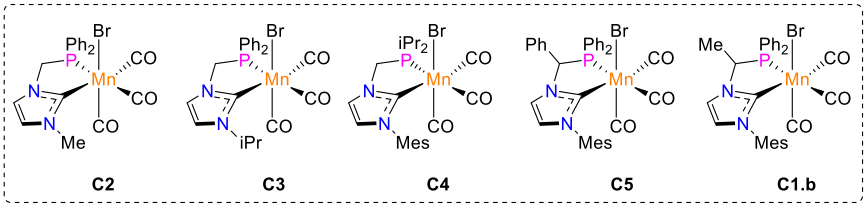

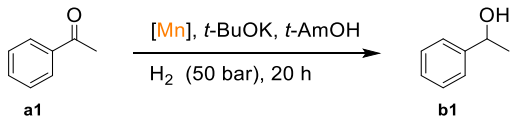

Entry	Complex	Cata. % mol	Method	Temp. °C	Conv. %[b]
1	**C2**	0.1	A	60	73
2	**C2**	0.1	B	60	74
3	**C2**	0.05	A	60	22
4	**C2**	0.05	A	100	74
5	**C3**	0.1	A	60	94
6	**C3**	0.1	B	60	62
7	**C3**	0.05	A	60	64
8	**C3**	0.05	A	100	96
9	**C4**	0.1	A	60	100
10	**C4**	0.1	B	60	82
11	**C4**	0.05	A	60	100
12	**C4**	0.01	A	60	57
13	**C5**	0.1	A	60	100
14	**C5**	0.1	B	60	100
15	**C5**	0.05	A	60	100
16	**C5**	0.01	A	60	88
17	**C5**	0.001	A	60	16
18	**C5**	0.005	A	60	43
19	**C5**	0.005	A	100	76
20	**C5**	0.001	A	100	21
21	**C1.b**	0.05	A	60	100
22	**C1.b**	0.1	B	60	4

[a] Acetophenone (2.0 mmol), base (1.0 mol%; **A**: *t*-BuOK, **B**: KHMDS), solvent (2 mL, **A**: *t*-AmOH, **B**: toluene).

[b] Conversion determined by GC and ^{1}H NMR spectroscopy.

2.1.9 Mechanistic studies

On the basis of the above discussed experimental and theoretical results, we proposed the catalytic cycle shown in **Scheme 45** for the hydrogenation of acetophenone with our NHC-phosphine Mn complexes. In a first step, the deprotonation of the bromide Mn complex **C1** leads to the formation of NHC-ylide complex **C1.d[1]** which is then transformed into hydride Mn complex **C1.a** under H_2 atmosphere. The nucleophilic addition of the hydride complex **C1.a** on the acetophenone substrate would then result in the formation of the corresponding alkoxy Mn complex **C1.f**. Finally, the deprotonation of the alkoxy complex **C1.f** would release the alcohol product regenerating the NHC-ylide complex **C1.d[1]**.

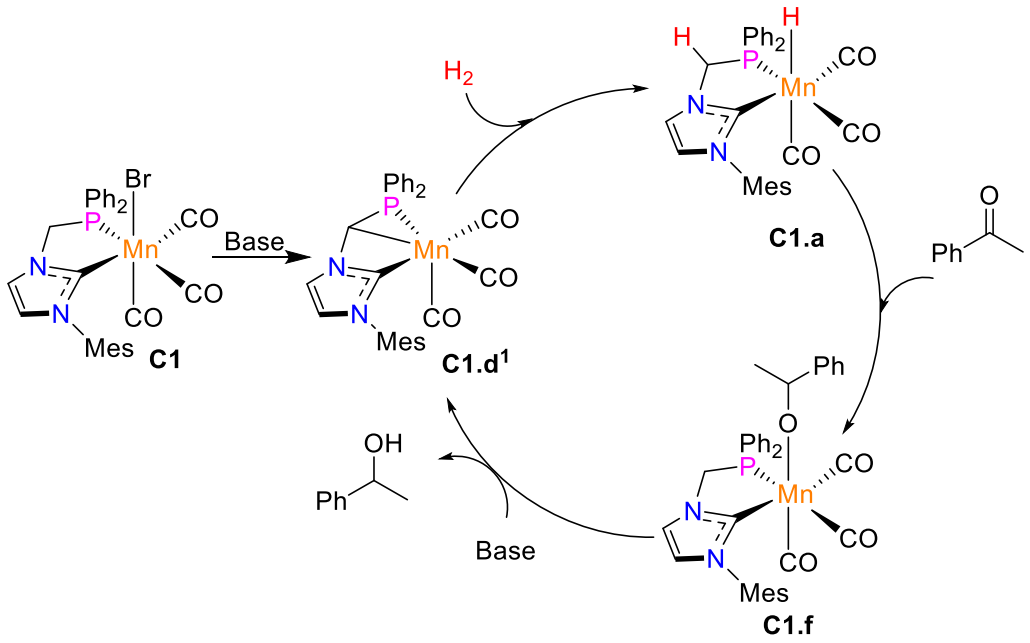

Scheme 45. Proposed mechanism for the catalytic hydrogenation of acetophenone with NHC-phosphine Mn(I) complex **C1**.

If the formation of Mn complexes **C1.d[1]** and **C1.a** was experimentally and theoretically evidenced, the involvement of alkoxy Mn complex **C1.f** was not confirmed to date. For this purpose, stoichiometric reactions were considered from hydride complex **C1.a** and bromide complex **C1**.

From hydride Mn complex **C1.a**, all attempts to isolate the postulated alkoxy complex **C1.f** have failed. Indeed, no reaction took place when a stoichiometric amount of complex **C1.a** was reacted with acetophenone in THF, even by heating the reaction mixture at 60 °C for 18 h, the ^{31}P and ^{1}H NMR spectra displaying only the characteristic signals of hydride complex **C1.a** (**Scheme 46**, *left*). To increase the nucleophilicity of hydride complex **C1.a** by forming in situ

a NHC-ylide species, 2.5 equiv. of KHMDS were added in toluene, followed by the addition of 1 equiv. of acetophenone. However, only the starting Mn complex **C1.a** was observed without visible decomposition, even after stirring the reaction mixture at room temperature for 18 h. (**Scheme 46**, *right*).

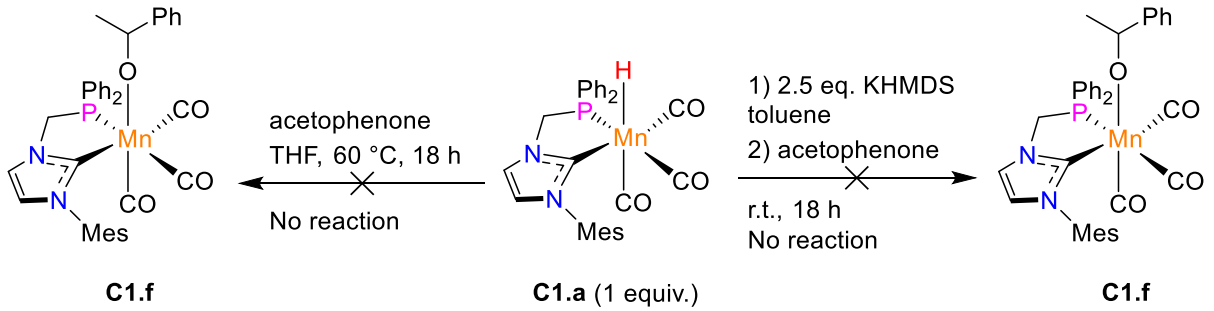

Scheme 46. Stoichiometric reactions between the hydride Mn complex **C1.a** and acetophenone.

The absence of apparent reactivity could indicate that the equilibrium between the alkoxy complex **C1.f** and the hydride complex **C1.a** is shifted toward the latter. Thus, in order to investigate this possibility, another strategy was considered based on the substitution of the bromide ligand in Mn complex **C1** by an alkoxide moiety. Treatment of complex **C1** with 1 equiv. of lithium 1-phenylethanolate in THF at room temperature, and after stirring the reaction mixture at 60 °C for 18 h, did not lead *a priori* to any reaction, the ^{31}P NMR spectrum indicating indeed a similar signal to the one of complex **C1** (**Scheme 47**, *left*). One possibility to explain this behavior could be that bromide complex **C1** and alkoxide complex **C1.f** present isochronous ^{31}P NMR chemical signals. To confirm or not this hypothesis, we have prepared the triflate analogue **C1.g** from bromide complex **C1** by addition of AgOTf in toluene at rt. This complex **C1.g** was characterized by ^{31}P NMR spectroscopy, showing a singlet at 74.2 ppm shifted by 3.1 ppm compared to complex **C1** (δ_P 71.1 ppm). As in the case of bromide complex **C1**, no reaction was observed between triflate complex **C1.g** and lithium 1-phenylethanolate excluding finally the formation of the alkoxy complex **C1.f**. (**Scheme 47**, *left*).

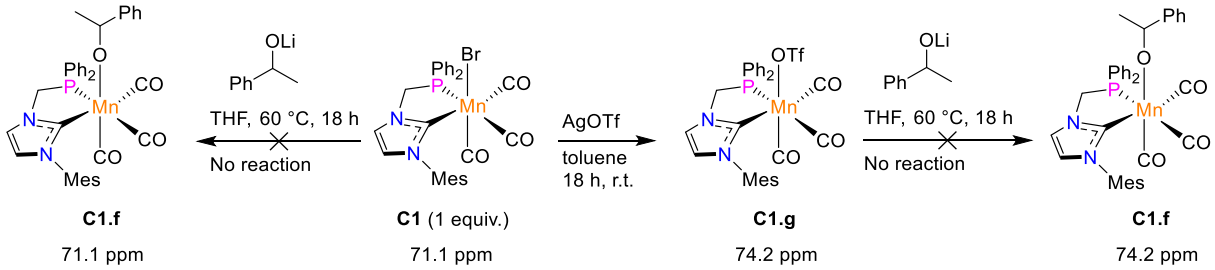

Scheme 47. Treatment of bromide Mn complex **C1** with 1 equiv. of lithium 1-phenylethanolate (*left*), and abstraction of the bromide ligand by AgOTf to form complex **C1.g**, following by the addition of the same alcoholate (*right*).

Moreover, the deprotonation of complex **C1** with 2.5 equiv. of KHMDS followed by addition of 1 equiv. of 1-phenylethanol gave several signals in the ^{31}P NMR spectrum at δ_P 140.8−196.7 ppm (**Scheme 48**). Similar chemical shift has been previously observed when the deprotonated form of complex **C1** was reacted with benzaldehyde. In both cases, we proposed that the products observed come from the formation of a C-C bond due to the nucleophilic addition of the ylidic species on the electrophilic subtrastes, as observed in the case of the CO_2 adduct (complex **C1.c**, see **Scheme 35**).

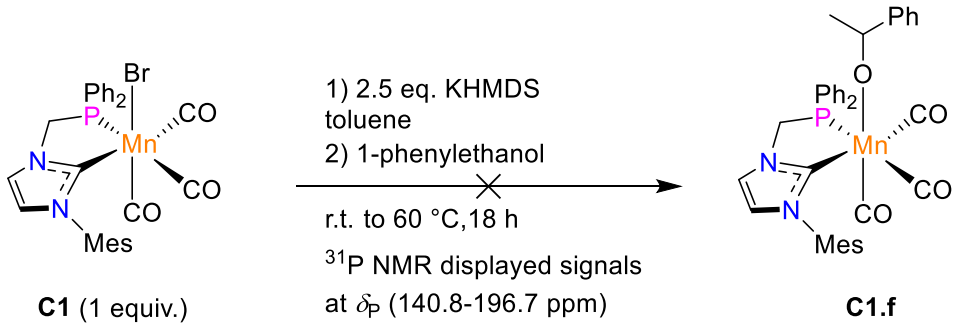

Scheme 48. Deprotonation of complex **C1** followed by addition of 1 equiv. of 1-phenylethanol.

Finally, replacing 1-phenylethanol with a more acidic substrate such as deuterated acetic acid. resulted after addition of 2.5 equiv. of KHMDS in the substitution of the bromide co-ligand by an acetate group. The latter complex **C1.h** displayed notably a singlet at δ_P 78.4 ppm in ^{31}P NMR spectroscopy (**Scheme 49**). The solid-state structure of complex **C1.h** was definitively confirmed by an X-ray diffraction study, showing a facial arrangement of the three carbonyls co-ligands with the acetate group coordinated to the Mn center (**Figure 9**).

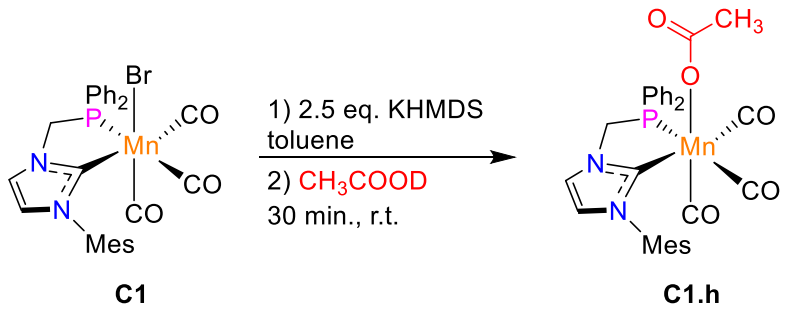

C1 **C1.h**

Scheme 49. Deprotonation of the bromide Mn complex **C1** followed by the addition of 1 equiv. of deuterated acetic acid.

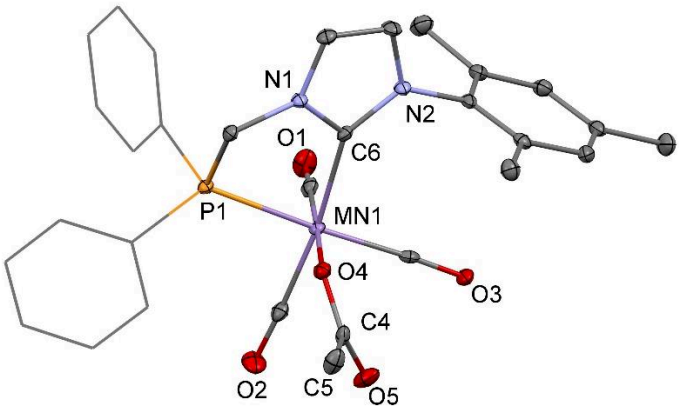

Figure 9. Molecular geometry of complex *fac*-**C1.h** (30% probability ellipsoids, aryl groups represented as a wireframe for clarity). Selected bond lengths (Å) and angles (°): Mn1–C6 2.048 (3), Mn1–P1 2.2997 (9), Mn1–O4 2.0623 (18), C6–Mn1–P1 79.10 (7), C6–Mn1–O4 84.07 (9), P1–Mn1–O4 84.58 (5).

These stoichiometric reactions did not therefore make it possible to demonstrate the involvement of the alkoxy Mn complex **C1.f** during the catalytic cycle. It therefore appears that a more complex mechanism probably operates here, such as an outer-sphere mechanism. A theoretical study is currently underway to specify the nature of the different species involved in this catalytic process.

2.1.10 Conclusion

Various Mn(I) complexes of easily accessible bidentate NHC-phosphine ligands were conveniently synthesized from corresponding imidazolium salts. Moreover, we have also shown that a Mn(I) complex **C1** of such phosphine-NHC ligand can be selectively deprotonated at the carbon position located between the two donor moieties to afford an original 18-e NHC-

phosphinomethanide complex. The latter can serve as a reservoir for an unconventional 16-e NHC-phosphonium ylide complex able to activate dihydrogen through a metal-ligand cooperation mode based on the formal interplay between λ^5- and λ^3-phosphorous species. Interestingly, homogeneous catalysis can take advantage of this new mode of H_2 activation, as demonstrated by the development of one of the most efficient Mn-based catalytic system for the hydrogenation of ketones. Noteworthy, changing the substituents on the N- and P- atoms has a small effect on complexes activity. Complex **C2** with a methyl group on the N-atom was found to be the less active in this process. By contrast, introducing a phenyl group at the methylene bridge increased significantly the catalytic activity of complex **C5**, which was found to be the most efficient pre-catalyst in this transformation. This catalytic activity was related to the acidity of the substituted methylene bridge linking the NHC and phosphine donor extremities.

2.2 Synthesis of Tridentate NHC-Phosphine Mn(I) Complexes

Based on the general structure of bidentate NHC-phosphine ligands of type **A**, we wondered about the possible impact on catalytic activity of changing the 'spectator' *N*-R substituent by a donor group capable of interacting with the metal center. For this purpose, we turned out attention to the preparation, the coordinating properties and the catalytic activity of the novel tridentate NHC core ligands of type **B** bearing phosphine and pyridine donor arms (**Scheme 50**). In a larger context, this comparative study also aimed to assess whether the improvement in catalytic performance necessarily involved the design of more complex architectures, as are pincer systems with respect to their bidentate versions.

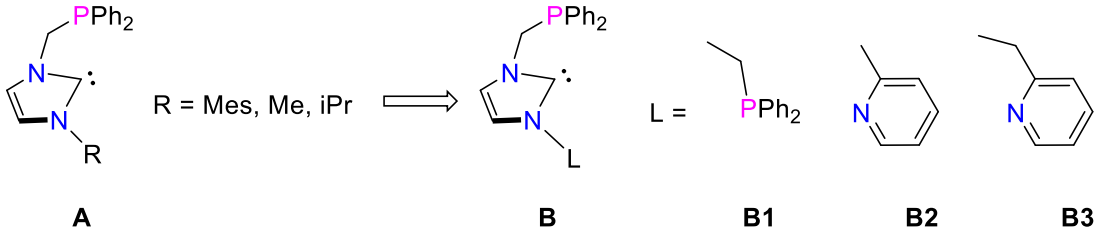

Scheme 50. Representation of previously prepared bidentate NHC-phosphine ligands **A**, and related targeted tridentate NHC core systems of type **B**.

2.2.1 *Synthesis and NMR characterization of NHC-based pre-ligands.*

The first representative **B1** of the family was prepared from the *N*-phosphine oxide substituted imidazole **L^{a}6(O)** isolated in 70% yield by treating 1*H*-imidazole with 1.0 equiv. of 1-[(diphenylphosphoryl)methylene]-4-methylbenzenesulfonate[71] in the presence of K_2CO_3 in DMSO at 90 °C (**Scheme 51**, *left*). The second phosphine oxide arm was then introduced by adding to the imidazole **L^{a}6(O)** an equiv. of the same tosylate precursor in toluene at 130 °C, allowing the bis(*N*-phosphine oxide)-imidazolium salt **L6(O)** to be isolated in 87% yield. The latter was finally reduced by an excess of triphenylsilane in the presence of a catalytic amount of bis(4-nitrophenyl) phosphate[110] in toluene at 110 °C affording the targeted bis(*N*-phosphino)-imidazolium salt **L6** in 89% yield. Typical methods of converting phosphine oxides into phosphines based on strong reducing conditions such as those requiring the use of an excess of $HSiCl_3$ in chlorobenzene at 80°C led also to salt **L6** but with a slightly lower yield (*ca.* 80%). The second representative **B2** was considered from 2-(1*H*-imidazol-1-yl)pyridine synthetized according to a well-known procedure (**Scheme 51**, *middle*).[111] From the *N*-pyridine substituted imidazole, following the same two-step strategy as that developed in the previous series, the imidazolium salts **L7(O)** and **L7** featuring phosphine oxide and phosphine arms were thus isolated in 90 and 89% yields, respectively. Gratifyingly, the application of similar reactivity pattern from reported 2-(1*H*-imidazol-1-yl-methyl)pyridine[112] enabled the formation of the representative **B3** in the form of imidazolium salt **L8** isolated in 86% yield from its P-oxidized precursor **L8(O)** (**Scheme 51**, *right*). Noteworthy in the case of *N*-pyridine substituted imidazole derivatives **L7(O)** and **L8(O)**, the reduction of the phosphine oxide moiety by using the strong reducing agent $HSiCl_3$ was found to be non-selective, resulting in partial reduction of the pyridine nucleus.

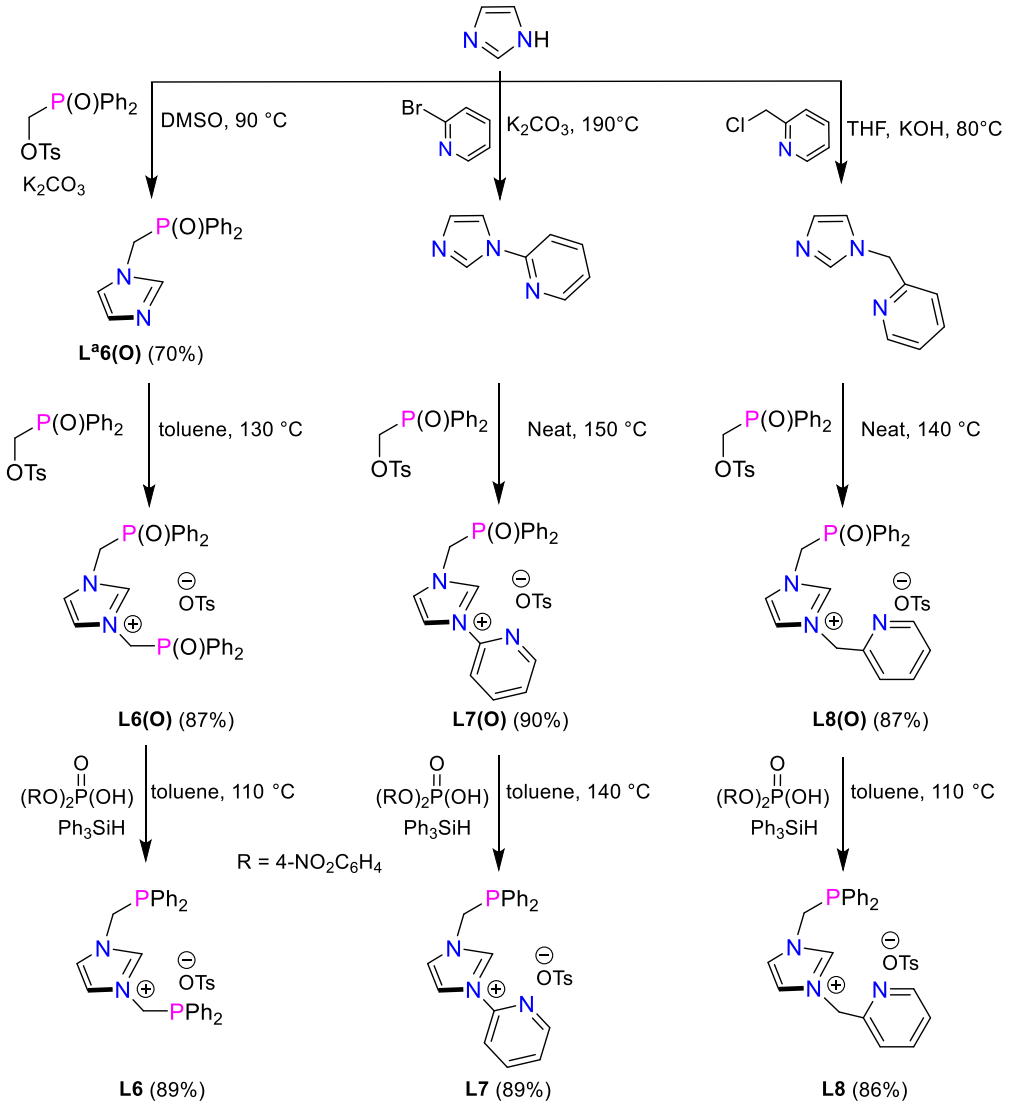

Scheme 51. Preparation of tridentate PCP and PCN pre-ligands **L6**, **L7** and **L8** from 1*H*-imidazole.

The identity of all salts was mainly established on the basis of their characteristic ^{31}P, ^{1}H and ^{13}C NMR resonances (**Table 8**). For imidazolium salts **L6(O)**, **L7(O)**, and **L8(O)** exhibiting a phosphine oxide moiety, the ^{31}P NMR spectrum displayed a single signal at δ_P 26.5−27.2 ppm in the typical range for such P(V)-based derivatives. As expected, the ^{31}P NMR singlet of imidazolium salts **L6**, **L7**, and **L8** appeared at higher field at δ_P –(11.1−12.4) ppm in agreement with the presence of P(III) donor extremities of alkyl(diphenyl)phosphine nature. The cationic character of these salts was confirmed by ^{1}H and ^{13}C NMR spectroscopy by the characteristic low field signals of the CH imidazolium fragment at δ_H 9.56−10.59 ppm and δ_{CH} 136.0−138.6 ppm.

Table 8. Selected ^{31}P, ^{1}H and ^{13}C NMR chemical shifts in $CDCl_3$ (ppm) for imidazolium salts **L6(O)**, **L6**, **L7(O)**, **L7**, **L8(O)** and **L8**.

	L6(O)	**L6**	**L7(O)**	**L7**	**L8(O)**	**L8**
δ_P	26.5	−12.4	27.1	−11.1	27.2	−12.2
δ_{CH}	9.85	9.62	10.44	10.59	9.95	9.56
δ_{CH}	138.6	138.1	135.6	136.0	138.5	137.5

2.2.2 *Synthesis and spectroscopic characterization of NHC-based Mn(I) complexes*

The complexation of P-reduced pre-ligands **L6**, **L7**, and **L8** was envisioned following a strategy developed recently in the case of the bidentate versions (see **Scheme 43**). Complexes **C6**, **C7, C7'**, and **C8** were thus readily obtained from the corresponding salt precursors through the sequential addition of equimolar quantities of KHMDS and $[Mn(CO)_5Br]$ in 71, 80, and 60% isolated yield, respectively (**Scheme 52**). While all neutral $Mn(CO)_3Br$ complexes formed appeared to be bidentate in nature, a difference in the coordination mode was observed between the two representatives bearing a pyridine extremity. From **L7** where the pyridine is directly connected to the imidazole core, two isomeric complexes **C7** and **C7'** in a 1/3 ratio were evidenced due to the possible formation of two thermodynamically favored five-membered metallacycles upon coordination of the phosphine or of the pyridine arm. By contrast in the case of **L8**, only the bidentate complex **C8** resulting from the concomitant coordination of NHC and diphenylphosphine extremities was observed, the coordination of pyridine would indeed have led to a less stable six-membered metallacycle.

All of the bromo NHC-based Mn(I) complexes were then easily converted in the presence of AgOTf in CH_2Cl_2 to their corresponding air-stable cationic tridentate complexes **C6^t**, **C7^t**, and **C8^t** isolated as single isomers in 88, 76, and 96 % yields, respectively.

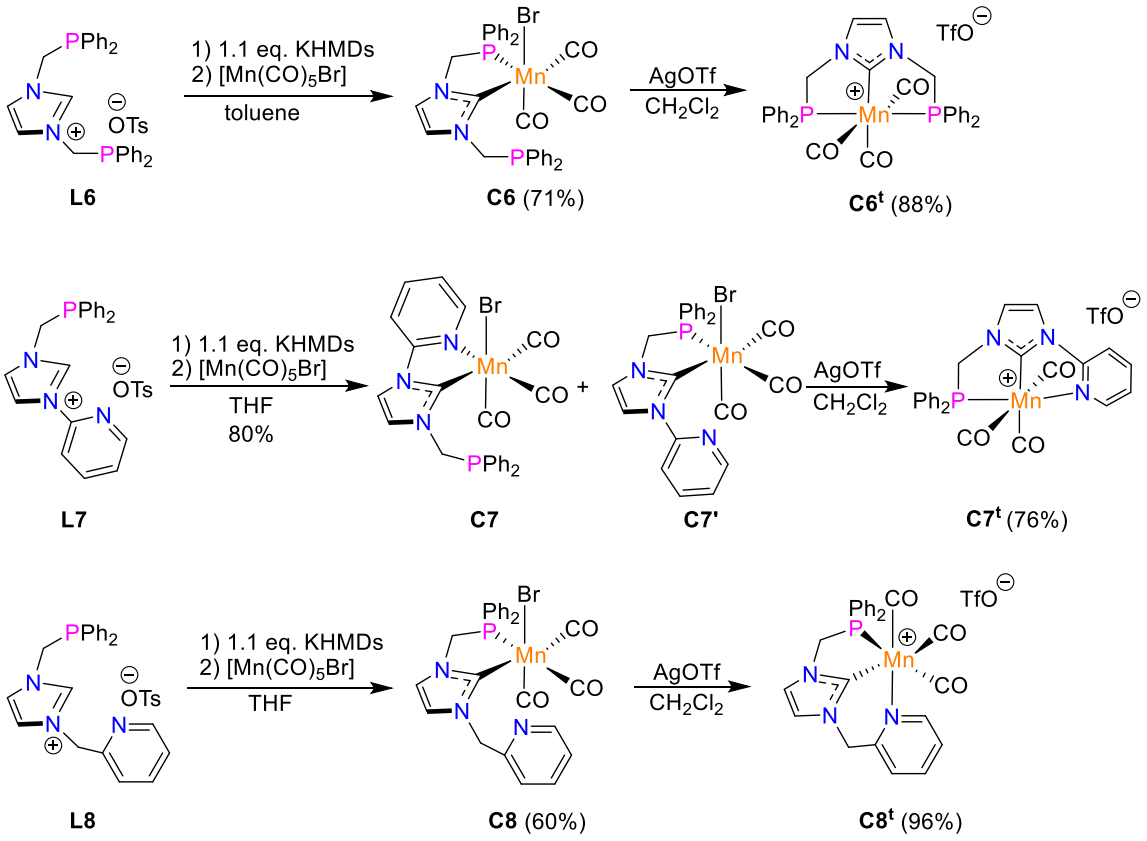

Scheme 52. Syntheses of cationic tridentate NHC core Mn(I) complexes **C6**^{t}, **C7**^{t}, and **C8**^{t} from corresponding PCP **L6** and PCN ligand precursors **L7** and **L8**.

The formation of NHC Mn complexes was clearly indicated by ^{1}H and ^{13}C NMR spectroscopy showing the disappearance of the C−H imidazolium signals of pre-ligands **L6**, **L7**, and **L8** (**Table 9**). Regardless of their coordination mode, in the ^{13}C NMR spectra, the N_2C−Mn carbon atoms of NHC core complexes (δ_{N2C} 195.6−206.5 ppm) were typically found to be strongly deshielded with proper multiplicity with respect to the N_2CH carbon atoms of corresponding precursors (δ_{CH} 136.0−138.6 ppm). The coordination of the *N*-substituted NHC-phosphine moiety was also apparent from the downfield shift of the ^{31}P NMR resonances, ranging from δ_P –(11.1−12.4) ppm in the pre-ligands to δ_P 71.0−71.8 ppm in the bidentate complexes and δ_P 89.6−97.4 ppm in their tridentate analogues. The IR spectrum of all bidentate NHC Mn complexes **C6**, **C7**, **C7'**, and **C8** exhibited three ν_{CO} bands consistent with the presence of three CO ligands in a facial arrangement. The small differences observed between these frequency values seem to indicate that the three ligands of interest have similar electronic properties. In the tridentate series, complexes **C6**^{t}, **C7**^{t}, and **C8**^{t} featured three νCO bands with different relative intensities suggesting two distinct CO ligand arrangements. In complement to these IR

frequency values, ^{13}C NMR data revealed for complexes **C6^t** and **C7^t** the presence of two CO resonances **C6^t**: δ_C 220.7 (brt, J_{PC} = 10.5 Hz), 213.6 (brt, J_{PC} = 19.0 Hz); **C7^t**: δ_C 218.4 (d, J_{PC} = 9.7 Hz), 212.7 (d, J_{PC} = 17.7 Hz)), and of three resonances (δ_C 219.6 (brd, J_{PC} = 25.5 Hz), 218.7 (d, J_{PC} = 18.5 Hz)), 216.9 (d, J_{PC} = 23.5 Hz)) for **C8^t**, suggesting that the NHC core backbone is *a priori* coordinated to the Mn center in a meridional fashion within complexes **C6^t** and **C7^t**, and adopts rather a tripodal coordination mode in **C8^t**.

Table 9. Selected ^{31}P and ^{13}C NMR chemical shifts in CD_2Cl_2 (ppm) with J_{CP} coupling constants (Hz), and IR ν_{CO} frequencies in THF (cm^{-1}) for NHC-based Mn(I) complexes of bidentate nature **C6**, **C7**, **C7'**, and **C8**, and of tridentate nature **C6^t**, **C7^t** and **C8^t**.

	C6[a]	**C6^t**	**C7**	**C7'**	**C7^t**[b]	**C8**	**C8^t**
δ_P	71.0 (s) −17.0 (s)	89.6 (s)	−15.9 (s)	71.8 (s)	97.4 (s)	71.2 (s)	93.3 (s)
δ_{N2C}	197.1 (d) J_{CP} = 16.5	195.6 (t) J_{CP} = 13.1	206.0 (s)	198.1 (d) J_{CP} = 15.1	206.5 (d) J_{CP} = 18.9	197.7 (d) J_{CP} = 17.5	202.9 (d) J_{CP} = 22.3
δ_{CO}	222.9 (d) 221.4 (d) 220.1 (d)	220.7 (brt) 213.6 (brt)	226.4 (s) 221.3 (s) 218.0 (s)	223.9 (d) 220.2 (d) 218.5 (d)	218.4 (d) 212.7 (d)	222.8 (brd) 220.8 (brd) 220.2 (brd)	219.6 (brd) 218.7 (brd) 216.9 (brd)
ν_{CO}	1910 1940 2015	2045 1942 1966	1907 1930 2016	1904 1939 2016	2052 1941 1969	1913 1941 2018	1929 1947 2024

[a] IR ν_{CO} frequencies were measured in a toluene solution.

[b] NMR data was recorded in $CDCl_3$.

2.2.3 *Solid-state structural studies*

Single-crystal X-ray diffraction studies allowed us to establish the solid-state structures of the imidazolium salt **L6**, the neutral bidentate Mn complexes **C7**, **C7'** and **C8**, and of the cationic tridentate Mn complexes **C6^t**, **C7^t** and **C8^t** (**Figure 10**, and **Table 10**). In all complexes, the hexacoordinate Mn(I) atom resides in a distorted octahedral environment. As anticipated by NMR and IR spectroscopy, the three carbonyl co-ligands adopt a facial arrangement in bidentate representatives. In the tridentate series, complexes **C6^t** and **C7^t** can be regarded as real pincers characterized by the meridional coordination of the NHC-based ligand with two

CO co-ligands positioned in *trans* with respect to each other, while in **C8^t** the PCN backbone acts as a tripodal ligand with the three CO co-ligands located *cis* to each other. In the pincer systems, the two coordinating heteroatoms are positioned in pseudo-*trans* position with respect to the metal center **C6^t**: P1−Mn1−P2 = 160.148(14); **C7^t**: P1−Mn1−N3 = 153.76(4)°) as opposed to the tripodal complex **C8^t** where the related coordination angle is much more acute (P1−Mn1−N3 = 91.92(3)°). As generally observed in meridional Mn(I) complexes, the C−O distances in the mutually *trans* CO ligands are shorter **C6^t**: 1.1407(17), 1.1383(17) Å; **C7^t**: 1.139(2), 1.138(2) Å) than in the CO *trans* to the ligand, in this case the NHC core **C6^t**: 1.1423(16) Å; **C7^t**: 1.151(2) Å).[113] As general trend, the C1−Mn1 bond distances are significantly shortened in the tridentate systems compared to their bidentate precursors, a difference that may be attributed to the existence of more constrained geometries in the pincer-type complexes. The PCP and PCN pincer structures **C6^t** and **C7^t** are defined by the presence of two fused 5-membered metallacyles with the PCP backbone in the former symmetrically linked to Mn through two quasi-equal P−Mn bonds (2.2627(3) and 2.2661(3) Å). The facial geometry observed in complex **C8^t** can be rationalized by the presence of a longer lateral chain which offers more flexibility accomodating the formation of a six-membered metallacycle upon pyridine coordination.

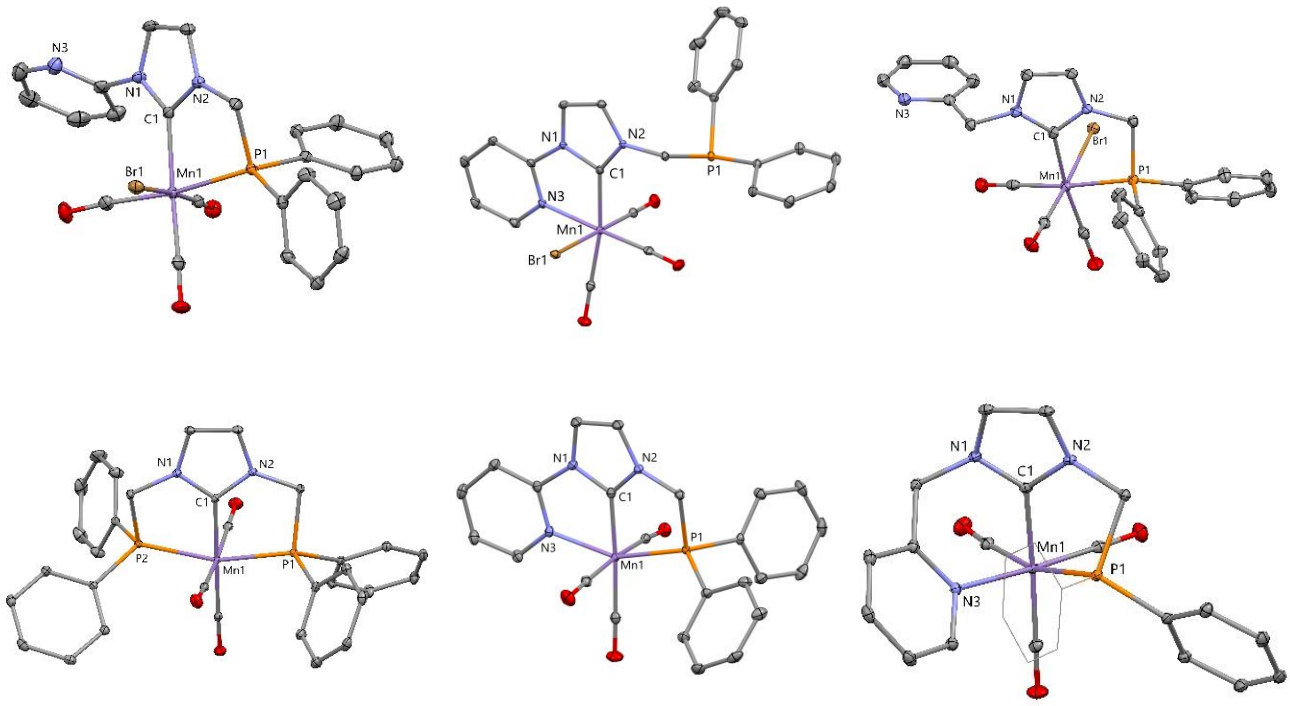

Figure 10. Perspective views of bidentate NHC Mn(I) complexes **C7**, **C7'**, and **C8** (*up*), and of tridentate NHC Mn(I) complexes **C6^t**, **C7^t** and **C8^t** (*down*) with thermal ellipsoids drawn at the 30% probability level. The H atoms are omitted for clarity.

Table 10. Selected bond lengths (Å) and bond angles (°) for bidentate Mn complexes **C7**, **C7'** and **C8**, and tridentate Mn complexes **C6^t**, **C7^t** and **C8^t**.

Complex	C7	C7'	C8	C6^t	C7^t	C8^t
C1−Mn1	2.054(2)	1.993(2)	2.049(3)	1.9726(12)	1.9360(16)	1.9881(11)
P1−Mn1	2.3175(7)	-	2.2861(9)	2.2627(3)	2.2712(5)	2.3348(3)
P2−Mn1	-	-	-	2.2661(3)	-	-
N3−Mn1		2.0753(17)	-	-	2.0894(14)	2.1095(9)
Mn1−Br	2.5510(5)	2.5354(4)	2.5527(5)	-	-	-
C1−Mn1−P1	79.02(7)	-	79.95(9)	79.88(4)	78.15(5)	75.16(6)
C1−Mn1−P2	-	-	-	80.30(4)	-	-
C1−Mn1−N3	-	78.17(8)	-	-	75.67(6)	82.90(4)
P1−Mn1−P2	-	-	-	160.148(14)	-	-
P1−Mn1−N3	-	-	-	-	153.76(4)	91.92(3)

2.2.4 *Catalytic investigations*

Based on the recent observation that a Mn(I) complex of the bidentate NHC-phosphine ligand **L1** behaves as one of the most efficient Mn-based catalytic system for the hydrogenation of ketones, this transformation was naturally selected to evaluate the influence of the introduction of an additional coordinating arm.[114] For such comparative study, the three pincer-type complexes **C6^t**, **C7^t** and **C8^t** differing only by the nature of one of the three donor ends were considered. The catalytic reactions were performed under H_2 pressure (50 bar) in *t*-AmOH at 60 or 100 °C, and in the presence of 10 mol% of *t*-BuOK (**Table 11**). Gratifyingly at 100 °C, in the presence of 1.0 mol% of **C8^t**, acetophenone was fully reduced to 1-phenylethanol (entry 9). The catalytic charge could be decreased to 0.5 mol% at the same temperature keeping a good conversion of 80% (entry 10). At 60 °C, the alcohol was produced in lower yields with a conversion of 30 and 20% by using 1.0 and 0.5 mol% of **C8^t**, respectively (entries 11-12). The two other selected complexes were found to be significantly less active in this process. For instance, at 100 °C, with a catalytic charge of 1.0 mol% of **C6^t** and **C7^t**, the acetophenone was only converted into the corresponding alcohol in 27 and 39% yields, respectively (entries 1 and 5). Between them, regardless of catalytic loading and temperature reaction, the pre-catalyst **C7^t** bearing a pyridine donor appeared to be slightly more efficient. These results indicate that the ligand structure of pincer-type Mn complexes influence to some extend the catalytic properties. The superiority of *fac*-complex **C8^t** was tentatively attributed to the presence of a six-membered

metallacycle which should result in greater lability of the pyridine arm and thus allows the release of a vacant site during the catalytic cycle. The lability of a donor extremity was also supported in other systems by the catalytic activities of the bidentate complexes **C6**, **C7** and **C8** which were found to be very close to those obtained with their corresponding tridentate forms **C6^t**, **C7^t** and **C8^t** (entries 13-15). This similarity in catalytic efficiency also suggests that the same type of catalytic active species is certainly involved in both series. Noteworthy, the performance of complex **C8^t** remains lower than that of the Mn complex of the bidentate NHC-phosphine ligand **L1**,[114] showing that the development of more elaborate structures is not always a prerequisite to reach higher activities in the field of catalysis.

Table 11. Catalytic hydrogenation of acetophenone with NHC core Mn(I) complexes **C6^t**, **C7^t** and **C8^t**.[a]

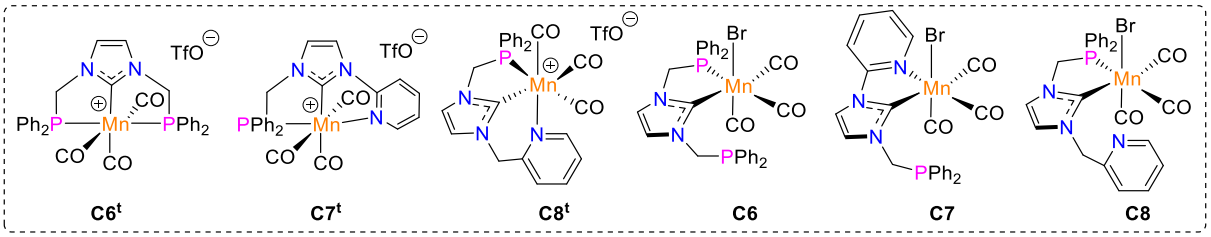

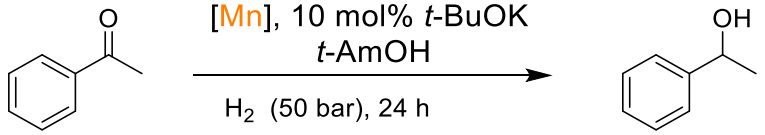

Entry	Complex	Cat. (mol%)	Temp. (°C)	Conv. %[b]
1	**C6^t**	1.0	100	27
2	**C6^t**	0.5	100	19
3	**C6^t**	1.0	60	6
4	**C6^t**	0.5	60	3
5	**C7^t**	1.0	100	39
6	**C7^t**	0.5	100	21
7	**C7^t**	1.0	60	22
8	**C7^t**	0.5	60	11
9	**C8^t**	1.0	100	100 (95)
10	**C8^t**	0.5	100	80
11	**C8^t**	1.0	60	30
12	**C8^t**	0.5	60	20
13	**C6**	1.0	100	42
14	**C7**	1.0	100	33
15	**C8**	1.0	100	98

[a] Procedure: an autoclave was charged with pre-catalyst (**C6^t**, **C7^t** or **C8^t**), acetophenone (1.0 mmol), *t*-BuOK (10 mol%) in *t*-AmOH (2 mL) under H_2 (50 bar) at 60 or 100 °C.

[b] Conversions determined by GC and ^{1}H NMR, isolated yield in parenthesis.

2.2.5 *Conclusion*

A family of NHC core, phosphine-based Mn(I) pincer-type complexes where the third donor extremity can be modified was described from 1*H*-imidazole according to a five-step procedure. Cationic symmetrical *mer*-[Mn(CO)$_3$(κ^3*P,C,P*)(OTf)] **C6^t**, and non-symmetrical *mer*-[Mn(CO)$_3$(κ^3*P,C,N*)(OTf)] **C7^t**, and *fac*-[Mn(CO)$_3$(κ^3*P,C,N*)(OTf)] **C8^t** complexes were thus selectively prepared, fully characterized including by X-ray diffraction analysis and evaluated in the catalytic hydrogenation of acetophenone. The *fac*-[Mn(CO)$_3$(κ^3*P,C,N*)(OTf)] pre-catalyst **C6^t** was found to be the most active system in the selected transformation, the efficiency of which was attributed to the presence of a 5,6-fused membered metallacyclic architecture promoting the dissociation of the pyridine arm and thereby releasing a vacant site beneficial to the catalytic process. Future studies will aim to engage these Mn(I) complexes in different catalytic processes, but also to implant this new class of NHC core pincer-type ligands on other abundant metal centers.

3. References

[1] J. R. Khusnutdinova, D. Milstein, *Angew. Chem. Int. Ed.* **2015**, *54*, 12236–12273.

[2] B. L. Conley, M. K. Pennington-Boggio, E. Boz, T. J. Williams, *Chem. Rev.* **2010**, *110*, 2294–2312.

[3] A. Quintard, J. Rodriguez, *Angew. Chem. Int. Ed.* **2014**, *53*, 4044–4055.

[4] D. W. Stephan, G. Erker, *Angew. Chem. Int. Ed.* **2015**, *54*, 6400–6441.

[5] E. von Grotthuss, M. Diefenbach, M. Bolte, H.-W. Lerner, M. C. Holthausen, M. Wagner, *Angew. Chem. Int. Ed.* **2016**, *55*, 14067–14071.

[6] J. W. Taylor, A. McSkimming, C. F. Guzman, W. H. Harman, *J. Am. Chem. Soc.* **2017**, *139*, 11032–11035.

[7] L. Stahl, *J. Am. Chem. Soc.* **2007**, *129*, 10297–10298.

[8] D. Wang, D. Astruc, *Chem. Rev.* **2015**, *115*, 6621–6686.

[9] C. Gunanathan, D. Milstein, *Chem. Rev.* **2014**, *114*, 12024–12087.

[10] A. Corma, J. Navas, M. J. Sabater, *Chem. Rev.* **2018**, *118*, 1410–1459.

[11] T. Irrgang, R. Kempe, *Chem. Rev.* **2019**, *119*, 2524–2549.

[12] M. Trincado, H. Grützmacher, in *Coop. Catal.*, John Wiley & Sons, Ltd, **2015**, pp. 67–110.

[13] B. Zhao, Z. Han, K. Ding, *Angew. Chem. Int. Ed.* **2013**, *52*, 4744–4788.

[14] T. Ohkuma, H. Ooka, S. Hashiguchi, T. Ikariya, R. Noyori, *J. Am. Chem. Soc.* **1995**, *117*, 2675–2676.

[15] R. Noyori, T. Ohkuma, *Angew. Chem. Int. Ed.* **2001**, *40*, 40–73.

[16] C. A. Sandoval, T. Ohkuma, K. Muñiz, R. Noyori, *J. Am. Chem. Soc.* **2003**, *125*, 13490–13503.

[17] M. Zimmer-De Iuliis, R. H. Morris, *J. Am. Chem. Soc.* **2009**, *131*, 11263–11269.

[18] S. Musa, I. Shaposhnikov, S. Cohen, D. Gelman, *Angew. Chem. Int. Ed.* **2011**, *50*, 3533–3537.

[19] G. A. Silantyev, O. A. Filippov, S. Musa, D. Gelman, N. V. Belkova, K. Weisz, L. M. Epstein, E. S. Shubina, *Organometallics* **2014**, *33*, 5964–5973.

[20] S. Musa, S. Fronton, L. Vaccaro, D. Gelman, *Organometallics* **2013**, *32*, 3069–3073.

[21] B. Saha, S. M. Wahidur Rahaman, P. Daw, G. Sengupta, J. K. Bera, *Chem. – Eur. J.* **2014**, *20*, 6542–6551.

[22] A. Bartoszewicz, R. Marcos, S. Sahoo, A. K. Inge, X. Zou, B. Martín-Matute, *Chem. – Eur. J.* **2012**, *18*, 14510–14519.

[23] W.-Y. Chu, X. Zhou, T. B. Rauchfuss, *Organometallics* **2015**, *34*, 1619–1626.

[24] Y. Blum, D. Czarkie, Y. Rahamim, Y. Shvo, *Organometallics* **1985**, *4*, 1459–1461.

[25] R. Karvembu, R. Prabhakaran, K. Natarajan, *Coord. Chem. Rev.* **2005**, *249*, 911–918.

[26] A. Comas-Vives, G. Ujaque, A. Lledós, *Organometallics* **2007**, *26*, 4135–4144.

[27] C. P. Casey, J. B. Johnson, *J. Org. Chem.* **2003**, *68*, 1998–2001.

[28] C. P. Casey, S. W. Singer, D. R. Powell, R. K. Hayashi, M. Kavana, *J. Am. Chem. Soc.* **2001**, *123*, 1090–1100.

[29] A. M. Poitras, S. E. Knight, M. W. Bezpalko, B. M. Foxman, C. M. Thomas, *Angew. Chem.* **2018**, *130*, 1513–1516.

[30] M. Xu, A. R. Jupp, Z.-W. Qu, D. W. Stephan, *Angew. Chem. Int. Ed.* **2018**, *57*, 11050–11054.

[31] A. T. Normand, C. G. Daniliuc, B. Wibbeling, G. Kehr, P. Le Gendre, G. Erker, *J. Am. Chem. Soc.* **2015**, *137*, 10796–10808.

[32] E. J. Derrah, D. A. Pantazis, R. McDonald, L. Rosenberg, *Organometallics* **2007**, *26*, 1473–1482.

[33] M. D. Fryzuk, Kiran. Bhangu, *J. Am. Chem. Soc.* **1988**, *110*, 961–963.

[34] Noel. Lugan, Guy. Lavigne, J. Jacques. Bonnet, Regis. Reau, Denis. Neibecker, Igor. Tkatchenko, *J. Am. Chem. Soc.* **1988**, *110*, 5369–5376.

[35] C. Gunanathan, D. Milstein, *Acc. Chem. Res.* **2011**, *44*, 588–602.

[36] L. Alig, M. Fritz, S. Schneider, *Chem. Rev.* **2019**, *119*, 2681–2751.

[37] C. Gunanathan, Y. Ben-David, D. Milstein, *Science* **2007**, *317*, 790–792.

[38] Y. Canac, C. Maaliki, I. Abdellah, R. Chauvin, *New J. Chem.* **2012**, *36*, 17–27.

[39] J. I. Bates, P. Kennepohl, D. P. Gates, *Angew. Chem.* **2009**, *121*, 10028–10031.

[40] D. Mendoza-Espinosa, B. Donnadieu, G. Bertrand, *J. Am. Chem. Soc.* **2010**, *132*, 7264–7265.

[41] D. Mendoza-Espinosa, B. Donnadieu, G. Bertrand, *Chem. Asian J.* **2011**, *6*, 1099–1103.

[42] J. Ruiz, A. F. Mesa, *Chem. – Eur. J.* **2012**, *18*, 4485–4488.

[43] J. I. Bates, D. P. Gates, *Organometallics* **2012**, *31*, 4529–4536.

[44] P. K. Majhi, S. Sauerbrey, G. Schnakenburg, A. J. Arduengo, R. Streubel, *Inorg. Chem.* **2012**, *51*, 10408–10416.

[45] A. A. Tolmachev, A. A. Yurchenko, A. S. Merculov, M. G. Semenova, E. V. Zarudnitskii, V. V. Ivanov, A. M. Pinchuk, *Heteroat. Chem.* **1999**, *10*, 585–597.

[46] A. P. Marchenko, H. N. Koidan, A. N. Huryeva, E. V. Zarudnitskii, A. A. Yurchenko, A. N. Kostyuk, *J. Org. Chem.* **2010**, *75*, 7141–7145.

[47] A. P. Marchenko, H. N. Koidan, I. I. Pervak, A. N. Huryeva, E. V. Zarudnitskii, A. A. Tolmachev, A. N. Kostyuk, *Tetrahedron Lett.* **2012**, *53*, 494–496.

[48] A. P. Marchenko, H. N. Koidan, A. N. Hurieva, I. I. Pervak, S. V. Shishkina, O. V. Shishkin, A. N. Kostyuk, *Eur. J. Org. Chem.* **2012**, *2012*, 4018–4033.

[49] E. Kühnel, I. V. Shishkov, F. Rominger, T. Oeser, P. Hofmann, *Organometallics* **2012**, *31*, 8000–8011.

[50] S. Gaillard, J.-L. Renaud, *Dalton Trans.* **2013**, *42*, 7255–7270.

[51] C. Yang, H. M. Lee, S. P. Nolan, *Org. Lett.* **2001**, *3*, 1511–1514.

[52] L. D. Field, B. A. Messerle, K. Q. Vuong, P. Turner, *Organometallics* **2005**, *24*, 4241–4250.

[53] J. Wolf, A. Labande, M. Natella, J.-C. Daran, R. Poli, *J. Mol. Catal. Chem.* **2006**, *259*, 205–212.

[54] J. Wolf, A. Labande, J.-C. Daran, R. Poli, *J. Organomet. Chem.* **2006**, *691*, 433–443.

[55] F. E. Hahn, M. C. Jahnke, T. Pape, *Organometallics* **2006**, *25*, 5927–5936.

[56] M. Brill, E. Kühnel, C. Scriban, F. Rominger, P. Hofmann, *Dalton Trans.* **2013**, *42*, 12861–12864.

[57] N. Tsoureas, A. A. Danopoulos, A. A. D. Tulloch, M. E. Light, *Organometallics* **2003**, *22*, 4750–4758.

[58] W. A. Herrmann, C. Köcher, L. J. Gooßen, G. R. J. Artus, *Chem. – Eur. J.* **1996**, *2*, 1627–1636.

[59] M. J. Bitzer, A. Pöthig, C. Jandl, F. E. Kühn, W. Baratta, *Dalton Trans.* **2015**, *44*, 11686–11689.

[60] H. Salem, M. Schmitt, U. Herrlich (née Blumbach), E. Kühnel, M. Brill, P. Nägele, A. L. Bogado, F. Rominger, P. Hofmann, *Organometallics* **2013**, *32*, 29–46.

[61] D. A. Valyaev, O. A. Filippov, N. Lugan, G. Lavigne, N. A. Ustynyuk, *Angew. Chem.* **2015**, *127*, 6413–6417.

[62] J. Willot, Elaboration de Ligands Hétéropolydentes à Motifs NHC-Phosphine En Sphère de Coordination Du Manganèse et Évaluation de Leurs Propriétés de Coordination, phd, Université de Toulouse, Université Toulouse III - Paul Sabatier, **2017**.

[63] H. M. Lee, J. Y. Zeng, C.-H. Hu, M.-T. Lee, *Inorg. Chem.* **2004**, *43*, 6822–6829.

[64] H. Willms, W. Frank, C. Ganter, *Chem. – Eur. J.* **2008**, *14*, 2719–2729.

[65] S. Gischig, A. Togni, *Organometallics* **2004**, *23*, 2479–2487.

[66] H. Seo, H. Park, B. Y. Kim, J. H. Lee, S. U. Son, Y. K. Chung, *Organometallics* **2003**, *22*, 618–620.

[67] F. Visentin, A. Togni, *Organometallics* **2007**, *26*, 3746–3754.

[68] J. Shi, P. Yang, Q. Tong, L. Jia, *Dalton Trans.* **2008**, *0*, 938–945.

[69] S. Gischig, A. Togni, *Eur. J. Inorg. Chem.* **2005**, *2005*, 4745–4754.

[70] A.-E. Wang, J. Zhong, J.-H. Xie, K. Li, Q.-L. Zhou, *Adv. Synth. Catal.* **2004**, *346*, 595–598.

[71] A. Plikhta, A. Pöthig, E. Herdtweck, B. Rieger, *Inorg. Chem.* **2015**, *54*, 9517–9528.

[72] D. A. Valyaev, J. Willot, L. P. Mangin, D. Zargarian, N. Lugan, *Dalton Trans.* **2017**, *46*, 10193–10196.

[73] T. Steinke, B. K. Shaw, H. Jong, B. O. Patrick, M. D. Fryzuk, *Organometallics* **2009**, *28*, 2830–2836.

[74] A. Bruneau-Voisine, D. Wang, T. Roisnel, C. Darcel, J.-B. Sortais, *Catal. Commun.* **2017**, *92*, 1–4.

[75] A. Bruneau-Voisine, D. Wang, V. Dorcet, T. Roisnel, C. Darcel, J.-B. Sortais, *Org. Lett.* **2017**, *19*, 3656–3659.

[76] D. Wang, A. Bruneau-Voisine, J.-B. Sortais, *Catal. Commun.* **2018**, *105*, 31–36.

[77] D. Wei, A. Bruneau-Voisine, T. Chauvin, V. Dorcet, T. Roisnel, D. A. Valyaev, N. Lugan, J.-B. Sortais, *Adv. Synth. Catal.* **2018**, *360*, 676–681.

[78] D. Wei, A. Bruneau-Voisine, D. A. Valyaev, N. Lugan, J.-B. Sortais, *Chem. Commun.* **2018**, *54*, 4302–4305.

[79] N. V. Kireev, O. A. Filippov, E. S. Gulyaeva, E. S. Shubina, L. Vendier, Y. Canac, J.-B. Sortais, N. Lugan, D. A. Valyaev, *Chem. Commun.* **2020**, *56*, 2139–2142.

[80] G. D. Vaughn, K. Alex. Krein, J. A. Gladysz, *Organometallics* **1986**, *5*, 936–942.

[81] E. Lindner, E. Ossig, M. Darmuth, *J. Organomet. Chem.* **1989**, *379*, 107–118.

[82] M. Devillard, C. A. Lamsfus, V. Vreeken, L. Maron, J. I. van der Vlugt, *Dalton Trans.* **2016**, *45*, 10989–10998.

[83] T. Simler, G. Frison, P. Braunstein, A. A. Danopoulos, *Dalton Trans.* **2016**, *45*, 2800–2804.

[84] S. Chakraborty, U. Gellrich, Y. Diskin-Posner, G. Leitus, L. Avram, D. Milstein, *Angew. Chem.* **2017**, *129*, 4293–4297.

[85] M. Devillard, A. Ehlers, M. A. Siegler, J. I. van der Vlugt, *Chem. – Eur. J.* **2019**, *25*, 3875–3883.

[86] E. Lindner, K. A. Starz, H.-J. Eberle, W. Hiller, *Chem. Ber.* **1983**, *116*, 1209–1218.

[87] Y. Nakajima, F. Ozawa, *Organometallics* **2012**, *31*, 2009–2015.

[88] Y. Canac, C. Lepetit, M. Abdalilah, C. Duhayon, R. Chauvin, *J. Am. Chem. Soc.* **2008**, *130*, 8406–8413.

[89] I. Benaissa, R. Taakili, N. Lugan, Y. Canac, *Dalton Trans.* **2017**, *46*, 12293–12305.

[90] C. Barthes, C. Bijani, N. Lugan, Y. Canac, *Organometallics* **2018**, *37*, 673–678.

[91] R. Taakili, C. Lepetit, C. Duhayon, D. A. Valyaev, N. Lugan, Y. Canac, *Dalton Trans.* **2019**, *48*, 1709–1721.

[92] C. H. Leung, C. D. Incarvito, R. H. Crabtree, *Organometallics* **2006**, *25*, 6099–6107.

[93] G. Sipos, A. Ou, B. W. Skelton, L. Falivene, L. Cavallo, R. Dorta, *Chem. – Eur. J.* **2016**, *22*, 6939–6946.

[94] C. Liu, R. van Putten, P. O. Kulyaev, G. A. Filonenko, E. A. Pidko, *J. Catal.* **2018**, *363*, 136–143.

[95] R. van Putten, E. A. Uslamin, M. Garbe, C. Liu, A. Gonzalez-de-Castro, M. Lutz, K. Junge, E. J. M. Hensen, M. Beller, L. Lefort, E. A. Pidko, *Angew. Chem. Int. Ed.* **2017**, *56*, 7531–7534.

[96] E. B. Hulley, M. L. Helm, R. M. Bullock, *Chem. Sci.* **2014**, *5*, 4729–4741.

[97] S. Elangovan, C. Topf, S. Fischer, H. Jiao, A. Spannenberg, W. Baumann, R. Ludwig, K. Junge, M. Beller, *J. Am. Chem. Soc.* **2016**, *138*, 8809–8814.

[98] F. Kallmeier, T. Irrgang, T. Dietel, R. Kempe, *Angew. Chem. Int. Ed.* **2016**, *55*, 11806–11809.

[99] M. B. Widegren, G. J. Harkness, A. M. Z. Slawin, D. B. Cordes, M. L. Clarke, *Angew. Chem. Int. Ed.* **2017**, *56*, 5825–5828.

[100] S. Weber, B. Stöger, K. Kirchner, *Org. Lett.* **2018**, *20*, 7212–7215.

[101] S. Elangovan, C. Topf, S. Fischer, H. Jiao, A. Spannenberg, W. Baumann, R. Ludwig, K. Junge, M. Beller, *J. Am. Chem. Soc.* **2016**, *138*, 8809–8814.

[102] F. Kallmeier, T. Irrgang, T. Dietel, R. Kempe, *Angew. Chem. Int. Ed.* **2016**, *55*, 11806–11809.

[103] M. B. Widegren, G. J. Harkness, A. M. Z. Slawin, D. B. Cordes, M. L. Clarke, *Angew. Chem. Int. Ed.* **2017**, *56*, 5825–5828.

[104] P. A. Dub, J. C. Gordon, *ACS Catal.* **2017**, *7*, 6635–6655.

[105] A. E. Stross, G. Iadevaia, C. A. Hunter, *Chem. Sci.* **2015**, *7*, 94–101.

[106] D. A. Valyaev, O. A. Filippov, N. Lugan, G. Lavigne, N. A. Ustynyuk, *Angew. Chem. Int. Ed.* **2015**, *54*, 6315–6319.

[107] H. J. Clark, R. Wang, H. Alper, *J. Org. Chem.* **2002**, *67*, 6224–6225.

[108] E. Alberico, P. Sponholz, C. Cordes, M. Nielsen, H.-J. Drexler, W. Baumann, H. Junge, M. Beller, *Angew. Chem. Int. Ed.* **2013**, *52*, 14162–14166.

[109] R. Langer, M. A. Iron, L. Konstantinovski, Y. Diskin-Posner, G. Leitus, Y. Ben-David, D. Milstein, *Chem. – Eur. J.* **2012**, *18*, 7196–7209.

[110] Y. Li, L.-Q. Lu, S. Das, S. Pisiewicz, K. Junge, M. Beller, *J. Am. Chem. Soc.* **2012**, *134*, 18325–18329.

[111] A. Raba, M. R. Anneser, D. Jantke, M. Cokoja, W. A. Herrmann, F. E. Kühn, *Tetrahedron Lett.* **2013**, *54*, 3384–3387.

[112] P. L. Chiu, C.-L. Lai, C.-F. Chang, C.-H. Hu, H. M. Lee, *Organometallics* **2005**, *24*, 6169–6178.

[113] A. Passera, A. Mezzetti, *Adv. Synth. Catal.* **2019**, *361*, 4691–4706.

[114] R. Buhaibeh, O. A. Filippov, A. Bruneau-Voisine, J. Willot, C. Duhayon, D. A. Valyaev, N. Lugan, Y. Canac, J.-B. Sortais, *Angew. Chem. Int. Ed.* **2019**, *58*, 6727–6731.

4. Experimental part

4.1 General information

All manipulations were carried out using Schlenk techniques under an atmosphere of dry nitrogen or in an argon-filled glovebox (MBraun Unilabplus Eco. Dry and oxygen-free organic solvents (THF, Et_2O, CH_2Cl_2, toluene, pentane) were obtained using LabSolv (Innovative Technology) solvent purification system. Organic solvents used for column chromatography and water were degassed by nitrogen bubbling during 15 min. Deuterated benzene, toluene, THF and CD_2Cl_2 for NMR experiments and *t*-AmOH for catalytic experiments were deoxygenated by three freeze-pump-thaw cycles and kept over 4Å molecular sieves. Liquid ketones and $CDCl_3$ were passed through a short column of basic alumina, deoxygenated by three freeze-pump-thaw cycles and kept over 4Å molecular sieves. Column chromatography purification for organic substrates was performed on Acros Organics Ultrapure silica gel (mesh size 40-60 μm, 60 Å). N-mesitylimidazole,[1] *N*- isopropylimidazole,[2] $Ph_2P(O)CH_2OTs$,[3] $Ph_2P(O)CHPhOH$,[4] 2-(1H-imidazol-1-yl)pyridine,[5] and 2-(1*H*-Imidazol-1-yl-methyl)pyridine,[6] were prepared according to known methods. Phosphine-imidazolium precursors **L1-L5** were obtained by the modification of literature procedure previously used for synthesis $[Ph_2PCH_2ImMes]Br$.[7] All other reagent grade chemicals purchased from commercial sources were used as received.

Solution IR spectra were recorded in 0.1 mm CaF_2 cells using a Perkin Elmer Frontier FT-IR spectrometer and given in cm^{-1} with relative intensity in parentheses. ^1H, ^{13}C, ^{19}F and ^{31}P NMR spectra were obtained on Bruker Avance 300, Bruker Avance 400, Avance III HD 400, and Bruker Avance NEO 600 spectrometers and referenced against the residual signals of deuterated solvents (^1H and ^{13}C), $BF_3{\times}OEt_2$ (^{19}F, external standard) and 85% H_3PO_4 (^{31}P, external standard), respectively. When necessary, signal attribution in 13C spectra was based on decoupled $^{13}C\{^{31}P, ^1H\}$ and $^{13}C–^1H$ HMQC experiments. GC analyses were performed with GC-2014 (Shimadzu) 2010 equipped with a capillary column (Supelco, SPBTM-20, fused silica capillary column, 30 m × 0.25 mm × 0.25 mm film thickness). High-resolution mass spectra (ESI positive mode) were obtained using a Xevo G2 QTof (Waters) spectrometer. Elemental analyses were carried out at the LCC-CNRS (Toulouse) using a Perkin Elmer 2400 series II analyzer. Non-stirred 'Autoclave Maxitech' autoclaves (50 mL) were used for the hydrogenation.

4.2 Synthesis of the Bidentate Ligands

4.2.1 Synthesis of the phosphine oxide ligands [L1(O)], [L2(O)], [L3(O)], [L4(O)], and [L5(O)]

General procedure (I)

A mixture of solid **N-X-imidazole** (1.2-1.5 equiv.) and **$R_2P(O)CHYOTs$** (1.0 equiv.) was heated under stirring at 130-150 °C overnight. After cooling to r.t., the resulting light-brown solid was dissolved in dichloromethane and then diethyl ether was added to precipitate the product. The resulting precipitate was triturated with diethyl ether until the formation of a white powder (*ca.* 30 min.), the supernatant was removed after decantation and the product was dried in vacuum to afford the desired product.

Synthesis of [$Ph_2P(O)CH_2ImMes$]OTs [L1(O)]

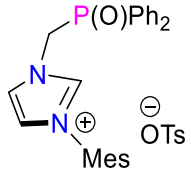

L1(O)

According to the general procedure (**I**), N-mesitylimidazole (0.72 g, 3.86 mmol) and $Ph_2P(O)CH_2OTs$ (1.00 g, 2.59 mmol), afforded the title compound **L1(O)** (1.28 g, 86%) as a white powder. **^{1}H NMR** (400.1 MHz, $CDCl_3$, 25 °C): δ 9.78 (s, 1H, C$H_{Im\text{-}2}$), 8.11 (dd, J_{PH} = 11.5 Hz, J_{HH} = 7.8 Hz 4H, C$H_{ortho\ Ph}$), 8.05 (s, 1H, C$H_{Im\text{-}4,5}$), 7.76 (d, J_{HH} = 7.5 Hz, 2H, CH_{Ts}), 7.57–7.44 (m, 6H, CH_{Ph}), 7.09 (d, J_{HH} = 7.5 Hz, 2H, CH_{Ts}), 6.97 (s, 1H, C$H_{Im\text{-}4,5}$), 6.90 (s, 2H, CH_{Mes}), 5.83 (d, J_{PH} = 6.0 Hz, 2H, $Ph_2P(O)CH_2$), 2.32 (s, 3H, C$H_{3para\ Mes}$), 2.30 (s, 3H, CH_{3Ts}), 1.68 ppm (s, 6H, C$H_{3ortho\ Mes}$); **^{31}P{^{1}H} NMR** (162.0 MHz, $CDCl_3$, 25 °C) δ 27.4 (s); **^{13}C{^{1}H} NMR** (100.6 MHz, $CDCl_3$, 25 °C) δ 143.6 (s, C_{Ts}), 141.5 (s, C_{Mes}), 139.3 (s, C_{Ts}), 139.1 (d, J_{PC} = 2.2 Hz, CH$_{Im\text{-}2}$), 134.2 (s, C_{Mes}), 133.1, (d, J_{PC} = 2.5 Hz, CH$_{para\ Ph}$), 131.6, (d, J_{PC} = 10.0 Hz, CH$_{Ph}$), 130.5 (s, $C_{ipso\ Mes}$), 129.9 (s, CH$_{Mes}$), 129.4 (d, J_{PC} = 12.6 Hz, CH_{Ph}), 128.7 (s, CH$_{Ts}$), 128.1 (d, J_{PC} = 103.2 Hz, $C_{ipso\ Ph}$), 126.1 (s, CH$_{Ts}$), 124.3 (s, CH$_{Im\text{-}4,5}$), 122.8 (s, CH$_{Im\text{-}4,5}$), 49.5 (d, J_{PC} = 66.5 Hz, $Ph_2P(O)CH_2$), 21.4, 21.2 (s, CH$_{3para\ Mes}$ and CH$_{3Ts}$), 17.1 (s, CH$_{3ortho\ Mes}$); **Anal.** Found: C, 65.29; H, 5.95; N, 4.70. Calcd. (%) for $C_{32}H_{33}N_2O_4PS$. 0.9(H_2O): C, 65.27; H, 5.96; N, 4.76; **LRMS** (ESI, POS): m/z calcd. for $C_{25}H_{26}N_2OP^+$ $[M - OTs]^+$ 401.2; found, 401.3.

Synthesis of [$Ph_2P(O)CH_2ImMe$]OTs ([L2(O)]

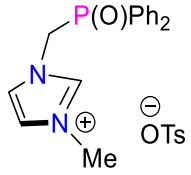

L2(O)

According to the general procedure (**I**), *N*-methylimidazole (0.10 mL, 0.10 mmol) and $Ph_2P(O)CH_2OTs$ (0.30 g, 0.78 mmol) in toluene (3 mL) afforded the title compound **L2(O)** (0.30 g, 83%) as a white powder. **^{1}H NMR** (400.1 MHz, $CDCl_3$, 25 °C): δ 10.01 (s, 1H, C$H_{Im\text{-}2}$), 7.98 (dd, J_{PH} = 11.6, J_{HH} =7.7 Hz, 4H, CH_{Ph}), 7.83 (d, J_{HH} = 8.0 Hz, 2H, CH_{Ts}), 7.76 (s, 1H, C$H_{Im\text{-}4,5}$), 7.59 – 7.43 (m, 6H, CH_{Ph}), 7.17 (d, J_{HH} = 7.9 Hz, 2H, CH_{Ts}), 7.08 (s, 1H, C$H_{Im\text{-}4,5}$), 5.53 (d, J_{PH} = 5.7 Hz, 2H, $Ph_2P(O)CH_2$), 3.81 (s, 3H, CH_{3Me}), 2.35 (s, 3H, CH_{3Ts}); **^{31}P{^{1}H} NMR** (162.0 MHz, $CDCl_3$, 25 °C): δ 27.01 (s); **^{13}C{^{1}H} NMR** (100.6 MHz, $CDCl_3$, 25 °C): δ 143.4 (s, C_{Ts}), 139.8 (s, C_{Ts}), 139.1 (d, J_{PC} = 2.2 Hz, CH$_{Im\text{-}2}$), 133.2 (d, J_{PC} =2.0 Hz, CH$_{Ph}$), 131.4 (d, J_{PC} =9.9 Hz, CH$_{Ph}$), 129.4 (d, J_{PC} =12.0 Hz, CH$_{Ph}$), 128.9 (s, CH$_{Ts}$), 128.1 (d, J_{PC} = 103.9 Hz, $C_{ipso\ Ph}$), 126.1 (s, CH$_{Ts}$), 123.8 (s, CH$_{Im\text{-}4,5}$), 122.6 (s, CH$_{Im\text{-}4,5}$), 48.7 (d, J_{PC} = 69.2 Hz, $Ph_2P(O)CH_2$), 36.61(s, CH$_{3Me}$), 21.48 (s, CH$_{3Ts}$); **Anal.** Found: C, 60.86; H, 5.16; N, 5.89. Calcd. (%) for $C_{24}H_{25}N_2O_4PS$: C, 61.53; H, 5.38; N, 5.98; **LRMS** (ESI, POS): m/z calcd. for $C_{17}H_{18}N_2OP^+$ $[M - OTs]^+$ 297.1; found, 297.2.

Synthesis of [$Ph_2P(O)CH_2ImiPr$]OTs ([L3(O)]

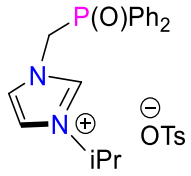

L3(O)

According to the general procedure (**I**), *N*-isopropylimidazole (1.70 g, 15.54 mmol) and $Ph_2P(O)CH_2OTs$ (3.00 g, 7.77 mmol) afforded the title compound **L3(O)** (3.40 g, 88%) as a white powder. **^{1}H NMR** (400 MHz, $CDCl_3$, 25 °C): δ 9.80 (s, 1H, C$H_{Im\text{-}2}$), 7.98 – 7.94 (m, 4H, CH_{Ph}), 7.80 (d, J_{HH} = 7.3 Hz, 2H, CH_{Ts}), 7.63 (s, 1H, C$H_{Im\text{-}4,5}$), 7.54 – 7.37 (m, 6H, CH_{Ph}), 7.21 (s, 1H, C$H_{Im\text{-}4,5}$), 7.12 (d, J_{HH} = 7.3 Hz, 2H, CH_{Ts}), 5.52 (d, J_{PH} = 4.8 Hz, 2H, $Ph_2P(O)CH_2$), 4.42 – 4.36 (sept, J_{HH} = 6 Hz 1H, CH_{iPr}), 2.31 (s, 3H, CH_{3Ts}), 1.31 (d, J_{HH} = 6.2 Hz, 6H, CH_{3iPr}); **^{31}P{^{1}H} NMR** (162 MHz, $CDCl_3$, 25 °C): δ 27.3 (s); **^{13}C{^{1}H} NMR** (101 MHz, $CDCl_3$, 25 °C): δ 143.7 (s, C_{Ts}), 139.4 (s, C_{Ts}), 136.9 (d, J_{PC} = 3.1 Hz, CH$_{Im\text{-}2}$), 133.0 (d, J_{PC} = 3.0 Hz, CH$_{Ph}$),

131.4 (d, J_{PC} = 9.9 Hz, CH_{Ph}), 129.2 (d, J_{PC} = 12.4 Hz, CH_{Ph}), 128.7 (s, CH_{Ts}),128.0 (d, J_{PC} = 103.0 Hz, $C_{ipso\ Ph}$), 126.0 (s, CH_{Ts}), 123.4 (s, $CH_{Im\text{-}4,5}$), 119.7 (s, $CH_{Im\text{-}4,5}$), 53.5 (s, CH_{iPr}), 49.1 (d, J_{PC} = 67.4 Hz, $Ph_2P(O)CH_2$), 22.8 (s, CH_{3iPr}), 21.4 (s, CH_{3Ts}); **Anal.** Found: C, 61.59; H, 5.88; N, 5.50. Calcd. (%) for $C_{26}H_{29}N_2O_4PS$. 0.5 (H_2O): C, 61.77; H, 5.98; N, 5.54; **HRMS** (ESI, POS): m/z: calcd. for $C_{19}H_{22}N_2OP^+$ [M – OTs]$^+$ 325.1479; found, 325.1470 (εr = 2.8 ppm); **LRMS** (ESI, POS): m/z calcd. for $C_{19}H_{22}N_2OP^+$ [M – OTs]$^+$ 325.1; found, 325.2.

Synthesis of *i*Pr$_2$P(O)CH$_2$OTs [L^{a}4(O)]

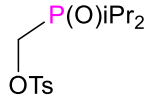

L^{a}4(O)

*i*Pr$_2$P(O)CH$_2$OTs was prepared following the method described for the synthesis of *t*Bu$_2$P(O)CH$_2$OTs.[8] To a solution of *i*Pr$_2$P(O)CH$_2$OH (0.53 g, 3.22 mmol) in THF (20 mL), 1 eq. of Et$_3$N (0.68 mL) was added at 0 °C, the reaction mixture was stirred at room temperature for 1 h. Tosyl chloride (0.74 g, 3.87 mmol) in THF (5 mL) was added slowly over 5 min.. The reaction mixture was stirred overnight at room temperature. The product was washed with distilled water (30 mL) and then extracted with ethyl acetate (3 × 15 mL). The resulting solution was dried with Na_2SO_4, filtered and evaporated under vacuum to afford *i*Pr$_2$P(O)CH$_2$OTs **L^{a}4(O)** as a white powder (0.59 g, 56%). **^{1}H NMR** (400 MHz, $CDCl_3$, 25 °C): δ 7.78 (d, J_{HH} = 8.0 Hz, 2H, CH_{Ts}), 7.37 (d, J_{HH} = 8.0 Hz, 2H, CH_{Ts}), 4.19 (d, J_{PH} = 7.3 Hz, 2H, $iPr_2P(O)CH_2$), 2.46 (s, 3H, CH_{3Ts}), 2.15 (d sept, J_{PH} = 9.7 Hz, J_{HH} = 7.2 Hz, 2H, CH_{iPr}), 1.22 (dd, J_{PH} = 15.3 Hz, J_{HH} = 7.2 Hz, 6H, CH_{3iPr}), 1.14 (dd, J_{PH} = 15.8 Hz, J_{HH} = 7.2 Hz, 6H, CH_{3iPr}); **^{31}P{^{1}H} NMR** (162 MHz, $CDCl_3$, 25 °C): δ 53.9 (s); **^{13}C{^{1}H} NMR** (101 MHz, $CDCl_3$, 25 °C): δ 146.0 (s, C_{Ts}), 131.2 (s, C_{Ts}), 130.3 (s, CH_{Ts}), 128.4 (s, CH_{Ts}), 60.4 (d, J_{PC} = 66.9 Hz, $iPr_2P(O)CH_2$), 24.5 (d, J_{PC} = 64.7 Hz, CH_{iPr}), 21.9 (s, CH_{3Ts}), 15.5 (s, CH_{3iPr}), 14.9 (s, CH_{3iPr}); **Anal.** Found: C, 51.77; H, 7.58. Calcd. (%) for $C_{14}H_{23}O_4PS$. 0.4 (H_2O): C, 51.65; H, 7.37; **LRMS** (ESI, POS): m/z calcd. for $C_{14}H_{24}O_4PS^+$ [M + H]$^+$ 319.2; found, 319.1.

Synthesis of [*i*Pr$_2$P(O)CH$_2$ImMes]OTs [L4(O)]

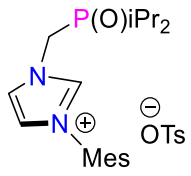

L4(O)

According to the general procedure (**I**), *N*-mesitylimidazole (0.15 g, 0.79 mmol) and iPr$_2$P(O)CH$_2$OTs (0.17 g, 0.53 mmol) in toluene (5 mL) afforded the title compound **L4(O)** (0.26 g, 99%) as a white powder. **^{1}H NMR** (400 MHz, $CDCl_3$, 25 °C): δ 9.75 (s, 1H, C$H_{Im\text{-}2}$), 8.34 (s, 1H, C$H_{Im\text{-}4,5}$), 7.70 (d, J_{HH} = 7.4 Hz, 2H, CH_{Ts}), 7.13 (s, 1H, C$H_{Im\text{-}4,5}$), 7.06 (d, J_{HH} = 7.4 Hz, 2H, CH_{Ts}), 6.97 (s, 2H, CH_{Mes}), 5.27 (br, 2H, iPr$_2$P(O)CH_2), 2.32 (s, 3H, CH_3), 2.29 (s, 3H, CH_3), 2.30-2.19 (m, 2H, CH_{iPr}), 2.00 (s, 6H, CH_{3Mes}), 1.18 (m, 12H, CH_{3iPr}); **^{31}P{^{1}H} NMR** (162 MHz, $CDCl_3$, 25 °C): δ 53.4 (s); **^{13}C{^{1}H} NMR** (101 MHz, $CDCl_3$, 25 °C): δ 143.7 (s, C_{Ts}), 141.4 (s, C_{Ts}), 139.2 (s, C_{Mes}), 138.6 (s, CH$_{Im\text{-}2}$), 134.2 (s, C_{Mes}), 130.7 (s, C_{Mes}), 130.0 (s, CH$_{Ar}$), 128.6 (s, CH$_{Ar}$), 126.0 (s, CH$_{Ar}$), 125.3 (s, CH$_{Im\text{-}4,5}$), 122.6 (s, CH$_{Im\text{-}4,5}$), 43.7 (d, J_{PC} = 51.4 Hz, iPr$_2$P(O)CH$_2$), 25.8 (d, J_{PC} = 64.4 Hz, CH$_{iPr}$), 21.3 (s, CH$_3$), 21.2 (s, CH$_3$), 17.5 (s, CH$_{3Mes}$), 15.6 (s, CH$_{3iPr}$), 15.3 (s, CH$_{3iPr}$); **Anal.** Found: C, 61.72; H, 7.55; N, 5.42. Calcd. (%) for $C_{26}H_{37}N_2O_4PS$: C, 61.88; H, 7.39; N, 5.55; **LRMS** (ESI, POS): m/z calcd. for $C_{19}H_{30}N_2OP^+$ [M – OTs]$^+$ 333.2; found, 333.2.

Synthesis of [Ph$_2$P(O)CH(Ph)OTs [L^{a}5(O)]

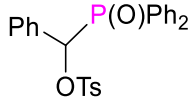

L^{a}5(O)

To a stirred solution of Ph$_2$P(O)CH(Ph)OH (1.00 g, 3.20 mmol) in THF (30 mL) was added *n*-BuLi (2.5 M solution in hexane, 1.4 mL, 3.52 mmol) dropwise at -40 °C over 10 min., then a solution of TsCl (0.64 g, 3.36 mmol) in THF was dropped to the orange solution, the color turned immediately to yellow. This mixture was stirred at r.t. for 18 hours. Then, all volatiles were removed under vacuum, and the solid residue was dissolved in dichloromethane (5 mL), and then diethyl ether (50 mL) was added to precipitate the product. The resulting precipitate was triturated with diethyl ether until the formation of a white powder (*ca.* 30 min), the supernatant was removed by decantation and the product was dried *in vacuo* to afford Ph$_2$P(O)CH(Ph)OTs **L^{a}5(O)** (0.90 g, 61%) as white powder. **^{1}H NMR** (400 MHz, $CDCl_3$, 25 °C) δ 7.87 – 7.83 (m, 2H, CH_{Ph}), 7.76 – 7.67 (m, 2H, CH_{Ph}), 7.60 – 7.56 (m, 1H, CH_{Ph}), 7.54 – 7.44 (m, 3H, CH_{Ph}), 7.42-7.40 (m, 2H, CH_{Ph}), 7.34 (d, J_{HH} = 8.3 Hz, 2H, CH_{Ts}), 7.16 – 7.09 (m, 1H, CH_{Ar}), 7.06 – 6.92 (m, 6H, CH_{Ar}), 6.19 (d, J_{PH} = 7.8 Hz, 1H, CH), 2.29 (s, 3H, CH_3); **^{31}P{^{1}H} NMR** (162 MHz, $CDCl_3$, 25 °C): δ 27.1 (s); **^{13}C{^{1}H} NMR** (101 MHz, $CDCl_3$, 25 °C) δ 144.8 (s, C_{Ts}), 133.5 (s, C_{Ts}), 132.7 (d, J_{PC} = 2.5 Hz, CH$_{Ph}$), 132.6 (s, CH$_{Ph}$), 132.5 (m, CH$_{Ph}$), 131.8 (d, J_{PC} = 8.9 Hz, CH$_{Ph}$), 130.9 (d, J_{PC} = 1.5 Hz, C_{Ph}), 129.9 (d, J_{PC} = 101.0 Hz, C_{Ph}),

129.5 (s, CH_{Ts}), 128.8 (d, J_{PC} = 2.2 Hz, CH_{Ph}), 128.7 (d, J_{PC} = 10.6 Hz, CH_{Ph}), 128.6 (d, J_{PC} = 10.6 Hz, CH_{Ph}), 128.4 (d, J_{PC} = 4.2 Hz, CH_{Ph}), 128.0 (s, CH_{Ph}), 127.7 (d, J_{PC} = 100.6 Hz, C_{Ph}), 127.9 (s, CH_{Ts}), 80.3 (d, J_{PC} = 82.7 Hz, *C*H), 21.6 (s, CH_3); **Anal.** Found: C, 65.58; H, 4.85. Calcd. (%) for $C_{26}H_{23}O_4PS$, 0.2 (CH_2Cl_2): C, 65.63; H, 4.92; **HRMS** (ESI, POS): m/z: calcd. for $C_{26}H_{24}O_4PS^+$ $[M + H]^+$ 463.1133; found, 463.1138 (εr = 1.1 ppm).

Synthesis of [$Ph_2P(O)CH(Ph)ImMes$]OTs [L5(O)]

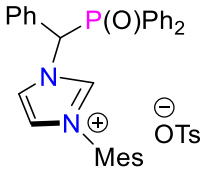

L5(O)

According to the general procedure (**I**), *N*-mesitylimidazole (1.30 g, 6.98 mmol) and $Ph_2P(O)CH(Ph)OTs$ (2.30 g, 4.97 mmol) in toluene (4 mL) heating this mixture at 180 °C for 24 h afforded the title compound **L5(O)** (2.40 g, 75%) as a white powder. **^{1}H NMR** (400 MHz, $CDCl_3$, 25 °C) δ 9.99 (s, 1H, $CH_{Im\text{-}2}$), 8.41 (s, 1H, CH_{Ar}), 8.29 – 8.20 (m, 2H, CH_{Ar}), 8.02 – 7.90 (m, 5H, $CH_{Ar + CHPh}$), 7.79 (d, J_{HH} = 8.1 Hz, 2H, CH_{Ts}), 7.42 – 7.29 (m, 6H, CH_{Ar}), 7.22 – 7.16 (m, 3H, CH_{Ar}), 7.07 (d, J_{HH} = 7.9 Hz, 2H, CH_{Ts}), 7.02 (s, 1H, CH_{Ar}), 6.84 – 6.83 (m, 2H, CH_{Ar}), 2.29 (s, 3H, CH_{3Ts}), 2.23 (s, 3H, CH_{3Mes}), 1.75 (s, 3H, CH_{3Mes}), 1.40 (s, 3H, CH_{3Mes}); **^{31}P{^{1}H} NMR** (162 MHz, $CDCl_3$, 25 °C): δ 30.2(s); **^{13}C{^{1}H} NMR** (101 MHz, $CDCl_3$, 25 °C) δ 143.7 (s, C_{Ts}), 141.0 (s, C_{Ts}), 140.7 (s, C_{Ar}), 139.1 (s, C_{Ar}), 138.0 (d, J_{PC} = 4.4 Hz, $CH_{Im\text{-}2}$), 134.3 (s, C_{Ar}),133.8 (s, C_{Ar}), 133.7 (s, C_{Ar}), 132.5-132.4 (m, 2C, CH_{Ph}), 131.57 (s, C_{Ar}), 131.55 (d, J_{PC} = 9.5 Hz, CH_{Ph}), 131.2 (d, J_{PC} = 9.5 Hz, CH_{Ph}), 130.2 (s, C_{Ar}), 130,0 (d, J_{PC} = 5.1 Hz, CH_{Ph}), 129.6-129.4 (m, 3C, CH_{Ar}), 129.46 (s, CH_{Ar}), 129.1 (d, J = 12.2 Hz, CH_{Ph}), 129.0 (s, CH_{Ar}), 128.7 (d, J_{PC} = 12.6 Hz, CH_{Ph}), 128.4 (s, CH_{Ar}), 125.9 (s, $CH_{Im\text{-}4,5}$), 123.1 (s, $CH_{Im\text{-}4,5}$), 60.5 (d, J_{PC} = 67.0 Hz, *C*HPh), 21.2 (s, CH_3), 20.9 (s, CH_3), 17.1 (s, CH_{3Mes}), 16.6 (s, CH_{3Mes}); **Anal.** Found: C, 67.75; H, 5.82; N, 4.14. Calcd. (%) for $C_{38}H_{37}N_2O_4PS$, 0.4 (CH_2Cl_2): C, 67.56; H, 5.58; N, 4.10; **HRMS** (ESI, POS): m/z: calcd. for $C_{31}H_{30}N_2OP^+$ $[M – OTs]^+$ 477.2096; found, 477.2107 (εr = 2.3 ppm); **LRMS** (ESI, POS): m/z: calcd for $C_{31}H_{30}N_2OP^+$ $[M – OTs]^+$ 477.2, found: 477.2.

4.2.2 Synthesis of the phosphine ligands [L1], [L2], [L3], [L4)], and [L5]

General procedure (II)

Method A:[9] A solution of the corresponding phosphine oxide [**L1(O)-L5(O)**] in chlorobenzene was heated to 80 °C and $HSiCl_3$ (20 equiv.) was added dropwise. The reaction mixture was stirred overnight, cooled to r.t. and the volatiles were removed under vacuum. The resulting light brown solid was dissolved in dichloromethane and deoxygenated 0.1M aqueous solution of sodium hydroxide was added. The resulting biphasic mixture was vigorously shaken, and the organic phase was then separated and washed with degassed water (3 × 20 mL). The resulting solution was dried with Na_2SO_4, filtered through Celite and evaporated under vacuum. The residue was washed with diethyl ether (3 × 20 mL) and dried under vacuum to afford the desired product.

Method B:[10]A dried Schlenk tube containing a stirring bar was charged with Bis(4-nitrophenyl) phosphate (10 mol %) and the corresponding phosphine oxide [**L1(O)-L5(O)**], under Ar flow, dry toluene and $PhSiH_3$ (4 equiv.) were added, and the mixture was stirred at 110 °C overnight, cooled to r.t. and the volatiles were removed under vacuum. The resulting solid was dissolved in degassed dichloromethane and then degassed diethyl ether was added to precipitate the product. The resulting precipitate was washed with degassed ether and dried under vacuum to afford the corresponding phosphine.

Synthesis of [Ph_2PCH_2ImMes]OTs [L1]

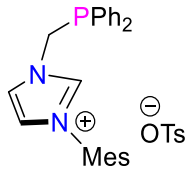

L1

According to the general procedure (**II**), (**Method A**): **L1(O)** (2.00 g, 3.49 mmol) afforded the title compound **L1** (1.81 g, 93%) as a white powder. According to the general procedure (**II**), (**Method B**): **L1(O)** (1.50 g, 2.62 mmol) afforded the title compound **L1** (1.40 g, 96%) as a white powder. **^{1}H NMR** (400.1 MHz, $CDCl_3$, 25 °C): δ 9.54 (m, 1H, C$H_{Im\text{-}2}$), 7.67 (d, J_{HH} = 8.0 Hz, 2H, CH_{Ts}), 7.61–7.54 (m, 4H, CH_{Ph}), 7.49 (br. s, 1H, C$H_{Im\text{-}4,5}$), 7.38–7.30 (m, 6H, CH_{Ph}), 7.01 (d, J_{HH} = 8.0 Hz, 2H, CH_{Ts}), 6.98 (br. s, 1H, C$H_{Im\text{-}4,5}$), 6.88 (m, 2H, CH_{Mes}), 5.39 (d, J_{PH} = 5.4 Hz, 2H, Ph_2PCH_2), 2.29 (s, 6H, C$H_{3\,para\ Mes}$ and CH_{3Ts}), 1.76 ppm (s, 6H, C$H_{3\,ortho\ Mes}$); **^{31}P{^{1}H} NMR** (162.0 MHz, $CDCl_3$, 25 °C): δ –11.7 ppm (s); **^{13}C{^{1}H} NMR** (100.6 MHz, $CDCl_3$, 25 °C): δ 144.2 (s, C_{Ts}), 141.1 (s, C_{Mes}), 138.8 (br. s, $CH_{Im\text{-}2}$), 138.8 (s, C_{Ts}), 134.4 (s,

C_{Mes}), 133.6 (d, J_{PC} = 20.2 Hz, CH_{Ph}), 133.0 (d, J_{PC} = 12.0 Hz, $C_{ipso\ Ph}$), 130.7 (s, $C_{ipso\ Mes}$), 130.3 (s, $CH_{para\ Ph}$), 129.7 (s, CH_{Mes}), 129.3 (d, J_{CP} = 7.5 Hz, CH_{Ph}), 128.5, 126.1 (s, CH_{Ar}), 123.1 (s, $CH_{Im\text{-}4,5}$), 122.9 (d, J_{CP} = 7.5 Hz, $CH_{Im\text{-}4,5}$), 49.1 (d, J_{PC} = 19.1 Hz, Ph_2PCH_2), 21.4, 21.2 (s, $CH_{3para\ Mes}$ and CH_{3Ts}), 17.3 ppm (s, $CH_{3ortho\ Mes}$); **Anal.** Found: C, 68.89; H, 5.93; N, 5.03. Calcd. (%) for $C_{32}H_{33}N_2O_3PS$: C, 69.05; H, 5.98; N, 5.03; **LRMS** (ESI, POS): m/z calcd. for $C_{25}H_{26}N_2P^+$ $[M - OTs]^+$ 385.2; found, 385.1.

Synthesis of [Ph_2PCH_2ImMe]OTs [L2]

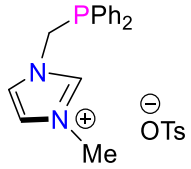

L2

According to the general procedure (**II**), (**Method A**): **L2(O)** (0.70 g, 1.50 mmol) afforded the title compound **L2** (0.6 g, 90%) as a white powder. **^{1}H NMR** (400 MHz, $CDCl_3$, 25 °C): δ 9.89 (s, 1H, $CH_{Im\text{-}2}$), 7.78 (d, J_{HH} = 8.1 Hz, 2H, CH_{Ts}), 7.51 – 7.49 (m, 4H, CH_{Ph}), 7.41 – 7.40 (m, 6H, CH_{Ph}), 7.16 (d, J_{HH} = 8.1 Hz, 2H, CH_{Ts}), 7.11 (s, 1H, $CH_{Im\text{-}4,5}$), 7.03 (s, 1H, $CH_{Im\text{-}4,5}$), 5.11 (d, J_{PH} = 4.0 Hz, 2H, Ph_2PCH_2), 3.91 (s, 3H, CH_{3Me}), 2.35 (s, 3H, CH_{3Ts}); **^{31}P{^{1}H} NMR** (162.0 MHz, $CDCl_3$, 25 °C): δ -12.2 (s); **^{13}C{^{1}H} NMR** (100.6 MHz, $CDCl_3$, 25 °C): δ 144.0 (s, C_{Ts}), 139.2 (s, C_{Ts}), 137.7 (s, $CH_{Im\text{-}2}$), 133.1 (d, J_{PC} = 12 Hz, $C_{ipso\ Ph}$),133.07 (d, J_{PC} = 19.7 Hz, CH_{Ph}), 130.1 (s, CH_{Ar}), 129.1 (d, J_{PC} = 7.2 Hz, CH_{Ph}), 128.6 (s, CH_{Ar}), 125.8 (s, CH_{Ar}), 123.7 (s, $CH_{Im\text{-}4,5}$), 122.0 (d, J_{PC} = 3.4 Hz, $CH_{Im\text{-}4,5}$), 48.7 (d, J_{PC} = 20.5 Hz, Ph_2PCH_2), 36.1 (s, CH_{3Me}), 21.3 (s, CH_{3Ts}); **Anal.** Found: C, 63.24; H, 5.49; N, 6.10. Calcd. (%) for $C_{24}H_{25}N_2O_3PS$: C, 63.70; H, 5.57; N, 6.19; **LRMS** (ESI, POS): m/z calcd. for $C_{17}H_{18}N_2P^+$ $[M - OTs]^+$ 281.1; found, 281.0.

Synthesis of [Ph_2PCH_2ImiPr]OTs [L3]

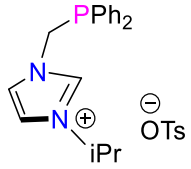

L3

According to the general procedure (**II**), (**Method A**): **L3(O)** (1.65 g, 3.32 mmol) afforded the title compound **L3** (1.33 g, 83%) as a white powder. According to the general procedure (**II**), (**Method B**): **L3(O)** (2.25 g, 4.50 mmol) afforded the title compound **L3** (1.97 g, 92%) as a

white powder. **^{1}H NMR** (400 MHz, $CDCl_3$, 25 °C): δ 9.42 (s, 1H, C$H_{Im\text{-}2}$), 7.71 (d, J_{HH} = 7.6 Hz, 2H, CH_{Ts}), 7.42 (s, 1H, C$H_{Im\text{-}4,5}$), 7.38 (m, 4H, CH_{Ph}), 7.29 (m, 6H, CH_{Ph}), 7.04-7.02 (m, 3H, C$H_{Im\text{-}4,5}$ + CH_{Ts}), 4.96 (d, J_{PH} = 5.5 Hz, 2H, $Ph_2P(O)CH_2$), 4.40 (sept, J_{HH} = 6.5 Hz, 1H, CH_{iPr}), 2.25 (s, 3H, CH_{3Ts}), 1.26 (d, J_{HH} = 6.5 Hz, 6H, CH_{3iPr}); **^{31}P{^{1}H} NMR** (162 MHz, $CDCl_3$, 25 °C): δ -12.1 (s); **^{13}C{^{1}H} NMR** (101 MHz, $CDCl_3$, 25 °C): δ 144.1 (s, C_{Ts}), 139.0 (s, C_{Ts}), 135.9 (s, CH$_{Im\text{-}2}$), 133.1 (d, J_{CP} = 13 Hz, $C_{ipso\ Ph}$), 133.1 (d, J_{PC} = 19.7 Hz, CH$_{Ph}$), 129.9 (s, CH$_{Ar}$), 129.0 (d, J_{PC} = 7.1 Hz, CH$_{Ph}$), 128.5 (s, CH$_{Ar}$), 125.9 (s, CH$_{Ar}$), 121.9 (d, J_{PC} = 3.9 Hz, CH$_{Im\text{-}4,5}$), 120.6 (s, CH$_{Im\text{-}4,5}$), 53.0 (s, CH_{iPr}), 48.4 (d, J_{PC} = 21.2 Hz, Ph_2PCH_2), 22.7 (s, CH$_{3iPr}$), 21.2 (s, CH$_{3Ts}$); **Anal.** Found: C, 64.87; H, 6.31; N, 5.83. Calcd. (%) for $C_{26}H_{29}N_2O_3PS$: C, 64.98; H, 6.08; N, 5.83; **LRMS** (ESI, POS): m/z calcd. for $C_{19}H_{22}N_2P^+$ [M – OTs]$^+$ 309.1; found, 309.0.

Synthesis of [*i*Pr$_2$PCH$_2$ImMes]OTs([L4]

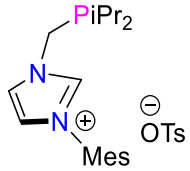

L4

According to the general procedure (**II**), (**Method A**): **L4(O)** (0.16 g, 0.32 mmol) afforded the title compound **L4** (0.097 g, 62%) as a white powder. According to the general procedure (**II**), (**Method B**): **L4(O)** (0.26 g, 0.51 mmol) afforded the title compound **L4** (0.20 g, 82%) as a white powder. **^{1}H NMR** (400 MHz, $CDCl_3$, 25 °C): δ 10.17 (s, 1H, C$H_{Im\text{-}2}$), 7.97 (s, 1H, C$H_{Im\text{-}4,5}$), 7.69 (d, J_{HH} = 8.0 Hz, 2H, CH_{Ts}), 7.13 (s, 1H, C$H_{Im\text{-}4,5}$), 7.07 (d, J_{HH} = 8.0 Hz, 2H, CH_{Ts}), 6.98 (s, 2H, CH_{Mes}), 5.08 (s, 2H, *i*Pr_2PCH_2), 2.33 (s, 3H, CH_3), 2.31 (s, 3H, CH_3), 2.18-2.08 (m, 2H, CH_{iPr}), 2.02 (s, 6H, CH_{3Mes}), 1.20 – 1.11 (m, 12H, CH_{3iPr}); **^{31}P{^{1}H} NMR** (162 MHz, $CDCl_3$, 25 °C): δ 11.5 (s); **^{13}C{^{1}H} NMR** (101 MHz, $CDCl_3$, 25 °C): δ 143.2 (s, C_{Ts}), 141.4 (s, C_{Ts}), 139.5 (s, C_{Mes}), 139.3 (s, CH$_{Im\text{-}2}$), 134.4 (s, C_{Mes}), 130.9 (s, C_{Mes}), 130.0 (s, CH$_{Ar}$), 128.6 (s, CH$_{Ar}$), 126.1 (s, CH$_{Ar}$), 123.5 (d, J_{PC} = 6.9 Hz, CH$_{Im\text{-}4,5}$), 123.1 (s, CH$_{Im\text{-}4,5}$), 45.2 (d, J_{PC} = 14.5 Hz, *i*Pr_2PCH_2), 22.9 (d, J_{PC} = 4.4 Hz, CH$_{iPr}$), 21.4 (s, CH$_3$), 21.2 (s, CH$_3$), 19.6 (d, J_{PC} = 13.0 Hz, CH$_{3iPr}$), 18.8 (d, J_{PC} = 6.1 Hz, CH$_{3iPr}$), 17.6 (s, CH$_{3Mes}$); **Anal.** Found: C, 63.23; H, 7.71; N, 5.65. Calcd. (%) for $C_{26}H_{37}N_2O_3PS$: C, 63.91; H, 7.63; N, 5.73; **LRMS** (ESI, POS): m/z calcd. for $C_{19}H_{30}N_2P^+$ [M – OTs]$^+$ 317.2; found, 317.2.

Synthesis of [Ph_2PCHPhImMes]OTs [L5]

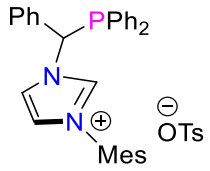

L5

According to the general procedure (**II**), (**Method B**): **L5(O)** (0.72 g, 1.12 mmol) in chlorobenzene as solvent afforded the title compound **L5** (0.48 g, 67%) as a white powder. **^{1}H NMR** (400 MHz, $CDCl_3$, 25 °C) δ 10.09 (s, 1H, C$H_{Im\text{-}2}$), 7.91-7.85 (m, 4H, CH_{Ar}), 7.71 (d, J_{HH} = 7.8 Hz, 2H, CH_{Ts}), 7.67 (s, 1H, CH_{CHPh}), 7.56 (t, J_{PH} = 7.7 Hz, J_{HH} = 7.1 Hz, 2H, CH_{Ar}), 7.45-7.42 (m; 1H, CH_{Ar}) 7.27 – 7.26 (m, 6H, CH_{Ar}), 7.19 – 7.17 (m, 3H, CH_{Ar}), 7.04 (d, J_{HH} = 7.8 Hz, 2H, CH_{Ts}), 6.97 (s, 1H, CH_{Ar}), 6.85 – 6.83 (m, 2H, CH_{Ar}), 2.30 (s, 3H, CH_{3Ts}), 2.26 (s, 3H, CH_{3Mes}), 1.81 (s, 3H, CH_{3Mes}), 1.42 (s, 3H, CH_{3Mes}); **^{31}P{^{1}H} NMR** (162 MHz, $CDCl_3$, 25 °C): δ -5.2 (s); **^{13}C{^{1}H} NMR** (101 MHz, $CDCl_3$, 25 °C) δ 143.5 (s, C_{Ts}), 141.1 (s, C_{Ts}),139.3 (s, C_{Mes}), 138.3 (s, CH_{Ar}), 135.6 (d, J_{PC} = 15.2 Hz, $C_{ipso\ Ph}$), 134.9 (d, J_{PC} = 15.2 Hz, CH_{Ph}), 134.2 (s, C_{Mes}), 134.1 (s, C_{Mes}),133.8 (s, CH_{Ar}), 132.9 (d, J_{PC} = 13.2 Hz, $C_{ipso\ Ph}$), 132.4 (d, J_{PC} = 8.5 Hz, $C_{ipso\ Ph}$), 130.7 (s, C_{Mes}), 129.9 (s, CH_{Ar}), 129.6 (d, J_{PC} = 9.9 Hz, CH_{Ph}), 129.5 (s, CH_{Ar}), 129.4 (s, CH_{Ar}), 129.3 (d, J_{PC} = 8.5 Hz, CH_{Ph}), 128.8 (d, J_{PC} = 8.3 Hz, CH_{Ph}), 128.6 (s, CH_{Ar}), 126.2 (s, CH_{Ar}), 123.6 (s, $CH_{Im\text{-}4,5}$), 120.9 (d, J_{PC} = 8.1 Hz, $CH_{Im\text{-}4,5}$), 61.8 (d, J_{PC} = 11.2 Hz, CH_{CHPh}), 21.4 (s, $CH_{3Mes,Ts}$), 21.2 (s, $CH_{3Mes,Ts}$), 17.5 (s, CH_{3Mes}), 17.0 (s, CH_{3Mes}); **Anal.** Found: C, 63.67; H, 5.06; N, 3.92. Calcd. (%) for $C_{38}H_{37}N_2O_3PS$. 1.3(CH_2Cl_2): C, 63.52; H, 5.37; N, 3.77; **HRMS** (ESI, POS): m/z: calcd. for $C_{31}H_{30}N_2P^+$ $[M - OTs]^+$ 461.2142; found, 461.2149 (εr = 1.5 ppm).

4.3 Synthesis of the Bidentate Complexes (C1-C5)

General procedure (III)

To a stirred suspension of ligands **(L1-L5)** in toluene/THF was added at r.t a solution of KHMDS (0.5 M in toluene, 1.1 equiv.). The resulting yellow suspension was sonicated during 5 min. and stirred for additional 15 min. $MnBr(CO)_5$ (1.0 equiv.) was added in one portion inducing a vigorous CO evolution. The resulting orange solution was stirred for 2 h at 60 °C and the progress of the reaction was monitored by liquid IR. The reaction mixture was cooled to r.t., filtered through Celite and evaporated under vacuum. The crude product was crystallized in THF/pentane mixture to afford complexes **(C1-C5)** as a yellow powder.

Synthesis of *fac*-[MnBr(CO)$_3$(κ^{2}P,Ĉ-Ph$_2$PCH$_2$NHC^{Mes})] (C1)

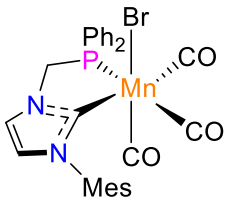

C1

According to the general procedure (**III**), **L1** (0.508 g, 0.91 mmol) in toluene (40 mL), afforded complex **C1** (0.470 g, 86%) as a yellow powder. Single crystals suitable for X-ray diffraction analysis were obtained by slow vapor diffusion of pentane into the solution of complex **C1** in THF at room temperature. **^{1}H NMR** (400.1 MHz, CD_2Cl_2, 25 °C): δ 8.05–7.98 (m, 2H, CH_{Ph}), 7.61–7.50 (m, 4H, CH_{Ph} + C$H_{Im\text{-}4,5}$), 7.41–7.32 (m, 3H, CH_{Ph}), 7.19–7.12 (m, 2H, CH_{Ph}), 7.09 (t, J_{HH} = J_{PH} = 1.8 Hz, 1H, C$H_{Im\text{-}4,5}$), 7.04 (s, 1H, CH_{Mes}), 7.01 (s, 1H, CH_{Mes}), 5.09 (dd, J_{HH} = 12.8 Hz, J_{PH} = 12.0 Hz, 1H, Ph$_2$PCH_2), 4.96 (dd, J_{HH} = 12.8 Hz, 1H, Ph$_2$PCH_2), 2.36 (s, 3H, CH_{3Mes}), 2.20 (s, 3H, CH_{3Mes}), 1.91 (s, 3H, CH_{3Mes}); **^{31}P{^{1}H} NMR** (162.0 MHz, CD_2Cl_2, 25 °C): δ 71.3 (s); ^{31}P{^{1}H} NMR (162.0 MHz, Tol-d^8, 25 °C): δ 71.7 (s); **^{13}C{^{1}H} NMR** (100.6 MHz, CD_2Cl_2, 25 °C): δ 222.5 (br. d, J_{PC} = 18.2 Hz, *C*O), 219.8 (br. d, J_{PC} = 20.4 Hz, *C*O), 216.8 (br. d, J_{PC} = 32.2 Hz, *C*O), 197.7 (d, J_{PC} = 17.5 Hz, *C*N$_2$), 139.7 (s, C_{Mes}), 137.4 (s, C_{Mes}), 136.5 (d, J_{PC} = 16.0 Hz, $C_{ipso\ Ph}$), 136.3 (d, J_{PC} = 20.8 Hz, $C_{ipso\ Ph}$), 135.2 (s, C_{Mes}), 134.7 (d, J_{PC} = 9.9 Hz, *C*H$_{Ph}$), 131.6 (d, J_{PC} = 2.0 Hz, *C*H$_{Ph}$), 129.9 (d, J_{PC} = 1.5 Hz, *C*H$_{Ph}$), 129.3 (s, *C*H$_{Mes}$), 128.8 (d, J_{PC} = 7.3 Hz, *C*H$_{Ph}$), 128.8 (s, *C*H$_{Ph}$), 128.7 (d, J_{PC} = 8.8 Hz, *C*H$_{Ph}$), 128.3 (s, $C_{ipso\ Mes}$), 125.1 (s, *C*H$_{Im\text{-}4,5}$), 120.7 (d, J_{PC} = 7.2 Hz, *C*H$_{Im\text{-}4,5}$), 51.9 (d, J_{PC} = 30.7 Hz, Ph$_2$P*C*H$_2$), 20.9 (s, *C*H$_{3Mes}$), 18.4 (s, *C*H$_{3Mes}$), 17.1 (s, *C*H$_{3Mes}$); **IR** (toluene): ν_{CO} 2020 (vs), 1948 (s), 1908 cm^{-1} (s); **Anal.** Found: C, 55.69; H, 3.93; N, 4.65. Calcd. (%) for $C_{28}H_{25}BrMnN_2O_3P$: C, 55.74; H, 4.18; N, 4.64; **LRMS** (ESI, POS): m/z calcd. for $C_{28}H_{25}MnN_2O_3P^+$ [M – Br]$^+$ 523.1; found, 523.1.

Synthesis of *fac*-[MnI(CO)$_3$(κ^2*P*,*Ĉ*-Ph$_2$PC(H)MeNHC^{Mes})] C1.b

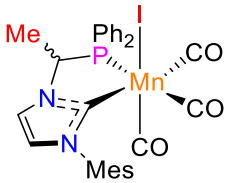

C1.b

To a solution of complex **C1** (85 mg, 0.14 mmol) in toluene (10 mL) a 0.5M toluene solution of KHMDS (0.7 mL, 0.35 mmol) was added dropwise and the reaction mixture was sonicated for 3 min. until the complete conversion of **C1** was evidenced by IR spectroscopy. The resulting solution was cooled to 0 °C and treated with excess of MeI (44 μL, 0.7 mmol). The reaction mixture was stirred at 0 °C for 1 h and then was allowed to warm to r.t. over 1 h until IR monitoring evidenced the formation of complex **C1.b** as a main component (ν_{CO} 2015 (s), 1946 (s), 1907 cm^{-1} (s)). The solution was filtered through Celite, the volatiles were removed under vacuum to afford the yellow residue containing according to ^{31}P NMR spectroscopy complex **C1.b** as a major component. The analytically pure sample was obtained by repetitive crystallizations in THF/hexane mixture to afford finally target product **C1.b** in a moderate yield (35 mg, 40%) as a yellow powder. According to NMR data compound **C1.b** contained a mixture of two isomers in *ca.* 6:1 ratio differing by the orientation of methyl group of the bridge *vs.* iodine ligand. Single crystals suitable for X-ray diffraction analysis were obtained by slow vapor diffusion of pentane into the solution of complex **C1.b** in toluene at room temperature. **^{1}H NMR** (400.1 MHz, THF-d^8, 25 °C): δ 8.28–8.20 (m, 2H, C$H_{\text{Ph major}}$), 8.06–7.98 (m, 2H, C$H_{\text{Ph minor}}$), 7.82 (s, 1H, C$H_{\text{Im-4,5 major}}$), 7.60–7.49 (m, 4H, C$H_{\text{Ph major+minor}}$), 7.40–7.35 (m, 2H, C$H_{\text{Ph minor}}$), 7.35–7.27 (m, 5H, C$H_{\text{Ph}}$ + C$H_{\text{Im-4,5 major+minor}}$), 7.20–7.13 (m, 2H, C$H_{\text{Ph minor}}$), 7.13–7.06 (m, 2H, C$H_{\text{Ph major+minor}}$), 7.05 (s, 1H, C$H_{\text{Mes minor}}$), 7.03 (s, 1H, C$H_{\text{Mes minor}}$), 7.00 (s, 1H, C$H_{\text{Mes major}}$), 6.96 (s, 1H, C$H_{\text{Mes major}}$), 5.60 (br dq, J_{HH} = 7.0 Hz, J_{PH} = 1.1 Hz, 1H, $Ph_2PCHCH_{3\ \text{minor}}$), 5.51 (dq, J_{PH} = 11.4 Hz, J_{HH} = 7.1 Hz, 1H, $Ph_2PCHCH_{3\ \text{major}}$), 2.34 (s, 3H, C$H_{\text{3Mes minor}}$), 2.31 (s, 6H, C$H_{\text{3Mes major}}$), 2.26 (s, 3H, C$H_{\text{3Mes minor}}$), 2.12 (s, 3H, C$H_{\text{3Mes minor}}$), 1.89 (s, 3H, C$H_{\text{3Mes major}}$), 1.66 (dd, J_{PH} = 11.0 Hz, J_{HH} = 7.1 Hz, 3H, $Ph_2PCHCH_{3\ \text{major}}$), 1.63 (dd overlapped with a signal of major isomer, J_{HH} = 7.1 Hz, 3H, $Ph_2PCHCH_{3\ \text{minor}}$); **^{31}P{^{1}H} NMR** (162.0 MHz, THF-d^8, 25 °C): δ 81.2 (s $_{\text{minor}}$), 74.5 (s $_{\text{major}}$); **^{13}C{^{1}H} NMR** (100.6 MHz, THF-d^8, 25 °C): δ 224.3 (br. d, J_{PC} = 16.8 Hz, CO_{major}), 221.2 (br. d, J_{PC} = 20.5 Hz, CO_{major}), 217.8 (br. d, J_{PC} = 28.6 Hz, CO_{major}), 195.7 (d, J_{PC} = 17.0 Hz, $CN_{2\ \text{major}}$), 195.6 (d overlapped with a signal of major isomer, J_{PC} = 17.5 Hz, $CN_{2\ \text{minor}}$), 141.9 (s, $C_{\text{Mes minor}}$), 141.6 (d, J_{PC} = 40.3 Hz, $C_{ipso\ \text{Ph major}}$), 140.3 (s, $C_{\text{Mes major}}$), 138.7 (s, $C_{\text{Mes minor}}$), 138.6 (s, $C_{\text{Mes major}}$), 138.3 (d, J_{PC} = 10.2 Hz, $CH_{\text{Ph major}}$), 137.8 (s, $C_{\text{Mes minor}}$), 137.7 (d, J_{PC} = 10.2 Hz, $CH_{\text{Ph minor}}$), 136.4 (s, $C_{\text{Mes major}}$), 136.3 (s, $C_{\text{Mes minor}}$), 135.6 (d, J_{PC} = 9.1 Hz, $CH_{\text{Ph minor}}$), 133.2 (d, J_{PC} = 9.0 Hz, $CH_{\text{Ph minor}}$), 132.6 (d, J_{PC} = 2.2 Hz, $CH_{\text{Ph major}}$), 132.0 (d, J_{PC} = 2.2 Hz, $CH_{\text{Ph minor}}$), 131.2 (s, $CH_{\text{Ph minor}}$), 130.5 (d, J_{PC} = 9.8 Hz, $CH_{\text{Ph major}}$), 130.4 (s, $C_{ipso\ \text{Mes major}}$), 130.2 (d, J_{PC} = 1.2 Hz, $CH_{\text{Ph major}}$), 130.0 (d, J_{PC} = 38.3 Hz, $C_{ipso\ \text{Ph major}}$), 129.7 (s, $CH_{\text{Ph major}}$), 129.6 (d, J_{PC} = 8.8 Hz, $CH_{\text{Ph major}}$),

129.4, 129.3 (s, $CH_{Mes\ major+minor}$), 127.1 (s, $CH_{Im\text{-}4,5\ major}$), 126.0 (s, $CH_{Im\text{-}4,5\ minor}$), 121.4 (d, J_{PC} = 8.1 Hz, $_{major}$), 120.7 (d, J_{PC} = 6.7 Hz, $_{minor}$), 60.6 (d, J_{PC} = 27.9 Hz, $Ph_2PCHCH_{3\ major}$), 58.8 (d, J_{PC} = 31.4 Hz, $Ph_2PCHCH_{3\ minor}$), 21.35 (s, $CH_{3Mes\ minor}$), 21.3 (s, $CH_{3Mes\ major}$), 20.4 (s, $CH_{3Mes\ major}$), 20.1 (br. s, $Ph_2PCHCH_{3\ major}$), 18.2 (s, $CH_{3Mes\ minor}$), 18.0 (s, $CH_{3Mes\ major+minor}$), 15.0 (d, J_{PC} = 6.2 Hz, $Ph_2PCHCH_{3\ minor}$); **IR** (toluene): ν_{CO} 2015 (vs), 1946 (s), 1907 cm^{-1} (s); **Anal**. Found: C, 55.69; H, 3.93; N, 4.65. Calcd. (%) for $C_{29}H_{27}IMnN_2NaO_3P$: C, 55.74; H, 4.18; N, 4.64; **HRMS** (ESI, POS): m/z calcd. for $C_{29}H_{27}MnN_2O_3P^+$ $[M - I]^+$ 537.1140; found, 537.1140 (ε_r = 0.0 ppm), calcd. for $C_{29}H_{27}MnN_2NaO_3P^+$ $[M + Na]^+$ 687.0085; found, 567.0882 (ε_r = 0.4 ppm).

Synthesis of [Mn(CO)$_3$(κ^3*P*,*Ĉ*,*O*-Ph$_2$PCH(CO$_2$)NHC^{Mes})] C1.c

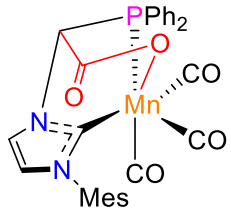

C1.c

To a solution of complex **C1** (90 mg, 0.15 mmol) in toluene (10 mL) a 0.5M toluene solution of KHMDS (0.8 mL, 0.37 mmol) was added dropwise. The reaction mixture was sonicated for 3 min until the complete conversion of **C1** was evidenced by IR spectroscopy and then a stream of CO_2 was bubbled through the solution. The reaction was stirred at r.t. for 2 h until IR analysis evidenced the formation of complex **C1.c** as only product (ν_{CO} 2024 (s), 1949 (s), 1910 cm^{-1} (s), ($\nu_{C=O}$ 1653 (m, br.). After filtration through Celite and evaporation of the solvent under vacuum, the crude product was crystallized in THF/hexane mixture to afford complex **C1.c** (75 mg, 89%) as a yellow powder. Single crystals suitable for X-ray diffraction analysis were obtained by slow vapor diffusion of pentane into the solution of complex **C1.c** in THF at room temperature. **^{1}H NMR** (400.1 MHz, $CDCl_3$, 25 °C): δ 7.69–7.62 (m, 2H, CH_{Ph}), 7.59–7.52 (m, 2H, CH_{Ph}), 7.51–7.41 (m, 7H, CH_{Ph} + $CH_{Im\text{-}4,5}$), 7.02 (s, 1H, CH_{Mes}), 6.90 (s, 1H, CH_{Mes}), 6.79 (d, J_{PH} = 1.4 Hz, 1H, $CH_{Im\text{-}4,5}$), 5.67 (d, J_{PH} = 9.2 Hz, 1H, Ph_2PCH), 2.34 (s, 3H, CH_{3Mes}), 2.07 (s, 3H, CH_{3Mes}), 1.49 (s, 3H, CH_{3Mes}); **^{31}P{^{1}H} NMR** (162.0 MHz, $CDCl_3$, 25 °C): δ 92.8 (s). **^{13}C{^{1}H} NMR** (100.6 MHz, $CDCl_3$, 25 °C): δ 224.2 (br. d, J_{PC} = 17.7 Hz, *C*O), 218.4 (br. d, J_{PC} = 18.2 Hz, *C*O), 217.1 (br. d, J_{PC} = 29.3 Hz, *C*O), 198.6 (d, J_{PC} = 16.9 Hz, CN_2), 173.0 (d, J_{PC} = 19.8 Hz, Ph_2PCHC=O), 139.8, 1360, 135.5 (s, C_{Mes}), 135.1 (s, $C_{ipso\ Mes}$), 133.0 (d, J_{PC} = 11.1 Hz, CH_{Ph}), 132.5 (d, J_{PC} = 10.6 Hz, CH_{Ph}), 132.0 (d, J_{PC} = 2.1 Hz, CH_{Ph}), 131.8 (d, J_{PC} = 1.9 Hz, CH_{Ph}), 129.5 (d, J_{PC} = 9.5 Hz, CH_{Ph}), 129.4 (d, J_{PC} = 7.6 Hz, CH_{Ph}), 129.3, 129.1 (s,

CH_{Mes}), 128.4 (d, J_{PC} = 31.4 Hz, $C_{ipso\ Ph}$), 127.5 (d, J_{PC} = 35.3 Hz, $C_{ipso\ Ph}$), 124.0 (s, $CH_{Im\text{-}4,5}$), 121.0 (d, J_{PC} = 1.3 Hz, $CH_{Im\text{-}4,5}$), 67.0 (d, J_{PC} = 23.8 Hz, $Ph_2PCHC{=}O$), 21.3 (s, CH_{3Mes}), 18.3 (s, CH_{3Mes}), 16.9 (s, CH_{3Mes}); **IR** (toluene): ν_{CO} 2024 (s), 1949 (s), 1910 (s), $\nu_{C=O}$ 1653 cm^{-1} (m, br.); **HRMS** (ESI, POS): m/z calcd. for $C_{29}H_{25}MnN_2O_5P^+$ $[M + H]^+$ 567.0881; found, 567.0882 (ε_r = 0.2 ppm).

Generation of complex [Mn(CO)$_3$(κ^3*P*,C,*Ĉ*-Ph$_2$PCHNHC^{Mes})] C1.d for NMR characterization.

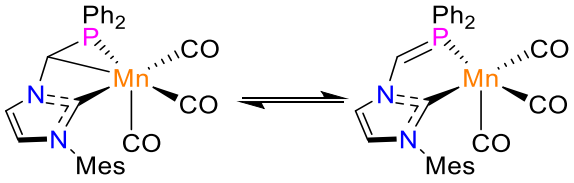

C1.d^1 **C1.d^2**

To a Schlenk tube charged in a glove box with solid complex **C1** (50 mg, 0.08 mmol) and KHMDS (40 mg, 0.2 mmol) [D_8]toluene (1 mL) was added at room temperature. The reaction mixture was sonicated for 3 min until the complete conversion of **C1** was evidenced by IR spectroscopy. The resulting orange solution was filtered through Celite directly to NMR tube and rapidly analyzed at low temperature. **^{1}H NMR** (600.1 MHz, Tol-d^8, –30 °C): δ 7.42–7.36 (m, 2H, CH_{Ph}), 7.18–6.14 (m overlapped with residual toluene protons, 2H, CH_{Ph}), 7.05 (br. s, 2H, CH_{Ph}), 6.98–6.91 (m overlapped with residual toluene protons, 4H, CH_{Ph}), 6.68 (s, 1H, CH_{Mes}), 6.51 (s, 1H, CH_{Mes}), 5.93 (s, 1H, C$H_{Im\text{-}4,5}$), 5.40 (s, 1H, C$H_{Im\text{-}4,5}$), 3.55 (d, J_{PH} = 8.6 Hz, 1H, Ph_2PCH), 2.02 (s, 3H, CH_{3Mes}), 2.01 (s, 3H, CH_{3Mes}), 1.49 (s, 3H, CH_{3Mes}); **^{31}P{^{1}H} NMR** (242.9 MHz, Tol-d^8, –30 °C): δ 51.6 (s); **^{13}C{^{1}H} NMR** (150.9 MHz, Tol-d^8, –30 °C): δ 228.9 (br. s, *C*O), 227.2 (br. s, *C*O), 223.6 (br. s, *C*O), 178.0 (d, J_{PC} = 14.2 Hz, CN_2), 138.4 (s, $C_{ipso\ Mes}$), 135.1 (s, C_{Mes}), 134.9 (s, C_{Mes}), 134.8 (d, J_{PC} = 14.0 Hz, CH_{Ph}), 134.5 (s, C_{Mes}), 137.7 (d, J_{PC} = 43.6 Hz, $C_{ipso\ Ph}$), 131.3 (d, J_{PC} = 9.3 Hz, CH_{Ph}), 131.1 (br. s, $C_{ipso\ Ph}$), 130.6, 129.9 (s, CH_{Ph}), 129.1 (s, CH_{Mes}), 128.4 (s overlapped with toluene signal, chemical shift obtained from ^{13}C–^{1}H HMQC, CH_{Mes}), 128.2, 125.3 (s, CH_{Ph}), 121.5, 120.6 (s, $CH_{Im\text{-}4,5}$), 22.7 (d, J_{PC} = 18.2 Hz, Ph_2PCH), 20.9 (s, CH_{3Mes}), 17.9 (s, CH_{3Mes}), 17.8 (s, CH_{3Mes}); **IR** (toluene): 1993 (s), 1901 (vs) cm^{-1}.

Synthesis of *fac*-[MnBr(CO)$_3$(κ^2P,Ĉ-Ph$_2$PCH$_2$NHC^{Me})] (C2)

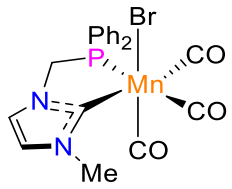

C2

According to the general procedure (**III**), **L2** (0.50 g, 1.11 mmol) in THF (40 mL, N.B.: the addition of the base was done at - 40 °C), afforded complex **C2** (0.51 g, 82%) as a yellow powder. Single crystals suitable for X-ray diffraction analysis were obtained by slow vapor diffusion of pentane into the solution of complex **C2** in CH_2Cl_2 at room temperature. **^{1}H NMR** (400 MHz, CD_2Cl_2, 25 °C): δ 7.94 – 7.90 (m, 2H, CH_{Ar}), 7.58 – 7.48 (m, 3H, CH_{Ar}), 7.42 – 7.27 (m, 4H, CH_{Ar}), 7.22 – 7.09 (m, 3H, CH_{Ar}), 4.99 – 4.90 (m, 2H, Ph$_2$PCH_2), 4.03 (s, 3H, CH_{3Me}); **^{31}P{^{1}H} NMR** (162 MHz, CD_2Cl_2, 25 °C): δ 72.1 (s); **^{13}C{^{1}H} NMR** (101 MHz, CD_2Cl_2, 25 °C): δ 223.1 (d, J_{PC}= 17.7 Hz, *C*O), 221.3 (d, J_{PC} = 29.7 Hz, *C*O), 220.0 (d, J_{PC} = 20.6 Hz, *C*O), 196.4 (d, J_{PC} = 16.9 Hz, *C*N$_2$), 135.6 (d, J_{PC} = 36.2 Hz, C_{ipso}) 134.7 (d, J_{PC} = 9.7 Hz, *C*H$_{Ph}$), 131.8 (d, J_{PC} = 1.8 Hz, *C*H$_{Ph}$), 130.56 (d, J_{PC} = 8.0 Hz, *C*H$_{Ph}$), 130.50 (s, *C*H), 129.21 (d, J_{PC} = 42.2 Hz, $C_{ipso\ Ph}$), 129.20 (d, J_{PC} = 9.0 Hz, *C*H$_{Ph}$) – 129.15 (d, J_{PC} = 9.0 Hz, *C*H$_{Ph}$),125.6 (s, *C*H$_{Im\text{-}4,5}$), 120.2 (d, J_{PC}= 7.4 Hz, *C*H$_{Im\text{-}4,5}$), 52.1 (d, J_{PC} = 31.9 Hz, Ph$_2$P*C*H$_2$), 39.4 (s, *C*H$_3$); **IR** (THF): ν_{CO} 2013; 1937; 1906 cm^{-1}; **Anal.** Found: C, 48.23; H, 3.30; N, 5.43. Calcd. (%) for $C_{20}H_{17}BrMnN_2O_3P$: C, 48.12; H, 3.43; N,5.61; **LRMS** (DCI-CH$_4$, POS): m/z calcd. for $C_{20}H_{17}MnN_2O_3P^+$ [M – Br]$^+$ 419.0; found, 419.0.

Synthesis of *fac*-[MnBr(CO)$_3$(κ^2P,Ĉ-Ph$_2$PCH$_2$NHC^{iPr})] (C3)

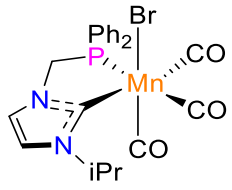

C3

According to the general procedure (**III**), **L3** (0.50 g, 1.04 mmol) in toluene (40 mL) afforded complex **C3** (0.37 g, 60%) as a yellow powder. Single crystals suitable for X-ray diffraction analysis were obtained by slow evaporation of a solution of complex **C3** in $CDCl_3$ at room temperature. **^{1}H NMR** (400 MHz, CD_2Cl_2, 25 °C): δ 7.94 (t, J_{PH} = 8.0 Hz, J_{HH} = 7.0 Hz, 2H, CH_{Ar}), 7.57 – 7.48 (m, 3H, CH_{Ar}), 7.37 – 7.34 (m, 4H, CH_{Ar}), 7.25 (s, 1H, CH_{Ar}), 7.13 (t, J_{PH} = 10 Hz, J_{HH} = 7.0 Hz, 2H, CH_{Ar}), 5.14 (sept, J_{HH} = 6.9 Hz, 1H, CH_{iPr}), 4.98 – 4.90 (m, 2H,

Ph_2PCH_2), 1.58 (d, J = 6.9 Hz, 3H, CH_{3iPr}), 1.51 (d, J = 6.9 Hz, 3H, CH_{3iPr}); **$^{31}P\{^1H\}$ NMR** (162 MHz, CD_2Cl_2, 25 °C): δ 70.6 (s); **$^{13}C\{^1H\}$ NMR** (101 MHz, CD_2Cl_2, 25 °C): δ 223.6 (d, J_{PC} = 17.2 Hz, *C*O), 221.3 (d, J_{PC} = 30.6 Hz, *C*O), 220.3 (d, J_{PC} = 21.3 Hz, *C*O), 194.9 (d, J_{PC} = 16.9 Hz, *C*N_2), 135.6 (d, J_{PC} = 36.5 Hz, $C_{ipso\ Ph}$), 134.8 (d, J_{PC} = 9.7 Hz, *C*H_{Ph}), 131.8 (s, *C*H_{Ph}), 130.5 – 130,4 (m, 2C, *C*H_{Ph}), 129.2 (d, J_{PC} = 8.0 Hz, *C*H_{Ph}), 129.1 (d, J_{PC} = 9.0 Hz, *C*H_{Ph}), 129.1 (d, J_{PC} = 42.9 Hz, $C_{ipso\ Ph}$), 121.1 (d, J = 6.9 Hz, *C*$H_{Im\text{-}4,5}$), 119.8 (s, *C*$H_{Im\text{-}4,5}$), 53.6 (s, *C*H_{iPr}), 51.6 (d, J_{PC} = 31.9 Hz, Ph_2PCH_2), 24.2 (s, *C*H_{3iPr}), 23.5 (s, *C*H_{3iPr}); **IR** (THF): ν_{CO} 2017; 1940; 1915 cm^{-1}; **Anal.** Found: C, 50.17; H, 3.86; N, 4.88. Calcd. (%) for $C_{26}H_{35}BrMnN_2O_3P$: C, 50.12; H, 4.01; N, 5.31; **LRMS** (DCI-CH_4, POS): m/z calcd. for $C_{22}H_{21}MnN_2O_3P^+$ $[M - Br]^+$ 447.0; found, 447.0.

Synthesis of *fac*-[MnBr(CO)$_3$(κ^2P,Ĉ-*i*Pr$_2$PCH$_2$NHC^{Mes})] (C4)

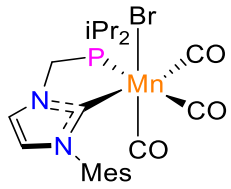

C4

According to the general procedure (**III**), **L4** (0.10 g, 0.20 mmol) in toluene (10 mL) afforded complex **C4** (0.083 g, 78%) as a yellow powder. Single crystals suitable for X-ray diffraction analysis were obtained by slow vapor diffusion of hexane into the solution of complex **C4** in THF at room temperature. **^{1}H NMR** (400 MHz, CD_2Cl_2, 25 °C): δ 7.35 (s, 1H, C*H*$_{Ar}$), 7.05 (s, 1H, C*H*$_{Ar}$), 7.03 (s, 1H, C*H*$_{Ar}$), 6.97 (s, 1H, C*H*$_{Ar}$), 4.39 (d, J_{HH} = 12.9 Hz, J_{PH} = 0 Hz, 1H, *i*Pr_2PCH_2), 4.33 (dd, J_{HH} = 12.9 Hz, J_{PH} = 10.2 Hz, 1H, *i*Pr_2PCH_2), 3.24 (d sept, J_{PH} = 7.3 Hz, J_{HH} = 6.9 Hz, 1H, C*H*$_{iPr}$), 2.59 (d sept, J_{PH} = 13.2 Hz, J_{HH} = 6.9 Hz, 1H, C*H*$_{iPr}$), 2.37 (s, 3H, C*H*$_{3Mes}$), 2.16 (s, 3H, C*H*$_{3Mes}$), 2.03 (s, 3H, C*H*$_{3Mes}$), 1.53 (dd, J_{PH}= 16.0, J_{HH} = 6.9 Hz, 3H, C*H*$_{3iPr}$), 1.34 (dd, J_{PH}= 11.0, J_{HH} = 6.9 Hz, 3H, C*H*$_{3iPr}$), 1.28 (dd, J_{PH}= 16.0, J_{HH} = 6.9 Hz, 3H, C*H*$_{3iPr}$), 0.98 (dd, J_{PH} = 14.0, J_{HH} = 6.9 Hz, 3H, C*H*$_{3iPr}$); **$^{31}P\{^1H\}$ NMR** (162 MHz, CD_2Cl_2, 25 °C): δ 91.0 (s); **$^{13}C\{^1H\}$ NMR** (101 MHz, CD_2Cl_2, 25 °C): δ 225.1 (d, J_{PC} = 18.5 Hz, *C*O), 220.4 (d, J_{PC} = 19.9 Hz, *C*O), 217.2 (d, J_{PC} = 28.5 Hz, *C*O), 197.9 (d, J_{PC} = 16.3 Hz, *C*N_2), 139.9 (s, *C*$_{Mes}$), 137.8 (s, *C*$_{Mes}$), 136.9 (s, *C*$_{Mes}$), 135.8 (s, *C*$_{Mes}$), 129.6 (s, *C*H$_{Ar}$), 129.2 (s, *C*H$_{Ar}$), 125.0 (s, *C*H$_{Ar}$), 120.9 (d, J_{PC} = 6.6 Hz, *C*H$_{Im\text{-}4,5}$), 49.5 (d, J_{PC} = 25.6 Hz, *i*Pr_2PCH_2), 25.5 (d, J_{PC} = 22.6 Hz, *C*H$_{iPr}$), 24.3 (d, J_{PC} = 16.5 Hz, *C*H$_{iPr}$), 21.3 (s, *C*H$_{3iPr}$), 19.8 (d, J_{PC} = 4.4 Hz, *C*H$_{3iPr}$), 19.2 (d, J_{PC} = 6.4 Hz, *C*H$_{3iPr}$), 19.1 (d, J_{PC} = 7.3 Hz, *C*H$_{3iPr}$), 18.8 (s, *C*H$_{3Mes}$), 18.2 (s, *C*H$_{3Mes}$), 17.7 (s, *C*H$_{3Mes}$); **IR** ν_{CO} (THF): 2018, 1943, 1899 cm^{-1}; **Anal.** Found: C, 49.40; H,

5.76; N, 5.22. Calcd. (%) for $C_{22}H_{29}BrMnN_2O_3P$: C, 49.36; H, 5.46; N, 5.23; **LRMS** (DCI-CH_4, POS): m/z calcd. for $C_{22}H_{29}MnN_2O_3P^+$ $[M - Br]^+$ 455.1; found, 455.1.

4.4 Synthesis of the Hydride Complexes (C1.a-C5.a)

General procedure (IV)

A stream of dihydrogen was bubbled through a solution of the selected complex in toluene cooled to –20°C and then a solution of KHMDS (2.5 equiv.) in toluene was added dropwise. The reaction mixture was allowed to warm to r.t. over *ca*. 30 minutes. The reaction was followed by IR analysis. The resulting orange solution was thoroughly washed with degassed water until the neutral pH of the aqueous phase was obtained. The organic phase was dried over Na_2SO_4, filtered through Celite, and all the volatiles were evaporated under vacuum. The residue was thoroughly dried under vacuum to afford the desired hydride complexes as a yellow powder.

General procedure (V)

To a solution of complexes **(C1-C3)** in ethanol, 2.0 equiv. of $NaBH_4$ was added and the reaction mixture was stirred at 80 °C for 2 h, the resulting yellow suspension was filtered through Celite and evaporated under vacuum to afford hydride complexes **(C1.a-C3.a)** as a yellow powder.

Synthesis of *fac*-[MnH(CO)$_3$(κ^2*P*,*Ĉ*-Ph$_2$PCH$_2$NHC^{Mes})]C1.a

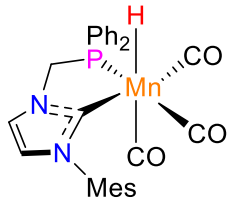

C1.a

According to the general procedure (**IV**), **C1** (100 mg, 0.17 mmol) in toluene (10 mL) afforded complex **C1.a** (75 mg, 78%) as a yellow powder. Single crystals suitable for X-ray diffraction analysis were obtained by the crystallization in concentrated toluene solution at room temperature. **^{1}H NMR** (400.1 MHz, [D$_8$]THF, 25 °C): δ 7.83–7.75 (m, 2H, C*H*$_{Ph}$), 7.63–7.56 (m, 2H, C*H*$_{Ph}$), 7.44 (s, 1H, C*H*$_{Im\text{-}4,5}$), 7.42–7.35 (m, 6H, C*H*$_{Ph}$), 7.01 (s, 1H, C*H*$_{Im\text{-}4,5}$), 6.98 (s, 1H, C*H*$_{Mes}$), 6.95 (s, 1H, C*H*$_{Mes}$), 4.99 (dd, J_{HH} = 13.7 Hz, J_{PH} = 7.3 Hz, 1H, Ph$_2$PC*H*$_2$), 4.50 (dd, J_{HH} = 13.7 Hz, J_{PH} = 3.6 Hz, 1H, Ph$_2$PC*H*$_2$), 2.31 (s overlapped with residual toluene signal, 3H, C*H*$_{3Mes}$), 2.02 (s, 3H, C*H*$_{3Mes}$), 1.99 (s, 3H, C*H*$_{3Mes}$), –7.25 (d, J_{PH} = 53.8 Hz, Mn–*H*); **^{31}P{^{1}H} NMR** (162.0 MHz, THF-d^8, 25 °C): δ 94.2 (s); **^{13}C{^{1}H} NMR** (100.6 MHz, THF-d^8, 25 °C): δ 226.3 (br. d, J_{PC} = 20.8 Hz, *C*O), 224.6 (br. d, J_{PC} = 17.7 Hz, *C*O), 222.4 (br. d,

J_{PC} = 13.9 Hz, *C*O), 205.4 (d, J_{PC} = 14.3 Hz, *C*N_2), 139.6 (s, $C_{ipso\ Mes}$), 138.8 (d, J_{PC} = 31.4 Hz, $C_{ipso\ Ph}$), 138.4 (s, C_{Mes}), 138.1 (d, J_{PC} = 44.8 Hz, $C_{ipso\ Ph}$), 137.6, 136.6 (s, C_{Mes}), 134.1 (d, J_{PC} = 10.8 Hz, *C*H_{Ph}), 132.4 (d, J_{PC} = 11.2 Hz, *C*H_{Ph}), 130.9 (d, J_{PC} = 1.7 Hz, *C*H_{Ph}), 130.5 (d, J_{PC} = 1.3 Hz, *C*H_{Ph}), 129.9, 129.8 (s, *C*H_{Mes}), 129.4 (d, J_{PC} = 9.0 Hz, *C*H_{Ph}), 129.1 (d, J_{PC} = 9.0 Hz, *C*H_{Ph}), 124.9 (s, *C*$H_{Im-4,5}$), 121.0 (d, J_{PC} = 8.1 Hz, *C*$H_{Im-4,5}$), 54.9 (d, J_{PC} = 29.6 Hz, Ph_2PCH_2), 21.4 (s, *C*H_{3Mes}), 18.6 (s, *C*H_{3Mes}), 18.2 (s, *C*H_{3Mes}); **IR** (toluene): ν_{CO} 1991 (s), 1913 (s), 1893 cm^{-1} (s); **Anal.** Found: C, 66.15; H, 5.39; N, 5.10. Calcd. (%) for $C_{28}H_{26}MnN_2O_3P$. 0.5(toluene): C, 66.32; H, 5.30; N, 4.91.

Synthesis of *fac*-[MnH(CO)$_3$(κ^2*P*,*Ĉ*-Ph$_2$PCH$_2$NHC^{Me})] (C2.a)

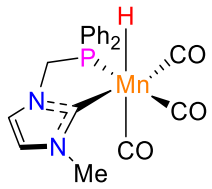

C2.a

According to the general procedure (**V**), **C2** (30mg, 0.060 mmol) in ethanol (5 mL) afforded complex **C2.a** (20 mg, 80%) as a yellow powder. **^{1}H NMR** (400 MHz, Tol-d^8, 25 °C) δ 7.76 (br s, 2H, C*H*$_{Ar}$), 7.32 (br s, 2H, C*H*$_{Ar}$), 7.15-6.80 (m, 6H, C*H*$_{Ph}$, overlap with tol-d^8 signals), 6.13 (br s, 1H, C*H*$_{Ar}$), 5.88 (br s, 1H, C*H*$_{Ar}$), 3.94 (t, J_{HH} = 12.4 Hz, J_{PH} = 10.8 Hz, 1H, Ph_2PCH_2), 3.46 (d, J_{HH} = 12.6 Hz, 1H, Ph_2PCH_2), 3.31 (s, 3H, C*H*$_{3Me}$), -7.12 (d, J_{PH} = 64.8 Hz, Mn–*H*); **^{31}P{^{1}H} NMR** (162 MHz, Tol-d^8, 25 °C) δ 98.3 (s); **^{13}C{^{1}H} NMR** (101 MHz, Tol-d8, 25 °C) δ 227.5 (br, *C*O), 225.6 (br, *C*O), 222.7 (br, *C*O), 203.3 (d, J_{PC} = 13.1 Hz, *C*N_2), 135.1 (d, J_{PC} = 47.8 Hz, $C_{ipso\ Ph}$), 133.5 (d, J_{PC} = 10.4 Hz, *C*H_{Ph}), 131.2 (d, J_{PC} = 11.8 Hz, *C*H_{Ph}), 130.4 (s, *C*H_{Ph}), 129.7 (s, *C*H_{Ph}), 128.7 (d, J_{PC} = 8.6 Hz, *C*H_{Ph}), 128.5 (d, J_{PC} = 9.1 Hz, *C*H_{Ph}), 123.2 (s, *C*$H_{Im-4,5}$), 118.0 (d, J_{PC}= 6.8 Hz, *C*$H_{Im-4,5}$), 54.4 (d, J_{PC} = 34.1 Hz, Ph_2PCH_2), 37.9 (s, *C*H_3); Some signals (*C*$H_{Ph-ipso}$) were undetected due to overlap with those of Tol-d^8; **IR** ν_{CO} (EtOH): 1987, 1905 cm^{-1}.

Synthesis of *fac*-[MnH(CO)$_3$(κ^2*P*,*Ĉ*-Ph$_2$PCH$_2$NHC$^{i\mathrm{Pr}}$)] (C3.a)

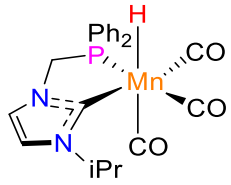

C3.a

According to the general procedure (**V**), **C3** (30 mg, 0.057 mmol) in ethanol (5 mL) afforded complex **C3.a** (18.6 mg, 73%) as a yellow powder. **^{1}H NMR** (400 MHz, Tol-d^8, 25 °C) δ 7.80 – 7.75 (m, 2H, CH_{Ph}), 7.37 – 7.32 (m, 2H, CH_{Ph}), 7.15-6.80 (m, 6H, CH_{Ph}, overlap with tol-d^8 signals), 6.24 (d, J_{PH} = 1.6 Hz, 1H, C$H_{\mathrm{Im\text{-}4,5}}$), 6.21 (t, J = 1.4 Hz 1H, C$H_{\mathrm{Im\text{-}4,5}}$), 5.23 (sept, J_{HH} = 6.6 1H, CH_{iPr}), 3.95 (dd, J_{HH} = 12.6 Hz, J_{PH} = 10.8 Hz, 1H, Ph$_2$PCH_2), 3.50 (d, J_{HH} = 13.6 Hz, 1H, Ph$_2$PCH_2), 1.16 (d, J_{HH} = 6.7 Hz, 3H, CH_{3iPr}), 0.98 (d, J_{HH} = 6.7 Hz, 3H, CH_{3iPr}), -7.12 (d, J_{PH} = 66.0 Hz, Mn–*H*); **^{31}P{^{1}H} NMR** (162 MHz, Tol-d^8, 25 °C) δ 97.3; **^{13}C{^{1}H} NMR** (101 MHz, Tol-d^8, 25 °C) δ 227.2 (br, *C*O), 225.9 (br, J_{PC} = 20.7 Hz, *C*O), 223.0 (br, *C*O), 201.6 (d, J_{PC} = 16.6 Hz, *C*N$_2$), 135.3 (d, J_{PC} = 48.1 Hz, $C_{ipso\ \mathrm{Ph}}$), 133.5 (d, J_{PC} = 10.5 Hz, *C*H$_{\mathrm{Ph}}$), 131.3 (d, J_{PC} = 11.5 Hz, *C*H$_{\mathrm{Ph}}$), 130.4 (s, *C*H$_{\mathrm{Ph}}$), 129.8 (s, *C*H$_{\mathrm{Ph}}$), 119.1 (d, J_{PC}= 6.1 Hz, *C*H$_{\mathrm{Im\text{-}4,5}}$), 117.9 (s, *C*H$_{\mathrm{Im\text{-}4,5}}$), 54.2 (d, J_{PC} = 34.6 Hz, Ph$_2$P*C*H$_2$), 52.7 (s, *C*H$_{\mathrm{iPr}}$), 23.2 (s, *C*H$_{\mathrm{3iPr}}$); Some signals were undetected due to overlap with those of Tol-d^8; **IR** ν_{CO} (EtOH): 1986, 1903 cm^{-1}.

Synthesis of *fac*-[MnH(CO)$_3$(κ^2*P*,*Ĉ*-*i*Pr$_2$PCH$_2$NHC$^{\mathrm{Mes}}$)] (C4.a)

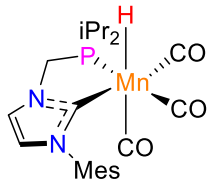

C4.a

According to general procedure (**V**), **C4** (30 mg, 0.056mmol) in ethanol (5 mL) afforded complex **C4.a** (18.2 mg, 71%) as a yellow powder. **^{1}H NMR** (400 MHz, Tol-d^8, 25 °C) δ 6.81 (s, 1H, CH_{Mes}), 6.80 (s, 1H, CH_{Mes}),6.28 (d, J = 1.7 Hz, 1H, C$H_{\mathrm{Im\text{-}4,5}}$), 6.07 (t, J = 1.7 Hz, 1H, C$H_{\mathrm{Im\text{-}4,5}}$), 3.10 (dd, J_{HH} = 13.0 Hz, J_{PH} = 4.3 Hz, 1H, iPr$_2$PCH_2), 3.03 (dd, J_{HH} = 13.0 Hz, J_{PH} = 5.0 Hz, 1H, *i*Pr$_2$PCH_2). 2.13 (s, 3H, CH$_{\mathrm{3Mes}}$), 2.11 (s, 3H, CH$_{\mathrm{3Mes}}$), 2.05 (s, 3H, CH$_{\mathrm{3Mes}}$), 1.93 – 1.81 (m, 2H, CH_{iPr}),1.12 (dd, J = 15.6, 7.0 Hz, 3H, CH_{3iPr}), 1.04 (dd, J = 15.3, 7.0 Hz, 3H, CH_{3iPr}), 0.90-0.82 (m, 3H, CH_{3iPr}) 0.80 (dd, J = 12.8, 6.9 Hz, 3H, CH_{3iPr}),-7.49 (d, J_{PH} = 49.8 Hz, Mn–*H*); **^{31}P{^{1}H} NMR** (162 MHz, Tol-d^8, 25 °C) δ 117.1; **^{31}P NMR** (162 MHz, THF-d^8,

25 °C) δ 114.21; **^{13}C{^{1}H} NMR** (101 MHz, THF-d^8, 25 °C) δ 227.1 (br, J_{PC} = 21.9 Hz, *C*O), 225.1 (br, *C*O), 224.3 (br, *C*O), 205.7 (d, J_{PC} = 14.2 Hz, *C*N$_2$), 139.4 (s, C_{Mes}), 138.4 (s, C_{Mes}) 137.5 (s, C_{Mes}), 136.6 (s, C_{Mes}), 129.9 (s, *C*H$_{Mes}$), 129.7 (s, *C*H$_{Mes}$), 124.6 (s, *C*H$_{Im-4,5}$), 120.6 (s, *C*H$_{Im-4,5}$), 47.34 (d, J = 23.2 Hz, *i*Pr$_2$P*C*H$_2$), 28.1 (d, J = 15.8 Hz, *C*H$_{iPr}$), 26.1 (d, J = 25.0 Hz, *C*H$_{iPr}$) 21.4 (s, *C*H$_{3iPr}$), 19.5 (d, J = 5.0 Hz, *C*H$_{3iPr}$), 18.7 (s, *C*H$_{3Mes}$), 18.5 (d, J = 5.0 Hz, *C*H$_{3iPr}$), 18.4 (d, J = 2.0 Hz, *C*H$_{3iPr}$), 18.3 (s, *C*H$_{3Mes}$), 18.2 (s, *C*H$_{3Mes}$); **IR** ν_{CO} (EtOH): 1984, 1903, 1882 cm^{-1}.

Synthesis of *fac*-[MnH(CO)$_3$(κ^2*P*,*Ĉ*-Ph$_2$PCH(Ph)NHC^{Mes})] (C5.a)

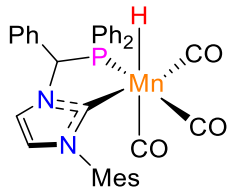

C5.a

According to general procedure (**V**), **C5** (30 mg, 0.044 mmol) in ethanol (5 mL) afforded complex **C5.a** (22 mg, 85%) as a yellow powder. **^{1}H NMR** (400.1 MHz, C_6D_6, 25 °C): δ 7.69-7.64 (m, 2H, C*H*$_{Ph\ major}$), 7.61-7.56 (m, 2H, C*H*$_{Ph\ minor}$), 7.54-7.50 (m, 2H, C*H*$_{Ph\ major}$), 7.48-7.46 (m, 2H, C*H*$_{Ph\ minor}$), 7.14-7.09 (m, 2H, C*H*$_{Ph}$), 7.07-7.03 (m, 2H, C*H*$_{Ph}$), 6.90 (br s, 1H, C*H*$_{Ph\ major}$), 6.88 (br s, 1H, C*H*$_{Ph\ minor}$), 6.86 (d, J_{HH} = 1.4 Hz, 1H, C*H*$_{Ph\ minor}$) 6.85 (d, J_{HH} = 1.8 Hz, 1H, C*H*$_{Ph\ major}$), 6.83-6.76 (m, 7H, C*H*$_{Ph\ major+minor}$), 6.71-6.62 (m, 3H, C*H*$_{Mes\ major+minor}$), 6.31 (d, J_{HH} = 2.0 Hz, 1H, C*H*$_{Im-4,5\ major}$), 6.30 (br. s, 1H, C*H*$_{Im-4,5\ minor}$), 6.07 (t, J = 1.8 Hz, 1H, C*H*$_{Im-4,5\ minor}$), 6.05 (t, J = 1.8 Hz, 1H, C*H*$_{Im-4,5\ major}$), 5.80 (d, J_{PH} = 7.7 Hz, 1H, C*H*Ph$_{major}$), 5.74 (d, J_{PH} = 5.6 Hz, 1H, C*H*Ph$_{minor}$), 2.35 (s, 3H, C*H*$_{3minor}$), 2.29 (s, 3H, C*H*$_{3major}$), 2.14 (s, 6H, C*H*$_{3major+minor}$), 2.10 (s, 3H, C*H*$_{3minor}$), 2.09 (s, 3H, C*H*$_{3major}$), –6.49 (d, J_{PH} = 52.3 Hz, 1H, Mn–*H*$_{major}$), –6.73 (d, J_{PH} = 51.7 Hz, 1H, Mn–*H*$_{minor}$); **^{31}P{^{1}H} NMR** (162 MHz, THF-d^8, 25 °C): δ 117.87 (s $_{major}$), 113.41 (s $_{minor}$); ^{31}P{^{1}H} NMR (162.0 MHz, C_6D_6, 25 °C): δ 119.2 (s $_{major}$), 115.5 (s $_{minor}$); **^{13}C NMR** (101 MHz, THF-d^8, 25 °C) δ 225.6 (br, J_{PC} = 22.4 Hz, *C*O), 225.0 (br, J_{PC} = 14.5 Hz, *C*O), 221.96 (br, *C*O), 205.8 (d, J_{PC} = 17.2 Hz, *C*N$_2$), 140.3 (d, J_{PC} = 27.9 Hz, $C_{ipso\ Ph}$), 139.5 (s, C_{Ar}), 138.2 (s, C_{Ar}), 137.6 (s, C_{Ar}), 137.3 (s, C_{Ar}), 136.3 (s, C_{Ar}), 136.2 (d, J_{PC} = 10.9 Hz, *C*H$_{Ph}$), 136.2 (d, J_{PC} = 11.0 Hz, *C*H$_{Ph}$), 135.9 (s, *C*H$_{Ar}$), 132.2 (d, J_{PC} = 9.8 Hz, *C*H$_{Ph}$) 132.0 (d, J_{PC} = 43.4 Hz, $C_{ipso\ Ph}$), 131.5 (d, J_{PC} = 10.4 Hz, *C*H$_{Ph}$), 130.8 (s, *C*H$_{Ar}$), 130.0 (s, *C*H$_{Ar}$), 129.9 (s, *C*H$_{Ar}$), 129.8 (s, *C*H$_{Ar}$), 129.4 (d, J_{PC} = 8.3 Hz, *C*H$_{Ph}$), 129.0 (d, J_{PC} = 8.9 Hz, *C*H$_{Ph\ minor}$), 128.8 (s, *C*H$_{Ar}$), 128.6 (s, *C*H$_{Ar}$), 128.4 (s, *C*H$_{Ar}$), 128.3 (s, *C*H$_{Ar}$), 128.2 (s, *C*H$_{Ar}$), 128.0 (d, J_{PC} = 8.6 Hz, *C*H$_{Ph}$), 128.03 (s, *C*H$_{Ar}$), 125.6 (s, *C*H$_{Ar}$), 125.2 (s, *C*H$_{Ar\ minor}$),

121.0 (d, J_{PC} = 7.7 Hz, $CH_{Im-4,5}$), 69.5 (d, J_{PC} = 21.8 Hz, *C*HPh), 21.3 (s, CH_3), 18.6 (s, CH_3), 18.1 (s, CH_3); **IR** (toluene): ν_{CO} 1991.0 (s), 1914.0 (s), 1896.5 cm^{-1} (s).

4.5 Catalytic ketone hydrogenation and characterization data for the alcohols b1-b20

Typical procedure for hydrogenation reactions

An autoclave was charged with complex **C1** (1.2 mg, 0.1%), solvent (2.0 mL), ketone (2.0 mmol) in this order. Then the base (1.0%) was added and the autoclave was immediately pressurized with hydrogen (50 bar) and kept under stirring in an oil bath at 60 °C for 20 hours. After cooling the reactor to room temperature and release of hydrogen, the reaction mixture was diluted with ethyl acetate (2.0 mL) and filtered through a small pad of silica (2 cm in a Pasteur pipette) with a subsequent washing with ethyl acetate. The filtrate was evaporated under vacuum and the crude product was purified by column chromatography on silica using petroleum ether/ethyl acetate mixtures as eluent to afford the corresponding alcohols with generally more than 95% purity according to NMR data.

Spectroscopic characterization data for the alcohols b1-b19

1-Phenylethanol (b1).[11]

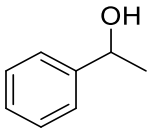

b1

According to general procedure, acetophenone **a1** (234 µL, 2.0 mmol) afforded the title compound **b1** as an oil (222 mg, 91%). **^{1}H NMR** (300.1 MHz, $CDCl_3$, 25 °C): δ 7.43–7.27 (m, 5H, Ph), 4.90 (q, $^3J_{HH}$ = 6.4 Hz, 1H, C*H*CH_3), 1.89 (br. s, 1H, OH), 1.50 (d, $^3J_{HH}$ = 6.5 Hz, 3H, C*H*CH_3); **^{13}C{^{1}H} NMR** (75.5 MHz, $CDCl_3$, 25 °C): δ 145.8, 128.5, 127.5, 125.4, 70.4, 25.2.

3-Methyl-1-phenyl-1-butanol (b2).[12]

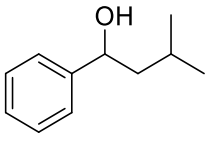

b2

According to general procedure, isovalerophenone **a2** (167 µL, 1.0 mmol) afforded the title compound **b2** as an oil (146 mg, 89%). **^{1}H NMR** (400.2 MHz, $CDCl_3$, 25 °C): δ 7.35 (m, 5H, Ph), 4.75 (t, $^3J_{HH}$ = 6.6 Hz, 1H, PhC*H*OH), 1.79–1.66 (m, 2H, CH_2CH(CH_3)$_2$), 1.62 (br. s, 2H,

OH overlapped with residual water), 1.52 (m, 1H, $CH_2CH(CH_3)_2$), 0.95 (d, $^3J_{HH}$ = 6.1 Hz, 6H, $CH_2CH(CH_3)_2$); **$^{13}C\{^1H\}$ NMR** (100.6 MHz, $CDCl_3$, 25 °C): δ 145.4, 128.6, 127.7, 126.0, 73.0, 48.5, 25.0, 23.3, 22.4.

2,2-dimethyl-1-phenylethanol (b3).[11]

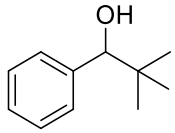

b3

According to general procedure, 2,2,2-trimethylacetophenone **a3** (167 μL, 1.0 mmol) afforded the title compound **b3** as an oil (50 mg, 30%). **^1H NMR** (400.1 MHz, $CDCl_3$, 25 °C): δ 7.41–7.19 (m, 5H, Ph), 4.40 (d, $^3J_{HH}$ = 2.5 Hz, 1H, PhC*H*OH), 1.89 (d, $^3J_{HH}$ = 2.5 Hz, 1H, PhC*H*OH), 0.93 (s, 9H, CH_3); **$^{13}C\{^1H\}$ NMR** (100.6 MHz, $CDCl_3$, 25 °C): δ 142.3, 127.75, 127.7, 127.4, 82.5, 35.8, 26.1.

1-(2-Methylphenyl)ethanol (b4).[11]

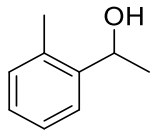

b4

According to general procedure, 2′-methylacetophenone **a4** (263 μL, 2.0 mmol) afforded the title compound **b4** as an oil (254 mg, 93%). **^1H NMR** (400.1 MHz, $CDCl_3$, 25 °C): δ 7.51 (d, J_{HH} = 7.6 Hz, 1H, C*H*$_{Ar}$), 7.28–7.12 (m, 3H, C*H*$_{Ar}$), 5.10 (q, $^3J_{HH}$ = 6.4 Hz, 1H, C*H*CH_3), 2.35 (s, 3H, C*H*$_{3\ Ar}$), 2.23 (br. s, 1H, OH), 1.46 (d, $^3J_{HH}$ = 6.5 Hz, 3H, CHC*H*$_3$); **$^{13}C\{^1H\}$ NMR** (100.6 MHz, $CDCl_3$, 25 °C): δ 143.9, 134.3, 130.4, 127.2, 126.4, 124.6, 66.8, 24.0, 19.0.

1-(3-Methylphenyl)ethanol (b5).[13]

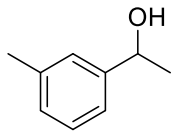

b5

According to general procedure, 3′-methylacetophenone **a5** (272 μL, 2.0 mmol) afforded the title compound **b5** as an oil (266 mg, 98%). **^1H NMR** (400.1 MHz, $CDCl_3$, 25 °C) δ 7.31–7.09 (m, 4H, C*H*$_{Ar}$), 4.88 (d, $^3J_{HH}$ = 6.0 Hz, 1H, C*H*CH_3), 2.40 (s, 3H, $CH_{3\ Ar}$), 2.05 (br. s, 1H, OH),

1.52 (d, $^3J_{HH}$ = 6.0 Hz, 3H, CHCH_3); **^{13}C{^{1}H} NMR** (100.6 MHz, $CDCl_3$, 25 °C): δ 145.9, 138.2, 128.5, 128.3, 126.2, 122.5, 70.5, 25.2, 21.6.

1-(4-Methylphenyl)ethanol (b6).[11]

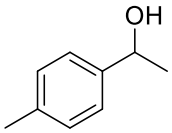

b6

According to general procedure, 4′-methylacetophenone **a6** (267 μL, 2.0 mmol) afforded the title compound **b6** as an oil (253 mg, 93%). **^{1}H NMR** (400.1 MHz, $CDCl_3$, 25 °C): δ 7.29 (d, $^3J_{HH}$ = 7.8 Hz, 2H, CH_{Tol}), 7.20 (d, $^3J_{HH}$ = 7.8 Hz, 2H, CH_{Tol}), 4.87 (q, $^3J_{HH}$ = 6.4 Hz, 1H, CHCH$_3$), 2.40 (s, 3H, CH_{3Tol} + OH), 1.51 (d, $^3J_{HH}$ = 6.4 Hz, 3H, CHCH$_3$); **^{13}C{^{1}H} NMR** (100.6 MHz, $CDCl_3$, 25 °C): δ 143.0, 137.1, 129.2, 125.4, 70.2, 25.1, 21.1.

1-(2,4,6-Trimethylphenyl)ethanol (b7).[11]

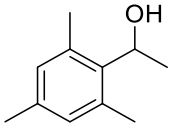

b7

According to general procedure, 2',4',6'-trimethylacetophenone **a7** (167 μL, 1.0 mmol) afforded the title compound **b7** as an oil (117.8 mg, 72%). **^{1}H NMR** (400.1 MHz, $CDCl_3$, 25 °C): δ 6.85 (s, 2H, CH_{Mes}), 5.36 (q, $^3J_{HH}$ = 6.7 Hz, 1H, CHCH$_3$), 2.44 (s, 6H, C$H_{3ortho\text{-}Mes}$), 2.29 (s, 3H, C$H_{3para\text{-}Mes}$), 2.13 (s, 1H, OH), 1.54 (d, $^3J_{HH}$ = 6.3 Hz, 3H, CHCH_3); **^{13}C {^{1}H} NMR** (100.6 MHz, $CDCl_3$, 25 °C): δ 137.8, 136.4, 135.7, 130.2, 21.6, 20.8, 20.6.

1-(4-Methoxyphenyl)ethanol (b8).[11]

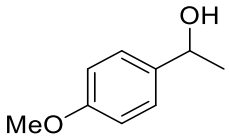

b8

According to general procedure, 4′-Methoxyacetophenone **a8** (600 mg, 4.0 mmol) afforded the title compound **b8** as an oil (596 mg, 98%). **^{1}H NMR** (400.1 MHz, $CDCl_3$, 25 °C): δ 7.29 (d, $^3J_{HH}$ = 8.2 Hz, 2H, CH_{Ar}), 6.88 (d, $^3J_{HH}$ = 8.2 Hz, 2H, CH_{Ar}), 4.85 (q, $^3J_{HH}$ = 6.4 Hz, 1H, CHCH$_3$), 3.80 (s, 1H, OCH_3), 1.99 (br. s, 1H, OH), 1.47 (d, $^3J_{HH}$ = 6.0 Hz, 3H, CHCH_3); **^{13}C{^{1}H} NMR** (100.6 MHz, $CDCl_3$, 25 °C): δ 158.2, 138.0, 126.3, 113.2, 69.2, 54.6, 24.8.

1-(4-Fluorophenyl)ethanol (b9).[11]

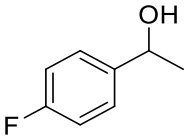

b9

According to general procedure, 4′-fluoroacetophenone **a9** (247.7 µL, 2.0 mmol) afforded the title compound **b9** as an oil (273.5 mg, 97%). **^{1}H NMR** (400.1 MHz, $CDCl_3$, 25 °C): δ 7.37–7.31 (m, 2H, CH_{Ar}), 7.06–6.99 (m, 2H, CH_{Ar}), 4.88 (q, $^3J_{HH}$ = 6.2 Hz, 1H, CHCH$_3$), 1.90 (br. s, 1H, OH), 1.48 (d, $^3J_{HH}$ = 6.5 Hz, 3H, CHCH_3); **^{19}F{^{1}H} NMR** (376.5 MHz, $CDCl_3$, 25 °C) δ –115.4; **^{13}C{^{1}H} NMR** (100.6 MHz, $CDCl_3$, 25 °C): δ 162.2 (d, $^1J_{FC}$ = 245.2 Hz) 141.6 (d, $^4J_{FC}$ = 3.1 Hz), 127.2 (d, $^3J_{FC}$ = 8.1 Hz), 115.4 (d, $^2J_{FC}$ = 21.3 Hz), 69.9, 25.4.

1-(4-Chlorophenyl)ethanol (b10).[11]

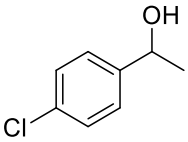

b10

According to general procedure, 4′-chroloacetophenone **a10** (129.5 µL, 1.0 mmol) afforded the title compound **b10** as a colorless oil (156 mg, 83%). **^{1}H NMR** (400.1 MHz, $CDCl_3$, 25 °C): δ 7.57–6.98 (m, 4H, CH_{Ar}), 4.85 (q, $^3J_{HH}$ = 6.4 Hz, 1H, CHCH$_3$), 2.15 (br. s, 1H, OH), 1.45 (d, $^3J_{HH}$ = 6.5 Hz, 3H, CHCH_3); **^{13}C{^{1}H} NMR** (100.6 MHz, $CDCl_3$, 25 °C): δ 144.4, 133.1, 128.7, 126.9, 69.8, 25.4.

1-(2-Bromophenyl)ethanol (b11).[14]

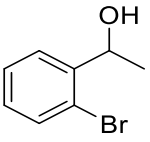

b11

According to general procedure, 2′-bromoacetophenone **a11** (269 µL, 2.0 mmol) afforded the title compound **b11** as a colorless oil (325 mg, 81%). **^{1}H NMR** (400.1 MHz, $CDCl_3$, 25 °C): δ 7.59 (dd, J_{HH} = 7.8 Hz, J_{HH} = 1.8 Hz, 1H, CH_{Ar}), 7.51 (J_{HH} = 8.0 Hz, J_{HH} = 1.2 Hz, 1H, CH_{Ar}), 7.37–7.31 (m, 1H, CH_{Ar}), 7.15–7.09 (ddd, J_{HH} = 8.0 Hz, J_{HH} = 7.3 Hz, J_{HH} = 1.2 Hz, 1H, CH_{Ar}), 5.24 (qd, $^3J_{HH}$ = 6.4 Hz, $^3J_{HH}$ = 3.3 Hz, 1H, CHCH$_3$), 2.06 (d, $^3J_{HH}$ = 3.3 Hz, 1H, OH), 1.48 (d, $^3J_{HH}$ = 6.4 Hz, 3H, CHCH_3); **^{13}C{^{1}H} NMR** (100.6 MHz, $CDCl_3$, 25 °C): δ 144.7, 132.7, 128.8, 127.9, 126.8, 121.7, 69.2, 23.7.

1-(4-Chlorophenyl)ethanol (b12).[15]

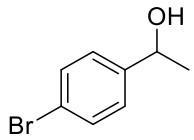

b12

According to general procedure, 4′-bromoacetophenone **a12** (796 mg, 4.0 mmol) afforded the title compound **b12** as a colorless oil (797 mg, 99%). **^{1}H NMR** (400.1 MHz, $CDCl_3$, 25 °C): δ 7.39 (d, $^3J_{HH}$ = 8.3 Hz, 2H, C*H*$_{Ar}$), 7.17 (d, $^3J_{HH}$ = 8.5 Hz, 2H, C*H*$_{Ar}$), 4.79 (q, $^3J_{HH}$ = 6.4 Hz, 1H, C*H*CH$_3$), 1.80 (br. s, 1H, OH), 1.39 (d, $^3J_{HH}$ = 6.4 Hz, 3H, CHC*H*$_3$); **^{13}C{^{1}H} NMR** (100.6 MHz, $CDCl_3$, 25 °C): δ 144.7, 131.3, 127.1, 120.9, 69.4, 25.1.

1-(4-Iodophenyl)ethanol (b13).[11]

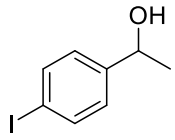

b13

According to general procedure, 4′-iodoacetophenone **a13** (246 mg, 1.0 mmol) afforded the title compound **b13** as an oil (195 mg, 79%). **^{1}H NMR** (400.1 MHz, $CDCl_3$, 25 °C): δ 7.65–7.68 (m, 2H, C*H*$_{Ar}$), 7.23–6.91 (m, 2H, C*H*$_{Ar}$), 4.84 (q, $^3J_{HH}$ = 6.5 Hz, 1H, C*H*CH$_3$), 1.89 (br. s, 1H, OH), 1.46 (d, $^3J_{HH}$ = 6.5 Hz, 3H, CHC*H*$_3$); **^{13}C{^{1}H} NMR** (100.6 MHz, $CDCl_3$, 25 °C): δ 145.6, 137.7, 127.5, 92.8, 70.0, 25.4.

1-(4-Trifluoromethyl)ethanol (b14).[11]

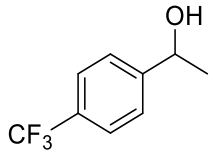

b14

According to general procedure, 4′-(trifluoromethyl)acetophenone **a14** (300 μL, 2.0 mmol) afforded the title compound **b14** as an oil (349 mg, 92%). **^{1}H NMR** (400.1 MHz, $CDCl_3$, 25 °C): δ 7.61 (d, $^3J_{HH}$ = 8.2 Hz, 2H, C*H*$_{Ar}$), 7.49 (d, $^3J_{HH}$ = 8.2 Hz, 2H, C*H*$_{Ar}$), 4.97 (qd, $^3J_{HH}$ = 6.5 Hz, $^3J_{HH}$ = 3.5 Hz, 1H, C*H*CH$_3$), 1.91 (d, $^3J_{HH}$ = 3.5 Hz, 1H, O*H*), 1.51 (d, $^3J_{HH}$ = 6.5 Hz, 3H, CHC*H*$_3$); **^{19}F{^{1}H} NMR** (376.5 MHz, $CDCl_3$, 25 °C) δ –62.5; **^{13}C{^{1}H} NMR** (100.6 MHz, $CDCl_3$, 25 °C): δ 149.8 (br s), 129.7 (q, J_{CF} = 32.4 Hz), 125.8 (s), 125.5 (q, J_{CF} = 3.8 Hz), 124.3 (q, J_{CF} = 271.5 Hz), 69.8, 25.3.

1-(2-Naphthyl)ethanol (b15).[11]

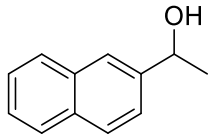

b15

According to general procedure, 2-acetonaphthone **a15** (680 mg, 4.0 mmol) afforded the title compound **b15** as a white solid (458 mg, 65%). **^{1}H NMR** (400.1 MHz, $CDCl_3$, 25 °C): δ 7.89–7.77 (m, 4H, CH_{Ar}), 7.55–7.45 (m, 3H, CH_{Ar}), 5.04 (q, $^3J_{HH}$ = 6.5 Hz, 1H, CHCH$_3$), 2.33 (br. s, 1H, OH), 1.58 (d, $^3J_{HH}$ = 6.4 Hz, 3H, CHCH_3); **^{13}C{^{1}H} NMR** (100.6 MHz, $CDCl_3$, 25 °C): δ 143.2, 133.2, 132.7, 128.1, 127.9, 127.6, 125.9, 125.6, 123.8, 123.7, 70.1, 25.0.

1-indanol (b16).[11]

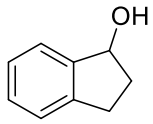

b16

According to general procedure, 1-indanone **a16** (528 mg, 4.0 mmol) afforded the title compound **b16** as an oil (280 mg, 92%). **^{1}H NMR** (400.1 MHz, $CDCl_3$, 25 °C): δ 7.44–7.40 (m, 1H, CH_{Ar}), 7.28–7.22 (m, 3H, CH_{Ar}), 5.25 (br t, $^3J_{HH}$ = 6.0 Hz, 1H, CHOH), 3.06 (ddd, $^2J_{HH}$ = 15.8 Hz, $^3J_{HH}$ = 8.3 Hz, $^3J_{HH}$ = 5.0 Hz, 1H, CH_2CHOH), 2.83 (ddd, $^2J_{HH}$ = 15.8 Hz, $^3J_{HH}$ = 8.3 Hz, $^3J_{HH}$ = 6.6 Hz, 1H, CH_2CHOH), 2.49 (dddd, $^2J_{HH}$ = 13.5 Hz, $^3J_{HH}$ = 8.6 Hz, $^3J_{HH}$ = 6.6 Hz, $^3J_{HH}$ = 5.0 Hz, 1H, CH_2CH$_2$CHOH), 1.95 (dddd, $^2J_{HH}$ = 13.5 Hz, $^3J_{HH}$ = 8.3 Hz, $^3J_{HH}$ = 6.8 Hz, $^3J_{HH}$ = 4.8 Hz, 1H, CH_2CH$_2$CHOH), 1.86 (br. s, 1H, OH); **^{13}C{^{1}H} NMR** (100.6 MHz, $CDCl_3$, 25 °C): δ 143.2, 133.2, 132.7, 128.1, 127.9, 127.6, 125.9, 125.6, 123.8, 123.7, 70.1, 25.0.

1,3-Diphenyl-1-propanol (b17).[11]

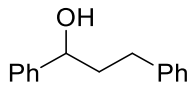

b17

According to general procedure, 3-phenylpropiophenone **a17** (528 mg, 4.0 mmol) afforded the title compound **b17** as an oil (280 mg, 92%). **^{1}H NMR** (400.1 MHz, $CDCl_3$, 25 °C): δ 7.42–7.18 (m, 10H, CH_{Ar}), 4.70 (dd, $^3J_{HH}$ = 7.7 Hz, $^3J_{HH}$ = 5.4 Hz, 1H, CH$_2$CH$_2$CHOH), 2.85–2.73

(m, 2H, CH_2CH_2CHOH), 2.24–1.97 (m, 3H, CH_2CH_2CHOH); **$^{13}C\{^1H\}$ NMR** (100.6 MHz, $CDCl_3$, 25 °C): δ 144.6, 141.9, 128.55, 128.50, 128.45, 127.6, 126.0, 125.9, 73.9, 40.5, 32.1.

α-Cyclopropylbenzyl alcohol (b18).[14]

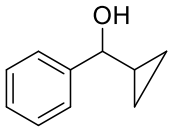

b18

According to general procedure, phenyl(cyclopropyl)ketone **a18** 276 µL, 2.0 mmol) afforded the title compound **b18** as an oil (109 mg, 37%). **^1H NMR** (400.1 MHz, $CDCl_3$, 25 °C): δ 7.48–7.41 (m, 2H, CH_{Ar}), 7.40–7.33 (m, 2H, CH_{Ar}), 7.32–7.26 (m, 1H, CH_{Ar}), 4.02 (dd, $^3J_{HH}$ = 8.3 Hz, $^3J_{HH}$ = 2.6 Hz, 1H, CHOH), 1.94 (br. d, $^3J_{HH}$ = 2.6 Hz, 1H, OH), 1.28–1.18 (m, 1H, C_3H_5), 0.70–0.61 (m, 1H, C_3H_5), 0.60–0.52 (m, 1H, C_3H_5), 0.52–0.44 (m, 1H, C_3H_5), 0.43–0.35 (m, 1H, C_3H_5); **$^{13}C\{^1H\}$ NMR** (100.6 MHz, $CDCl_3$, 25 °C): δ 144.0, 128.3, 127.5, 126.1, 78.5, 19.2, 3.7, 2.8.

2-undecanol (b19).[11]

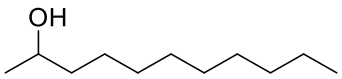

b19

According to general procedure, 2-undecanone **a19** (246 mg, 1.0 mmol) afforded the title compound **b19** as an oil (195 mg, 98%). **^1H NMR** (400.1 MHz, $CDCl_3$, 25 °C): δ 3.84–3.74 (m, 1H, $CH_2CH(OH)CH_3$), 1.48–1.36 (m, 5H, CH_2 + OH), 1.33–1.22 (m, 12H, CH_2), 1.18 (d, $^3J_{HH}$ = 6.2 Hz, 3H, $CH_2CH(OH)CH_3$), 0.88 (d, $^3J_{HH}$ = 6.5 Hz, 3H, CH_2CH_3); **$^{13}C\{^1H\}$ NMR** (100.6 MHz, $CDCl_3$, 25 °C): δ 68.3, 39.5, 32.0, 29.8, 29.75, 29.7, 29.4, 25.9, 23.6, 22.8, 14.2.

4.6 Synthesis of the Tridentate Ligands

4.6.1 Synthesis of the Phosphine Oxide Ligands [L6(O)], [L7(O)], and [L8(O)]

Synthesis of [$Ph_2P(O)CH_2Im$] [$L^a6(O)$]

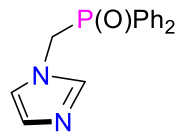

$L^a6(O)$

A Schlenk tube was charged with $Ph_2P(O)CH_2OTs$ (4.0 g, 10.4 mmol), 1*H*-imidazole (0.71 g, 10.4 mmol) and K_2CO_3 (9.67 g, 70.0 mmol) under an air atmosphere. After addition of DMSO (40 mL), the suspension was vigorously stirred at 90 °C for 24 h. The reaction mixture was cooled to 50 °C and DMSO was removed under reduced pressure. The solid residue was dissolved in $CHCl_3$ (20 mL), the solution was washed several times with H_2O, dried over $MgSO_4$ and evaporated under reduced pressure. The resulting solid was washed with Et_2O (20 mL) and dried under vacuum to afford **L^{a}6(O)** as a white powder (1.98 g, 70%). **^{1}H NMR** (400 MHz, $CDCl_3$, 25 °C): δ 7.70–7.65 (m, 4H, CH_{Ph}), 7.61–7.57 (m, 2H, CH_{Ph}), 7.52–7.47 (m, 4H, CH_{Ph}), 7.30 (br s, 1H, C$H_{Im\text{-}2}$), 6.96 (br s, 1H, C$H_{Im\text{-}4,5}$), 6.91 (br s, 1H, C$H_{Im\text{-}4,5}$), 4.77 (d, J_{PH} = 4.5 Hz, 2H, CH_2); **^{31}P{^{1}H} NMR** (162 MHz, $CDCl_3$, 25 °C): δ 25.7 (s); **^{13}C{^{1}H} NMR** (101 MHz, $CDCl_3$, 25 °C): δ 137.9 (br s, $CH_{Im\text{-}2}$), 132.9 (d, J_{PC} = 2.5 Hz, CH_{Ph}), 131.2 (d, J_{PC} = 9.5 Hz, CH_{Ph}), 129.7 (s, $CH_{Im\text{-}4,5}$), 129.1 (d, J_{PC} = 103.7 Hz, $C_{ipso\ Ph}$), 129.0 (d, J_{PC} = 18.0 Hz, CH_{Ph}), 120.3 (s, $CH_{Im\text{-}4,5}$), 47.8 (d, J_{PC} = 73.9 Hz, CH_2); **Anal.** Found: C, 65.58; H, 5.63; N, 9.48. Calcd. (%) for $C_{16}H_{15}N_2OP$. 0.25 (DMSO): C, 65.66; H, 5.51; N, 9.28; **HRMS** (ESI, POS): m/z calcd. for $C_{16}H_{16}N_2OP^+$ $[M + H]^+$ 283.1000, found, 283.1006 (ε_r = 2.1 ppm).

Synthesis of [(Ph$_2$P(O)CH$_2$)$_2$Im]OTs [L6(O)]

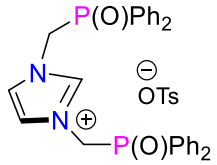

L6(O)

A mixture of **L^{a}6(O)** (1.26 g, 4.5 mmol) and $Ph_2P(O)CH_2OTs$ (1.70 g, 4.5 mmol) was heated under stirring in toluene (5 mL) at 130 °C for 16 h. After cooling to room temperature, the light-brown solid formed was dissolved in CH_2Cl_2 (5 mL) and then Et_2O (50 mL) was added. The resulting precipitate was triturated with Et_2O (20 mL) until the formation of a white powder (*ca*. 30 min). The supernatant was then removed by decantation and the precipitate was washed with Et_2O (10 mL) and dried under vacuum to afford **L6(O)** as a white powder (2.6 g, 87%). **^{1}H NMR** (400 MHz, $CDCl_3$, 25 °C): δ 9.85 (s, 1H, C$H_{Im\text{-}2}$), 7.82–7.77 (m, 10H, CH_{Ar}), 7.48–7.42 (m, 6H, CH_{Ar}), 7.34–7.30 (m, 8H, CH_{Ar}), 7.08 (d, J_{HH} = 7.8 Hz, 2H, CH_{Ts}), 5.28 (d, J_{PH} = 6.3 Hz, 4H, CH_2), 2.30 (s, 3H, CH_{3Ts}); **^{31}P{^{1}H} NMR** (162 MHz, $CDCl_3$, 25 °C): δ 26.5 (s). **^{13}C{^{1}H} NMR** (101 MHz, $CDCl_3$, 25 °C): δ 143.6 (s, C_{Ts}), 139.6 (s, C_{Ts}), 138.6 (s, $CH_{Im\text{-}2}$), 133.0 (d, J_{PC} = 2.0 Hz, CH_{Ph}), 131.3 (d, J_{PC} = 9.9 Hz, CH_{Ph}), 129.2 (d, J_{PC} = 12.5 Hz, CH_{Ph}), 128.8 (s, CH_{Ts}), 127.9 (d, J_{PC} = 103.8 Hz, $C_{ipso\ Ph}$), 126.0 (s, CH_{Ts}), 123.2 (s, $CH_{Im\text{-}4,5}$), 48.6 (d, J_{PC} = 66.0 Hz, CH_2), 21.4 (s, CH_{3Ts}); **Anal.** Found: C, 59.71; H, 4.97; N, 3.84. Calcd. (%) for

$C_{36}H_{34}N_2O_5P_2S$. 0.85 (CH_2Cl_2): C, 59.74; H, 4.86; N, 3.78; **HRMS** (ESI, POS): m/z calcd. for $C_{29}H_{27}N_2O_2P_2^+$ $[M - OTs]^+$ 497.1548; found, 497.1534 (ε_r = 2.8 ppm).

Synthesis of [$Ph_2P(O)CH_2ImPy$]OTs [L7(O)]

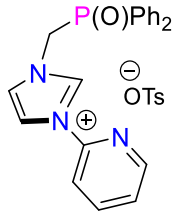

L7(O)

A mixture of 2-(1H-imidazol-1-yl)pyridine (0.68 g, 4.7 mmol) and $Ph_2P(O)CH_2OTs$ (1.5 g, 3.9 mmol) was heated under stirring at 150 °C for 16 h. After cooling to room temperature, the resulting brown solid was dissolved in CH_2Cl_2 (5 mL) and then Et_2O (100 mL) was added. The resulting precipitate was triturated with Et_2O (30 mL) until the formation of a white powder (*ca.* 30 min). The supernatant was removed by decantation and the precipitate was washed with Et_2O (10 mL) and dried under vacuum to afford **L7(O)** as a very hygroscopic white powder (1.8 g, 90%). **^{1}H NMR** (400 MHz, $CDCl_3$, 25 °C): δ 10.44 (s, 1H, C*H*$_{Im\text{-}2}$), 8.34 (d, J_{HH} = 4.6 Hz, 1H, C*H*$_{Ar}$), 8.08 (s, 1H, C*H*$_{Ar}$), 7.99–7.94 (m, 5H, C*H*$_{Ar}$), 7.86 (s, 1H, C*H*$_{Ar}$), 7.79–7.82 (m, 3H, C*H*$_{Ar}$), 7.47–7.39 (m, 6H, C*H*$_{Ar}$), 7.32–7.28 (m, 1H, C*H*$_{Ar}$), 7.08 (d, J_{HH} = 7.8 Hz, 2H, C*H*$_{Ts}$), 5.75 (d, J_{PH} = 6.3 Hz, 2H, P(O)C*H*$_2$), 2.27 (s, 3H, C*H*$_{3Ts}$); **^{31}P{^{1}H} NMR** (162 MHz, $CDCl_3$, 25 °C): δ 27.1 (s); **^{13}C{^{1}H} NMR** (101 MHz, $CDCl_3$, 25 °C): δ 148.8 (s, *C*H$_{Py}$), 145.7 (s, *C*$_{Py}$), 143.3 (s, *C*$_{Ts}$), 140.5 (s, *C*H$_{Py}$), 139.5 (s, *C*$_{Ts}$), 135.6 (d, J_{PC} = 2.6 Hz, *C*H$_{Im\text{-}2}$), 133.0 (d, J_{PC} = 2.6 Hz, *C*H$_{Ph}$), 131.3 (d, J_{PC} = 9.9 Hz, *C*H$_{Ph}$), 129.2 (d, J_{PC} = 12.5 Hz, *C*H$_{Ph}$), 128.7 (s, *C*H$_{Ts}$), 127.9 (d, J_{PC} = 103.6 Hz, *C*$_{ipso\ Ph}$), 125.9 (s, *C*H$_{Ts}$), 125.0 (s, *C*H$_{Py}$), 124.3 (s, *C*H$_{Py}$), 118.6 (s, *C*H$_{Im\text{-}4,5}$), 114.4 (s, *C*H$_{Im\text{-}4,5}$), 49.2 (d, J_{PC} = 66.5 Hz, P(O)*C*H$_2$), 21.3 (s, *C*H$_{3Ts}$); **Anal.** Found: C, 61.26; H, 4.87; N, 7.76. Calcd. (%) for $C_{28}H_{26}N_3O_4PS$. 0.25 (CH_2Cl_2): C, 61.38; H, 4.83; N, 7.60; **HRMS** (ESI, POS): m/z calcd. for $C_{21}H_{19}N_3OP^+$ $[M - OTs]^+$ 360.1266; found, 360.1266 (ε_r = 0.0 ppm).

Synthesis of [$Ph_2P(O)CH_2ImCH_2Py$]OTs [L8(O)]

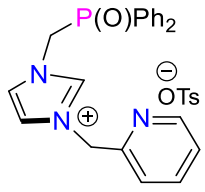

L8(O)

A mixture of 2-(1H-imidazol-1-yl-methyl)pyridine (1.98 g, 12.4 mmol) and $Ph_2P(O)CH_2OTs$ (4.00 g, 10.4 mmol) was heated under stirring at 140 °C for 16 h. After cooling to room temperature, the brown solid formed was dissolved in CH_2Cl_2 (5 mL) and then Et_2O (100 mL) was added. The resulting precipitate was triturated with Et_2O (30 mL) until the formation of a white/brown powder (*ca.* 30 min). The supernatant was removed by decantation and the precipitate was washed with Et_2O (10 mL) and dried under vacuum to afford **L8(O)** (4.8 g, 87%) as very hygroscopic brown crystals. **^{1}H NMR** (400 MHz, $CDCl_3$, 25 °C): δ 9.95 (s, 1H, C$H_{Im\text{-}2}$), 8.43 (d, J = 4.8 Hz, 1H, CH_{Ar}), 7.97–7.88 (m, 4H, CH_{Ar}), 7.79 (d, J_{HH} = 7.7 Hz, 2H, CH_{Ts}), 7.65 (s, 1H, CH_{Ar}), 7.63–7.58 (m, 1H, CH_{Ar}), 7.51–7.45 (m, 2H, CH_{Ar}), 7.43–7.35 (m, 4H, CH_{Ar}), 7.36–7.29 (m, 2H, CH_{Ar}), 7.24–7.19 (m, 1H, CH_{Ar}), 7.12 (d, J_{HH} = 7.8 Hz, 2H, CH_{Ts}), 5.46 (d, J_{PH} = 6.2 Hz, 2H, P(O)CH_2), 5.33 (s, 2H, PyCH_2), 2.32 (s, 3H, CH_{3Ts}); **^{31}P{^{1}H} NMR** (162 MHz, $CDCl_3$, 25 °C): δ 27.2 (s); **^{13}C{^{1}H} NMR** (101 MHz, $CDCl_3$, 25 °C): δ 152.3 (s, C_{Py}), 149.9 (s, CH$_{Py}$), 143.5 (s, C_{Ts}), 139.6 (s, C_{Ts}), 138.5 (d, J_{PC} = 2.3 Hz, CH$_{Im\text{-}2}$), 137.7 (s, CH$_{Py}$), 133.1 (d, J_{PC} = 2.3 Hz, CH$_{Ph}$), 131.4 (d, J_{PC} = 10.0 Hz, CH$_{Ph}$), 129.3 (d, J_{PC} = 12.5 Hz, CH$_{Ph}$), 128.8 (s, CH$_{Ts}$), 127.9 (d, J_{PC} = 103.3 Hz, $C_{ipso\ Ph}$), 126.0 (s, CH$_{Ts}$), 124.0 (s, CH$_{Py}$), 123.5 (s, CH$_{Py}$), 123.4 (s, CH$_{Im\text{-}4,5}$), 122.3 (s, CH$_{Im\text{-}4,5}$), 54.3 (s, PyCH$_2$), 48.9 (d, J_{PC} = 66.0 Hz, P(O)CH$_2$), 21.4 (s, CH$_{3Ts}$); **Anal.** Found: C, 61.20; H, 5.02; N, 7.64. Calcd. (%) for $C_{29}H_{28}N_3O_4PS$. 0.35 (CH_2Cl_2): C, 61.27; H, 5.03; N, 7.30; **HRMS** (ESI, POS): m/z calcd. for $C_{22}H_{21}N_3OP^+$ (M – OTs]$^+$ 374.1422; found, 374.1431 (ε_r = 2.4 ppm).

4.6.2 Synthesis of the Phosphine Ligands [L6], [L7], and [L8]

Synthesis of [(Ph$_2$PCH$_2$)$_2$Im]OTs [L6]

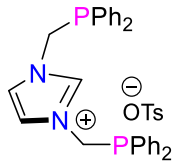

L6

According to the general procedure (**II**), (**Method A**): **L6(O)** (0.50 g, 0.75 mmol) afforded the title compound **L6** (0.38 g, 80%) as a white powder. According to the general procedure (**II**), (**Method B**): **L6(O)** (4.0 g, 6.0 mmol) afforded the title compound **L6** (3.4 g, 89%).as a beige powder. Single crystals suitable for X-ray diffraction analysis were obtained by slow evaporation of a concentrated CH_2Cl_2 solution at room temperature. **^{1}H NMR** (400 MHz, $CDCl_3$, 25 °C): δ 9.62 (s, 1H, C$H_{Im\text{-}2}$), 7.79 (d, J_{HH} = 8.1 Hz, 2H, CH_{Ts}), 7.43–7.30 (m, 20H,

C*H*$_{Ph}$), 7.10 (d, J_{HH} = 7.9 Hz, 2H, C*H*$_{Ts}$), 6.88 (brs, 2H, C*H*$_{Im\text{-}4,5}$), 4.92 (d, J_{PH} = 5.5 Hz, 4H, C*H*$_2$), 2.31 (s, 3H, C*H*$_{3Ts}$); **^{31}P{^{1}H} NMR** (162 MHz, $CDCl_3$, 25 °C): δ –12.4 (s); **^{13}C{^{1}H} NMR** (101 MHz, $CDCl_3$, 25 °C): δ 143.9 (s, *C*$_{Ts}$), 139.3 (s, *C*$_{Ts}$), 138.1 (s, *C*H$_{Im\text{-}2}$), 133.1 (d, J_{PC} = 19.8 Hz, *C*H$_{Ph}$), 133.0 (d, J_{PC} = 13.1 Hz, *C*$_{*ipso* Ph}$), 130.2 (s, *C*H$_{Ph}$), 129.3 (d, J_{PC} = 7.0 Hz, *C*H$_{Ph}$), 128.7 (s, *C*H$_{Ts}$), 126.2 (s, *C*H$_{Ts}$), 121.9 (d, J_{PC} = 4.2 Hz, *C*H$_{Im\text{-}4,5}$), 48.9 (d, J_{PC} = 21.1 Hz, *C*H$_2$), 21.4 (s, *C*H$_{3Ts}$); **Anal.** Found: C, 65.83; H, 5.19; N, 4.25. Calcd. (%) for $C_{36}H_{34}N_2O_3P_2S$. 0.30 (CH_2Cl_2): C, 65.84; H, 5.27; N, 4.23; **HRMS** (ESI, POS): m/z calcd. for $C_{29}H_{27}N_2P_2$ [M – OTs]$^+$ 465.1649; found, 465.1648 (ε_r = 0.2 ppm).

Synthesis of [Ph$_2$PCH$_2$ImPy]OTs [L7].

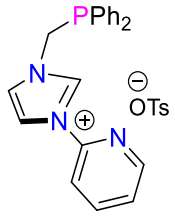

L7

According to the general procedure (**II**), **(Method B)**: **L7(O)** (2.0 g, 3.8 mmol) afforded the title compound **L7** (1.7 g, 89%).as a beige powder. **^{1}H NMR** (600 MHz, $CDCl_3$, 25 °C): δ 10.59 (s, 1H, C*H*$_{Im\text{-}2}$), 8.40 (d, *J* = 4.5 Hz, 1H, C*H*$_{Ar}$), 8.26 (d, *J* = 8.2 Hz, 1H, C*H*$_{Ar}$), 8.08 (s, 1H, C*H*$_{Ar}$), 7.90–7.88 (m, 1H, C*H*$_{Ar}$), 7.79 (d, J_{HH} = 7.8 Hz, 2H, C*H*$_{Ts}$), 7.54–7.51 (m, 4H, C*H*$_{Ar}$), 7.37–7.32 (m, 7H, C*H*$_{Ar}$), 7.22 (s, 1H, C*H*$_{Ar}$), 7.09 (d, J_{HH} = 7.8 Hz, 2H, C*H*$_{Ts}$), 5.34 (d, J_{PH} = 5.3 Hz, 2H, P(O)C*H*$_2$), 2.30 (s, 3H, C*H*$_{3Ts}$). **^{31}P{^{1}H} NMR** (162 MHz $CDCl_3$, 25 °C): δ –11.1 (s); **^{13}C{^{1}H} NMR** (151 MHz, $CDCl_3$, 25 °C): δ 148.9 (s, *C*H$_{Py}$), 146.0 (s, *C*$_{Py}$), 143.6 (s, *C*$_{Ts}$), 140.8 (s, *C*H$_{Py}$), 139.5 (s, *C*$_{Ts}$), 136.0 (s, *C*H$_{Im\text{-}2}$), 133.4 (d, J_{PC} = 19.8 Hz, *C*H$_{Ph}$), 132.9 (d, J_{PC} = 12.0 Hz, *C*$_{*ipso* Ph}$), 130.3 (s, *C*H$_{Ph}$), 129.3 (d, J_{PC} = 7.3 Hz, *C*H$_{Ph}$), 128.8 (s, *C*H$_{Ts}$), 126.1 (s, *C*H$_{Ts}$), 125.0 (s, *C*H$_{Py}$), 122.7 (s, *C*H$_{Py}$), 118.7 (s, *C*H$_{Im\text{-}4,5}$), 115.0 (s, *C*H$_{Im\text{-}4,5}$), 49.7 (d, J_{PC} = 21.9 Hz, P*C*H$_2$), 21.4 (s, *C*H$_{3Ts}$); **Anal.** Found: C, 61.43; H, 4.91; N, 7.31. Calcd. (%) for $C_{28}H_{26}N_3O_3PS$. 0.50 (CH_2Cl_2): C, 61.34; H, 4.88; N, 7.53; **HRMS** (ESI, POS): m/z calcd. for $C_{21}H_{19}N_3P^+$ [M – OTs]$^+$ 344.1317; found, 344.1317 (ε_r = 0.0 ppm).

Synthesis of [$Ph_2PCH_2ImCH_2Py$]OTs [L8]

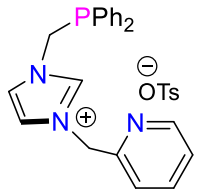

L8

According to the general procedure (**II**), **(Method B)**: **L8(O)** (2.8 g, 5.3 mmol) afforded the title compound **L8** (2.4 g, 86%) as very hygroscopic brown crystals. **^{1}H NMR** (400 MHz, $CDCl_3$, 25 °C): δ 9.56 (s, 1H, C$H_{Im\text{-}2}$), 8.37 (d, J = 4.8 Hz, 1H, CH_{Ar}), 7.74 (d, J_{HH} = 7.7 Hz, 2H, CH_{Ts}), 7.55–7.52 (m, 1H, CH_{Ar}), 7.44 (s, 1H, CH_{Ar}), 7.39–7.36 (m, 5H, CH_{Ar}), 7.30–7.20 (m, 6H, CH_{Ar}), 7.18–7.10 (m, 2H, CH_{Ar}), 7.04 (d, J_{HH} = 7.7 Hz, 2H, CH_{Ts}), 5.36 (s, 2H, PyCH_2), 4.95 (d, J_{PH} = 5.4 Hz, 2H, PCH_2), 2.26 (s, 3H, CH_{3Ts}); **^{31}P{^{1}H} NMR** (162 MHz, $CDCl_3$, 25 °C): δ –12.2 (s); **^{13}C{^{1}H} NMR** (101 MHz, $CDCl_3$, 25 °C): δ 152.6 (s, C_{Py}), 149.5 (s, CH_{Py}), 143.9 (s, C_{Ts}), 139.0 (s, C_{Ts}), 137.5 (s, $CH_{Im\text{-}2}$), 137.3 (s, CH_{Py}), 133.0 (d, J_{PC} = 19.4 Hz, CH_{Ph}), 132.9 (d, J_{PC} = 11.4 Hz, $C_{ipso\ Ph}$), 129.9 (s, CH_{Ph}), 128.9 (d, J_{PC} = 7.4 Hz, CH_{Ph}), 128.5 (s, CH_{Ts}), 125.9 (s, CH_{Ts}), 123.5 (s, CH_{Py}), 123.4 (s, CH_{Py}), 122.7 (s, $CH_{Im\text{-}4,5}$), 121.9 (s, $CH_{Im\text{-}4,5}$), 53.7 (s, PyCH_2), 48.7 (d, J_{PC} = 22.1 Hz, PCH_2), 21.2 (s, CH_{3Ts}); **Anal.** Found: C, 63.25; H, 5.06; N, 8.15. Calcd. (%) for $C_{29}H_{28}N_3O_3PS$. $0.3CH_2Cl_2$: C, 63.40; H, 5.19; N, 7.57; **HRMS** (ESI, POS): m/z calcd. for $C_{22}H_{21}N_3P^+$ $[M - OTs]^+$ 358.1473; found, 358.1482 (ε_r = 2.5 ppm).

4.7 Synthesis of the Bidentate Complexes C6, C7, C7' and C8

Synthesis of PCP Bidentate Complex C6

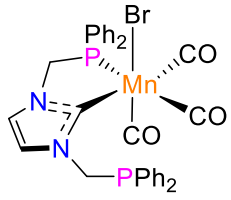

C6

According to the general procedure (**III**), **L6** (0.40 g, 0.63 mmol) in toluene (30 mL), afforded complex **C6** (0.32 g, 71%) as a yellow powder. **^{1}H NMR** (400 MHz, CD_2Cl_2, 25 °C): δ 7.93 (t, J = 8.7 Hz, 2H, CH_{Ph}), 7.56–7.35 (m, 16H, CH_{Ph}), 7.21–7.13 (m, 3H, CH_{Ph}), 6.99 (br s, 1H, C$H_{Im\text{-}4,5}$), 5.22 (dd, J_{HH} = 14.2 Hz, J_{PH} = 4.4 Hz, 1H, PCH_2), 5.07 (dd, J_{HH} = 14.2 Hz, J_{PH} = 3.5 Hz, 1H, PCH_2), 4.88–4.98 (m, 2H, PCH_2).**^{31}P{^{1}H} NMR** (162 MHz, CD_2Cl_2, 25 °C): δ 71.0 (s), –17.0 (s); **^{13}C{^{1}H} NMR** (101 MHz, CD_2Cl_2, 25 °C): δ 222.9 (d, J_{PC} = 17.8 Hz, CO), 221.4 (d, J_{PC} = 31.0 Hz, CO), 220.1 (d, J_{PC} = 21.5 Hz, CO), 197.1 (d, J_{PC} = 16.5 Hz, CN_2), 135.6 (d,

J_{PC} = 3.0 Hz, $C_{ipso\ Ph}$), 135.4 (d, J_{PC} = 21.2 Hz, $C_{ipso\ Ph}$), 135.2 (d, J_{PC} = 8.1 Hz, $C_{ipso\ Ph}$), 134.7 (d, J_{PC} = 9.9 Hz, CH$_{Ph}$), 133.6 (d, J_{PC} = 19.8 Hz, CH$_{Ph}$), 133.2 (d, J_{PC} = 19.1 Hz, CH$_{Ph}$), 131.8 (s, CH$_{Ph}$), 130.6 (d, J_{PC} = 10.1 Hz, CH$_{Ph}$), 130.5 (s, CH$_{Ph}$), 130.1 (s, CH$_{Ph}$), 129.9 (s, CH$_{Ph}$), 129.4 (s, CH$_{Ph}$), 129.2 (d, J_{PC} = 6.1 Hz, CH$_{Ph}$), 129.1 (s, CH$_{Ph}$), 124.2 (d, J_{PC} = 9.9 Hz, CH$_{Im\text{-}4,5}$), 120.5 (d, J_{PC} = 6.8 Hz, CH$_{Im\text{-}4,5}$), 52.3 (d, J_{PC} = 30.3 Hz, PCH$_2$), 52.2 (d, J_{PC} = 17.2 Hz, PCH$_2$); **IR** (toluene): ν_{CO} 2015 (s), 1940 (s), 1910 (s) cm^{-1}; **Anal.** Found: C, 54.50; H, 3.33; N, 4.13. Calcd. (%) for $C_{32}H_{26}BrMnN_2O_3P_2$. 0.35 ($CH_2Cl_2$): C, 54.49; H, 3.77; N, 3.93; **HRMS** (ESI, POS): m/z calcd. for $C_{32}H_{26}MnN_2O_3P_2^+$ [M – Br]$^+$ 603.0799; found, 603.0799 (ε_r = 0.0 ppm).

Synthesis of PCN Bidentate Complexes C7 and C7'

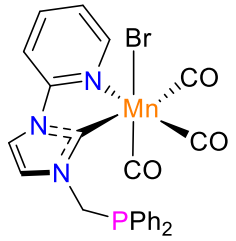

C7

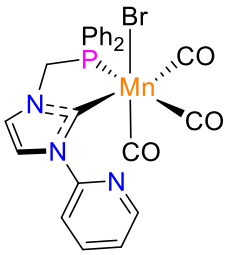

C7'

To a stirred suspension of **L7** (0.20 g, 0.39 mmol) in THF (30 mL), a solution of KHMDS (0.5 M in Toluene, 0.9 mL, 0.43 mmol) was added at r.t. and then the resulting brown suspension was sonicated during 5 min and stirred for additional 5 min. Solid [Mn(CO)$_5$Br] (0.11 g, 0.39 mmol) was added in one portion inducing a vigorous CO evolution. The resulting orange solution was then stirred for 15 min at room temperature. After filtration through Celite and evaporation of the solvent under vacuum, a mixture of two complexes **C7** and **C7'** in a 3:1 ratio was obtained as yellow-orange powder (0.16 g, 80%). The crude residue was recrystallized in THF/Et$_2$O mixture affording complex **C7** as a yellow-orange powder (0.11 g, 51%). Single crystals for both complexes suitable for X-ray diffraction analysis were obtained by slow evaporation of CH_2Cl_2 solutions at room temperature. **C7**: **^{1}H NMR** (400 MHz, CD_2Cl_2, 25 °C): δ 8.97 (d, J = 5.5 Hz, 1H, CH_{Ar}), 7.94 (t, J = 8.0 Hz, 1H, CH_{Ar}), 7.60–7.48 (m, 6H, CH_{Ar}), 7.45–7.37 (m, 6H, CH_{Ar}), 7.30 (t, J = 4.0 Hz, 1H, CH_{Ar}), 6.83 (s, 1H, CH_{Ar}), 5.37 (dd, J = 14.1, 8.2 Hz, 1H, PCH_2), 4.99 (dd, J = 14.1, 1.8 Hz, 1H, PCH_2); **^{31}P{^{1}H} NMR** (162 MHz, CD_2Cl_2, 25 °C): δ –15.9 (s); **^{13}C{^{1}H} NMR** (101 MHz, CD_2Cl_2, 25 °C): δ 226.4 (s, CO), 221.3 (s, CO), 218.0 (s, CO), 206.0 (s, CN$_2$), 153.9 (s, CH$_{Py}$), 153.0 (s, C_{Py}), 140.6 (s, CH$_{Py}$), 135.4 (d, J_{PC} = 13.2 Hz, $C_{ipso\ Ph}$), 135.0 (d, J_{PC} = 14.0 Hz, $C_{ipso\ Ph}$), 134.1 (d, J_{PC} = 19.9 Hz, CH$_{Ph}$), 132.9 (d, J_{PC} = 18.8 Hz, CH$_{Ph}$), 130.5 (s, CH$_{Ph}$), 129.9 (s, CH$_{Ph}$), 129.5 (d, J_{PC} = 7.3 Hz, CH$_{Ph}$), 129.3 (d,

J_{PC} = 6.5 Hz, CH_{Ph}), 125.1 (d, J_{PC} = 5.8 Hz, $CH_{Im\text{-}4,5}$), 122.8 (s, $CH_{Im\text{-}4,5}$), 115.9 (s, CH_{Py}), 111.7 (s, CH_{Py}), 51.9 (d, J_{PC} = 17.5 Hz, PCH_2); **IR** (THF): ν_{CO} 2016 (s), 1930 (s), 1907 (s) cm^{-1}; **Anal.** Found: C, 51.28; H, 2.71; N, 7.46. Calcd. (%) for $C_{24}H_{18}BrMnN_3O_3P$: C, 51.27; H, 3.23; N, 7.47; **HRMS** (ESI, POS): m/z calcd. for $C_{24}H_{19}MnBrN_3O_3P^+$ $[M + H]^+$ 561.9728; found, 561.9730 (ε_r = 0.4 ppm).

The NMR and IR data of complex **C7'** were deduced from the **C7/C7'** mixture. **C7'**: **^{1}H NMR** (400 MHz, CD_2Cl_2, 25 °C): δ 8.67 (d, J = 4.0 Hz, 1H, CH_{Ar}), 7.98–7.94 (m, 3H, CH_{Ar}), 7.61–7.24 (m, 12H, CH_{Ar}), 5.11 (t, J = 12.0 Hz, 1H, PCH_2), 4.97 (d, J = 12.0 Hz, 1H, PCH_2); **^{31}P{^{1}H} NMR** (162 MHz, CD_2Cl_2, 25 °C): δ 71.8 (s); **^{13}C{^{1}H} NMR** (101 MHz, CD_2Cl_2): δ 223.9 (d, J_{PC} = 18.2 Hz, CO), 220.2 (d, J_{PC} = 18.2 Hz, CO), 218.5 (d, J_{PC} = 32.3 Hz, CO), 198.1 (d, J_{PC} = 15.1 Hz, CN_2), 153.1 (s, C_{Py}), 150.0 (s, CH_{Py}), 139.3 (s, CH_{Py}), 136.1 (d, J_{PC} = 37.4 Hz, $C_{ipso\ Ph}$), 135.0 (d, J_{PC} = 10.1 Hz, CH_{Ph}), 131.9 (d, J_{PC} = 2.0 Hz, CH_{Ph}), 130.5 (s, CH_{Ph}), 130.4 (d, J_{PC} = 10.1 Hz, CH_{Ph}), 129.3 (d, J_{PC} = 9.1 Hz, CH_{Ph}), 129.2 (d, J_{PC} = 9.1 Hz, CH_{Ph}), 125.2 (s, CH_{Py}), 125.1 (s, CH_{Py}), 122.2 (s, $CH_{Im\text{-}4,5}$), 120.9 (d, J_{PC} = 4.0 Hz $CH_{Im\text{-}4,5}$), 52.2 (d, J_{PC} = 30.3 Hz, PCH_2); **IR** (THF): ν_{CO} 2016 (s), 1939 (s), 1904 (s) cm^{-1}.

Synthesis of PCN Bidentate Complex C8

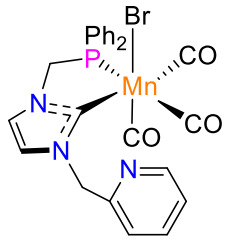

C8

According to the general procedure (**III**), **L8** (0.32 g, 0.60 mmol) in THF (20 mL), afforded complex **C8** as a yellow-orange powder (0.21 g, 60%). The crude product was purified by column chromatography on basic activated aluminium oxide using THF/toluene mixture as eluent. Single crystals suitable for X-ray diffraction analysis were obtained by slow evaporation of complex solution in CH_2Cl_2/toluene mixture at room temperature. **^{1}H NMR** (400 MHz, CD_2Cl_2, 25 °C): δ 8.57 (d, J = 4.7 Hz, 1H, CH_{Ar}), 8.00–7.91 (m, 2H, CH_{Ar}), 7.68–7.65 (m, 1H, CH_{Ar}), 7.57–7.50 (m, 3H, CH_{Ar}), 7.43–7.32 (m, 4H, CH_{Ar}), 7.27–7.13 (m, 5H, CH_{Ar}), 5.74 (d, J_{HH} = 16.0 Hz, 1H, $PyCH_2$), 5.64 (d, J_{HH} = 16.0 Hz, 1H, $PyCH_2$), 4.96–5.05 (m, 2H, PCH_2); **^{31}P{^{1}H} NMR** (162 MHz, $CDCl_3$, 25 °C): δ 71.2 (s); **^{13}C{^{1}H} NMR** (101 MHz, CD_2Cl_2, 25 °C): δ 222.8 (br d, J_{PC} = 16.8 Hz, CO), 220.8 (br d, J_{PC} = 30.1 Hz, CO), 220.2 (br d, J_{PC} = 20.8 Hz, CO), 197.7 (d, J_{PC} = 17.5 Hz, CN_2), 156.5 (s, C_{Py}), 150.0 (s, CH_{Ar}), 137.6 (s, CH_{Ar}), 135.7 (d,

J_{PC} = 36.6 Hz, $C_{ipso\ Ph}$), 134.9 (d, J_{PC} = 9.8 Hz, CH_{Ar}), 132.0 (s, CH_{Ar}), 130.7 (m, 2 CH_{Ar}), 129.4 (d, J_{PC} = 9.0 Hz, CH_{Ar}), 129.3 (d, J_{PC} = 9.0 Hz, CH_{Ar}), 125.2 (s, CH_{Ar}), 123.4 (s, CH_{Ar}), 122.3 (s, $CH_{Im\text{-}4,5}$), 121.3 (d, J_{PC} = 7.2 Hz, $CH_{Im\text{-}4,5}$), 57.1 (s, PyCH_2), 52.3 (d, J_{PC} = 31.5 Hz, PCH_2); **IR** (THF): ν_{CO} 2018 (s), 1941 (s), 1913 (s) cm^{-1}; **Anal.** Found: C, 51.61; H, 3.38; N, 7.03. Calcd. (%) for $C_{25}H_{20}BrMnN_3O_3P$: C, 52.11; H, 3.50; N, 7.29; **HRMS** (ESI, POS): m/z calcd. for $C_{25}H_{21}BrMnN_3O_3P$ $[M + H]^+$ 575.9884; found, 575.9893 (ε_r = 1.6 ppm).

4.8 Synthesis of the Tridentate complexes C6^t, C7^t, and C8^t

General procedure (VI)

To a solution of the selected complex (**C6**-**C8**) in CH_2Cl_2, 1.1 equiv. of AgOTf was added as a solid. The reaction mixture was then stirred at r.t. for 2 h. After filtration through Celite and evaporation of the solvent under vacuum, the desired pincer complexes (**C6^t**, **C7^t**, and **C8^t**) were obtained as pale-yellow powder.

Synthesis of PCP Tridentate Complex C6^t

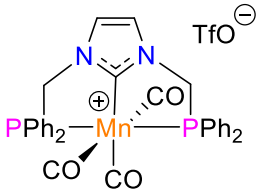

C6^t

According to the general procedure (**VI**), **C6** (0.4 g, 0.58 mmol) in CH_2Cl_2 (30 mL), afforded complex **C6^t** as a pale-yellow powder (0.39 g, 88%). Single crystals suitable for X-ray diffraction analysis were obtained by slow evaporation of a CH_2Cl_2/toluene solution at room temperature. **^{1}H NMR** (400 MHz, CD_2Cl_2, 25 °C): δ 7.82 (br s, 2H, CH_{Ar}), 7.58−7.50 (m, 20H, CH_{Ar}), 5.26–5.24 (m, 4H, PCH_2); **^{31}P{^{1}H} NMR** (162 MHz, CD_2Cl_2, 25 °C): δ 89.6 (s); **^{13}C{^{1}H} NMR** (101 MHz, CD_2Cl_2, 25 °C): δ 220.7 (br t, J_{PC} = 10.5 Hz, CO), 213.6 (br t, J_{PC} = 19.0 Hz, CO), 195.6 (t, J_{PC} = 13.1 Hz, CN_2), 133.8 (m, $C_{ipso\ Ph}$) 132.2 (s, CH_{Ph}), 131.7–132.0 (m, CH_{Ph}), 129.8–130.2 (m, CH_{Ph}), 124.9 (s, $CH_{Im\text{-}4,5}$), 121.6 (q, J_{CF} = 321.4 Hz, CF_3), 56.2 (m, PCH_2); **IR** (THF): ν_{CO} 1966 (s), 1942 (s) cm^{-1}; **Anal.** Found: C, 52.34; H, 3.82; N, 3.60. Calcd. (%) for $C_{33}H_{26}F_3MnN_2O_6P_2S$: C, 52.67; H, 3.48; N, 3.72; **HRMS** (ESI, POS): m/z calcd. for $C_{32}H_{26}MnN_2O_3P_2^+$ $[M – TfO]^+$ 603.0799; found, 603.0816 (ε_r = 2.8 ppm).

Synthesis of PCN Tridentate Complex C7^t

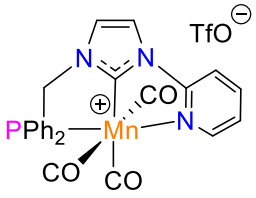

C7^t

According to the general procedure (**VI**), a mixture of complexes **C7** and **C7'** (0.20 g, 0.36 mmol) in CH_2Cl_2 (20 mL), afforded complex **C7^t** as a green-yellow powder (0.17 g, 76%) after crystallization of the crude in THF/Et_2O mixture. Single crystals suitable for X-ray diffraction analysis were obtained by slow evaporation of the complex solution in CH_2Cl_2 at room temperature. **^{1}H NMR** (400 MHz, $CDCl_3$, 25 °C): δ 8.58 (br s, 2H, C*H*$_{Ar}$), 8.25 (br s, 1H, C*H*$_{Ar}$), 8.10 (br s, 2H C*H*$_{Ar}$), 7.46–7.44 (m, 11H, C*H*$_{Ar}$), 5.51 (br s, 2H, PC*H*$_2$); **^{31}P{^{1}H} NMR** (162 MHz, CD_2Cl_2, 25 °C): δ 97.4 (s); **^{13}C{^{1}H} NMR** (101 MHz, $CDCl_3$, 25 °C): δ 218.4 (d, J_{PC} = 9.7 Hz, *C*O), 212.7 (d, J_{PC} = 17.7 Hz, *C*O), 206.5 (d, J_{PC} = 18.9 Hz, *C*N$_2$), 156.0 (s, *C*H$_{Py}$), 154.6 (s, *C*$_{Py}$), 141.8 (s, *C*H$_{Ar}$), 133.8 (d, J_{PC} = 42.8 Hz, *C*$_{ipso\ Ph}$), 131.6 (d, J_{PC} = 2.4 Hz, *C*H$_{Ph}$), 131.4 (d, J_{PC} = 11.0 Hz, *C*H$_{Ph}$), 129.5 (d, J_{PC} = 10.4 Hz, *C*H$_{Ph}$), 125.4 (d, J_{PC} = 6.0 Hz, *C*H$_{Im\text{-}4,5}$), 123.4 (s, *C*H$_{Im\text{-}4,5}$), 120.8 (s, *C*H$_{Py}$), 114.2 (s, *C*H$_{Py}$), 58.1 (d, J_{PC} = 37.4 Hz, P*C*H$_2$); **IR** (THF): ν_{CO} 1969, 1941 cm^{-1}; **Anal.** Found: C, 47.60; H, 2.45; N, 6.45. Calcd. (%) for $C_{25}H_{18}F_3MnN_3O_6PS$: C, 47.56; H, 2.87; N, 6.66; **HRMS** (ESI, POS): m/z calcd. for $C_{24}H_{18}MnN_3O_3P^+$ [M – TfO]$^+$ 482.0466; found, 482.0466 (ε_r = 0 ppm).

Synthesis of PCN Tridentate Complex C8^t

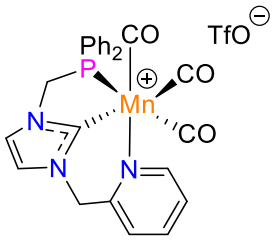

C8^t

According to the general procedure (**VI**), **C8** (0.20 g, 0.34 mmol) in CH_2Cl_2 (20 mL), afforded complex **C8^t** as a yellow-brown powder (0.21 g, 96%). Single crystals suitable for X-ray diffraction analysis were obtained by slow evaporation of the concentrated CH_2Cl_2 solution at room temperature. **^{1}H NMR** (400 MHz, CD_2Cl_2, 25 °C): δ 8.02 (dd, J = 7.4 and 10.9 Hz, 2H, C*H*$_{Ar}$), 7.88 (s, 1H, C*H*$_{Ar}$), 7.82–7.70 (m, 5H, C*H*$_{Ar}$), 7.66–7.61 (m, 2H, C*H*$_{Ar}$), 7.16 (t, J = 7.5 Hz, 1H, C*H*$_{Ar}$), 6.96 (t, J = 7.8 Hz, 2H, C*H*$_{Ar}$), 6.60 (t, J = 6.6 Hz, 1H, C*H*$_{Ar}$), 5.95 (t, J = 8.0

Hz, 2H, CH_{Ar}), 5.89 (d, J = 16.0 Hz, 1H, PyCH_2), 5.54 (d, J = 16.0 Hz, 1H, PyCH_2), 5.36 (t, J = 12.0 Hz, 1H, PCH_2), 4.91 (dd, J = 8.9 and 12.0 Hz, 1H, PCH_2); **^{31}P{^{1}H} NMR** (162 MHz, CD_2Cl_2, 25 °C): δ 93.3 (s); **^{13}C{^{1}H} NMR** (101 MHz, CD_2Cl_2, 25 °C): δ 219.6 (br d, J_{PC} = 25.5 Hz, CO), 218.7 (br d, J_{PC} = 18.5 Hz, CO), 216.9 (br d, J_{PC} = 23.5 Hz, CO), 202.9 (d, J_{PC} = 22.3 Hz, CN$_2$), 157.7 (d, J_{PC} = 3.4 Hz, CH$_{Ar}$), 156.9 (s, C_{Py}), 139.5 (s, CH$_{Ar}$), 134.4 (d, J_{PC} = 10.7 Hz, CH$_{Ar}$), 133.6 (d, J_{PC} = 2.0 Hz, CH$_{Ar}$), 131.2 (d, J_{PC} = 2.4 Hz, CH$_{Ar}$), 130.4 (d, J_{PC} = 9.9 Hz, CH$_{Ar}$), 129.7 (d, J_{PC} = 9.7 Hz, CH$_{Ar}$), 129.6 (d, J_{PC} = 9.4 Hz, CH$_{Ar}$), 127.5 (d, J_{PC} = 36.6 Hz, $C_{ipso\ Ph}$), 127.4 (s, CH$_{Ar}$), 126.3 (s, CH$_{Ar}$), 124.7 (s, CH$_{Ar}$), 123.1 (d, J_{PC} = 1.7 Hz, CH$_{Ar}$), 55.8 (d, J_{PC} = 37.9 Hz, PCH$_2$), 55.6 (s, PyCH$_2$); **IR** (THF): ν_{CO} 2024 (s), 1947 (s), 1929 (s) cm^{-1}; **Anal.** Found: C, 47.17; H, 2.84; N, 6.34. Calcd. (%) for $C_{26}H_{20}F_3MnN_3O_6PS$. 0.25 ($CH_2Cl_2$): C, 47.29; H, 3.10; N, 6.30; **HRMS** (ESI, POS): m/z calcd. for $C_{25}H_{20}MnN_3O_3P$ [M – TfO]$^+$ 496.0623; found, 496.0626 (ε_r = 0.6 ppm).

4.9 X-Ray Diffraction Studies

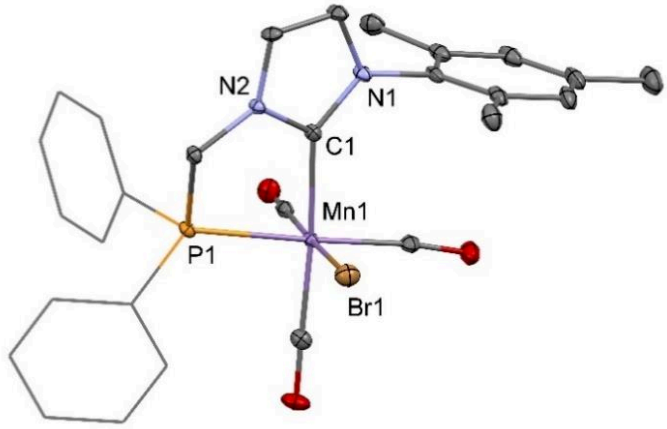

Table 1. Crystal data and structure refinements for Mn(I) complex **C1**.

Empirical formula	$C_{28}H_{25}BrMnN_2O_3P \times C_4H_8O$
Formula mass	675.41
Crystal system	Triclinic
Space group	P -1
T [K]	173
a [Å]	8.1114 (4)
b [Å]	14.0387 (7)
c [Å]	15.0360 (8)
α [°]	103.318 (2)
β [°]	105.057 (2)
γ [°]	100.045 (2)
V [Å^3]	1558.15 (14)
D_c	1.44
Z	2
μ[mm^{-1}]	1.795
Refl. measured	67478
Refl. unique/R_{int}	6371/0.025
Refl. with $I > n\sigma(I)$	5899, n=2
Nb parameters	419
Refinement on	F^2
R with $I > n\sigma(I)$	0.0568
R_w with $I > n\sigma(I)$	0.1907
GooF	1.07
$\Delta\rho_{max}/\Delta\rho_{min}$ [e.Å^{-3}]	1.60/–1.61

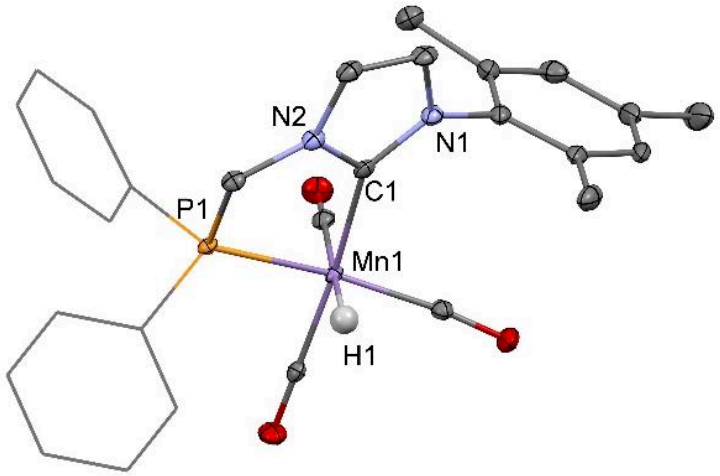

Table 2. Crystal data and structure refinements for Mn(I) complex **C1.a**.

Empirical formula	$C_{28}H_{26}MnN_2O_3P$
Formula mass	524.43
Crystal system	Monoclinic
Space group	P 2_1/c
T [K]	100
a [Å]	16.7499(5)
b [Å]	10.2552(3)
c [Å]	16.3493(4)
α [°]	90
β [°]	90.630(2)
γ [°]	90
V [Å^3]	2808.21(14)
D_c	1.24
Z	4
μ[mm^{-1}]	0.556
Refl. measured	30394
Refl. unique/R_{int}	6947/0.104
Refl. with $I > n\sigma(I)$	3860, n=3
Nb parameters	320
Refinement on	F
R with $I > n\sigma(I)$	0.0454
R_w with $I > n\sigma(I)$	0.0487
GooF	1.11
$\Delta\rho_{max}/\Delta\rho_{min}$ [e.Å^{-3}]	0.35/–0.34

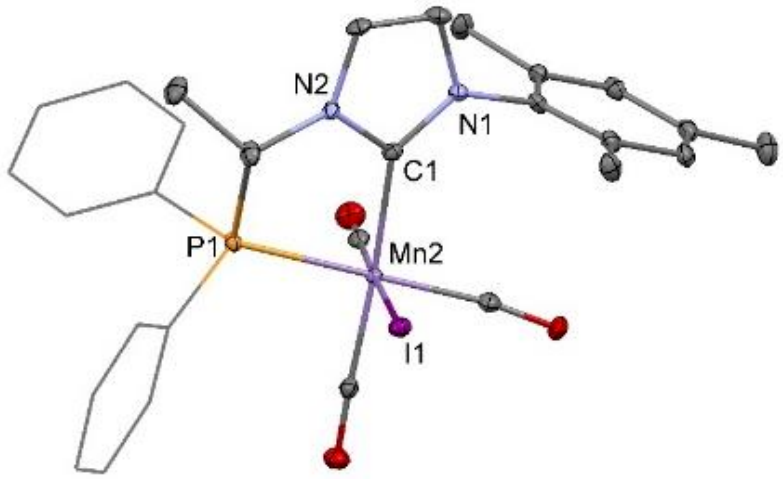

Table 3. Crystal data and structure refinements for Mn(I) complex **C1.b**.

Empirical formula	$C_{29}H_{27}IMnN_2O_3P$
Formula mass	664.35
Crystal system	Triclinic
Space group	P -1
T [K]	108
a [Å]	8.1734(4)
b [Å]	11.3495(5)
c [Å]	16.2623(8)
α [°]	109.5825(16)
β [°]	93.8479(18)
γ [°]	104.3593(16)
V [Å^3]	1358.12(11)
D_c	1.62
Z	2
μ[mm^{-1}]	1.715
Refl. measured	31509
Refl. unique/R_{int}	6763/0.118
Refl. with $I > n\sigma(I)$	4714, n=3
Nb parameters	334
Refinement on	F
R with $I > n\sigma(I)$	0.0362
R_w with $I > n\sigma(I)$	0.0403
GooF	1.05
$\Delta\rho_{max}/\Delta\rho_{min}$ [e.Å^{-3}]	0.89/–1.38

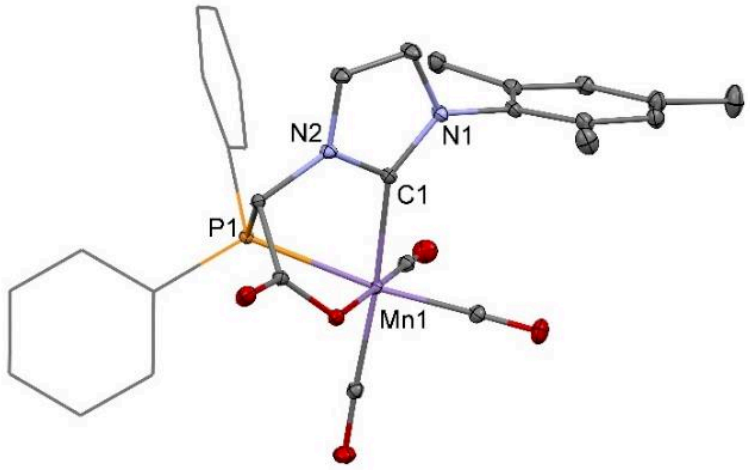

Table 4. Crystal data and structure refinements for Mn(I) complex **C1.c**.

Empirical formula	$C_{29}H_{24}MnN_2O_5P$
Formula mass	566.42
Crystal system	Triclinic
Space group	P -1
T [K]	107
a [Å]	9.9284(5)
b [Å]	11.0574(5)
c [Å]	12.2366(9)
α [°]	78.1555(19)
β [°]	78.3389(15)
γ [°]	86.3487(11)
V [Å^3]	1287.28(13)
D_c	1.46
Z	2
μ[mm^{-1}]	0.618
Refl. measured	51564
Refl. unique/R_{int}	7783/0.030
Refl. with $I > n\sigma(I)$	7064, n=3
Nb parameters	343
Refinement on	F
R with $I > n\sigma(I)$	0.0276
R_w with $I > n\sigma(I)$	0.0287
GooF	1.03
$\Delta\rho_{max}/\Delta\rho_{min}$ [e.Å^{-3}]	0.47/–0.27

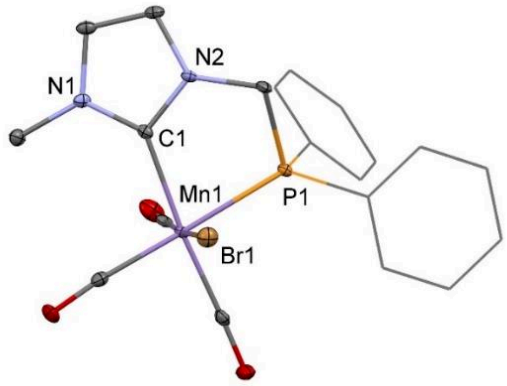

Table 5. Crystal data and structure refinements for Mn(I) complex **C2**

Empirical formula	C_{20} H_{17} Br_1 Mn_1 N_2 O_3 P_1
Formula mass	499.17
Crystal system	Monoclinic
Space group	P -1
T [K]	100
a [Å]	17.0859(7)
b [Å]	10.5413(4)
c [Å]	23.0838(9)
α [°]	90
β [°]	107.1723(14)
γ [°]	90
V [Å^3]	3972.2(3)
D_c	1.67
Z	8
μ[mm^{-1}]	2.781
Refl. measured	49854
Refl. unique/R_{int}	8120/0.0422
Refl. with $I > n\sigma(I)$	6481, n=3
Nb parameters	505
Refinement on	F
R with $I > n\sigma(I)$	0.043
R_w with $I > n\sigma(I)$	0.045
GooF	1.01
$\Delta\rho_{max}/\Delta\rho_{min}$ [e.Å^{-3}]	1.28/–1.64

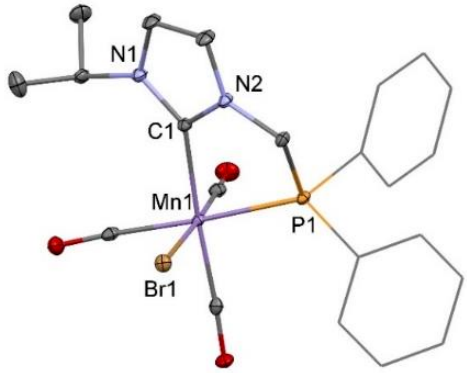

Table 6. Crystal data and structure refinements for Mn(I) complex **C3**

Empirical formula	C_{23} H_{23} Br_1 Cl_2 Mn_1 N_2 O_3 P_1
Formula mass	612.16
Crystal system	Triclinic
Space group	P -1
T [K]	100
a [Å]	12.4553(12)
b [Å]	14.0061(15)
c [Å]	16.6430(17)
α [°]	76.242(3)
β [°]	87.906(3)
γ [°]	65.332(3)
V [Å^3]	2556.2(5)
D_c	1.59
Z	4
μ[mm^{-1}]	2.379
Refl. measured	117361
Refl. unique/R_{int}	12841/0.0546
Refl. with $I > n\sigma(I)$	9667, n=3
Nb parameters	622
Refinement on	F
R with $I > n\sigma(I)$	0.032
R_w with $I > n\sigma(I)$	0.032
GooF	1.11
$\Delta\rho_{max}/\Delta\rho_{min}$ [e.Å^{-3}]	0.89/–1.61

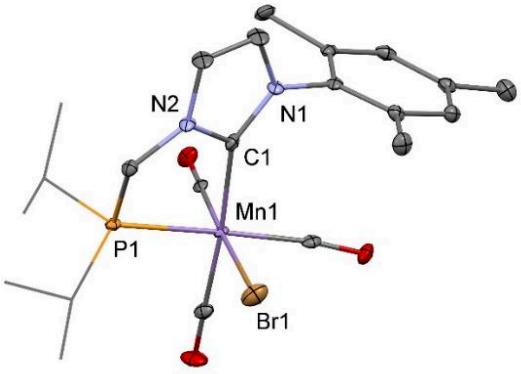

Table 7. Crystal data and structure refinements for Mn(I) complex **C4**

Empirical formula	C_{22} H_{29} Br_1 Mn_1 N_2 O_3 P_1
Formula mass	535.29
Crystal system	Monoclinic
Space group	P -1
T [K]	100
a [Å]	8.2962(5)
b [Å]	22.9441(12)
c [Å]	13.2050(7)
α [°]	90
β [°]	105.737(2)
γ [°]	90
V [Å^3]	2419.3(2)
D_c	1.47
Z	4
μ[mm^{-1}]	2.288
Refl. measured	39750
Refl. unique/R_{int}	4785/0.0421
Refl. with $I > n\sigma(I)$	3880, n=3
Nb parameters	271
Refinement on	F
R with $I > n\sigma(I)$	0.062
R_w with $I > n\sigma(I)$	0.065
GooF	1.02
$\Delta\rho_{max}/\Delta\rho_{min}$ [e.Å^{-3}]	1.32/–2.32

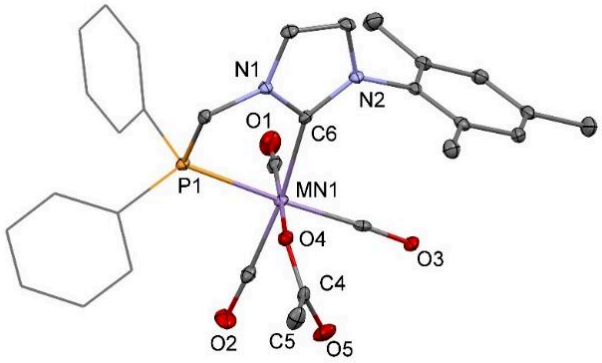

Table 8. Crystal data and structure refinements for Mn(I) complex **C1.h**

Empirical formula	$C_{30}H_{28}MnN_2O_5P \cdot 0.5(C_6H_6)$
Formula mass	646
Crystal system	Triclinic
Space group	P -1
T [K]	100
a [Å]	8.682 (3)
b [Å]	12.897 (4)
c [Å]	14.386 (4)
α [°]	84.629 (9)
β [°]	84.617 (8)
γ [°]	73.023 (9)
V [Å^3]	1530.2 (8)
D_c	1.34
Z	2
μ[mm^{-1}]	0.53
Refl. measured	36670
Refl. unique/R_{int}	5782/0.087
Refl. with $I > n\sigma(I)$	4236, n=2
Nb parameters	383
Refinement on	F
R with $I > n\sigma(I)$	0.042
R_w with $I > n\sigma$ (I)	0.098
GooF	1.05
$\Delta\rho_{max}/\Delta\rho_{min}$ [e.Å^{-3}]	0.34/–0.42

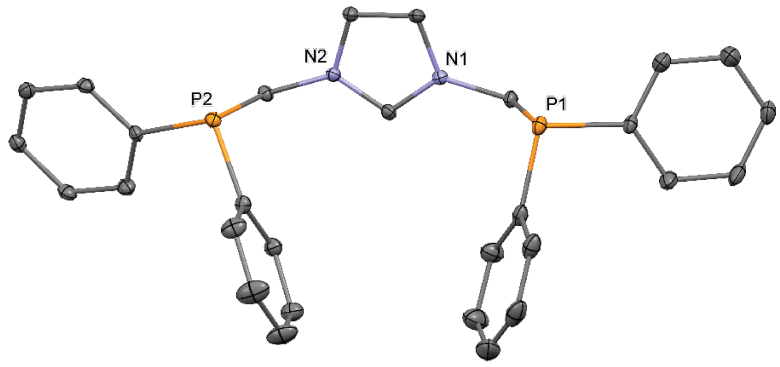

Table 9. Crystal data and structure refinements for PCP ligand **L6**

Empirical formula	$C_{36}\ H_{34}\ N_2\ O_3\ P_2\ S_1$
Formula mass	636.69
Crystal system	Orthorhombic
Space group	P 2_1 2_1 2_1
T [K]	100
a [Å]	9.2843(13)
b [Å]	16.587(3)
c [Å]	21.263(3)
α [°]	90
β [°]	90
γ [°]	90
V [Å^3]	3274.5(9)
D_c	1.29
Z	4
μ[mm^{-1}]	0.235
Refl. measured	39408
Refl. unique/R_{int}	8120/0.1165
Refl. with $I > n\sigma(I)$	5463, n=3
Nb parameters	398
Refinement on	F
R with $I > n\sigma(I)$	0.042
R_w with $I > n\sigma$ (I)	0.098
GooF	1.12
$\Delta\rho_{max}/\Delta\rho_{min}$ [e.Å^{-3}]	0.27/–0.28

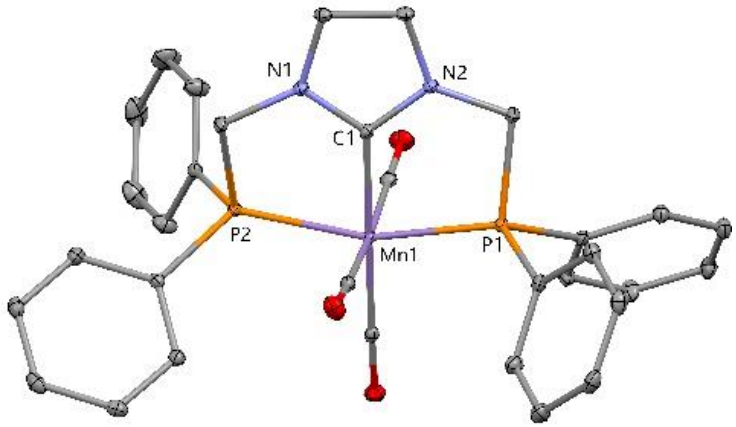

Table 10. Crystal data and structure refinements for Mn(I) complex **C6^{t}**

Empirical formula	C_{40} H_{34} F_3 Mn_1 N_2 O_6 P_2 S_1
Formula mass	844.65
Crystal system	Monoclinic
Space group	P 2_1/c
T [K]	100
a [Å]	11.7912(7)
b [Å]	11.3395(7)
c [Å]	28.8752(19)
α [°]	90
β [°]	100.519(3)
γ [°]	90
V [Å^3]	3795.9(4)
D_c	1.48
Z	4
μ[mm^{-1}]	0.552
Refl. measured	188387
Refl. unique/R_{int}	9461/0.0495
Refl. with $I > n\sigma(I)$	7791, n=3
Nb parameters	496
Refinement on	F
R with $I > n\sigma(I)$	0.028
R_w with $I > n\sigma(I)$	0.033
GooF	1.07
$\Delta\rho_{max}/\Delta\rho_{min}$ [e.Å^{-3}]	0.54/–0.41

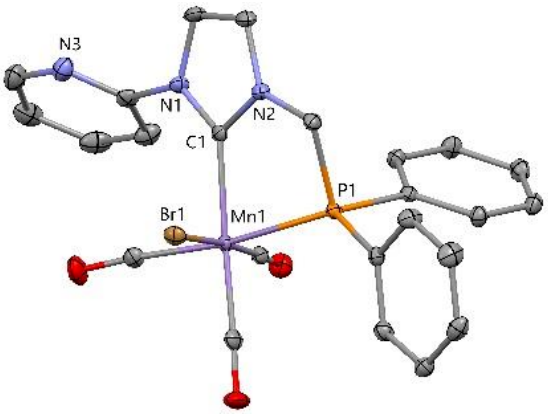

Table 11. Crystal data and structure refinements for Mn(I) complex **C7**

Empirical formula	$C_{24}\ H_{18}\ Br_1\ Mn_1\ N_3\ O_3\ P_1$
Formula mass	562.23
Crystal system	Monoclinic
Space group	P 1 2_1/c 1
T [K]	140
a [Å]	10.34980(5)
b [Å]	12.42640(6)
c [Å]	18.26690(7)
α [°]	90
β [°]	101.172(5)
γ [°]	90
V [Å^3]	2304.80(5)
D_c	1.62
Z	2
μ[mm^{-1}]	2.408
Refl. measured	62052
Refl. unique/R_{int}	7442/0.0876
Refl. with $I > n\sigma(I)$	5800, n=3
Nb parameters	298
Refinement on	F
R with $I > n\sigma(I)$	0.054
R_w with $I > n\sigma(I)$	0.097
GooF	1.02
$\Delta\rho_{max}/\Delta\rho_{min}$ [e.Å^{-3}]	0.74/–0.84

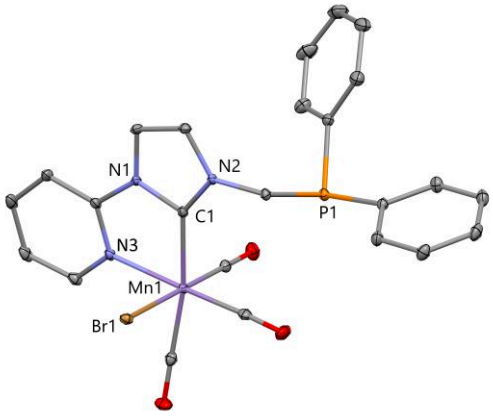

Table 12. Crystal data and structure refinements for Mn(I) complex **C7'**

Empirical formula	$C_{49}\ H_{38}\ Br_2\ Cl_2\ Mn_2\ N_6\ O_6\ P_2$
Formula mass	1209.39
Crystal system	Monoclinic
Space group	P 2_1/n
T [K]	110
a [Å]	12.88140(3)
b [Å]	15.57420(4)
c [Å]	25.05660(5)
α [°]	90
β [°]	99.639(3)
γ [°]	90
V [Å^3]	4955.83(5)
D_c	1.62
Z	4
μ[mm^{-1}]	2.350
Refl. measured	163166
Refl. unique/R_{int}	15107/0.0733
Refl. with $I > n\sigma(I)$	10044, n=3
Nb parameters	622
Refinement on	F
R with $I > n\sigma(I)$	0.032
R_w with $I > n\sigma$ (I)	0.066
GooF	1.00
$\Delta\rho_{max}/\Delta\rho_{min}$ [e.Å^{-3}]	0.54/–0.57

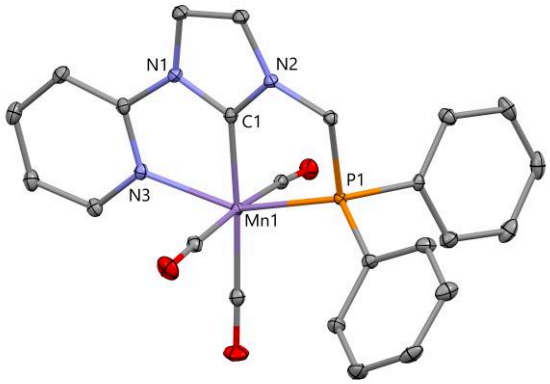

Table 13. Crystal data and structure refinements for Mn(I) complex **C7^{t}**

Empirical formula	C_{27} H_{20} Cl_6 F_3 Mn_1 N_3 O_6 P_1 S_1
Formula mass	870.15
Crystal system	Triclinic
Space group	P -1
T [K]	110
a [Å]	12.17490(4)
b [Å]	13.34250(4)
c [Å]	13.62890(4)
α [°]	66.278(4)
β [°]	65.043(4)
γ [°]	63.264(4)
V [Å^3]	1729.79(7)
D_c	1.67
Z	2
μ[mm^{-1}]	1.013
Refl. measured	93587
Refl. unique/R_{int}	10514/0.0559
Refl. with $I > n\sigma(I)$	7272, n=3
Nb parameters	433
Refinement on	F
R with $I > n\sigma(I)$	0.031
R_w with $I > n\sigma(I)$	0.080
GooF	0.95
$\Delta\rho_{max}/\Delta\rho_{min}$ [e.Å^{-3}]	0.5/–0.60

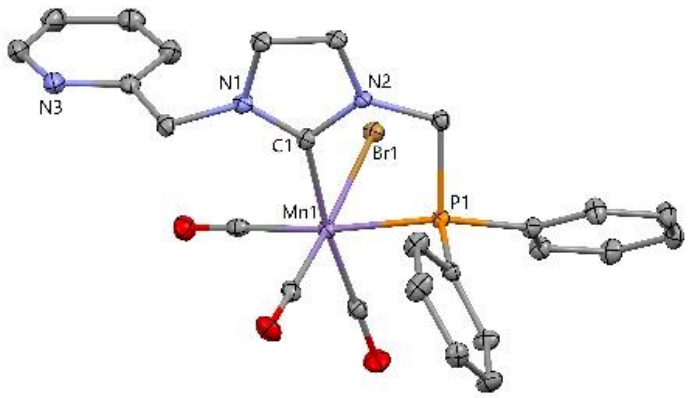

Table 14. Crystal data and structure refinements for Mn(I) complex **C8**

Empirical formula	$C_{25}\ H_{20}\ Br_1\ Mn_1\ N_3\ O_3\ P_1$
Formula mass	576.26
Crystal system	Monoclinic
Space group	P 2_1/c
T [K]	100
a [Å]	11.2844(9)
b [Å]	14.2144(10)
c [Å]	15.6717(12)
α [°]	90
β [°]	106.749(2)
γ [°]	90
V [Å^3]	2407.1(3)
D_c	1.59
Z	4
μ[mm^{-1}]	2.308
Refl. measured	57255
Refl. unique/R_{int}	5556/0.0783
Refl. with $I > n\sigma(I)$	3852, n=3
Nb parameters	307
Refinement on	F
R with $I > n\sigma(I)$	0.033
R_w with $I > n\sigma\ (I)$	0.039
GooF	1.09
$\Delta\rho_{max}/\Delta\rho_{min}$ [e.Å^{-3}]	0.67/–0.69

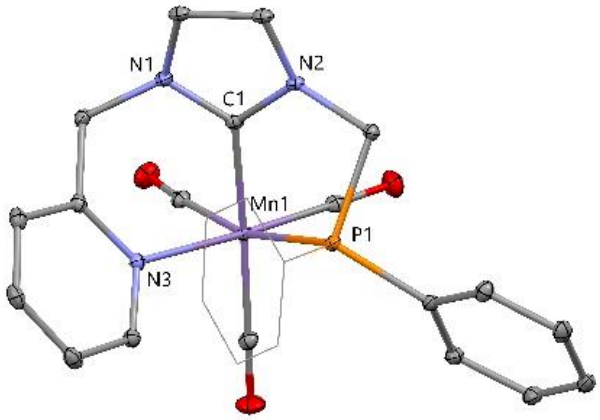

Table 15. Crystal data and structure refinements for Mn(I) complex **C8^{t}**

Empirical formula	C_{26} H_{20} F_3 Mn_1 N_3 O_6 P_1 S_1
Formula mass	645.42
Crystal system	Monoclinic
Space group	P 1 2_1/n 1
T [K]	113
a [Å]	11.7203(9)
b [Å]	15.7693(11)
c [Å]	14.4518(10)
α [°]	90
β [°]	94.081(2)
γ [°]	90
V [Å^3]	2664.2(3)
D_c	1.61
Z	4
μ[mm^{-1}]	0.703
Refl. measured	65015
Refl. unique/R_{int}	6601/0.0419
Refl. with $I > n\sigma(I)$	5923, n=3
Nb parameters	370
Refinement on	F
R with $I > n\sigma(I)$	0.026
R_w with $I > n\sigma(I)$	0.027
GooF	1.05
$\Delta\rho_{max}/\Delta\rho_{min}$ [e.Å^{-3}]	0.41/–0.39

4.10 References

[1] A. Szadkowska, E. Zaorska, S. Staszko, R. Pawłowski, D. Trzybiński, K. Woźniak, *Eur. J. Org. Chem.* **2017**, *2017*, 4074–4084.

[2] T. Chatterjee, N. T. Kumar, S. K. Das, *Polyhedron* **2017**, *127*, 68–83.

[3] A. Plikhta, A. Pöthig, E. Herdtweck, B. Rieger, *Inorg. Chem.* **2015**, *54*, 9517–9528.

[4] H. J. Clark, R. Wang, H. Alper, *J. Org. Chem.* **2002**, *67*, 6224–6225.

[5] A. Raba, M. R. Anneser, D. Jantke, M. Cokoja, W. A. Herrmann, F. E. Kühn, *Tetrahedron Lett.* **2013**, *54*, 3384–3387.

[6] P. L. Chiu, C.-L. Lai, C.-F. Chang, C.-H. Hu, H. M. Lee, *Organometallics* **2005**, *24*, 6169–6178.

[7] M. J. Bitzer, A. Pöthig, C. Jandl, F. E. Kühn, W. Baratta, *Dalton Trans.* **2015**, *44*, 11686–11689.

[8] A. E. Stross, G. Iadevaia, C. A. Hunter, *Chem. Sci.* **2015**, *7*, 94–101.

[9] H. Salem, M. Schmitt, U. Herrlich (née Blumbach), E. Kühnel, M. Brill, P. Nägele, A. L. Bogado, F. Rominger, P. Hofmann, *Organometallics* **2013**, *32*, 29–46.

[10] Y. Li, L.-Q. Lu, S. Das, S. Pisiewicz, K. Junge, M. Beller, *J. Am. Chem. Soc.* **2012**, *134*, 18325–18329.

[11] D. Wei, T. Roisnel, C. Darcel, E. Clot, J.-B. Sortais, *ChemCatChem* **2017**, *9*, 80–83.

[12] C.-H. Xing, Q.-S. Hu, *Tetrahedron Lett.* **2010**, *51*, 924–927.

[13] P. Schaaf, V. Gojic, T. Bayer, F. Rudroff, M. Schnürch, M. D. Mihovilovic, *ChemCatChem* **2018**, *10*, 920–924.

[14] D. Wang, A. Bruneau-Voisine, J.-B. Sortais, *Catal. Commun.* **2018**, *105*, 31–36.

[15] D. Wei, A. Bruneau-Voisine, T. Chauvin, V. Dorcet, T. Roisnel, D. A. Valyaev, N. Lugan, J.-B. Sortais, *Adv. Synth. Catal.* **2018**, *360*, 676–681.

Chapter 3: Hydrosilylation of Carboxylic Acids and Esters to Aldehydes Catalyzed by $Mn_2(CO)_{10}$ and $Re_2(CO)_{10}$

Chapter 3: Hydrosilylation of Carboxylic Acids and Esters to Aldehydes Catalyzed by $Mn_2(CO)_{10}$ and $Re_2(CO)_{10}$

Chapter 3: Hydrosilylation of Carboxylic Acids and Esters to Aldehydes Catalyzed by $Mn_2(CO)_{10}$ and $Re_2(CO)_{10}$

1. Introduction

The reduction of carboxylic acids and esters to the corresponding aldehydes is one of the most important and challenging transformations in synthetic chemistry. Due to the higher reactivity of aldehydes with respect to their acids/esters precursors towards nucleophilic addition of hydride species, the undesired formation of alcohols resulting from over-reduction of aldehydes is generally difficult to avoid. Stoichoimetric reducing reagents involving bulky substituents,[1–3] such as diisobutylaluminum hydride (DIBALH),[4] have been widely employed, usually at low temperature but these reagents proved to be difficult to handle in both laboratorial and industrial scales, because of their dangerous nature. Therefore, the development of safer or/and greener catalytic processes is highly preferable and of primary interest.

In the field of heterogeneous catalysis, a few systems based on γ-Al_2O_3,[5] Y_2O_3,[6] Mn/Al,[7–10] Mn–K/CeO_2–Al_2O_3[11] were developed for the direct hydrogenation of carboxylic acids and esters into aldehydes. However high reaction temperatures (260 – 420 °C) were generally required. As an alternative, catalytic reductions using hydrosilanes as a hydride source, i.e. *via* hydrosilylation, are more attractive from both selectivity and safety points of view.[12] For example, Motoyama and coll. reported Pd/C as catalyst for the hydrosilylation of esters to silyl acetals at 50 °C with 2.5 equiv. of 1,1,3,3-tetramethyldisiloxane (TMDS), the acetals being then easily converted to aldehydes after hydrolysis.[13]

In homogeneous catalysis, a limited number of systems capable of catalyzing the hydrosilylation of esters into aldehydes have been described. The first example, was reported by Piers and coll., involving the organo-catalyst $B(C_6F_5)_3$ and Ph_3SiH as reducing agent.[14,15] A few examples were also described with noble metals such as palladium,[16] ruthenium[17] and iridium[18,19] (**Scheme 1a**). On the other hand, only two catalysts involving Earth abundant metals were developed to date: a system based on cobalt described by Michon and coll.[20] and another involving iron described by our group (**Scheme 1b**).[21]

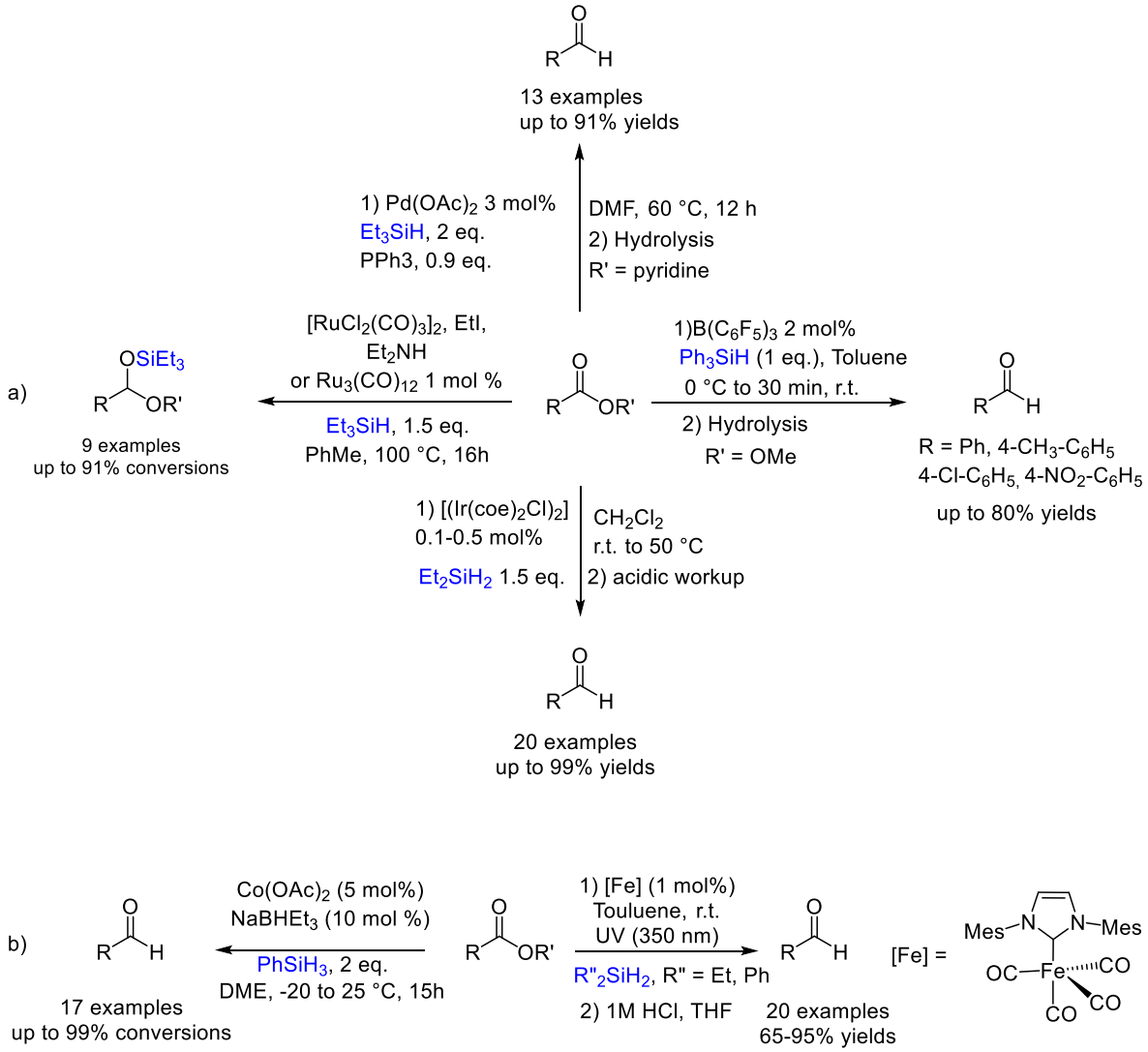

Scheme 1. Hydrosilylation of esters into aldehydes.

For the hydrosilylation of carboxylic acids into aldehydes, the first example was reported by Nagashima et *al.*, using ruthenium carbonyl catalysts in the presence of 1,2-bis(dimethylsilyl)benzene.[22] From iron-based catalysts, our group developed a selective and switchable method to form either alcohols in the presence of phenylsilane under UV irradiation or aldehydes with TMDS under thermal activation.[23] In addition, the Brookhart group demonstrated that the borane $B(C_6F_5)_3$ acts as an effective catalyst for the reduction of aliphatic and aromatic carboxylic acids to disilylacetals in the presence of bulky tertiary silanes (**Scheme 2**).[24]

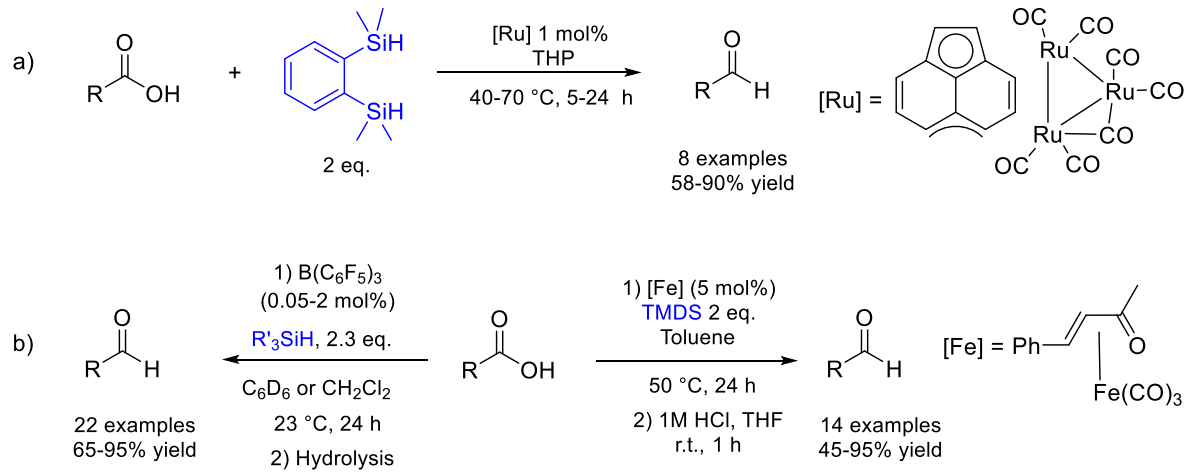

Scheme 2. Hydrosilylation of carboxylic acids into aldehydes.

Lately, the use of manganese in (transfer)hydrogenation reactions of various unsaturated compounds has grown exponentially including the reduction of carbonyl compounds (see Chapter I). Meanwhile, manganese has also been proven to be effective in the hydrosilylation of carbonyl and carboxylic acid derivatives.[25–28]

Compared with manganese, its lighter analogue, rhenium has been more rarely used in this field and in particular in hydrosilylation-type reactions.[29,30]

Some of the development of manganese and rhenium catalysis in the hydrosilylation of carboxylic acid derivatives will be discussed in this introductive Chapter.

2. Manganese catalyzed hydrosilylation of carboxylic acid derivatives.

The first manganese catalyzed hydrosilylation reaction was reported by Yates[31] in 1982, for ketones reduction under UV irradiation (365 nm), using $Mn_2(CO)_{10}$, as catalyst which was found to be poor catalyst for photohydrosilylation of acetone. Eight years later, Cutler's[32] group has intensively studied the hydrosilylation of carbonyl compounds with manganese acyl catalysts $L(CO)_4MnCOR$ [L = CO, R = CH_3, Ph; L = PPh_3, PEt_3, R = CH_3] for the hydrosilylation of organoiron acyl compounds. In 1995,[33] the same author reported the first example for the catalytic hydrosilylation of esters using manganese carbonyl acetyl complexes, $L(CO)_4MnCOCH_3$ [L = CO, PPh_3] to afford the corresponding ethers (**Scheme 3a**). Using 1.5 - 3.0 mol% of $(PPh_3)(CO)_4MnCOCH_3$ catalyst and 1.2 equiv. of $PhSiH_3$ in C_6D_6 solution, ethyl acetate was transformed to diethyl ether in good yield (85%) within 15 min. at room temperature. The pre-catalyst $(CO)_5MnCOCH_3$ needed more reaction's time (1.5 h) to produce diethyl ether quantitatively. Complexes $Mn(CO)_5CH_3$ and $Mn(CO)_5Br$ were found to be less

active catalysts, giving the desired product in 85 and 55% yields, respectively, over 4 h, while no catalytic activity has been observed with $Mn(CO)_5(SiMe_2Ph)$, $Mn(CO)_5(SiHPh_2)$, and $Mn_2(CO)_{10}$ complexes. With the optimized conditions, alkyl esters were reduced to the corresponding ethers within less than 1 h in moderate to good NMR yields (69-96%), the reduction of aromatic and cyclic esters yielded a mixture of the desired product and alkoxysilanes. A mechanism was proposed for the hydrosilylation of esters starting by the reaction of manganese complex $L(CO)_4MnCOCH_3$ with the silane to generate the active catalyst, $L(CO)_4MnSiR_3$ through ligand metathesis, followed by the coordination of the C=O bond to the manganese center, and then insertion into the Mn─Si bond, to give the manganese alkyl complex **1** which underwent oxidative addition of the Si─H bond to the manganese center to obtain complex **2** followed by reductive elimination reaction to produce the desired compound and regenerate the active catalyst (**Scheme 3b**).

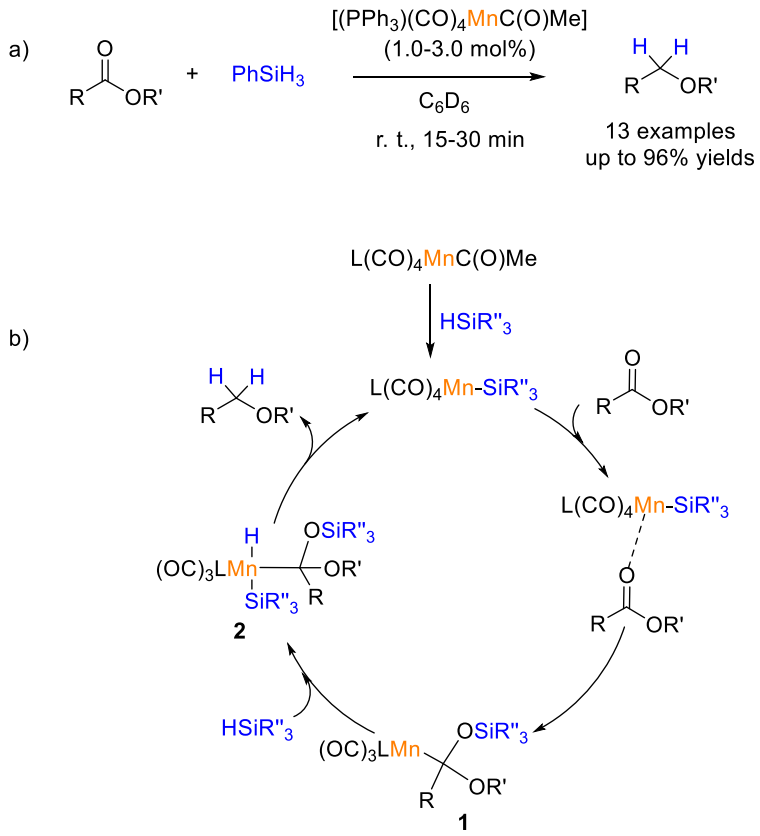

Scheme 3. Manganese-acyl catalyzed hydrosilylation of esters.

Trovitch and co-workers have developed a series of pyridine diimine (PDI) manganese complexes for the hydrosilylation of carbonyl and carboxyl acids derivatives (ketones, esters, aldehydes, and formates).[34–38] (^{Ph_2PPr}PDI)Mn complex **3** (**Scheme 4**) was found to be extremely active for the hydrosilylation of ketones. A variety of ketones were efficiently

reduced with TOFs of up to 1280 min^{-1} (76800 h^{-1}) in the absence of solvent. The same complex could also catalyze the hydrosilylation of esters with relatively modest TOF of 18 h^{-1}. Treating MeOAc with 1 mol% of **3** and 1 equiv. of $PhSiH_3$ in benzene, at room temperature for 24 h yielded a mixture of quaternary silanes that included $PhSi(OMe)_3$, $PhSi(OEt)_3$, $PhSi(OMe)_2(OEt)$, and $PhSi(OEt)_2(OMe)$. Repeating the same reaction with $PhSiD_3$ confirmed that ethoxide substituents are produced from carbonyl reduction following reductive cleavage of the MeOAc acyl C−O bond (**Scheme 4**).[36]

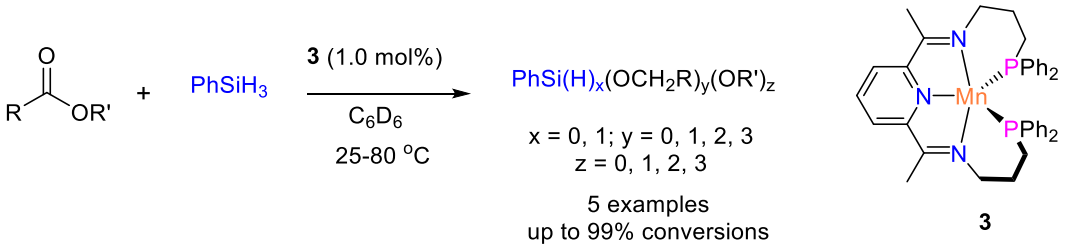

Scheme 4. Hydrosilylation of esters catalyzed by Mn complex **3**.

The dimer complex **4** has a similar activity to the monomeric complex **3**, both complexes are extremely active for the hydrosilylation of aldehydes with TOFs up to 4900 and 4950 min^{-1} respectively, which is the highest TOF reported for base metal catalyzed carbonyl hydrosilylation. Complex **4** was also found to be active for the hydrosilylation of formates under mild conditions: a neat equimolar mixture of alkyl or aryl formate and $PhSiH_3$ was added to 0.01 mol % of **4** and stirred at room temperature for 30 min to produce quantitatively the corresponding silyl ethers, which gave the corresponding alcohols after hydrolysis (**Scheme 5**).[38]

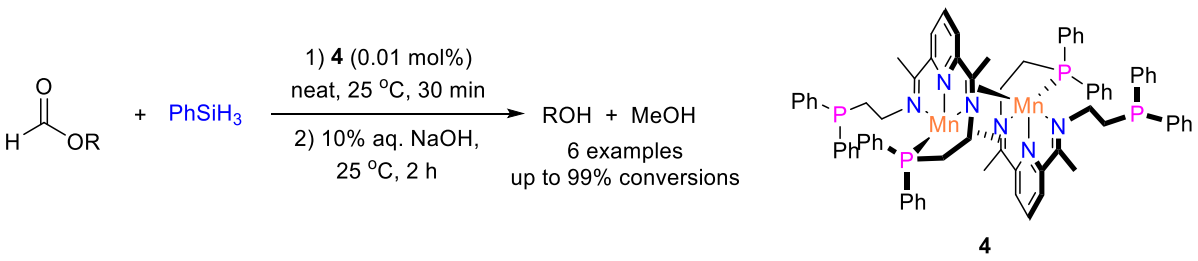

Scheme 5. Manganese-acyl catalyzed hydrosilylation of formates.

In 2017, Stradiotto and Turculet[39] reported the (N-phosphinoamidinate) manganese complex **5** for the reduction of carbonyl compounds and esters derivatives. The reaction proceeded at room temperature, with a catalyst loading of 1 mol% in the presence of phenylsilane. Within 4

h., a series of methyl benzoate derivatives bearing electron-donating or electron-withdrawing groups were efficiently reduced to the corresponding alcohols (**Scheme 6**).

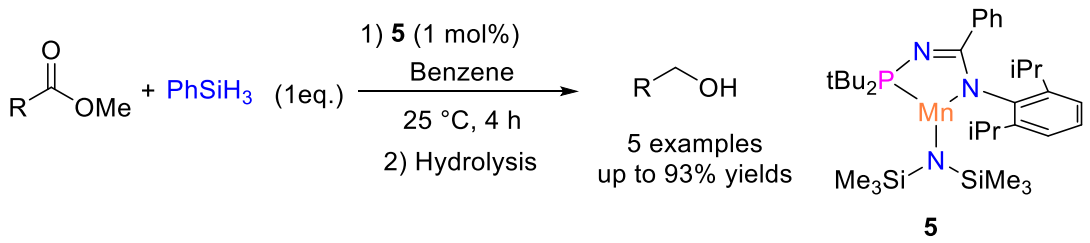

Scheme 6. Manganese complex catalyzed hydrosilylation of methyl benzoate derivatives.

Recently, manganese complexes bearing triazole ligands **6-9** were reported by Werlé and Leitner[40] for the hydrosilylation of ketones, esters, and carboxylic acids. All complexes were found to be effective catalysts for the hydrosilylation of ketones into alcohols. Using 1 mol% of catalyst loading and 1 equiv. of $PhSiH_3$ at 80 °C within 3 h, the desired product could be obtained quantitatively. When the reaction's times were reduced to 1 h and the catalyst loading to 0.1 mol%, complex **7** showed the best performance (55% yield), followed by complex **6** (30% yield), while no catalytic activity was observed with complexes **8** and **9** under the same conditions. Esters were reduced into alcohols with high conversions in moderate to good selectivity toward alcohols, using the tridentate complex **6** (2 mol%), while the bidentate complex **7** favored the formation of ether products, the others catalysts were less efficient. Interestingly, complex **6** provides the first example for effective manganese(I) catalyzed hydrosilylation of carboxylic acids to alcohols. Alkyl and aryl carboxylic acids substrates were reduced in high yields with excellent selectivity, using 2 mol% of **6**, at 80 °C in 2 h (**Scheme 7a**).

Mechanistic studies were performed for the hydrosilylation of carboxylic derivatives (**Scheme 7b**). The reaction between complex **6** and $PhSiH_3$ resulted in the formation of the hydride complex **10** which was characterized by HRMS analysis indicating a molecular formula $[C_{31}H_{25}MnN_4O_2P]^+$ and ^1H NMR spectroscopy by displaying a hydride signal at −8.56 ppm. Hydride transfer step between the hydride complex **10** and $PhSiH_3$ to the activated silyl substrate afforded the intermediate **A** which can give the corresponding aldehyde after hydrolysis or **A** undergoes a second Mn-catalyzed hydride transfer to the silylether derivatives yielding after hydrolysis the corresponding alcohol **B** or ether **C**.

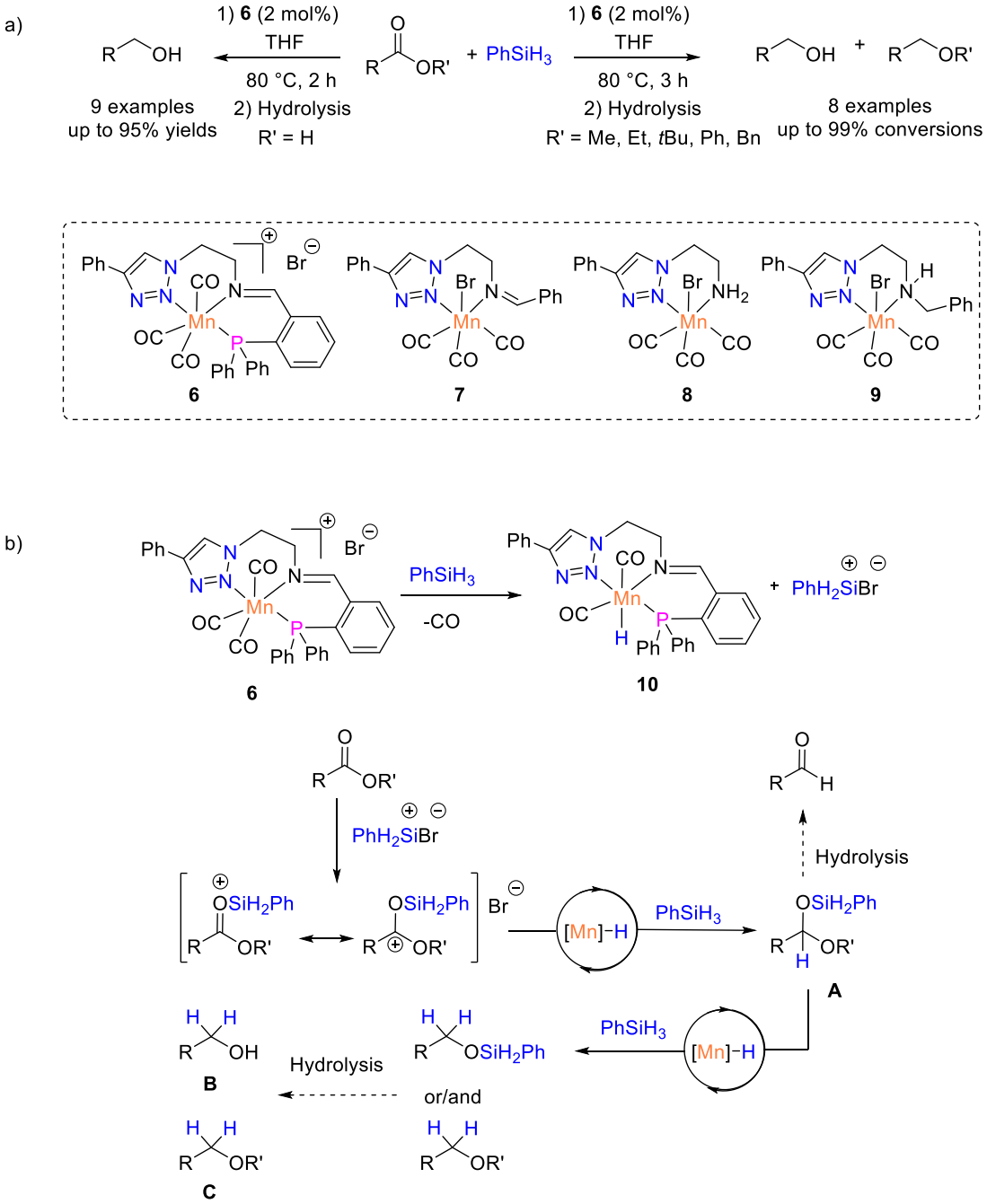

Scheme 7. Hydrosilylation of carboxylic acid derivatives catalyzed by Mn(I) complexes bearing triazole ligands.

From commercially available bisphosphine ligand, another Mn(I) complex catalyzed hydrosilylation of esters to alcohols was synthesized by Khamari and Bagh[41] affording a very selective and efficient hydrosilylation reaction compared to the tridentate (PNN)-iminotriazole Mn(I) complex **6** reported by Werlé and Leitner. A large reaction scope was demonstrated, with 1 mol % of catalyst **11** and 1 equiv. of $PhSiH_3$ at 100 °C under solvent free conditions. Various aromatic esters, methyl and ethyl benzoate derivatives, methyl 2-furoate, electron-

donating and electron-withdrawing functionalities, and benzyl acetate derivatives were reduced to the corresponding alcohols within 6 h in high isolated yields (73-97%). Interestingly, long-chain fatty alcohols which are very important products for chemical industry were obtained in excellent isolated yields (95-97%), using (1-2 mol%) of catalyst **11** and (1-3 eq.) of $PhSiH_3$ at (100-120 °C) within (6-24 h). Under the same reaction conditions, unsaturated esters substrates, methyl undecenoate and methyl oleate were tolerated as the corresponding alcohols were produced in good yields (71 and 83 % respectively), the C=C bond remaining intact. Keto ester, methyl levulinate, dimethyl adipate, six- and seven membered lactones, and poly(1,6-hexamethylene adipate), were reduced to the corresponding diols in good isolated yields (67-81%) (**Scheme 8**).

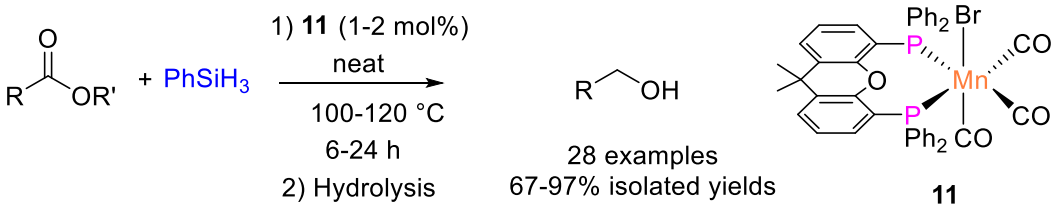

Scheme 8. Bisphosphine manganese(I) complex **11** catalyzed hydrosilylation of esters into alcohols.

Manganese complexes catalyzed amides reduction in the presence of silane are rare. In 2001, the group of Fuchikami[42] reported the reaction of amides with hydrosilanes catalyzed by a variety of transition-metal carbonyl complexes including manganese ones. With 1 mol% of $Mn_2(CO)_{10}$ in the presence of Et_2NH as co-catalyst, N-acetylpiperidine was reduced to N-ethylpiperidine in good yield 89% (**Scheme 9a**). In 2012, Pannell and co-workers[43] demonstrated the catalytic activity of $CpMn(CO)_3$ for the reduction of DMF and *N,N*-diethylformamide under UV irradiation or thermal conditions in the presence of $PhMe_2SiH$ as reducing agent (**Scheme 9b**).

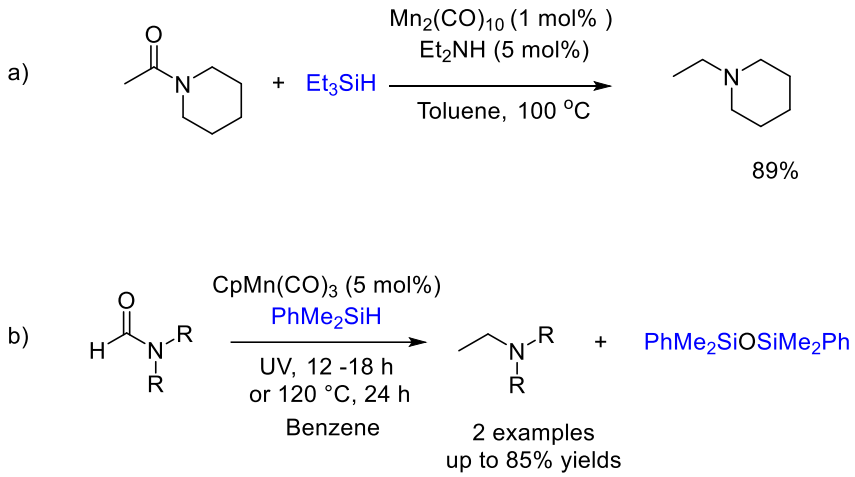

Scheme 9. Manganese-catalyzed reduction of amides with hydrosilanes.

Complex **5** was also found to be an active catalyst for the reduction of tertiary amides to tertiary amines in the presence of phenylsilane. A variety of aromatic and aliphatic tertiary amides were reduced in relatively short reaction times (75 ˚C, 1 h) with 5 mol% catalyst loading of **5**, or at room temperature within 18 h, using 2 mol% of **5** (**Scheme 10**).

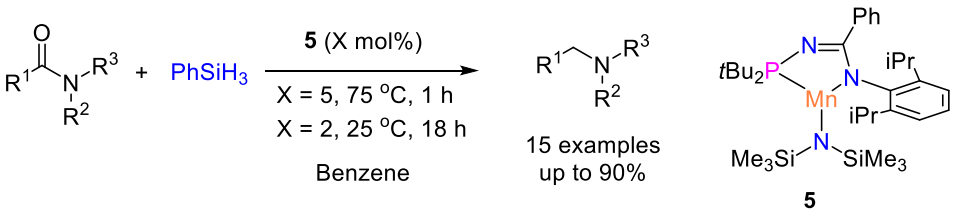

Scheme 10. Manganese complex **5** catalyzed hydrosilylation of amides.

The first and only example of manganese catalyzed hydrosilylation of carboxylic acids into aldehydes was described by our group[44] in 2013, using commercially available manganese carbonyl complex $Mn_2(CO)_{10}$ (5 mol%) in the presence of triethylsilane (3.3 equiv.) as reducing agent under UV irradiation at room temperature. A large variety of aromatic and aliphatic carboxylic acids were reduced to the corresponding aldehydes after acidic hydrolysis in good to excellent yields (**Scheme 11**).

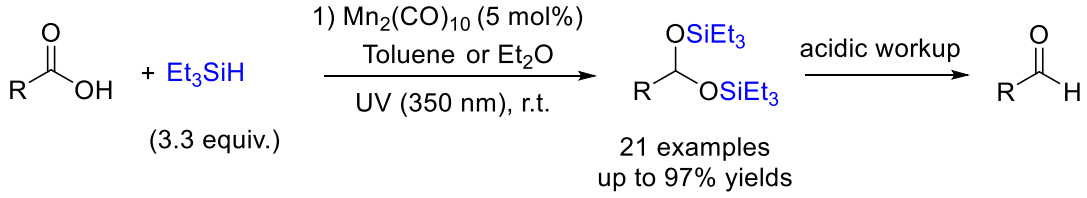

Scheme 11. Manganese carbonyl complex catalyzed hydrosilylation of carboxylic acids.

3. Rhenium catalyzed hydrosilylation of carboxylic acid derivatives

The first rhenium-catalyzed hydrosilylation reaction was developed by Toste *et al.* in 2003,[45] highlighting a new reactivity of a rhenium-dioxo complex as a catalyst for the reduction of organic functional groups, which exhibits a complete reversal from the traditional role of these complexes as oxidation catalysts. Large variety of aromatic or aliphatic ketones and aldehydes were reduced using iododioxo(bistriphenylphosphine)rhenium(V) [$(PPh_3)_2Re(O)_2I$] as catalyst in the presence of Me_2PhSiH. This reaction was compatible with many functional groups such as amino, cyano, nitro, aryl halo, ester, and no side products were produced (**Scheme 12a**).

A detailed mechanism for this new type of reaction was proposed. The first step involves a formal [2 + 2] addition of silane to the Re=O bond in **12** to produce metal hydride **D** which was confirmed by NMR analysis. The addition of the hydride complex **D** to the carbonyl group yielded the intermediate **E**, transfer of the silyl group to the alkoxy ligand, followed by formally a retro- [2 + 2] reaction, produced the silyl ether product and regenerates the dioxo-catalyst (**Scheme 12b**).

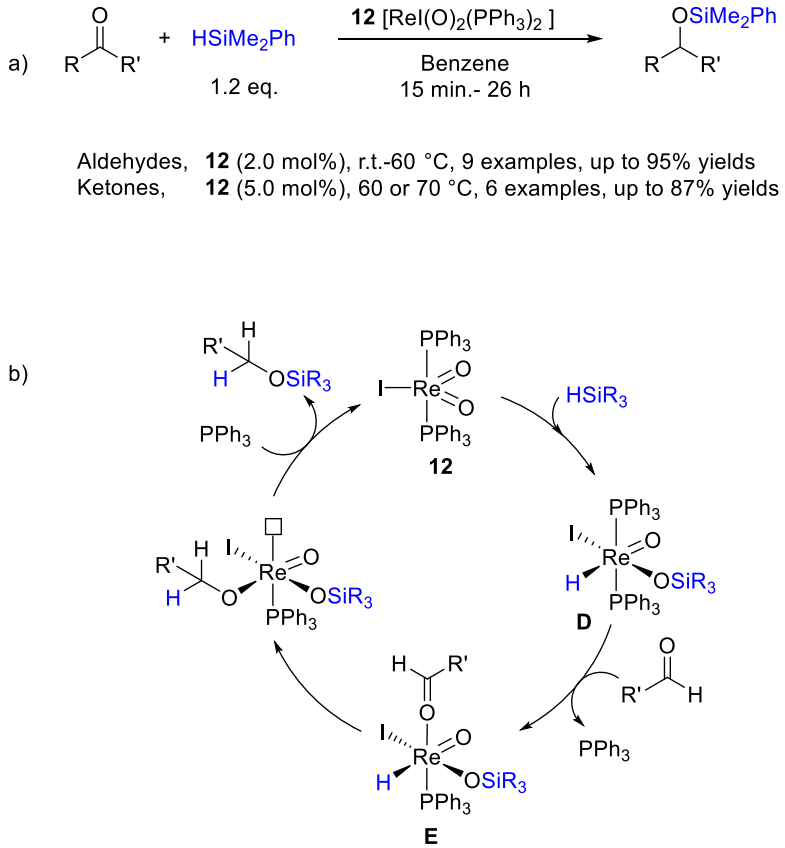

Scheme 12. Rhenium(V)-dioxo complex catalyzed hydrosilylation reaction of ketones and aldehydes.

Rhenium complexes that catalyze hydrosilylation of carboxylic derivatives are quite rare. In 2011, the group of Fernandes[46] described a new catalytic system for the reduction of nitriles into the corresponding amines, with rhenium(V)-dioxo complex **12** (10 mol%) and 3 equiv. of phenylsilane in refluxing toluene under air atmosphere. Under these conditions, high chemoselectivity was obtained and a wide range of functional groups, such as halogen derivatives, OCH_3, SCH_3, SO_2CH_3 and NHTs were well tolerated (**Scheme 13a**).

The proposed mechanism is depicted on **Scheme 13b**. First, the coordination of two nitriles to the rhenium center, with liberation of two phosphines, afford the complex $ReIO_2(nitrile)_2$ **F**. The addition of the Si-H bond to one of the oxo-rhenium bond results in the formation of the hydride species $(nitrile)_2(O)IRe(H)OSiR_3$ **G**. Dihydrosilylation of the nitrile to the corresponding N-disilylamine **H**, followed by hydrolysis forms the desired product.

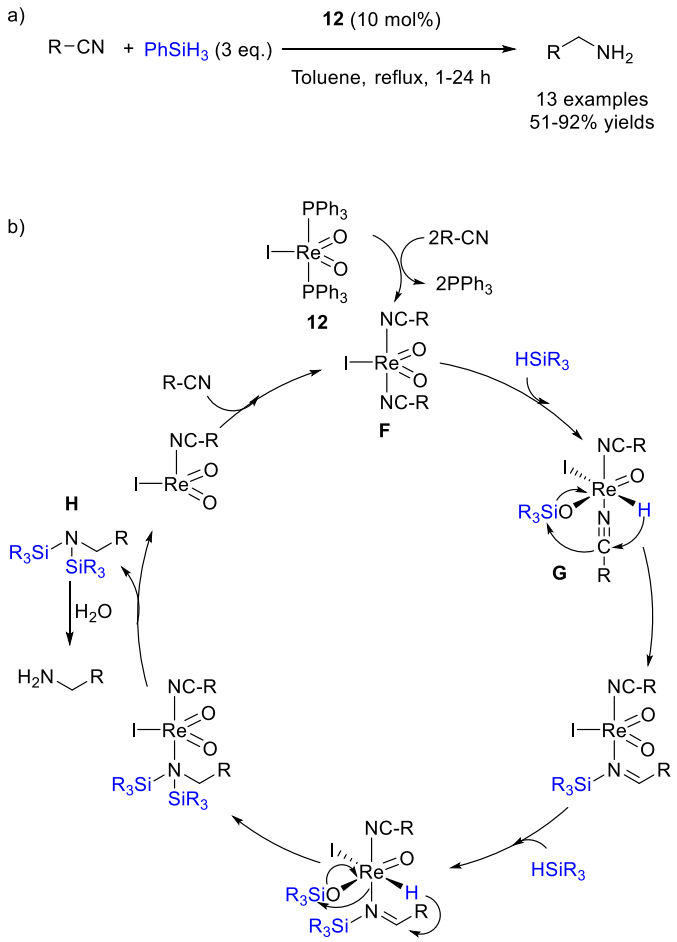

Scheme 13. Oxo-rhenium complex catalyzed hydrosilylation reduction of nitriles.

The commercially available rhenium(I) complexes $Re(CO)_5Cl$ and $Re_2(CO)_{10}$ were described by Fan and co-workers[47] as effective catalysts for the hydrosilylation of carbonyl substrates such as aldehyde, ketone, ester, and carbonate (**Scheme 14a**). The reaction proceeds in the presence of Et_3SiH, under UV irradiation at room temperature, with 1 mol% of $Re(CO)_5Cl$, various aromatic or aliphatic aldehydes and ketones were thus reduced with TOF of 20−25 h^{-1} for aldehydes. Esters and carbonates have been also reduced in the presence of $Re(CO)_5Cl$, with lower rate compared to that for the aldehydes. Under the previous conditions, the reaction of ethyl acetate and Et_3SiH produced ethoxytriethylsilane as the main product with a trace amount of diethyl ether. Similar results have been obtained for methyl phenylacetate and methyl formate. The reaction of Et_3SiH with diethyl carbonate afforded a mixture of $EtOCH_2OSiEt_3$ as a major product and Et_3SiOEt, a trace amount of ethyl formate, EtOCHO, has been detected.

A catalytic cycle for the hydrosilylation of carbonyl compounds was proposed to account for the experimental observations. The photolysis reaction of $Re(CO)_5Cl$ with Et_3SiH results in the formation of a dimeric rhenium carbonyl species with a bridging hydride $HRe_2(CO)_9(SiEt_3)$, which was characterized by IR and NMR spectroscopy analysis, its bridging hydride signal has been found at −9.03 ppm in the NMR spectrum. Another hydride signal at −5.77 ppm found in the reaction mixture has been attributed to $HRe(CO)_5$.

Upon photolysis, the dimer dissociates to afford $Et_3SiRe(CO)_4$ **I** and $HRe(CO)_5$ which was proved to be sluggish in catalysis. Coordination of the carbonyl substrate onto the vacant site of **I** facilitates the silyl ligand shift onto the oxygen atom to form **J**. Another silane molecule undergoes coordination *via* a η^2-silyl complex or a σ-silyl (σ_H) complex **K**. The H atom migrates from the silane to the alkyl group, thus regenerating the catalyst **I** and giving the silyl ether product (**Scheme 14b**).

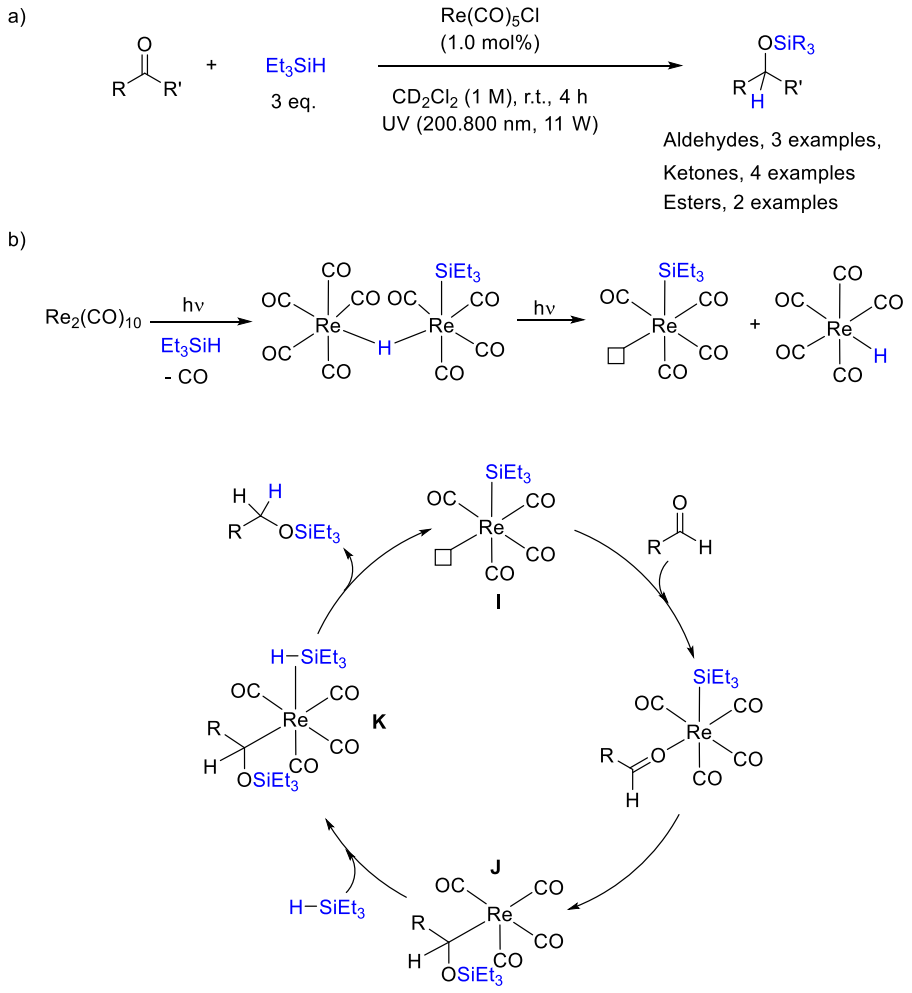

Scheme 14. Catalytic hydrosilylation of carbonyl compounds using $Re(CO)_5Cl$ as catalyst.

In summary, in this short survey of the literature, we have shown that carboxylic acid derivatives could be selectively reduced to alcohols, ethers, or aldehydes (**Scheme 15**). However, the hydrosilylation of esters into aldehydes remains unknown to date with manganese, while only one example was described with rhenium.[47] In the case of carboxylic acids, a sole example has been reported by our group,[44] however, high catalyst loading (5 mol%) and excess of silane (3.3 equiv.) were required. Therefore in this part of this thesis, we focused on the selective formation of aldehydes either from carboxylic acids with $Re_2(CO)_{10}$ or from esters with $Mn_2(CO)_{10}$ and $Re_2(CO)_{10}$ complexes.

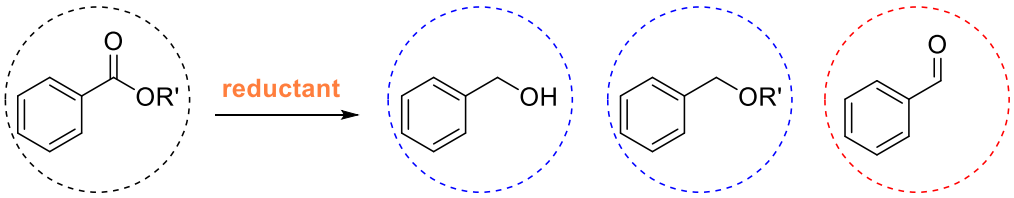

Scheme 15. Reduction of carboxylic acids and esters into alcohols, ethers, or aldehydes.

4. Results and discussions

4.1 $Re_2(CO)_{10}$ catalyzed hydrosilylation of carboxylic acids

Contributions in this part: Optimization: Duo Wei, Scope and Mechanistic studies: Duo Wei and Ruqaya Buhaibeh.

Publication: D. Wei, R. Buhaibeh, Y. Canac, J.-B. Sortais, *Org. Lett.* **2019**, *21*, 7713-7716.

4.1.1 Optimization of the reaction conditions

Based on the previous results obtained in the group for the reduction of carboxylic acids into aldehydes with $Mn_2(CO)_{10}$,[44] our first objective was to investigate the catalytic activity of its heavier analogue $Re_2(CO)_{10}$ and compare their reactivity in term of conditions and selectivity. Thus, the first conditions used here are based on those recently developed with $Mn_2(CO)_{10}$.[44] Using the complex $Re_2(CO)_{10}$ as pre-catalyst (5 mol%) and the tertiary silane Et_3SiH (4 equiv.) as reducing agent, a full conversion of 2-naphthyl acetic acid **a1** to the corresponding disilylacetal product **b1** was observed after 3 h of irradiation at 395 nm (LED, 45 W), at r.t. (ca. 30 °C) in toluene (Table 1, entry 1). The conditions were further optimized to decrease both the catalytic charge to 0.5 mol% (entry 2 and even up to 0.2 mol%, entries 3-4) and the amount of Et_3SiH to 2.2 equiv. (entries 5-6). After 9 h of irradiation, under these conditions ($Re_2(CO)_{10}$ 0.5 mol%, Et_3SiH 2.2 equiv.), the desired product **b1** was finally obtained with high conversion and selectivity (97%, entry 6).

Following these results, a series of control experiment was then performed (entries 7-13). In the absence of any light, under thermal conditions, or even in the presence of visible light, no conversion of **a1** was detected after 9 h (entries 7-9). With 0.5 mol% catalytic charge and 2.2 equiv. of Et_3SiH, the highest conversion of **a1** (ca. 98%) was observed when the reaction was performed under UV irradiations (350 nm) in a Rayonnet RPR100 apparatus (entry 10). Noteworthy, the use of a medium pressure UV mercury lamp (150 W) led to a 69% yield of **b1+c1** after only 1 hour and with good selectivity (ratio **b1**:**c1** = 94:6, entry 11). Changing the $Re_2(CO)_{10}$ catalyst to $Re(CO)_5Br$ (1.0 mol%) does not affect the outcome of the reaction,[47] the disilylacetal **b1** being formed in 95% yield under UV irradiation (350 nm) (entry 12). In the absence of any Re-based catalyst, no conversion of the 2-naphthyl acetic acid **a1** could be detected (entry 13).

Table 1. Optimization of the parameters for the reduction of 2-naphthyl acetic acid **a1**.[a]

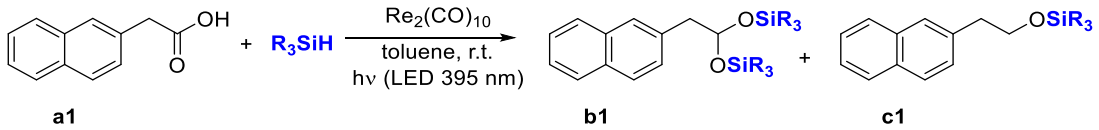

a1 b1 c1

Entry	$Re_2(CO)_{10}$ (mol%)	Silane (equiv.)	Time (h)	Yield **b1**+**c1**	Selectivity	
					b1	**C1**
1	5	Et_3SiH (4)	3	>98	99	1
2	0.5	Et_3SiH (4)	3	77	95	5
3	0.2	Et_3SiH (4)	3	44	95	5
4	0.2	Et_3SiH (4)	6	84	93	7
5	0.5	Et_3SiH (2.2)	6	69	97	3
6	0.5	Et_3SiH (2.2)	9	97	97	3
7[b]	0.5	Et_3SiH (2.2)	9	0	-	-
8[c]	0.5	Et_3SiH (2.2)	9	0	-	-
9[d]	0.5	Et_3SiH (2.2)	9	0	-	-
10[e]	0.5	Et_3SiH (2.2)	9	>98	98	2
11[f]	0.5	Et_3SiH (2.2)	1	69	94	6
12[e,g]	1	Et_3SiH (2.2)	9	95	95	5
13[e]	0	Et_3SiH (2.2)	9			

[a] General condition: In a Schlenk tube, $Re_2(CO)_{10}$, toluene, the silane and **a1** were added in that order. The reaction was stirred under irradiation (395 nm, 45W) at r.t.. Conversion and selectivity were detected by ^1H NMR on the crude reaction mixture.

[b] In the dark.

[c] At 100 °C, no irradiation.

[d] Visible light irradiation (30 W).

[e] Under UV irradiations (350 nm) in a Rayonet RPR100 apparatus.

[f] Under UV irradiation with a medium pressure lamp (150 W).

[g] $Re(CO)_5Br$ (1 mol%) as catalyst.

4.1.2 Optimization of the silanes for the reduction of 2-naphthyl acetic acid a1

The nature of the silane was shown to be crucial for the selectivity of the reaction (Table 2). Indeed, the use of Et_2SiH_2 and $PhSiH_3$ (4 equiv., entries 1 and 3) lowered the conversion of **a1**, while Ph_2SiH_2 reversed the selectivity in favor of the silylether **c1**, obtained in 80% yield after 3 h of exposure time (entry 2). For its part, TMDS (4 equiv.) led to a full conversion of **a1** but

as a 55/45 mixture of adducts **b1** and **c1** (entry 4). Among other tertiary silanes tested (Me_2PhSiH, Ph_2MeSiH, Ph_3SiH and, $(EtO)_3SiH$, entries 5-9), only Me_2PhSiH led to the formation of **b1** with satisfying selectivity (entry 5, 91%), albeit being less efficient than Et_3SiH under optimized conditions (entry 6, Table 1).

Table 2. Optimization of the silane for the reduction of 2-naphthyl acetic acid a1.[a]

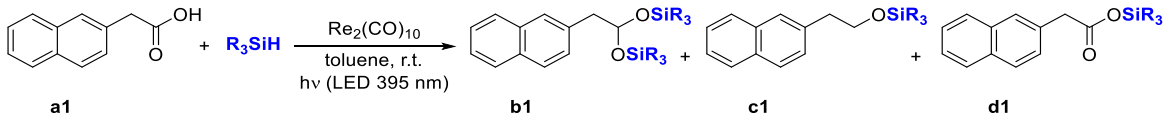

Entry	$Re_2(CO)_{10}$ (mol%)	Silane (equiv.)	Time (h)	Conv. (%)	Selectivity			Yield **b1**+**c1** (Selectivity **b1**:**c1**)
					b1	**c1**	**d1**	
1	0.5	Et_2SiH_2 (4)	3	26	69	31	-	26 (69:31)
2	0.5	Ph_2SiH_2 (4)	3	81	1	99	-	81 (1:99)
3	0.5	$PhSiH_3$ (4)	3	45	49	18	33	31 (73:27)
4	0.5	TMDS (4)	3	> 98	55	45	-	> 98 (55:45)
5	0.5	Me_2PhSiH (4)	3	>98	91	9	-	> 98 (91:9)
6	0.5	Me_2PhSiH (2.2)	9	>98	67	8	25-	> 74 (90:10)
7	0.5	Ph_2MeSiH (4)	3	85	-	-	>98	0
8	0.5	$(EtO)_3SiH$ (4)	3	>98	-	-	92[b]	0
9	0.5	Ph_3SiH	3	73	-	-	>98	0

[a] General conditions: In a Schlenk tube, $Re_2(CO)_{10}$, toluene, the silane and **1a** were added in that order. The reaction was stirred under irradiation (395 nm, 45W) at r.t.. Conversion and selectivity were detected by ^1H NMR on the crude reaction mixture.

[b] 8% of aldehyde was detected.

4.1.3 Scope of the reaction

With the optimized conditions in hand, *i.e.* $Re_2(CO)_{10}$ (0.5 mol%), Et_3SiH (2.2 equiv.) under irradiation (395 or 350 nm, Table 1, entries 6 and 10), the synthetic scope of this Re-catalyzed reduction of carboxylic acids to disilylacetals was investigated. As shown in **Scheme 16**, 2-naphthyl acetic acid **a1**, 1-naphthyl acetic acid **a2**, 2-phenyl acetic acid **a3**, methyl substituted 2-phenyl acetic acids **a4-a6** and 2-(4-methoxyphenyl) acetic acid **a8** were smoothly converted in the corresponding disilyl acetal products in good yields (up to 97%), although the reaction was shown to be less effective in the case of the *ortho*-substituted acid **a6** (ca. in 62% isolated

yield). Sterically hindered acids such as 2-phenylbutanoic acid **a7** could be also reduced but with lower efficiency (ca. 22 %). The reaction is tolerant to amino, fluoro and chloro groups, as demonstrated with the formation of **a9** in 75% yield without any evidence of silylamine species, and of products **a10** and **a11** bearing fluorine and chlorine atoms formed in 92% and 98% yield, respectively. On the opposite, 2-(4-bromophenyl)acetic acid **a12** inhibited the reaction, and debromination of **a12** was detected (c.a. 3%). Interestingly, hetero-aromatic substituted acetic acids based on thiophene **a13** and 1*H*-indole **a14** rings were reduced affording related products **b13** and **b14** in 59% and 89% yield, respectively. Carboxylic acids with longer carbon chains (**a15-a20**) gave also the corresponding acetals in excellent yield up to 98%. Notably, dicarboxylic acid **a18** led to the reduction product **b18** in 99% yield. The internal C=C bond in precursors **a19** and **a20** was not altered while the conjugated C=C bond of cinnamic acid was fully reduced yielding the saturated product **b15**. The latter was also formed by direct reduction of 3-phenylpropionic acid **a15**. The scope of the reaction was successfully extended to cyclohexane **a21** and cyclopentane **a22** carboxylic acids. Corresponding products **b21** and **b22** were formed in good yields (ca. 90-91%). It is worth mentioning that acetic and formic acids were also reactive in the current reaction, producing **b23** and **b24** in about 90% yield. Noteworthy, a series of substrates were not tolerated under the selected catalytic conditions, such as 2-pyridine carboxylic acid, mandelic acid and 4-nitrophenyl- acetic acid.

Scheme 16. Scope of the Re-catalyzed reduction of carboxylic acids **a** to disilylacetals **b**

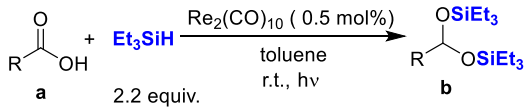

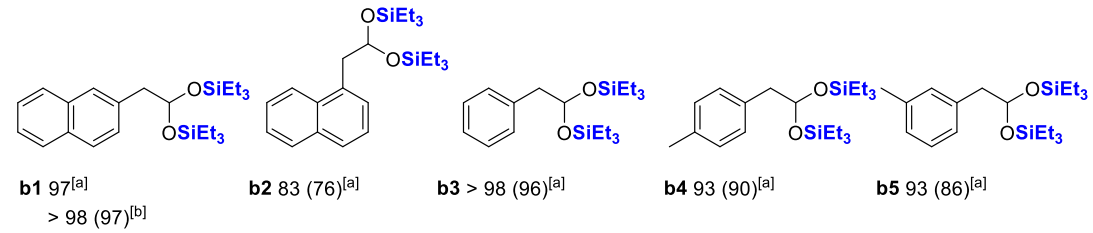

b1 97[a] > 98 (97)[b] **b2** 83 (76)[a] **b3** > 98 (96)[a] **b4** 93 (90)[a] **b5** 93 (86)[a]

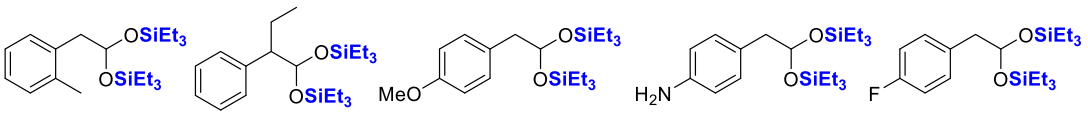

b6 75 (62)[a] **b7** 23 (22)[a,c] **b8** > 98 (95)[a] **b9** 94 (75)[a] **b10** > 98 (92)[a]

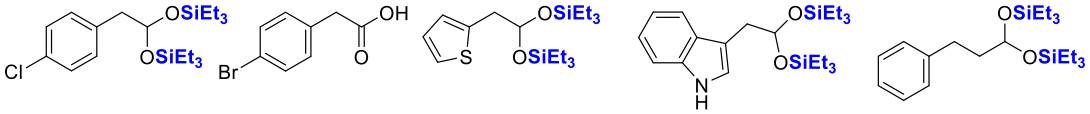

b11 > 98 (98)[a] **b12** 0 **b13** 66 (59)[a] **b14** 92 (89)[a] **b15** > 98 (93)[a] > 98[b] > 98[d]

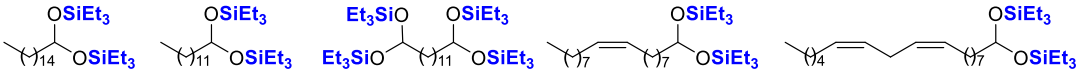

b16 > 98 (97)[a] > 98[b] **b17** > 98 (97)[a] **b18** > 98 (99)[a,e] **b19** > 98 (93)[a] > 98[b] **b20** > 98 (87)[a]

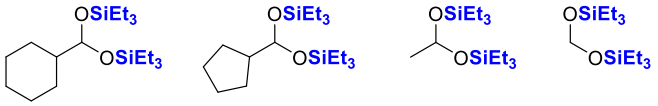

b21 93 (91)[a] >98[b] **b22** 98 (90)[a] **b23** > 98 (92)[a] > 98[b] **b24** > 98 (90)[a]

General conditions: carboxylic acid (0.5 mmol), Et_3SiH (176 µL, 1.1 mmol, 2.2 equiv.), $Re_2(CO)_{10}$ (1.6 mg, 0.5 mol%), r.t., toluene (1.0 mL), irradiation, 9 h; Conversion of **a** was detected by ^1H NMR of the crude mixture; and isolated yields of **b** were shown in parentheses.

[a] UV irradiation at 350 nm (Rayonet).

[b] Irradiation at 395 nm (LED).

[c] NMR Yield.

[d] Starting from cinnamic acid.

[e] $Re_2(CO)_{10}$ (1 mol%), Et_3SiH (4.4 equiv.).

In the perspective of synthetic applications, a gram-scale experiment was performed from 3-phenylpropionic acid **a15** (1.0 g, 6.7 mmol). After 24h reaction, **a15** was fully converted into the diacetal **b15** along with the silylether **c15** obtained in 72% and 28% NMR yield, respectively. After acid treatment (1N aqueous HCl),[22] the related 3-phenylpropionaldehyde was finally isolated in 61% yield.

4.1.4 Optimization for the reduction of aromatic carboxylic acids to aldehydes

Given the efficiency of the catalytic system, the reduction of more challenging benzoic acid derivatives was then investigated. Indeed, it has been reported that iron-based catalysts[48] are not active in the reduction of aromatic acids while $Mn_2(CO)_{10}$[44] lead to low yields and that in the case of $B(C_6F_5)_3$, a higher catalytic charge compared to aliphatic acids is required.[49]

The first catalytic tests carried out under the conditions developed for the aliphatic acids did not lead to any reaction with benzoic acid **e1**, even after 48 h. Increasing the catalyst loading to (5 mol%) and the amount of Et_3SiH (4 equiv.) enabled the formation of the corresponding benzaldehyde **f1** as evidenced by ^1H NMR of the crude mixture (25% conversion, Table 3, entry 3). In order to improve the conversion of benzoic acid **e1** into benzaldehyde **f1**, other silanes were then tested, no conversion of **e1** was observed with Ph_3SiH and $PhMe_2SiH$ (entries 4 and 5) while a satisfactory conversion (71%) was obtained in the presence of Ph_2MeSiH (4 equiv.) after 48 h under irradiation (350 nm) at r.t in Et_2O (entry 6).

Table 3. Optimization of the parameters for the reduction of benzoic acid **e1**.[a]

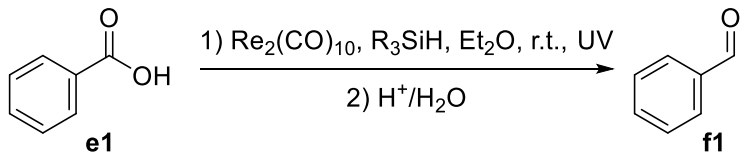

e1 **f1**

Entry	$Re_2(CO)_{10}$ (mol%)	Silane (equiv.)	Time (h)	Conv. [a] (%)	NMR-yields[b] Silylacetal	Aldehyde
1	5	Et_3SiH (2.2)	48	16	0	16
2	5	Et_3SiH (3.3)	48	17	0	17
3	5	Et_3SiH (4)	48	25	0	25
4	5	Ph_3SiH (4)	48	0	-	-
5	5	$PhMe_2SiH$ (4)	48	0	-	-
6	5	Ph_2MeSiH (4)	48	71	45	26
7	2	Ph_2MeSiH (4)	48	5	5	0
8	1	Ph_2MeSiH (4)	48	0	-	-

[a] General conditions: A 20 mL Schlenk tube was charged with $Re_2(CO)_{10}$ (1.0 - 5.0 mol%), benzoic acid (0.25 mmol) under argon atmosphere, followed by Et_2O (0.5 mL) and silane, then irradiated under UV irradiations (350 nm) in a Rayonet RPR100 apparatus at r.t. for 48 h. Then reaction mixture was hydrolysed at r.t. with trifluoroacetic acid (99%, 0.25 mL) for 3 h. Conversion of benzoic acid was detected by ^1H NMR of the crude mixture.

[b] NMR-yields of silylacetal and aldehyde detected by ^1H NMR of the crude mixture before hydrolysis.

4.1.5 Scope of the reduction of aromatic carboxylic acids

The general scope of the present reaction is presented on (**Scheme 17**). 2-Naphthoic acid **e1** afforded the corresponding aldehyde **f1** in 82% isolated yield. Aromatic acids **e3-e4** bearing electron-donating -OMe and $-NMe_2$ groups led to the related aldehydes **f3-f4** in good yields. Hetero-aromatic acids based on furane, thiophene and pyrrole rings (**e6-e8**) and 4-cyanobenzoic acid **e5** gave also the corresponding aldehydes but with moderate yields (23-58%). Low conversions were observed from acid precursors containing an electron-withdrawing group, such 4-(trifluoromethyl)benzoic acid **e9** and 4-chlorobenzoic acid **e10**. No conversion was detected for **e11**.

Scheme 17. Scope of the reduction of aromatic carboxylic acids to aldehydes.[a]

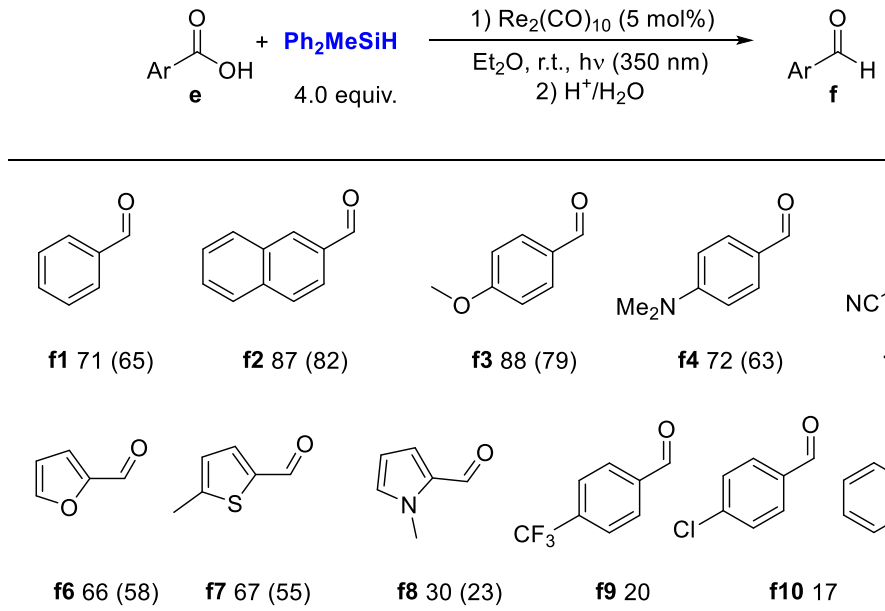

[a] General conditions: carboxylic acid **e** (0.5 mmol), Ph_2MeSiH (200 µL, 1.0 mmol, 4.0 equiv.), $Re_2(CO)_{10}$ (8.2 mg, 5.0 mol%), r.t., Et_2O (1.0 mL), UV irradiation (350 nm)), 48 h, then hydrolysed at r.t. with trifluoroacetic acid (99%, 0.25 mL) for 3 h. NMR-yield of **f** was detected by ^1H NMR of the crude mixture after hydrolysis, and isolated yields of **f** were shown in parentheses.

4.1.6 Reduction of aliphatic α,β-unsaturated carboxylic acids to aldehydes

Since α,β-unsaturated aldehydes are of significant interest in the fragrance, vitamins, and flavour industries,[50–52] some aliphatic α,β-unsaturated carboxylic acids were tested in this catalytic transformation. With 0.5 mol% of $Re_2(CO)_{10}$ and Et_3SiH 2.2 equiv. in Et_2O, after irradiation for 9 h at room temperature, butenoic acid **e12** and 3-methyl-2 butenoic acid **e13** were fully reduced directly to aldehydes to give the corresponding saturated aldehydes **f12** and **f13** in 82% and 91% isolated yields, respectively after hydrolysis (**Scheme 18**).

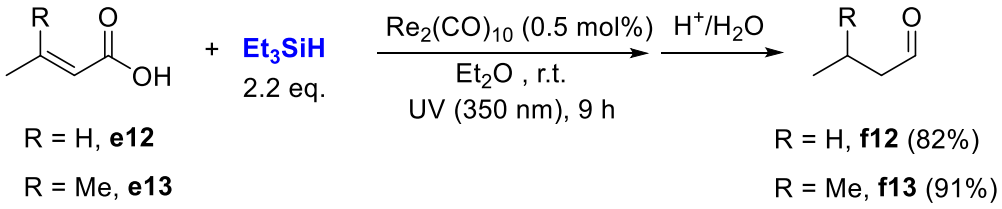

Scheme 18. $Re_2(CO)_{10}$ catalyzed hydrosilylation of aliphatic α,β-unsaturated carboxylic acids to aldehydes.

4.1.7 Conclusion

In this part, we have demonstrated that $Re_2(CO)_{10}$ does catalyze the reduction of carboxylic acids in the presence of Et_3SiH into disilylacetals that can be easily converted to aldehydes upon hydrolysis. On interest, in comparison with $Mn_2(CO)_{10}$, the catalytic loading is divided by ten from 5 mol% to 0.5 mol% and the quantity of silanes reduced from 3.3 to 2.2 equivalents. These results prompted us to investigate the more challenging, or at least unreported, reduction of esters into aldehydes with both catalytic systems.

4.2 Manganese and Rhenium-catalyzed Selective Hydrosilylation of Esters to Aldehydes

Contributions in this part: Duo Wei, Ruqaya Buhaibeh, equal contribution.
Publication: D. Wei, R. Buhaibeh, Y. Canac, J.-B. Sortais, *Chem. Commun.* **2020**, *56*, 11617-11620.

4.2.1 Optimization of the reaction conditions with $Mn_2(CO)_{10}$

We firstly reacted methyl 2-naphthylacetate **g1** with Et_3SiH (4 equiv.) in the presence of $Mn_2(CO)_{10}$ (5.0 mol%) under irradiation (LED, 365 nm, 4*10 W) in toluene at room temperature (Table 4). To our delight, within 3 h, **g1** was converted to the corresponding alkyl silyl acetal **h1** obtained as a major product in 92% conversion and 82% selectivity, while only 18% of the undesired silyl ether **i1** was formed simultaneously due to over reduction (entry 1). Lowering the amount of silane from 4 to 1.1 equiv. induced a decrease of the conversion (from 92% to 60%) but enhanced significantly the selectivity toward the desired product **h1** (entries 2-4). With only 1.1 equiv. of Et_3SiH, in 9 h, **h1** was obtained in 89% NMR yield with an excellent selectivity (90% conversion, ratio **h1**: **i1** over >95: <5, entry 6).

Then a series of control experiments were performed. Under visible light irradiation (LED, 400-800 nm, 30 W) using 2 equiv. of Et_3SiH, 56% conversion of **g1** was observed, with a ratio of >95: <5 for products **h1**: **i1** (entry 7). Replacing the UV-LED devices by a Rayonnet RPR100 apparatus (350 nm) had little influence on both reactivity and selectivity (entry 8). Noteworthy, under the same conditions, the use of a medium pressure UV mercury lamp (150 W) led to a 86% conversion after only 1 h but the selectivity **h1**: **i1** dropped to 85: 15 (entry 9). In the absence of any light or under thermal conditions[17] (100 °C), no conversion of **g1** was detected after 6 h (entries 10 and 11), demonstrating that the photo irradiation is essential to reduce methyl 2-naphthylacetate **g1**. No reaction took place using $Mn(CO)_5Br$ and $CpMn(CO)_3$ as catalysts (entries 12 and 13).

Table 4. Optimization of the parameters for the reduction of **g1** with $Mn_2(CO)_{10}$.[a]

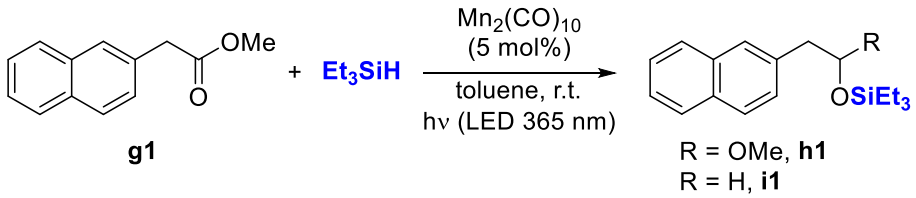

g1

R = OMe, **h1**
R = H, **i1**

Entry	Et_3SiH (equiv.)	Time (h)	Conv. of **g1** (%)[b]	Selectivity **h1** : **i1** (%)[b]
1	4	3	92	82: 18
2	3	3	82	>95: <5
3	2	3	73	>95: <5
4	1.1	3	60	>95: <5
5	1.1	6	70	>95: <5
6	1.1	9	90	>95: <5
7[c]	2	6	56	>95: <5
8[d]	2	9	92	99: 1
9[e]	2	1	86	85: 15
10[f]	2	6	<1	-
11[g]	2	6	<1	-
12[h]	1.1	9	0	-
13[i]	1.1	9	0	-

[a] General conditions: In a Schlenk tube, $Mn_2(CO)_{10}$ (4.9 mg, 5.0 mol%), toluene (0.5 mL), Et_3SiH, and **g1** (50 mg, 0.25 mmol) were added in that order, then stirred under irradiation (LED 365 nm, 40W) at r.t. (c.a. 30 °C).

[b] Conversion of **g1** and yields of **h1** and **i1** detected by ^1H NMR.

[c] Irradiation (400-800 nm, 30 W).

[d] UV irradiations (350 nm) in a Rayonet RPR100 apparatus.

[e] With UV lamp (medium pressure mercury lamp,150 W).

[f] In the dark.

[g] At 100 °C.

[h] $Mn(CO)_5Br$ (10 mol%) as catalyst.

[i] $CpMn(CO)_3$ (10 mol%) as catalyst.

4.2.2 Optimization of the reaction conditions with $Re_2(CO)_{10}$

Having optimized the reduction of **g1** with $Mn_2(CO)_{10}$, we then investigated the catalytic efficiency of the related complex $Re_2(CO)_{10}$, applying the optimized conditions, albeit using a lower loading of catalyst (0.5 mol %) as in the case of carboxylic acids, **g1** was thus quasi-quantitatively converted (96%) and the corresponding acetal **h1** was obtained in good yield

with high selectivity (>95%, entry 3, Table 5). Using 4 equiv. of Et_3SiH, full conversion of **g1** was obtained after 6 h with lower selectivity 85% of the desired product **h1** and 15 % of silyl ether **i1** (entry 2). With $Re(CO)_5Br$ as catalyst, 72% conversion of **g1** was detected (entry 5). Finally, in the absence of catalyst, no conversion of **g1** was observed (entry 6).

Table 5. Optimization of the parameters for the reduction of methyl 2-naphthylacetate **g1** with $Re_2(CO)_{10}$.[a]

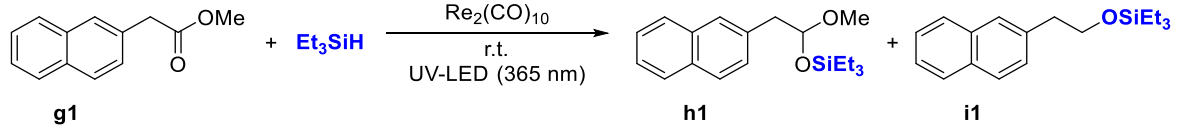

g1 **h1** **i1**

Entry	$Re_2(CO)_{10}$ (mol%)	Silane (equiv.)	Time (h)	Conv. (%)	Selectivity (%) h1 : i1
1	0.5	Et_3SiH (4)	3	75	96:4
2	0.5	Et_3SiH (4)	6	>99	85:15
3	0.5	Et_3SiH	9	96	99:1
4	1	Et_3SiH	6	92	94:6
5[b]	1	Et_3SiH	9	72	87:13
6	None	Et_3SiH	9	0	-

[a] General conditions: In a Schlenk tube, $Re_2(CO)_{10}$, toluene (1 mL), silane, and **g1** (100 mg, 0.5 mmol) were added in that order, then stirred under irradiation (LED 365 nm, 40W) at r.t. (c.a. 30°C); Conversion of **g1** and yields of **h1** and **i1** detected by ^1H NMR.

[b] $Re(CO)_5Br$ (1 mol%) as catalyst.

4.2.3 Optimization of the silanes for the reduction methyl 2-naphthylacetate g1

As in the case of carboxylic acids, the nature of the silane was found to be crucial for the selectivity of the reaction (Table 6). Indeed, the use of the secondary silane Et_2SiH_2 led to partial conversion of **g1** (41%) with the formation of a mixture of products **h1** and **i1** with a ratio 49: 51. On the contrary, Ph_2SiH_2, $PhSiH_3$ and TMDS reversed the selectivity of the reaction and **i1** was detected as the sole product. With other tertiary silanes such as Ph_3SiH and $MePh_2SiH$, no reaction was observed.

Table 6. Optimization of the silane for the reduction of methyl 2-naphthylacetate **g1**.

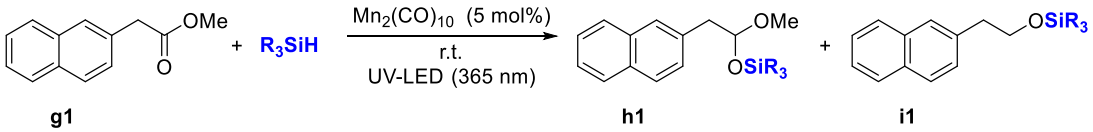

g1 h1 i1

Entry	Silane (equiv.)	Time (h)	Conv. (%)	Selectivity (%)	
				h1	**i1**
1	Et_2SiH_2 (3)	3	41	49	51
2	Ph_2SiH_2 (3)	3	>99	1	99
3	$PhSiH_3$ (3)	3	>99	1	99
4	TMDS (3)	3	>99	1	99
5	Ph_3SiH (1.1)	16	0	-	-
6	$MePh_2SiH$ (1.1)	16	0	-	-

[a] General conditions: In a Schlenk tube, $Mn_2(CO)_{10}$ (4.9 mg, 5 mol%), toluene (0.5 mL), silane, and **g1** (50 mg, 0.25 mmol) were added in that order, then stirred under irradiation (LED 365 nm, 40W) at r.t. (c.a. 30°C); Conversion of **g1** and yields of **h1** and **i1** detected by ^{1}H NMR.

4.2.4 Scope of the reaction

With the optimized conditions in hand (Method **A** ($Mn_2(CO)_{10}$, 5.0 mol%, table 4, entry 6) or Method **B** ($Re_2(CO)_{10}$, 0.5 mol%, table 5, entry 3), 1.1 equiv. of Et_3SiH, toluene, room temperature, 9 h, photo irradiation (365 nm, 40W), we then explored the scope of this transformation (**Scheme 19**). Noteworthy, since the two methods generally give similar results, we will detail below only those obtained with method **A**. The results observed with method **B** will only be mentioned, if there is a significant difference between the two metals. Methyl 2-naphthylacetate **g1**, 1-naphthylacetate **g3** and 2-phenylacetate **g5** were readily converted into the corresponding alkyl silyl acetals **h1**, **h3** and **h5** in 71-82% isolated yields. In general, ethyl esters were found to be more reactive than their methylated analogues, as demonstrated with the quantitative reduction of esters **g2**, **g4** and **g6** into the corresponding acetals **h2**, **h4** and **h6** obtained in high yields (94-99%). *p*-, *m*-, *o*-Methyl substituted methyl 2-phenylacetates **g7**, **g8** and **g9** were reduced in reasonable yields (59-83%). Increasing the steric hindrance at the phenyl ring barely affects the efficiency of this reaction, as illustrated with the ester **h10** featuring a mesityl group formed in 77% yield. Methyl 2-phenylacetate **g11** bearing a *p*-

methoxy substituent and its ethyl analogue **g12** were smoothly converted into the corresponding alkyl silyl acetals **h11** and **h12** isolated in 87% and 97%, respectively. From esters bearing halogen atoms (**g13**-**g16**), the corresponding products **h13**-**h16** were obtained in moderate to excellent yields (68-99%). It must be noted that the acetal **h14** decomposed into the corresponding aldehyde **j14** (**Scheme 23**) during its purification on silica gel. While $Mn_2(CO)_{10}$ afforded product **h15** in 59% yield, no conversion of the ester **g15** exhibiting a *p*-bromo substituent was observed with $Re_2(CO)_{10}$, in line with the results obtained for the reduction of carboxylic acids. In the same way, iodo derivatives were found to be not compatible with these catalytic systems. However, the reaction is tolerant to an electron-withdrawing group such as a *p*-trifluoromethyl substituent yielding the product **h16** in 75% yield.

Increasing the steric hindrance at the α-position of the ester decreased the reactivity, as observed with the methyl 2-phenylbutanoate **g17** converted into **h17** in 68% yield in the presence of 4 equiv. Et_3SiH. The reactions between Et_3SiH and methyl/ethyl/benzyl 3-phenylpropanoate substrates **g18**-**g20** afforded the corresponding acetals **h18**-**h20** in 88%, 99% and 99% yields, respectively. Esters bearing aliphatic chains like methyl decanoate **g21**, ethyl acetate **g22** and butyl formate **g23** gave full conversion affording the corresponding products **h21**, **h22**, and **h23** in 96%, 99% and 99% yields, respectively.

Dimethyl tridecanedioate **g24** was proved to be a suitable substrate since diacetal **h24** was formed in 92% isolated yield with 2.2 equiv. of Et_3SiH and $Re_2(CO)_{10}$ (1.0 mol%). The internal C=C bond in methyl oleate **g25** was also tolerated, as the acetal **h25** was produced in 56% yield with the C=C bond remaining intact.[53–56] On the opposite, when methyl 5-hexynoate was engaged as substrate, even in the presence of 2 equiv. of Et_3SiH, the hydrosilylation took place only at the terminal triple bond in line with the results reported by Wang *and coll.*[57]

Good isolated yields were generally obtained from benzoate derivatives, methyl and ethyl benzoate (**g26, g27)** and ethyl 4-methoxybenzoate **g28** were thus transformed into the acetals **h26, h27** and **h28** in 99%, 75%, and 95% yields with $Mn_2(CO)_{10}$. With $Re_2(CO)_{10}$ slightly lower conversions were observed for **h26** and **h28** (75% and 90%, respectively). Methyl 4-chlorobenzoate **g29** was reduced with a conversion of 37% and 80%, by using Mn and Re based-catalysts, respectively. Heteroaromatic substrates such as methyl (or ethyl) furan-2-carboxylate **g30** (**g31**) can be transformed into **h30** (**h31**) in 40% (96%) isolated yield.

Scheme 19. Scope of the catalyzed reduction of carboxylic esters **g** to alkyl silyl acetals **h**.[a]

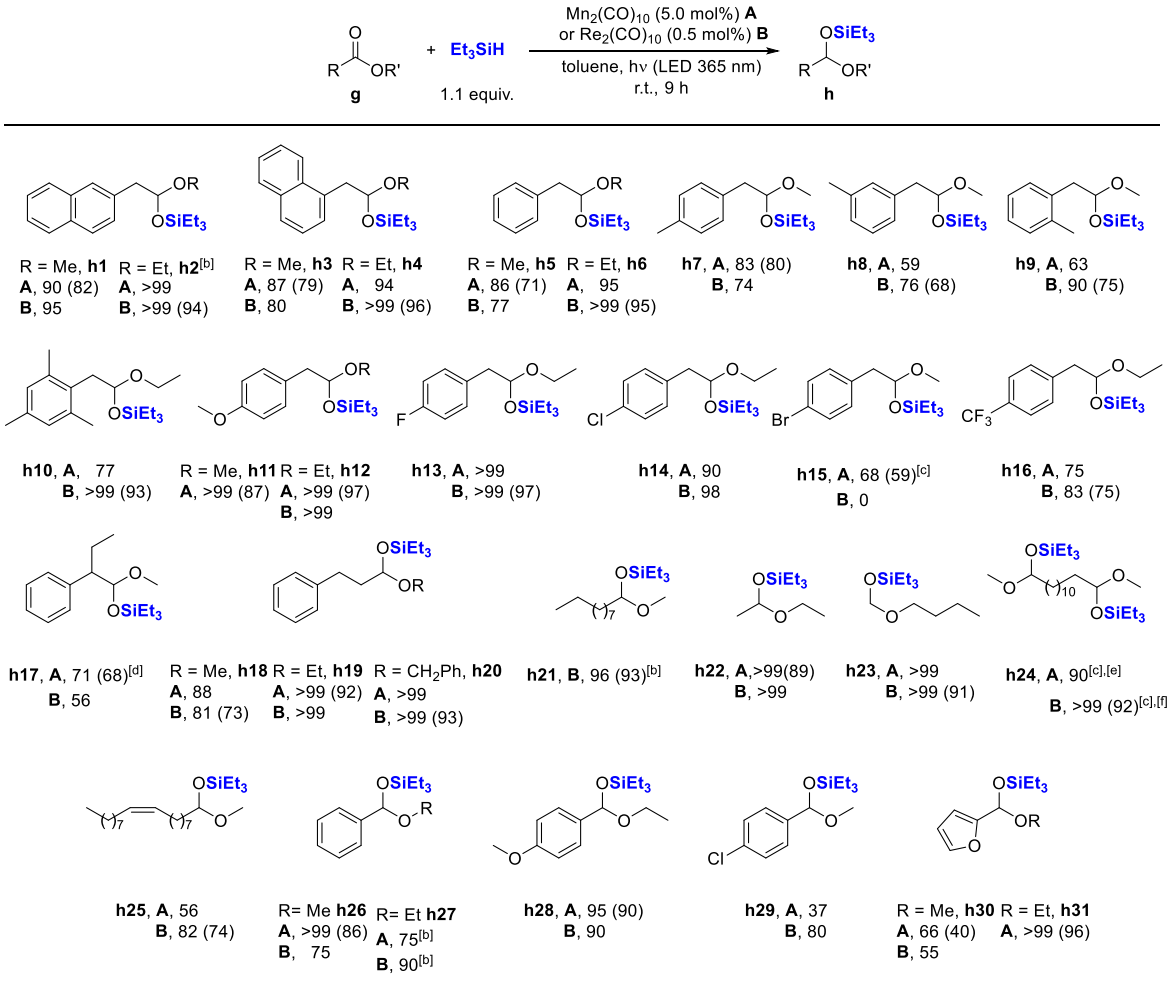

[a] General conditions: ester (0.5 mmol), Et_3SiH (88 µL, 0.55 mmol), $Mn_2(CO)_{10}$ (9.8 mg, 5.0 mol%, method A) or $Re_2(CO)_{10}$ (1.6 mg, 0.5 mol%, method B), r.t., toluene (1.0 mL), irradiation (LED 395 nm, 45W), 9 h; Conversion of **g** detected by ^1H NMR and isolated yields of **h** in parentheses.

[b] 1.0 mmol scale, toluene (1.0 mL).

[c] 2.2 equiv. Et_3SiH.

[d] 4.0 equiv. Et_3SiH.

[e] $Mn_2(CO)_{10}$ (10.0 mol%).

[f] $Re_2(CO)_{10}$ (1.0 mol%).

4.2.5 Limitations of the scope

Some substrates were found to be not compatible with this catalytic system, such as nitro and cyano derivatives and ethyl aminoacetate (**Scheme 20**), under optimal conditions, no conversion of **g32**, **g33**, and **g34** was obtained neither by $Mn_2(CO)_{10}$ or $Re_2(CO)_{10}$.

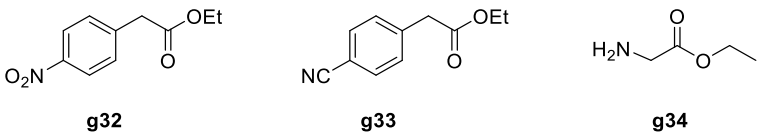

Scheme 20. Substrates did not reduce.

In order to study more in detail the functional group tolerance, ethyl 2-naphthylacetate **g2** was reduced in the presence of potential inhibitors such as nitrobenzene, cyanobenzene, pyridine and N-methylimidazole in the presence of 1.1 equiv. of Et_3SiH. After irradiation only starting material **2g** and the additive were detected, which confirms that the presence of such groups inhibits the catalytic reaction (**Scheme 21**).

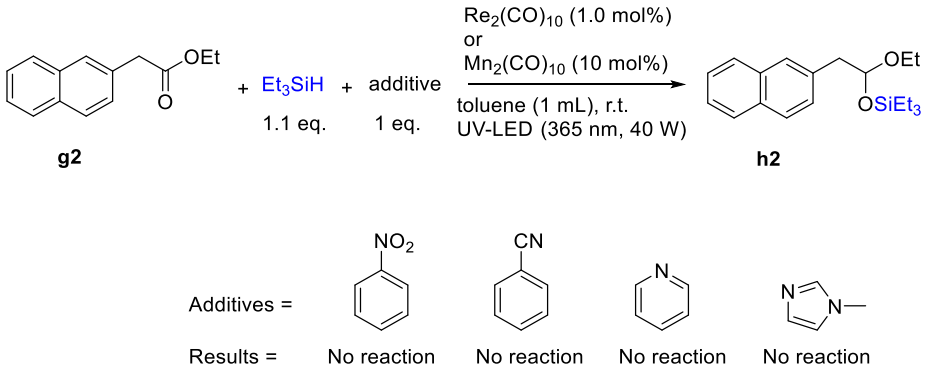

Scheme 21. Competitive experiments.

As in the case of carboxylic acids, the conjugated C=C bond of ethyl cinnamate was fully reduced with 3.3 equiv. of Et_3SiH yielding the saturated product ethyl-3-phenylpropanoate in 73% and 27% of the corresponding silyl acetal with $Mn_2(CO)_{10}$ as catalyst, in the case of $Re_2(CO)_{10}$ 100% yield of ethyl-3-phenylpropanoate was observed. (**Scheme 22**).

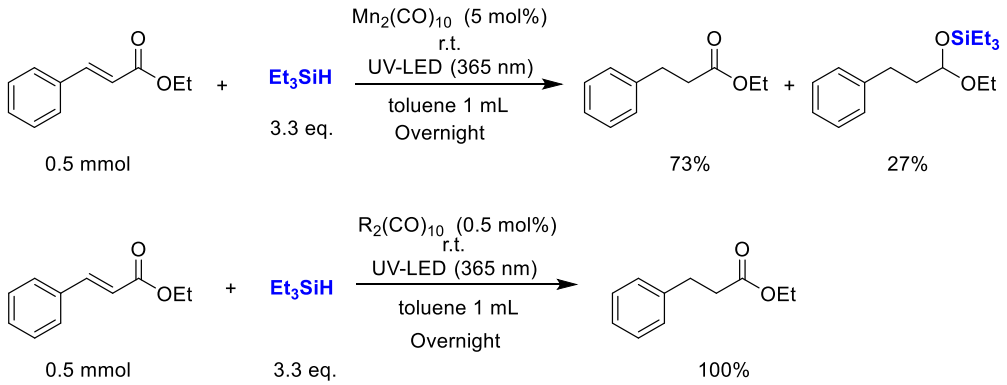

Scheme 22. Reduction of ethyl cinnamate.

4.2.6 Scope of the reduction of carboxylic esters to aldehydes

In order to directly obtain the aldehyde products from the esters, we then performed an one-pot synthesis consisting in carrying out the hydrosilylation of the esters followed by the acidic hydrolysis of the formed acetals into aldehydes. The general scope of the present reaction is presented on **Scheme 23**. Overall, the ester substrates were readily converted under these standard conditions. For instance, the 2-(2-Naphthalenyl)acetaldehyde **j1** was isolated in 93% yield, with $Mn_2(CO)_{10}$ as catalyst. Furthermore, from ethyl 2-(1-naphthaleneyl)acetate **j4**, we have demonstrated the synthetic utility of this methodology in the preparation of aldehyde in gram scale, as evidenced with the corresponding aldehyde **j4** produced in 75% yield after purification by bulb to bulb distillation. In addition, 2-phenylacetaldehyde **j5** and its derivatives bearing methyl- **j9**, **j10**, methoxy- **j12**, fluoro- **j13**, chloro- **j14** and trifluoromethyl- **j16** groups were isolated in 61-93% yields. 3-Phenylpropanal **j19**, decanal **j21**, tridecandial **j24** and benzaldehyde **j27** could be prepared in over 80% yields.

Scheme 23. Scope of the reduction of carboxylic esters **g** to aldehydes **j**.[a]

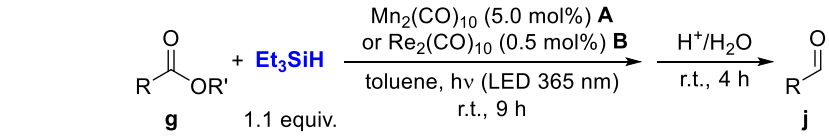

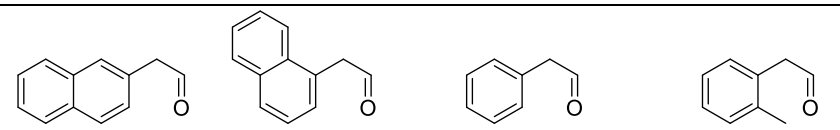

j1, **A**, >99 (93) **j4**, **B**, >99 (75) **j5**, **A**, >85 (84)[e] R=Me **B**, >99 (75)[c] R=Et **j9**, **B**, 90 (70)

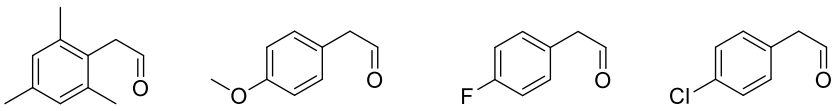

j10, **B**, >99 (93) **j12**, **A**, >99(>99)[d,e] **j13**, **A**, >99 (>99)[d,e] **B**, >99 (>99)[d,e] **j14**, **B**, 92 (76)

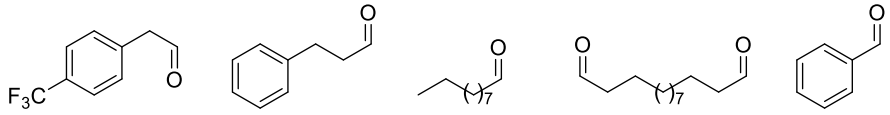

j16, **B**, 91 (61)[c][d] **j19**, **A**, >99 (85)[c] **j21**, **B**, 97 (83) **j24**, **B**, >99 (>99)[e] **j27**, **B**, 90 (86)[d,e]

[a] General conditions: ester (0.5 mmol), Et_3SiH (88 µL, 0.55 mmol), $Mn_2(CO)_{10}$ (9.8 mg, 5.0 mol%, method **A**) or $Re_2(CO)_{10}$ (1.6 mg, 0.5 mol%, method **B**), r.t., toluene (1.0 mL),

irradiation (LED 395 nm, 45W), 9 h; then hydrolysis (THF/HCl 1 N), 4 h. Conversions of **g** detected by ^{1}H NMR and isolated yields of **j** in parentheses;

[b] 4.67 mmol (1 gram) scale.

[c] Slowly evolved towards solid trioxane derivatives.

[d] 1.0 mmol scale, toluene (1.0 mL).

[e] NMR yield determined with internal standard.

4.2.7 Mechanistic studies

To gain some insights about the mechanism of this catalyzed reaction, kinetic monitoring of the reaction was performed. In the case of 2-phenyl acetic acid **a3** (**Table 7** and **Figure 1**), after 30 min. of the reaction, the formation of a silyl ester intermediate **d3** was observed in 10%, continuing the irradiation for 4 h resulted in the full conversion of **a3** to 95% silyl ester **d3** and 5% acetal **b3**. Finally, the desired product **b3** was detected in 98% yield after 24 h with only 1% of the undesired product **c3**.

Table 7. Monitoring over time of the reduction of phenyl acetic acid a3.[a]

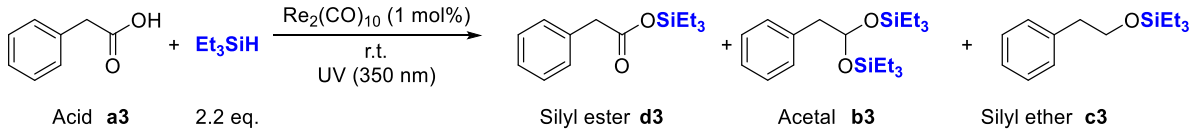

Entry	Time/h	Acid **a3** (%)	Silyl Ester **d3**(%)	Acetal **b3** (%)	Silyl ether **c3** (%)
1	0	100	0	0	0
2	0.3	90	10	0	0
3	1	58	41	1	0
4	2	13	85	2	0
5	4	0	95	5	0
6	5	0	81	19	0
7	10	0	17	83	0
8	24	0	1	98	1

[a] General conditions: a Young type NMR tube was charged with $Re_2(CO)_{10}$ (1.0 mol%), phenyl-acetic acid (0.1 mmol) in a glove box, followed by C_6D_6 (0.5 mL) and Et_3SiH (0.22

mmol, 2.2 equiv.), then irradiated under UV irradiations (350 nm) in a Rayonet RPR100 apparatus at r.t. for indicated hours. The selectivities were obtained from *in situ* NMR of this Young-type NMR tube. Note: H_2 was observed in ^1H NMR spectrum.

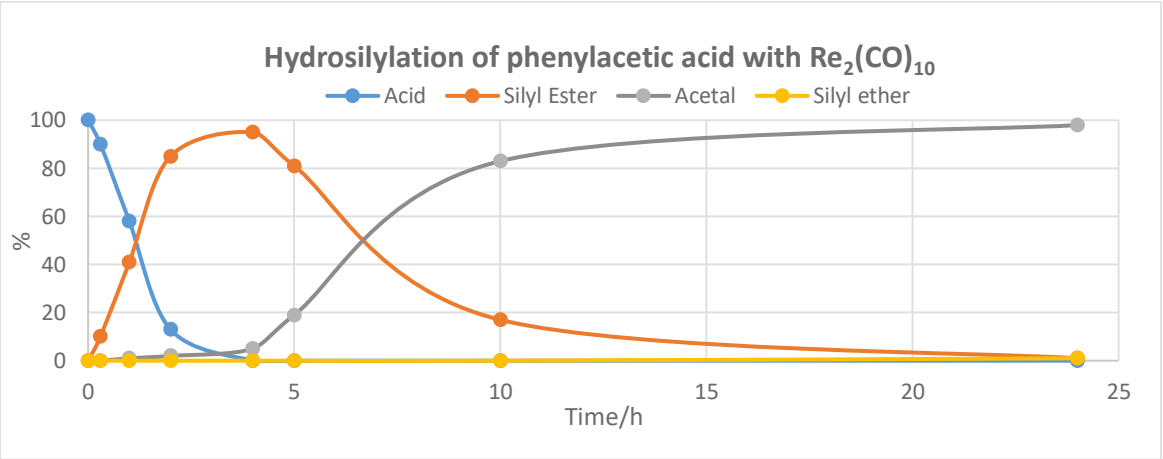

Figure 1. Monitoring over time of the reduction of phenyl acetic acid **a3**.

In the case of esters (**Table 8** and **Figure 2**), 9% conversion of the 2-phenylacetate **g5** towards silyl ester **h5** was detected after 30 min. of irradiation (entry 2). The yield of **h5** increased to 78% after 4 h of reaction (entry 6). Prolonging the reaction time to 10 h gave the desired product **h5** in 87% yield and the silyl ether **i5** in 5%.

Table 8. Monitoring over time of the reduction of phenyl acid g5.

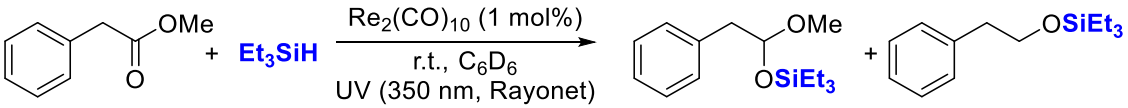

g5 1.1 eq. **h5** **i5**

Entry	Time/h	Ester **g5** (%)	Acetal **h5**(%)	Silyl ether **i5** (%)
1	0	100	0	0
2	0.3	91	9	0
3	1	68	32	0
4	2	44	56	0
5	3	29	71	0
6	4	22	78	0
7	10	8	87	5
8	24	3	88	9

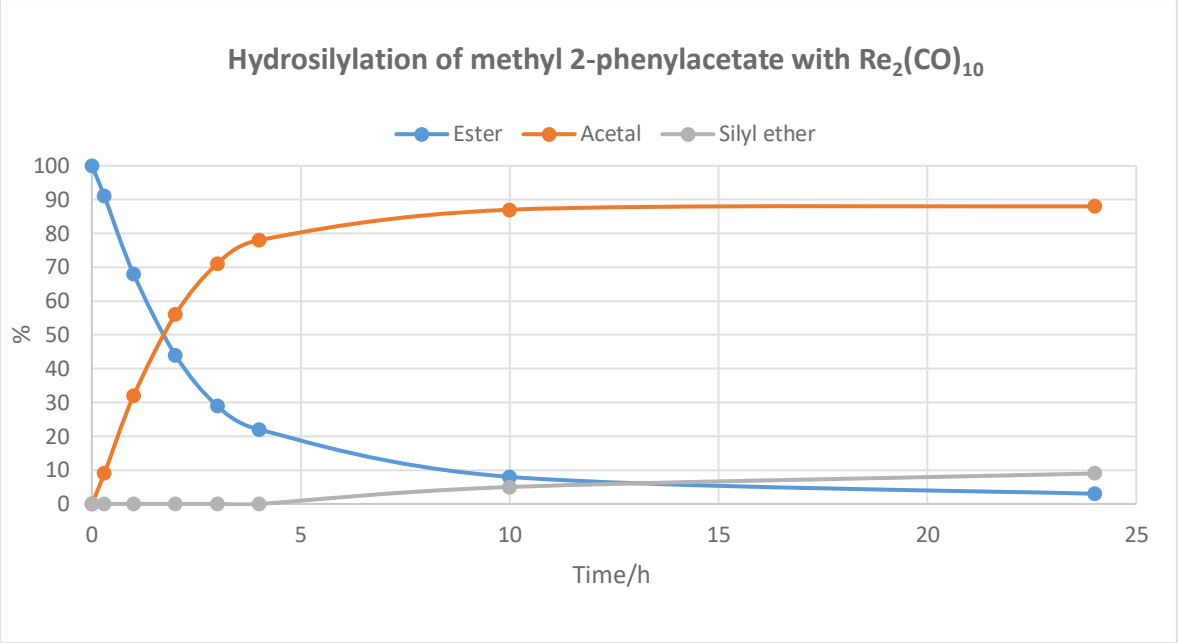

Figure 2. Kinetic monitoring of reaction between 2-phenylacetate **g5** and Et_3SiH catalyzed by $Re_2(CO)_{10}$.

4.2.7.1 On-Off experiments monitored by ^{1}H NMR

In order to investigate the role and the need of continuous irradiation, "On−Off" experiments were carried out using (0.1 mmol) of carboxylic acid **a3** [or **g2** as model ester], $Re_2(CO)_{10}$ (1.0 mol%, 0.7 mg) [or $Mn_2(CO)_{10}$ (10 mol%, 3.9 mg)] and Et_3SiH (2.2 equiv. with **a3** and 1.1 equiv. with **g2**) in C_6D_6 (0.5 mL), and toluene (internal standard, 0.066 mmol, 7 µL). The reactions were followed by ^{1}H NMR.

In the case of carboxylic acid, with 2-phenyl acetic acid **a3** using $Re_2(CO)_{10}$ as catalyst, no evolution of the reaction was observed in the absence of any light which confirms that continuous irradiation is mandatory for the reduction to proceed (**Figure 3**).

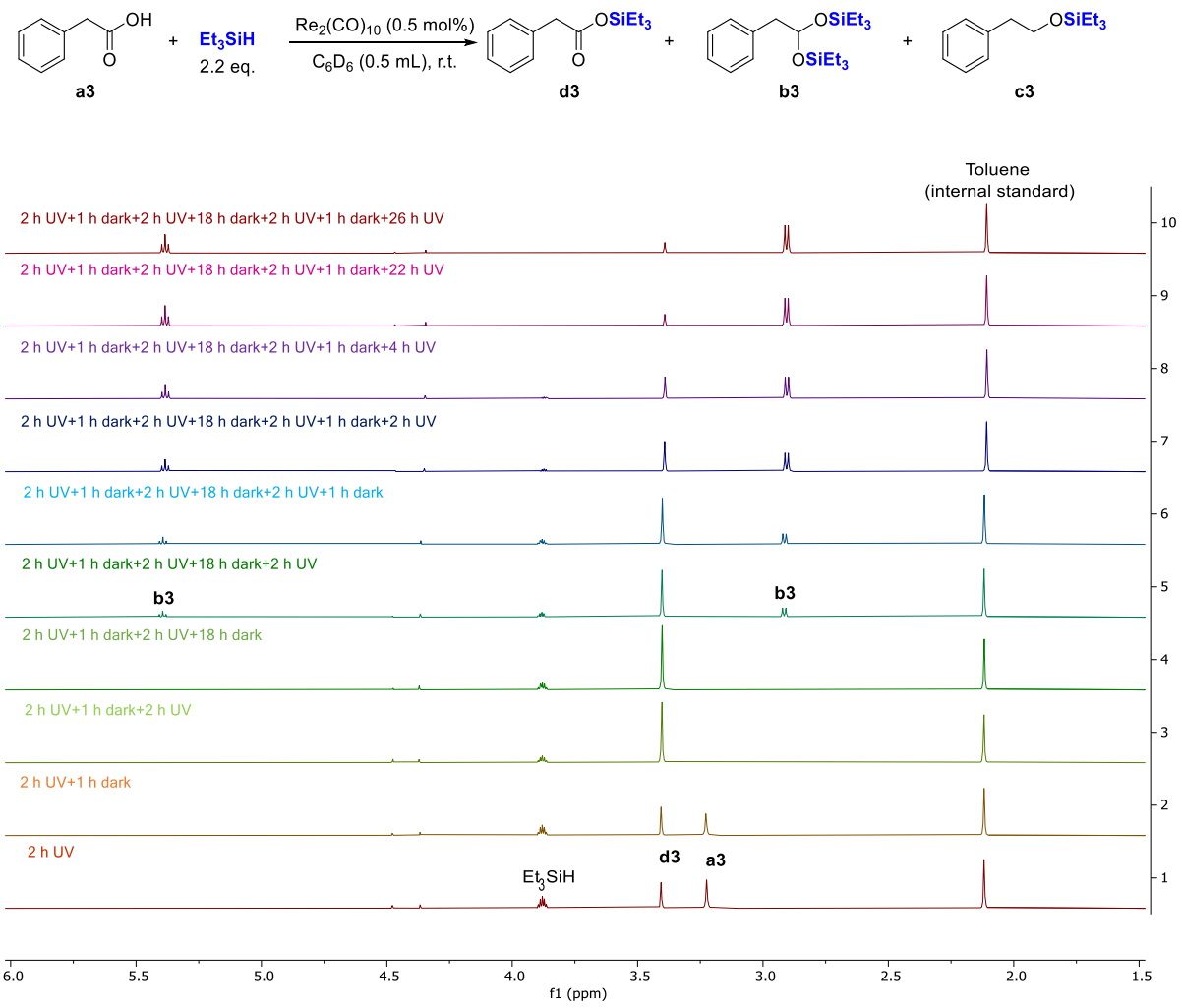

Figure 3. Monitoring over time of the "On-Off" experiment for the reduction of the carboxylic acid **a3**.

As in the case of acids, continuous irradiation was found necessary for the reduction of esters to proceed with both $Re_2(CO)_{10}$ and $Mn_2(CO)_{10}$ (**Figures 4** and **5**).

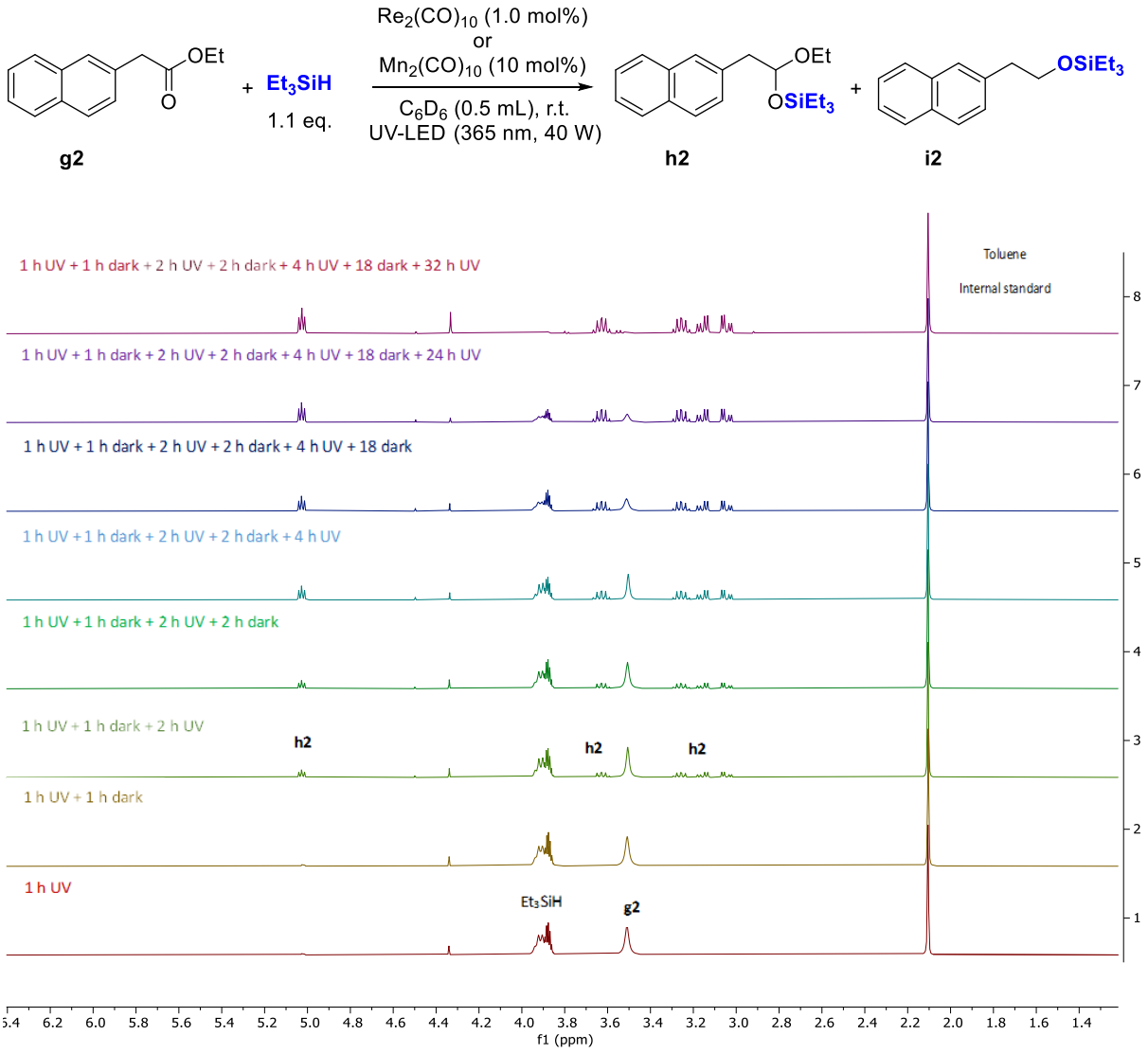

Figure 4. Monitoring over time of the "On-Off" experiment for the reduction of ester **g2** with $Re_2(CO)_{10}$ as catalyst.

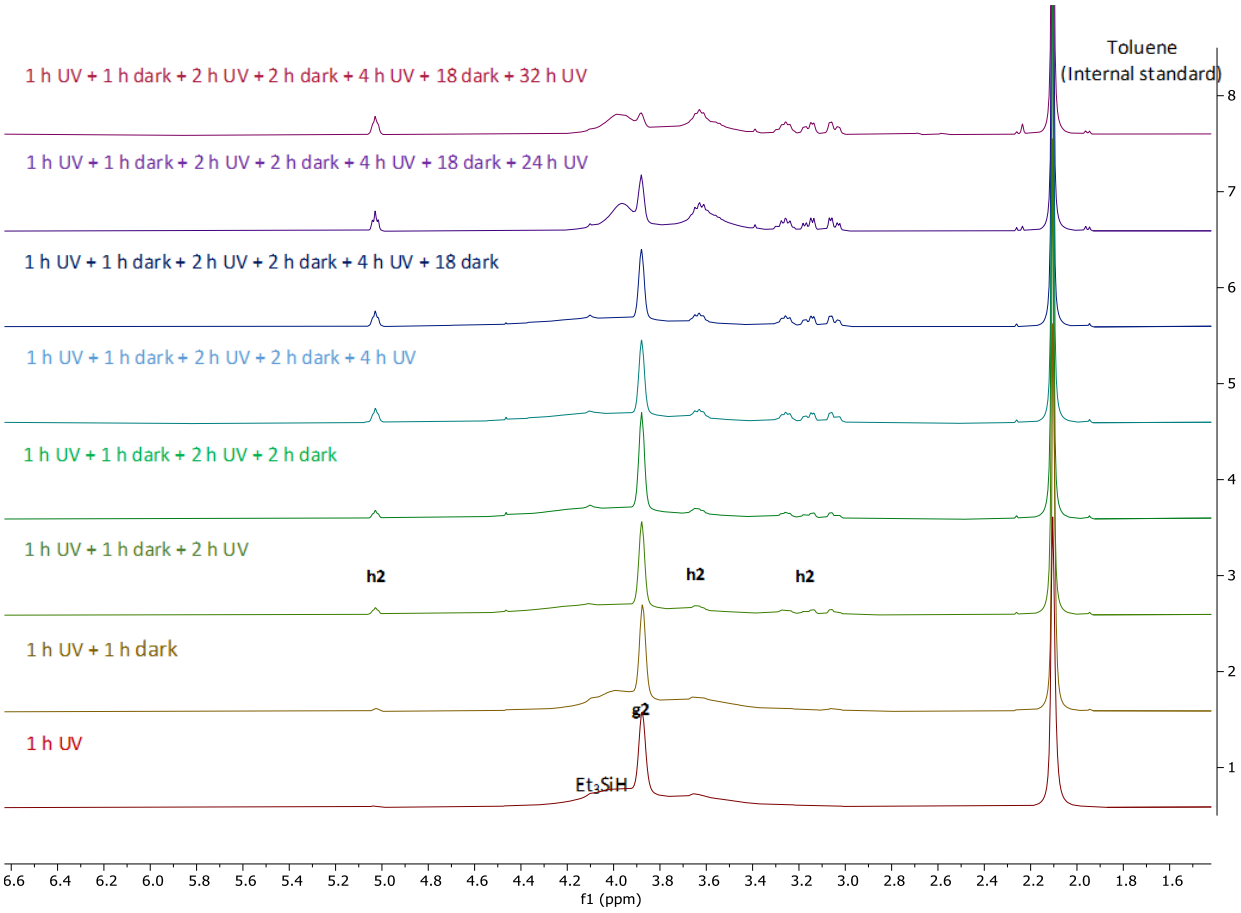

Figure 5. Monitoring over time of the "On-Off" experiment for the reduction of ester **g2** with $Mn_2(CO)_{10}$ as catalyst.

4.2.7.2 Stoichiometric and catalytic reactions

Stoichiometric reactions between metal precursors and Et_3SiH were performed under light irradiation (Figures 5-8).

- Stoichiometric reactions between metal precursor and Et_3SiH

In the case of $Mn_2(CO)_{10}$, a very weak signal at −7.9 ppm was detected which could be attributed to $HMn(CO)_5$, along with significant decomposition (black precipitate). When a stoichiometric amount of substrate was added, no product was detected with or without irradiation (**Figure 6**).

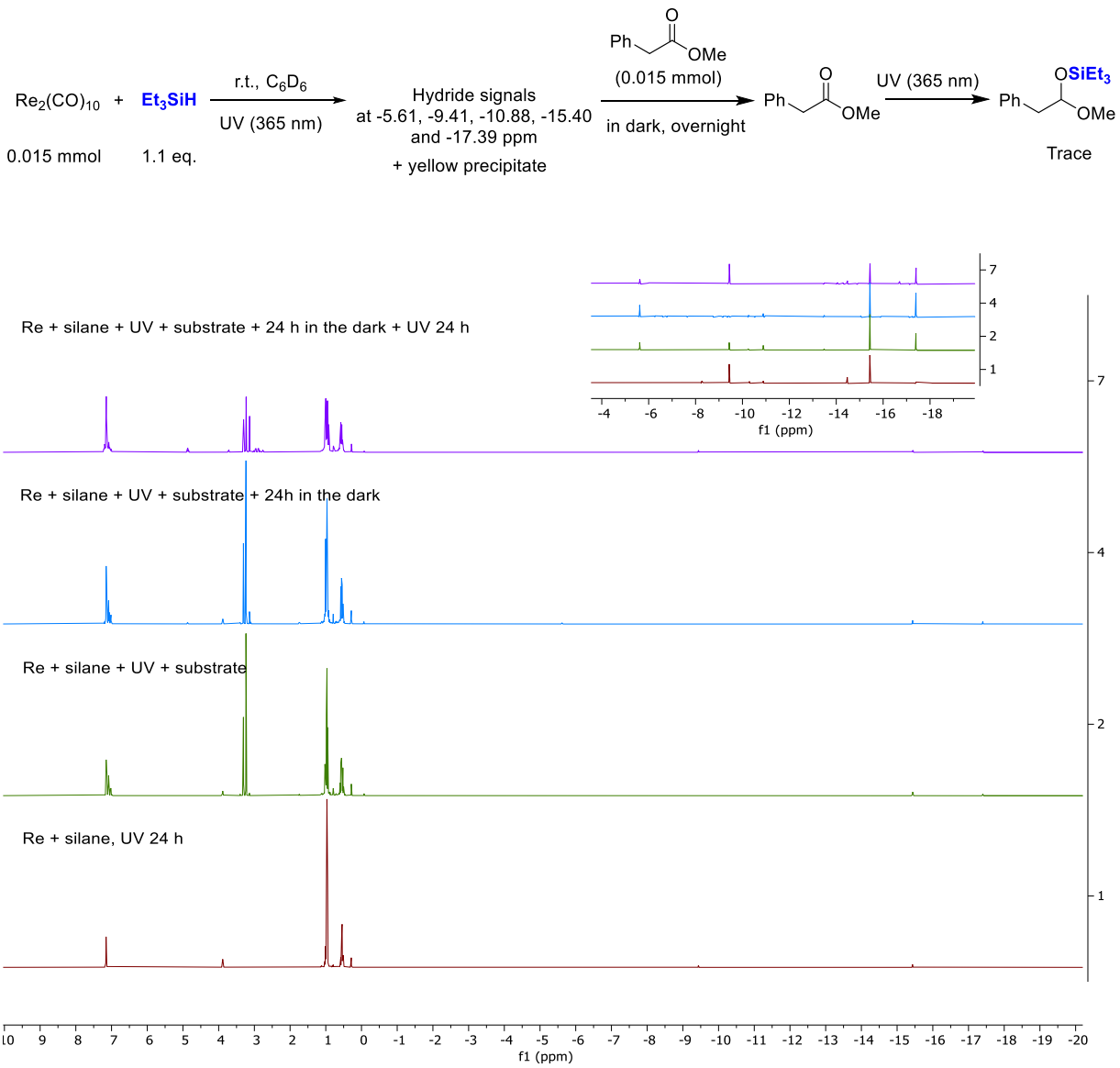

Figure 6. Monitoring over time of the reaction between $Re_2(CO)_{10}$ and Et_3SiH (1 equiv.).

In the case of $Re_2(CO)_{10}$, a series of signals was observed at negative chemical shifts, accompanied by significant precipitation (yellow precipitate). Some of these signals have been previously reported by Fan,[47] including $HRe(CO)_5$ (−5.7 ppm) and $HRe_2(CO)_9(SiEt_3)$ (−9.0 ppm). After addition of a stoichiometric amount of substrate, very low conversion was detected after UV irradiation (**Figure 7**).

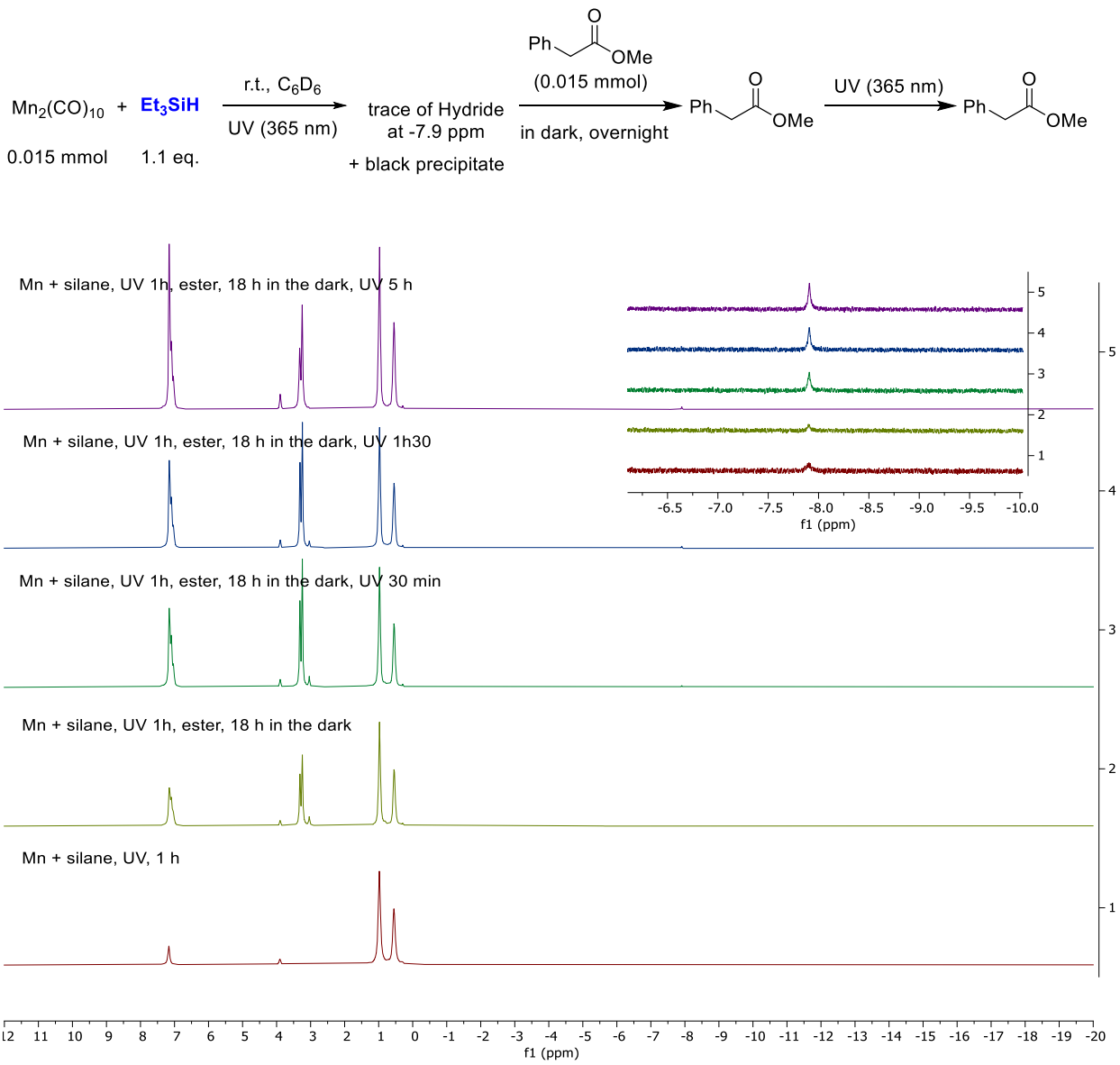

Figure 7. Monitoring over time of the reaction between $Mn_2(CO)_{10}$ and Et_3SiH (1 equiv.).

- Stoichiometric reactions of metal precursors with an excess of silane (10 equiv.)

Then, the same stepwise experiments were conducted in the presence of 10 equiv. of silane. As in the previous case, hydrides were detected (**Figures 8** and **9**), but the catalytic activity was recovered after irradiation.

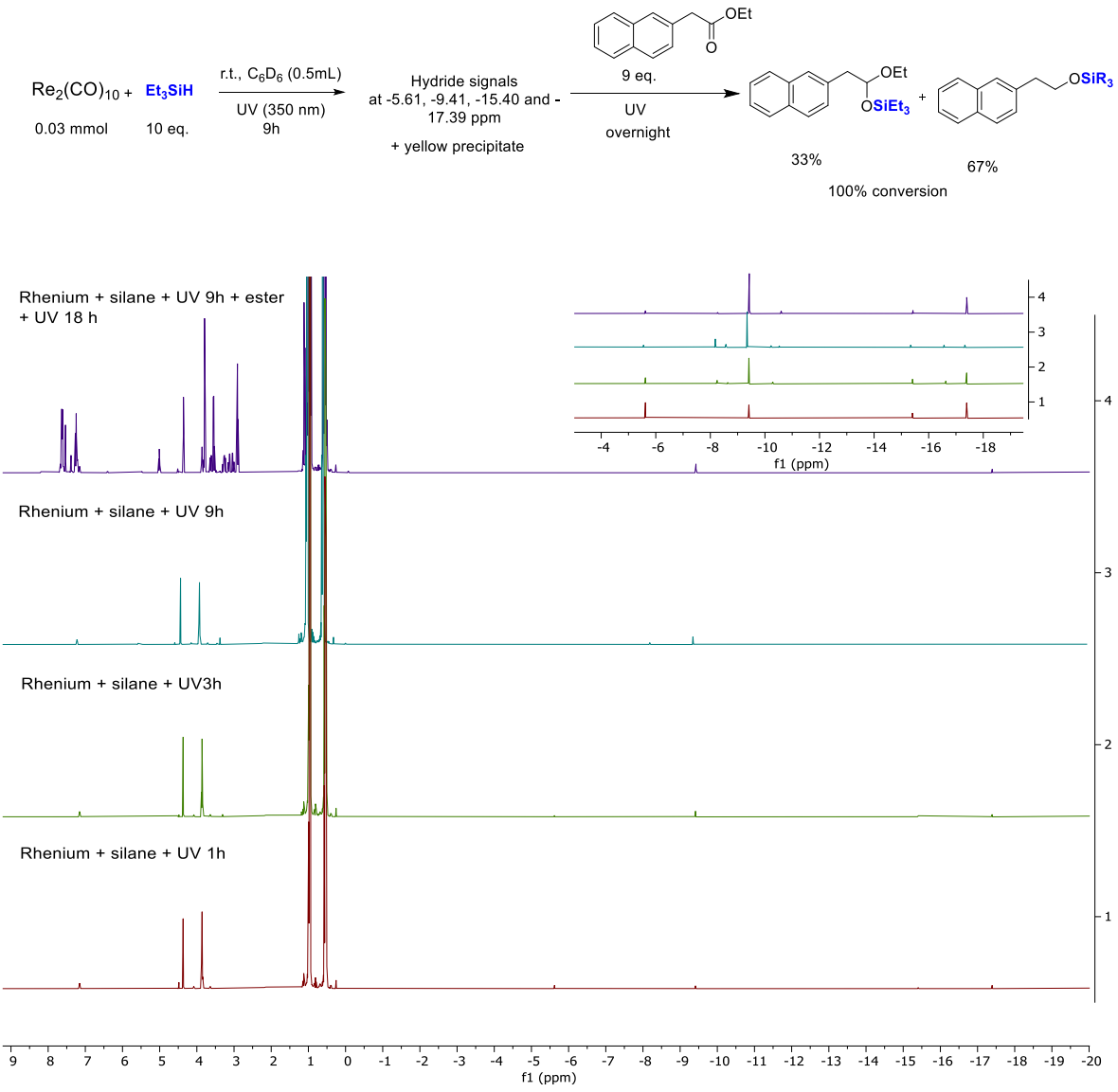

Figure 8. Monitoring over time of the reaction between $Re_2(CO)_{10}$ and Et_3SiH (10 equiv.).

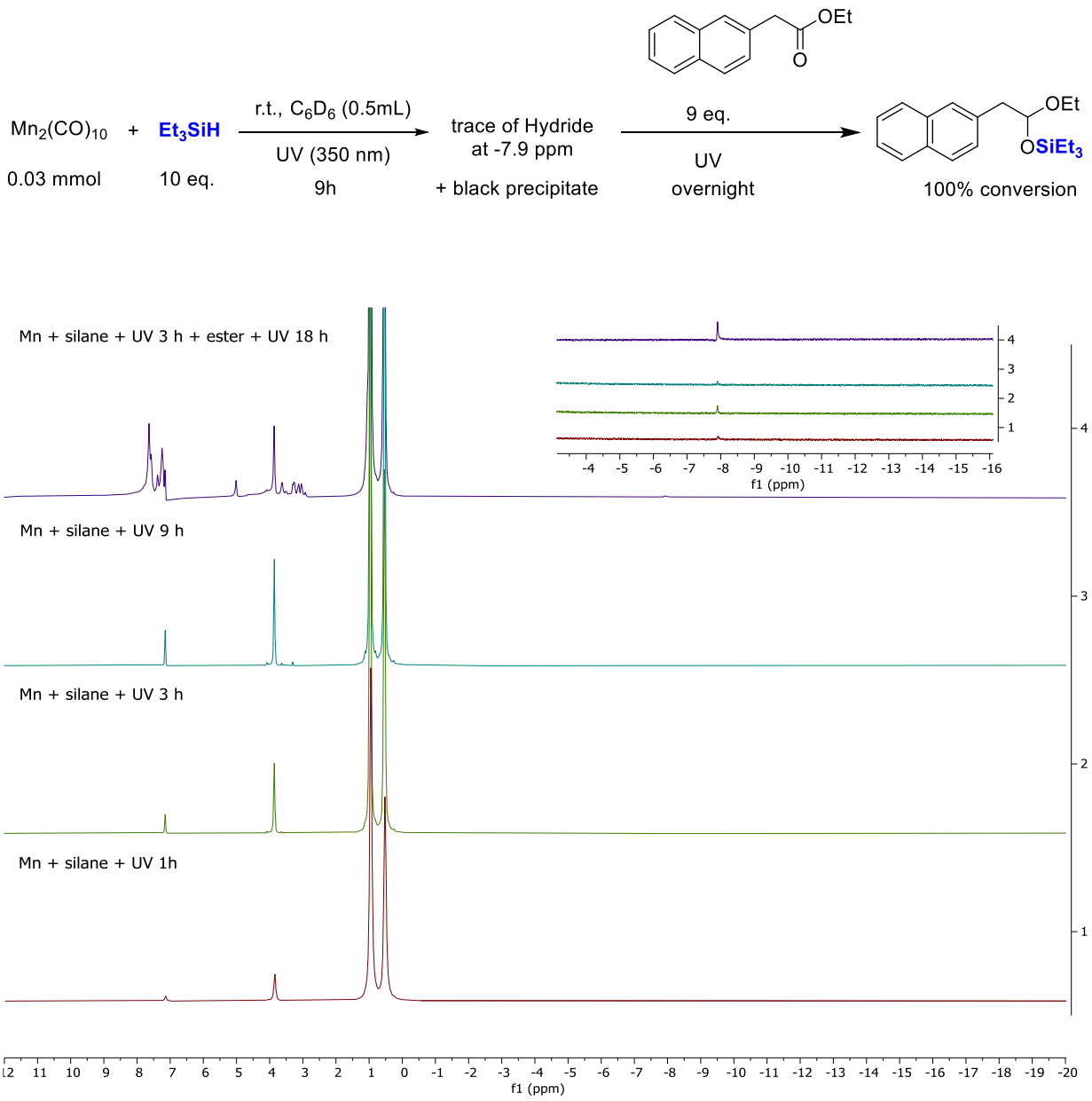

Figure 9. Monitoring over time of the reaction between $Mn_2(CO)_{10}$ and Et_3SiH (10 equiv.).

- Catalytic reactions with high loading of catalyst

Finally, under catalytic conditions (*i.e.* in the presence of the substrate from the beginning of the reaction) but with 10 mol% of catalyst, crude NMR mixture analysis revealed the presence of hydride species after the full conversion of the ester (**Figures 10** and **11**).

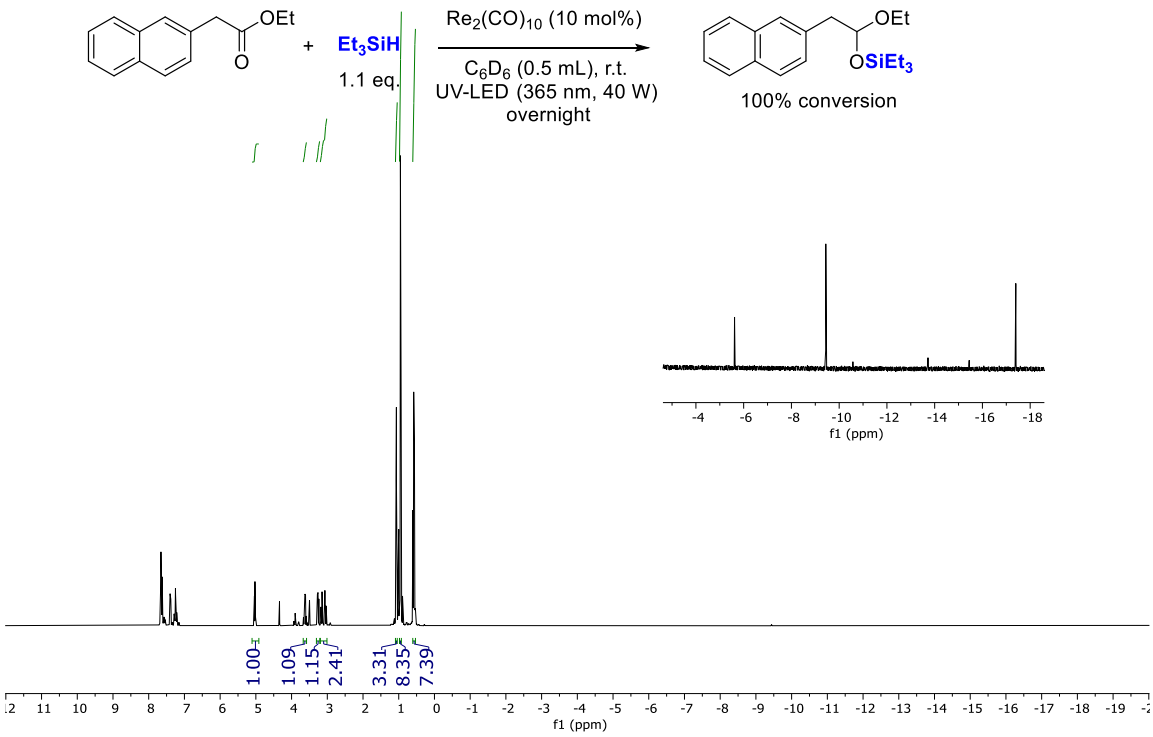

Figure 10. Crude NMR spectra of the catalytic mixture with 10 mol% $Re_2(CO)_{10}$.

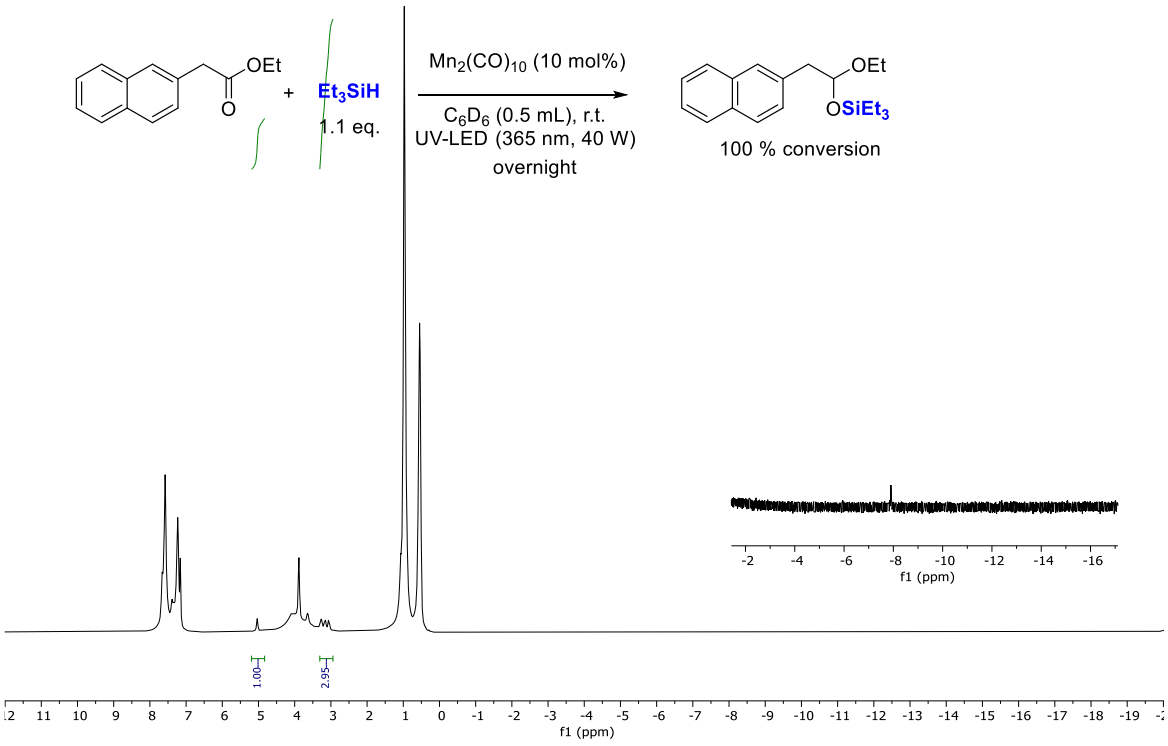

Figure 11. Crude NMR spectra of the catalytic mixture with 10 mol% $Mn_2(CO)_{10}$.

4.2.8 Proposed mechanism

The catalytic reactions were found to be inhibited by the addition of TEMPO, 2-phenyl acetic acid **a3**, was converted completely to the silyl ester **d3** and no conversion of **g2** was detected (**Scheme 24**). The homolytic cleavage of decacarbonyl manganese and rhenium complexes into [$M(CO)_5$] radicals upon irradiation has been studied in detail previously and reported.[58–61] Therefore, it is likely that the initiation step of the catalytic cycle is the homolytic cleavage of the metal pre-catalysts.

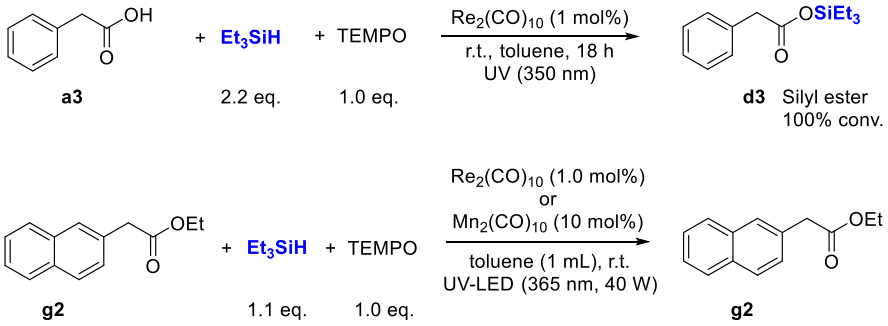

Scheme 24. Reduction of **a3** and **g2** in the presence of TEMPO.

For manganese catalysis, based on our results, we assumed that the radical mechanism proposed by Wang[62,63] or by Zhang[64] is likely to operate in our case.

The initiation step is Mn−Mn bond homolysis resulting in the formation of $(CO)_5Mn$ radical which reacts with Et_3SiH to give silyl radical and $HMn(CO)_5$. The addition of the silyl radical to the C=O bond yielded the alkyl radical, which undergo hydrogenolysis with $HMn(CO)_5$ to form the desired product and regenerate the $(CO)_5Mn$ species (**Scheme 25**).

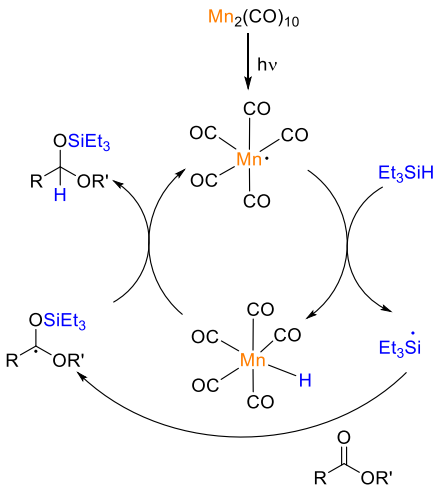

Scheme 25. Proposed catalytic cycle for the hydrosilylation of acids and esters with $Mn_2(CO)_{10}$.

In the case of rhenium catalysis, it is likely that the mechanism proposed by Fan[47] is operating in our case (**Scheme 26**).

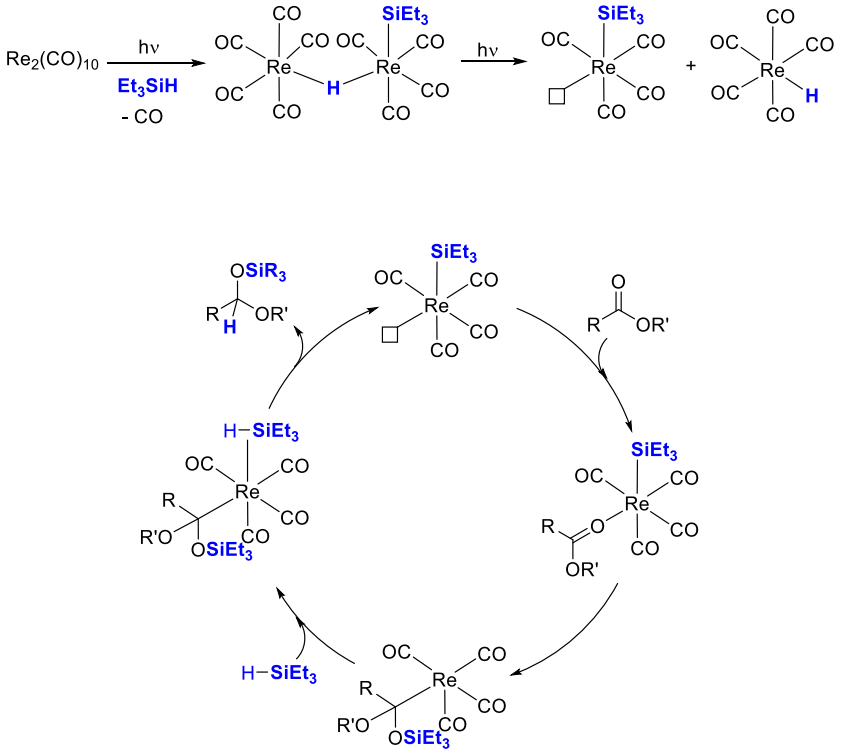

Scheme 26. Proposed catalytic cycle for the hydrosilylation of acids and esters with $Re_2(CO)_{10}$.

5. Conclusion

In conclusion, the commercially available $Mn_2(CO)_{10}$ and $Re_2(CO)_{10}$ were able to reduced carboxylic acids and esters with high chemoselectivity into corresponding silyl acetals, which can then be easily converted into aldehydes by acid treatment. Under mild conditions, with $Mn_2(CO)_{10}$ (5 mol%) or $Re_2(CO)_{10}$ (0.5 mol%) catalysts, in the presence of a stoichiometric amount of Et_3SiH as reducing agent, at room temperature under irradiation, a large variety of carboxylic acids and esters was thus reduced in moderate to good yields to the corresponding protected aldehydes without noticeable formation of silylethers arising from over-reduction. Upon hydrolysis, aromatic and aliphatic aldehydes, including di-aldehydes, were easily produced and isolated in good yields. For future developments in this competitive field, the two metallic systems reported here will have to be envisaged in a complementary manner, the catalytic loading 10 times lower used with rhenium having to be opposed with the lower price of manganese.

6. References

[1] L. I. Zakharkin, V. V. Gavrilenko, D. N. Maslin, I. M. Khorlina, *Tetrahedron Lett.* **1963**, *4*, 2087–2090.

[2] M. J. Chae, J. I. Song, D. K. An, *Bull.-KOREAN Chem. Soc.* **2007**, *28*, 2517.

[3] M. S. Kim, Y. M. Choi, D. K. An, *Tetrahedron Lett.* **2007**, *48*, 5061–5064.

[4] L. I. Zakharkin, I. M. Khorlina, *Tetrahedron Lett.* **1962**, *3*, 619–620.

[5] A. Feinstein, E. K. Fields, *Vapor Phase Conversion of Aromatic Esters to Aromatic Aldehydes*, **1976**, US3935265A.

[6] S. T. King, E. J. Strojny, *J. Catal.* **1982**, *76*, 274–284.

[7] A. Chen, H. Xu, W. Hua, W. Shen, Y. Yue, Z. Gao, *Top. Catal.* **2005**, *35*, 177–185.

[8] A. Chen, H. Xu, Y. Yue, W. Shen, W. Hua, Z. Gao, *Ind. Eng. Chem. Res.* **2004**, *43*, 6409–6415.

[9] H.-L. Xu, W. Shen, Y.-T. Yang, *Chin. J. Chem.* **2001**, *19*, 647–651.

[10] A. Chen, H. Xu, Y. Yue, W. Hua, W. Shen, Z. Gao, *J. Mol. Catal. Chem.* **2003**, *203*, 299–306.

[11] D. Cheng, C. Hou, F. Chen, X. Zhan, *React. Kinet. Catal. Lett.* **2009**, *97*, 217–223.

[12] D. Addis, S. Das, K. Junge, M. Beller, *Angew. Chem. Int. Ed.* **2011**, *50*, 6004–6011.

[13] S. Hosokawa, M. Toya, A. Noda, M. Morita, T. Ogawa, Y. Motoyama, *ChemistrySelect* **2018**, *3*, 2958–2961.

[14] D. J. Parks, W. E. Piers, *J. Am. Chem. Soc.* **1996**, *118*, 9440–9441.

[15] D. J. Parks, J. M. Blackwell, W. E. Piers, *J. Org. Chem.* **2000**, *65*, 3090–3098.

[16] J. Nakanishi, H. Tatamidani, Y. Fukumoto, N. Chatani, *Synlett* **2006**, *2006*, 869–872.

[17] M. Igarashi, R. Mizuno, T. Fuchikami, *Tetrahedron Lett.* **2001**, *42*, 2149–2151.

[18] C. Cheng, M. Brookhart, *Angew. Chem. Int. Ed.* **2012**, *51*, 9422–9424.

[19] Y. Corre, V. Rysak, F. Capet, J.-P. Djukic, F. Agbossou-Niedercorn, C. Michon, *Chem. – Eur. J.* **2016**, *22*, 14036–14041.

[20] V. Rysak, A. Descamps-Mandine, P. Simon, F. Blanchard, L. Burylo, M. Trentesaux, M. Vandewalle, V. Collière, F. Agbossou-Niedercorn, C. Michon, *Catal. Sci. Technol.* **2018**, *8*, 3504–3512.

[21] H. Li, L. C. Misal Castro, J. Zheng, T. Roisnel, V. Dorcet, J.-B. Sortais, C. Darcel, *Angew. Chem. Int. Ed.* **2013**, *52*, 8045–8049.

[22] K. Miyamoto, Y. Motoyama, H. Nagashima, *Chem. Lett.* **2012**, *41*, 229–231.

[23] L. C. M. Castro, H. Li, J.-B. Sortais, C. Darcel, *Chem. Commun.* **2012**, *48*, 10514–10516.

[24] D. Bézier, S. Park, M. Brookhart, *Org. Lett.* **2013**, *15*, 496–499.

[25] R. J. Trovitch, *Acc. Chem. Res.* **2017**, *50*, 2842–2852.

[26] X. Yang, C. Wang, *Chem. – Asian J.* **2018**, *13*, 2307–2315.

[27] R. J. Trovitch, *Synlett* **2014**, *25*, 1638–1642.

[28] B. Royo, in *Adv. Organomet. Chem.* (Ed.: P.J. Pérez), Academic Press, **2019**, pp. 59–102.

[29] R. G. Harms, W. A. Herrmann, F. E. Kühn, *Coord. Chem. Rev.* **2015**, *296*, 1–23.

[30] Y. Kuninobu, K. Takai, *Chem. Rev.* **2011**, *111*, 1938–1953.

[31] R. L. Yates, *J. Catal.* **1982**, *78*, 111–115.

[32] P. K. Hanna, B. T. Gregg, A. R. Cutler, *Organometallics* **1991**, *10*, 31–33.

[33] Z. Mao, B. T. Gregg, A. R. Cutler, *J. Am. Chem. Soc.* **1995**, *117*, 10139–10140.

[34] R. J. Trovitch, *Acc. Chem. Res.* **2017**, *50*, 2842–2852.

[35] R. J. Trovitch, *Synlett* **2014**, *25*, 1638–1642.

[36] T. K. Mukhopadhyay, M. Flores, T. L. Groy, R. J. Trovitch, *J. Am. Chem. Soc.* **2014**, *136*, 882–885.

[37] C. Ghosh, T. K. Mukhopadhyay, M. Flores, T. L. Groy, R. J. Trovitch, *Inorg. Chem.* **2015**, *54*, 10398–10406.

[38] T. K. Mukhopadhyay, C. Ghosh, M. Flores, T. L. Groy, R. J. Trovitch, *Organometallics* **2017**, *36*, 3477–3483.

[39] C. M. Kelly, R. McDonald, O. L. Sydora, M. Stradiotto, L. Turculet, *Angew. Chem. Int. Ed.* **2017**, *56*, 15901–15904.

[40] O. Martínez-Ferraté, B. Chatterjee, C. Werlé, W. Leitner, *Catal. Sci. Technol.* **2019**, *9*, 6370–6378.

[41] R. R. Behera, R. Ghosh, S. Panda, S. Khamari, B. Bagh, *Org. Lett.* **2020**, *22*, 3642–3648.

[42] M. Igarashi, T. Fuchikami, *Tetrahedron Lett.* **2001**, *42*, 1945–1947.

[43] R. Arias-Ugarte, H. K. Sharma, A. L. C. Morris, K. H. Pannell, *J. Am. Chem. Soc.* **2012**, *134*, 848–851.

[44] J. Zheng, S. Chevance, C. Darcel, J.-B. Sortais, *Chem. Commun.* **2013**, *49*, 10010–10012.

[45] J. J. Kennedy-Smith, K. A. Nolin, H. P. Gunterman, F. D. Toste, *J. Am. Chem. Soc.* **2003**, *125*, 4056–4057.

[46] I. Cabrita, A. C. Fernandes, *Tetrahedron* **2011**, *67*, 8183–8186.

[47] C. K. Toh, Y. N. Sum, W. K. Fong, S. G. Ang, W. Y. Fan, *Organometallics* **2012**, *31*, 3880–3887.

[48] L. C. M. Castro, H. Li, J.-B. Sortais, C. Darcel, *Chem. Commun.* **2012**, *48*, 10514–10516.

[49] D. Bézier, S. Park, M. Brookhart, *Org. Lett.* **2013**, *15*, 496–499.

[50] L. Stahl, *J. Am. Chem. Soc.* **2007**, *129*, 10297–10298.

[51] P. GALLEZOT, D. RICHARD, *Catal. Rev.* **1998**, *40*, 81–126.

[52] D. J. Ager, A. H. M. de Vries, J. G. de Vries, *Chem. Soc. Rev.* **2012**, *41*, 3340–3380.

[53] X. Yang, C. Wang, *Chin. J. Chem.* **2018**, *36*, 1047–1051.

[54] S. L. Pratt, R. A. Faltynek, *J. Organomet. Chem.* **1983**, *258*, C5–C8.

[55] H. S. Hilal, M. Abu-Eid, M. Al-Subu, S. Khalaf, *J. Mol. Catal.* **1987**, *39*, 1–11.

[56] H. S. Hilal, M. A. Suleiman, W. J. Jondi, S. Khalaf, M. M. Masoud, *J. Mol. Catal. Chem.* **1999**, *144*, 47–59.

[57] X. Yang, C. Wang, *Angew. Chem. Int. Ed.* **2018**, *57*, 923–928.

[58] M.-A. Tehfe, J. Lalevée, D. Gigmes, J. P. Fouassier, *J. Polym. Sci. Part Polym. Chem.* **2010**, *48*, 1830–1837.

[59] M. S. Wrighton, D. S. Ginley, *J. Am. Chem. Soc.* **1975**, *97*, 2065–2072.

[60] D. M. Allen, A. Cox, T. J. Kemp, Q. Sultana, R. B. Pitts, *J. Chem. Soc. Dalton Trans.* **1976**, 1189–1193.

[61] S. A. Hallock, A. Wojcicki, *J. Organomet. Chem.* **1973**, *54*, C27–C29.

[62] X. Yang, C. Wang, *Angew. Chem. Int. Ed.* **2018**, *57*, 923–928.

[63] X. Yang, C. Wang, *Chin. J. Chem.* **2018**, *36*, 1047–1051.

[64] H. Liang, Y.-X. Ji, R.-H. Wang, Z.-H. Zhang, B. Zhang, *Org. Lett.* **2019**, *21*, 2750–2754.

7. Experimental part

7.1 General information

All reagents were obtained from commercial sources and used as received. All reactions were carried out with dried glassware using standard Schlenk techniques under an inert atmosphere of dry argon. Technical grade petroleum ether and ethyl acetate were used for column chromatography. Dry and oxygen-free organic solvents (Et_2O, toluene) were obtained using LabSolv (Innovative Technology) solvent purification system. Analytical TLC was performed on Merck $^{60}F_{254}$ silica gel plates (0.25 mm thickness). Column chromatography was performed on Acros Organics Ultrapure silica gel (mesh size 40-60 µm, 60 Å).

^1H, $^{13}C\{^1H\}$, $^{19}F\{^1H\}$ and $^{29}Si\{^1H\}$ NMR spectra were recorded in $CDCl_3$ at 298 K unless otherwise stated, on Bruker, AVANCE 400 and AVANCE 300 spectrometers. ^1H and $^{13}C\{^1H\}$ NMR spectra were calibrated using the residual solvent signal as internal standard (^1H: $CDCl_3$ 7.26 ppm, C_6D_6 7.16 ppm ^{13}C: $CDCl_3$, central peak is 77.16 ppm C_6D_6 128.06 ppm). Chemical shift (δ) and coupling constants (J) are given in ppm and in Hz, respectively. The peak patterns are indicated as follows: (s, singlet; d, doublet; t, triplet; q, quartet; quin, quintet; m, multiplet, and br. for broad).

$Re_2(CO)_{10}$ and $Re(CO)_5Br$ were purchased from Strem Chemicals.

HR–MS spectra (ESI positive mode) were carried out by the corresponding facilities at the CRMPO (Centre Régional de Mesures Physiques de l'Ouest), University of Rennes 1.

Irradiation were performed using a Rayonet RPR100 apparatus equipped with UV lamps (350 nm) or homemade system equipped with 9*5W LEDs (395-400 nm).

7.2 Typical procedure for $Re_2(CO)_{10}$ catalyzed hydrosilylation of carboxylic acids to disilylacetals

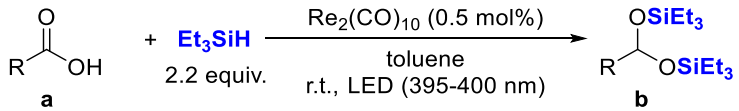

$Re_2(CO)_{10}$ (1.6 mg, 0.5 mol%) and carboxylic acid (0.5 mmol) were charged in a 20 mL Schlenk tube under argon atmosphere, followed by tol uene (1 mL), Et_3SiH (176 µL, 1.1 mmol, 2.2 equiv.), then the Schlenk tube was stirred at room temperature under LED irradiation (395-400 nm, 9*5 W) for 9 h. The crude solution was then diluted with ethyl acetate (2.0 mL) and

filtered through a small pad of celite (2 cm in a Pasteur pipette). The celite was washed with ethyl acetate (2×2.0 mL). The filtrate was evaporated and the crude residue was purified by column chromatography (SiO_2, mixture of petroleum ether/ethyl acetate as eluent) to afford the desired disilylacetal product.

7.2.1 *"1 mmol scale" procedure for $Re_2(CO)_{10}$ catalyzed hydrosilylation of carboxylic acid a1 to disilylacetal b1.*

$Re_2(CO)_{10}$ (3.3 mg, 0.5 mol%) and carboxylic acid **a1** (186 mg, 1 mmol) were charged in a 20 mL Schlenk tube under argon atmosphere, followed by toluene (2 mL), Et_3SiH (350 µL, 2.2 mmol, 2.2 equiv.), then the Schlenk tube was stirred at room temperature under LED irradiation (395-400 nm, 9*5 W) for 9 h. The crude solution was then diluted with ethyl acetate (4.0 mL) and filtered through a small pad of celite (2 cm in a Pasteur pipette). The celite was washed with ethyl acetate (2×2.0 mL). The filtrate was evaporated and the crude residue was purified by column chromatography (SiO_2, mixture of petroleum ether/ethyl acetate as eluent) to afford the desired disilylacetal product **b1** (400 mg, 96% yield).

7.2.2 *Typical procedure for $Re_2(CO)_{10}$ catalyzed hydrosilylation of aliphatic α,β-unsaturated carboxylic acids to aldehydes*

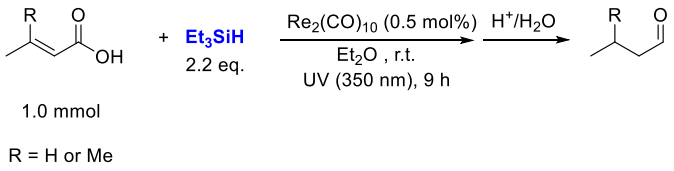

$Re_2(CO)_{10}$ (3.3 mg, 0.5 mol%) and carboxylic acid (1.0 mmol) were charged in a 20 mL Schlenk tube under argon atmosphere, followed by Et_2O (2 mL), Et_3SiH (350 µL, 2.2 mmol, 2.2 equiv.), then the Schlenk tube was stirred at room temperature under UV irradiations (350 nm) in a Rayonet RPR100 apparatus for 9 h. The crude solution was then hydrolysed at r.t. with HCl (aq., 1 M, 5 mL) for 3 h, then extracted with 3×5 mL of Et_2O. The combined fractions were dried over anhydrous Na_2SO_4 for 0.5 h. Then purified by filtration through a small pad of celite (2 cm in a Pasteur pipette) to afford the desired aldehyde product.

7.2.3 *Typical procedure for $Re_2(CO)_{10}$ catalyzed hydrosilylation of aromatic carboxylic acids to aldehydes*

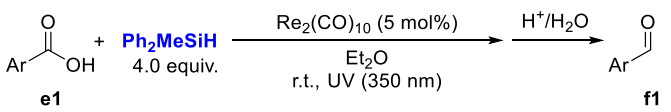

$Re_2(CO)_{10}$ (8.2 mg, 5 mol%) and aromatic carboxylic acid (0.25 mmol) was charged in a 20 mL Schlenk tube under argon atmosphere, followed by Et_2O (0.5 mL), Ph_2MeSiH (200 µL, 1.0 mmol, 4.0 equiv.), then the Schlenk tube was stirred at room temperature under UV irradiations (350 nm) in a Rayonet RPR100 apparatus for 48 h. The crude solution was then hydrolysed at r.t. with trifluoroacetic acid (99%, 0.25 mL) for 3 h. Then the mixture was evaporated and the crude residue was purified by column chromatography (SiO_2, mixture of petroleum ether/ethyl acetate as eluent) to afford the desired product.

7.2.4 *Characterization data for disilyl acetals*

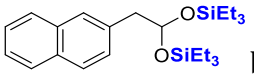

b1

The compound **b1** was prepared as described in the general procedure (202.2 mg) in 97% yield. **^{1}H NMR** (400 MHz, C_6D_6) δ 7.73 – 7.61 (m, 4H), 7.38 (dd, *J* = 8.4, 1.6 Hz, 1H), 7.31 – 7.21 (m, 2H), 5.50 (t, *J* = 5.3 Hz, 1H), 3.08 (d, *J* = 5.3 Hz, 2H), 0.97 (t, *J* = 7.9 Hz, 18H), 0.62 (q, *J* = 7.9 Hz, 12H); **^{13}C{^{1}H} NMR** (101 MHz, C_6D_6) δ 135.5, 134.1, 132.9, 128.9 (2C), 128.0, 127.92, 127.86, 126.2, 125.6, 94.6, 48.3, 7.2, 5.8; **^{29}Si{^{1}H} NMR** (79 MHz, C_6D_6) δ 15.78; **HRMS** (ESI): m/z calcd for C24H40O2NaSi$_2$ [M + Na$^+$] 439.2465, found 439.2467 (0.5 ppm).

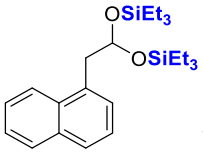

b2

The compound **b2** was prepared as described in the general procedure (158.4 mg) in 76% yield.[1] **^{1}H NMR** (300 MHz, C_6D_6) δ 8.19 (d, *J* = 8.4 Hz, 1H), 7.67 (d, *J* = 8.2 Hz, 1H), 7.59 (d, *J* = 8.1 Hz, 1H), 7.38 – 7.32 (m, 2H), 7.29 – 7.24 (m, 2H), 5.63 (t, *J* = 5.4 Hz, 1H), 3.41 (d, *J* = 5.3 Hz, 2H), 0.93 (t, *J* = 7.9 Hz, 18H), 0.56 (q, *J* = 8.2 Hz, 12H); **^{13}C{^{1}H} NMR** (75 MHz, C_6D_6) δ 134.5, 134.4, 133.3, 129.0, 128.5, 127.6, 125.9, 125.7 (2C), 124.8, 94.2, 45.0, 7.1, 5.8; **^{29}Si{^{1}H} NMR** (79 MHz, C_6D_6) δ 15.84.

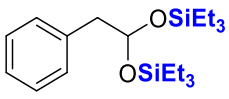

b3

The compound **b3** was prepared as described in the general procedure in 96% yield (176.0 mg).[1] **^{1}H NMR** (400 MHz, C_6D_6) δ 7.21 – 7.14 (m, 4H), 7.12 – 7.06 (m, 1H), 5.38 (t, *J* = 5.3 Hz, 1H), 2.90 (d, *J* = 5.3 Hz, 2H), 0.98 (t, *J* = 8.0 Hz, 18H), 0.61 (q, *J* = 8.0 Hz, 12H); **^{13}C{^{1}H}**

NMR (101 MHz, C_6D_6) δ 138.0, 130.3, 128.4, 126.6, 94.6, 48.3, 7.2, 5.8; **^{29}Si{^{1}H} NMR** (79 MHz, C_6D_6) δ 15.64.

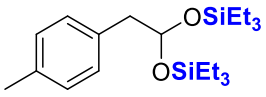

b4

The compound **b4** was prepared as described in the general procedure in 90% yield (171.3 mg).[1] **^{1}H NMR** (400 MHz, C_6D_6) δ 7.17 (d, *J* = 7.8 Hz, 2H), 7.02 (d, *J* = 7.8 Hz, 2H), 5.41 (t, *J* = 5.3 Hz, 1H), 2.93 (d, *J* = 5.3 Hz, 2H), 2.14 (s, 3H), 1.00 (t, *J* = 7.9 Hz, 18H), 0.65 (q, *J* = 8.0 Hz, 12H); **^{13}C{^{1}H} NMR** (75 MHz, C_6D_6) δ 135.9, 135.0, 130.2, 129.1, 94.8, 47.9, 21.1, 7.2, 5.8; **^{29}Si{^{1}H} NMR** (79 MHz, C_6D_6) δ 15.59.

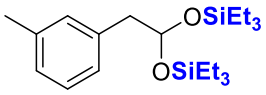

b5

The compound **b5** was prepared as described in the general procedure in 86% yield (163.7 mg).[1] **^{1}H NMR** (400 MHz, C_6D_6) δ 7.13 – 7.05 (m, 3H), 6.94 (d, *J* = 7.4 Hz, 1H), 5.42 (t, *J* = 5.3 Hz, 1H), 2.94 (d, *J* = 5.3 Hz, 2H), 2.19 (s, 3H), 1.00 (t, *J* = 7.9 Hz, 18H), 0.63 (q, *J* = 7.9 Hz, 12H); **^{13}C{^{1}H} NMR** (75 MHz, C_6D_6) δ 137.9, 137.6, 131.3, 127.4, 94.7, 48.2, 21.4, 7.2, 5.8. (Signals of C_6D_6 overlapped with two signals of **b5**); **^{29}Si{^{1}H} NMR** (79 MHz, C_6D_6) δ 15.60.

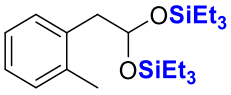

b6

The compound **b6** was prepared as described in the general procedure in 62% yield (118.0 mg).[1] **^{1}H NMR** (400 MHz, C_6D_6) δ 7.21 – 7.19 (m, 1H), 7.10 – 7.03 (m, 3H), 5.44 (t, *J* = 5.5 Hz, 1H), 2.97 (d, *J* = 5.5 Hz, 2H), 2.29 (s, 3H), 0.98 (t, *J* =8.0 Hz, 18H), 0.62 (q, *J* = 8.0 Hz, 12H); **^{13}C{^{1}H} NMR** (101 MHz, C_6D_6) δ 137.0, 136.4, 131.1, 130.4, 126.8, 126.1, 94.3, 45.1, 20.1, 7.1, 5.7; **^{29}Si{^{1}H} NMR** (79 MHz, C_6D_6) δ 15.75.

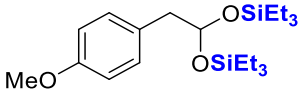

b8

The compound **b8** was prepared as described in the general procedure (188.4 mg) in 95% yield.[1] **^{1}H NMR** (400 MHz, C_6D_6) δ 7.16 (d, *J* = 8.5 Hz, 2H), 6.82 (d, *J* = 8.5 Hz, 2H), 5.40 (t, *J* = 5.2 Hz, 1H), 3.33 (s, 3H), 2.91 (d, *J* = 5.2 Hz, 2H), 1.01 (t, *J* = 8.0 Hz, 18H), 0.65 (q, *J*

= 8.1 Hz, 12H); **^{13}C{^{1}H} NMR** (75 MHz, C_6D_6) δ 159.0, 131.2, 130.0, 114.0, 94.8, 54.8, 47.4, 7.2, 5.8; **^{29}Si{^{1}H} NMR** (79 MHz, C_6D_6) δ 15.60.

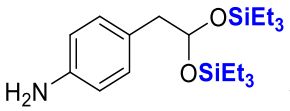

b9

The compound **b9** was prepared as described in the general procedure (143.1 mg) in 75% yield.[1] **^{1}H NMR** (400 MHz, C_6D_6) δ 7.07 (d, *J* = 8.3 Hz, 2H), 6.36 (d, *J* = 8.3 Hz, 2H), 5.39 (t, *J* = 5.3 Hz, 1H), 2.89 (d, *J* = 5.3 Hz, 2H), 2.77 (br, 2H), 1.02 (t, *J* = 7.9 Hz, 18H), 0.65 (q, *J* = 8.1 Hz, 12H); **^{13}C{^{1}H} NMR** (101 MHz, C_6D_6) δ 145.7, 131.0, 127.4, 114.9, 95.1, 47.5, 7.2, 5.8; **^{29}Si{^{1}H} NMR** (79 MHz, C_6D_6) δ 15.41.

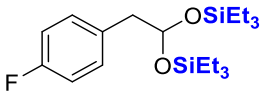

b10

The compound **b10** was prepared as described in the general procedure (177.0 mg) in 92% yield.[1] **^{1}H NMR** (400 MHz, C_6D_6) δ 6.99 (dd, *J* = 8.5, 5.6 Hz, 2H), 6.83 (t, *J* = 8.7 Hz, 2H), 5.29 (t, *J* = 5.2 Hz, 1H), 2.79 (d, *J* = 5.2 Hz, 2H), 0.97 (t, *J* = 7.9 Hz, 18H), 0.60 (q, *J* = 8.2 Hz, 12H); **^{13}C{^{1}H} NMR** (75 MHz, C_6D_6) δ 162.3 (d, *J* = 243.9 Hz), 133.6 (d, *J* = 3.2 Hz), 131.7 (d, *J* = 7.7 Hz), 115.1 (d, *J* = 21.0 Hz), 94.3, 47.2, 7.1, 5.7; **^{19}F NMR** (376 MHz, C_6D_6) δ -116.76; **^{29}Si{^{1}H} NMR** (79 MHz, C_6D_6) δ 15.88.

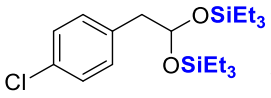

b11

The compound **b11** was prepared as described in the general procedure (196.6 mg) in 98% yield.[1] **^{1}H NMR** (400 MHz, C_6D_6) δ 7.16 – 7.13 (m, 2H), 6.94 (d, J = 8.3 Hz, 2H), 5.28 (t, *J* = 5.2 Hz, 1H), 2.75 (d, *J* = 5.2 Hz, 2H), 0.97 (t, *J* = 7.9 Hz, 18H), 0.59 (q, *J* = 8.2 Hz, 12H); **^{13}C{^{1}H} NMR** (101 MHz, C_6D_6) δ 136.4, 132.6, 131.7, 128.5, 94.1, 47.3, 7.1, 5.7; **^{29}Si{^{1}H} NMR** (79 MHz, C_6D_6) δ 15.98.

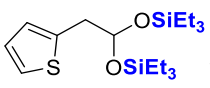

b13

The compound **b13** was prepared as described in the general procedure (109.0 mg) in 59% yield.[1] **^{1}H NMR** (300 MHz, C_6D_6) δ 6.88 (dd, *J* = 4.8, 1.5 Hz, 1H), 6.78 – 6.75 (m, 2H), 5.41 (t, *J* = 5.0 Hz, 1H), 3.09 (d, *J* = 4.9 Hz, 2H), 1.00 (t, *J* = 7.9 Hz, 18H), 0.64 (q, *J* = 8.0 Hz,

12H); **$^{13}C\{^{1}H\}$ NMR** (75 MHz, C_6D_6) δ 139.5, 126.7, 126.5, 124.4, 93.9, 42.2, 7.2, 5.8; **$^{29}Si\{^{1}H\}$ NMR** (79 MHz, C_6D_6) δ 16.16.

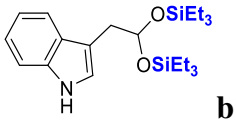

b14

The compound **b14** was prepared as described in the general procedure (180.5 mg) in 89% yield.[1] **^{1}H NMR** (300 MHz, C_6D_6) δ 7.81 – 7.78 (m, 1H), 7.24 – 7.19 (m, 2H), 7.09 – 7.05 (m, 1H), 6.72 (s, 2H), 5.58 (t, *J* = 5.3 Hz, 1H), 3.18 (d, *J* = 5.3 Hz, 2H), 1.00 (t, *J* = 7.9 Hz, 18H), 0.65 (q, *J* = 8.0 Hz, 12H); **$^{13}C\{^{1}H\}$ NMR** (75 MHz, C_6D_6) δ 136.6, 128.6, 123.0, 122.1, 119.6, 119.5, 112.0, 111.3, 94.2, 37.8, 7.2, 5.8; **$^{29}Si\{^{1}H\}$ NMR** (79 MHz, C_6D_6) δ 15.52.

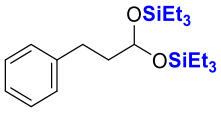

b15

The compound **b15** was prepared as described in the general procedure (177.0 mg) in 93% yield.[1] **^{1}H NMR** (400 MHz, C_6D_6) δ 7.20 – 7.16 (m, 4H), 7. 08 – 7.04 (m, 1H), 5.29 (t, *J* = 4.9 Hz, 1H), 2.84 – 2.80 (m, 2H), 2.00 – 1.95 (m, 2H), 1.03 (t, *J* = 7.9 Hz, 18H), 0.67 (q, *J* = 7.9 Hz, 12H); **$^{13}C\{^{1}H\}$ NMR** (101 MHz, C_6D_6) δ 142.5, 128.8 (2C), 126.2, 93.2, 43.0, 31.4, 7.2, 5.9; **$^{29}Si\{^{1}H\}$ NMR** (79 MHz, C_6D_6) δ 15.36.

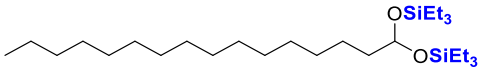

b16

The compound **b16** was prepared as described in the general procedure (236.2 mg) in 97% yield.[1] **^{1}H NMR** (400 MHz, C_6D_6) δ 5.29 (t, *J* = 5.0 Hz, 1H), 1.69 – 1.64 (m, 2H), 1.53-1.50 (m, 2H), 1.34 – 1.30 (m, 24H), 1.04 (t, *J* = 8.0 Hz, 18H), 0.91 (t, *J* = 6.8 Hz, 3H), 0.68 (q, *J* = 7.9 Hz, 12H); **$^{13}C\{^{1}H\}$ NMR** (101 MHz, C_6D_6) δ 94.0, 41.5, 32.4, 30.3, 30.23, 30.17, 30.1, 29.9, 25.2, 23.2, 14.4, 7.3, 6.0. (some signals are overlapping); **$^{29}Si\{^{1}H\}$ NMR** (79 MHz, C_6D_6) δ 14.79.

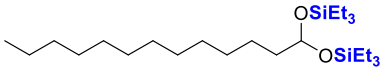

b17

The compound **b17** was prepared as described in the general procedure (218.0 mg) in 97% yield.[1] **^{1}H NMR** (400 MHz, C_6D_6) δ 5.34 (t, *J* = 5.0 Hz, 1H), 1.75 – 1.70 (m, 2H), 1.59-1.53 (m, 2H), 1.37– 1.30 (m, 18H), 1.07 (t, *J* = 7.9 Hz, 18H), 0.92 (t, *J* = I6.4 Hz, 3H), 0.72 (q, *J* =

7.9 Hz, 12H); **^{13}C{^{1}H} NMR** (101 MHz, C_6D_6) δ 94.0, 41.4, 32.4, 30.22, 30.17, 30.14, 30.13, 30.10, 30.0, 29.8, 25.1, 23.1, 14.4, 7.3, 5.9; **^{29}Si{^{1}H} NMR** (79 MHz, C_6D_6) δ 14.94.

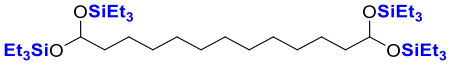

b18

The compound **b18** was prepared as described in the general procedure (349.2 mg) in 99% yield.[1] **^{1}H NMR** (500 MHz, C_6D_6) δ 5.32 – 5.29 (m, 2H), 1.70 – 1.67 (m, 4H), 1.34 – 1.30 (m, 18H), 1.06 (t, *J* = 8.0 Hz, 36H), 0.70 (q, *J* = 7.9 Hz, 24H); **^{13}C{^{1}H} NMR** (126 MHz, C_6D_6) δ 94.0, 41.5, 30.2, 30.15, 30.13, 30.0, 25.1, 7.3, 6.0; **^{29}Si{^{1}H} NMR** (79 MHz, C_6D_6) δ 14.86.

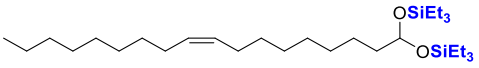

b19

The compound **b19** was prepared as described in the general procedure (238.5 mg) in 93% yield.[1] **^{1}H NMR** (400 MHz, C_6D_6) δ 5.54 – 5.46 (m, 2H), 5.33 (t, *J* = 5.0 Hz, 1H), 2.13 – 2.08 (m, 4H), 1.74 – 1.69 (m, 2H), 1.56-1.53 (m, 2H), 1.42 – 1.21jk (m, 20H), 1.07 (t, *J* = 7.9 Hz, 18H), 0.92 (t, *J* = 6.7 Hz, 3H), 0.72 (q, *J* = 8.0 Hz, 12H); **^{13}C{^{1}H} NMR** (126 MHz, C_6D_6) δ 130.3, 130.2, 93.9, 41.4, 32.3, 30.3, 30.2, 30.1, 30.00, 29.98, 29.79, 29.77, 29.69, 27.7, 25.1, 23.1, 14.4, 7.3, 5.9; **^{29}Si{^{1}H} NMR** (79 MHz, C_6D_6) δ 14.93.

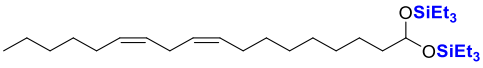

b20

The compound **b20** was prepared as described in the general procedure (222.3 mg) in 87% yield. **^{1}H NMR** (400 MHz, C_6D_6) δ 5.53 – 5.43 (m, 4H), 5.32 (t, *J* = 5.0 Hz, 1H), 2.89 (t, *J* = 6.0 Hz, 2H), 2.11 – 2.05 (m, 4H), 1.73 – 1.68 (m, 2H), 1.50 – 1.25 (m, 16H), 1.07 (t, *J* = 7.9 Hz, 18H), 0.89 (t, *J* = 6.9 Hz, 3H), 0.71 (q, *J* = 7.9 Hz, 12H); **^{13}C{^{1}H} NMR** (101 MHz, C_6D_6) δ 130.4, 130.4, 128.5, 128.4, 93.9, 41.4, 31.9, 30.14, 30.12, 30.0, 29.8, 29.7, 27.71, 27.66, 26.2, 25.1, 23.0, 14.3, 7.3, 5.9; **^{29}Si{^{1}H} NMR** (79 MHz, C_6D_6) δ 14.92; **HRMS** (ESI): m/z calcd for C30H62O2NaSi$_2$ [M + Na$^+$] 533.41806, found 533.4176 (1 ppm).

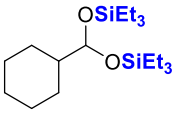

b21

The compound **b21** was prepared as described in the general procedure (163.2 mg) in 91% yield. **^{1}H NMR** (400 MHz, C_6D_6) δ 5.09 (d, *J* = 3.1 Hz, 1H), 1.89 – 1.66 (m, 5H), 1.47 – 1.21 (m, 6H), 1.05 (t, *J* = 7.9 Hz, 18H), 0.70 (q, *J* = 7.9 Hz, 12H); **^{13}C{^{1}H} NMR** (101 MHz, C_6D_6) δ 96.4, 47.7, 27.5, 27.2, 26.7, 7.3, 5.9; **^{29}Si{^{1}H} NMR** (79 MHz, C_6D_6) δ 14.71.

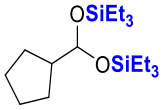

b22

The compound **b22** was prepared as described in the general procedure (155.1 mg) in 90% yield. **^{1}H NMR** (400 MHz, C_6D_6) δ 5.21 (d, *J* = 4.1 Hz, 1H), 2.15 – 2.06 (m, 1H), 1.70 – 1.66 (m, 8H), 1.05 (t, *J* = 7.9 Hz, 18H), 0.69 (q, *J* = 7.9 Hz, 12H); **^{13}C{^{1}H} NMR** (75 MHz, C6D6) δ 95.9, 48.8, 27.8, 26.6, 7.3, 5.9; **^{29}Si{^{1}H} NMR** (79 MHz, C_6D_6) δ 14.69.

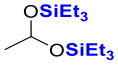

b23

The compound **b23** was prepared as described in the general procedure (133.7 mg) in 92% yield.[1] **^{1}H NMR** (500 MHz, C_6D_6) δ 5.40 (q, *J* = 4.9 Hz, 1H), 1.33 (d, *J* = 4.9 Hz, 3H), 1.03 (t, *J* = 8.0 Hz, 18H), 0.66 (q, *J* = 8.0 Hz, 12H); **^{13}C{^{1}H} NMR** (126 MHz, C_6D_6) δ 90.9, 27.8, 7.2, 5.8; **^{29}Si{^{1}H} NMR** (79 MHz, C_6D_6) δ 14.83.

b24

The compound **b24** was prepared as described in the general procedure (124.5 mg) in 90% yield.[1] **^{1}H NMR** (400 MHz, C_6D_6) δ 5.05 (s, 2H), 1.02 (t, *J* = 7.9 Hz, 18H), 0.64 (q, *J* = 8.0 Hz, 12H); **^{13}C{^{1}H} NMR** (101 MHz, C_6D_6) δ 84.5, 7.0, 5.3; **^{29}Si{^{1}H} NMR** (79 MHz, C_6D_6) δ 18.33.

7.2.5 *Characterization data for aldehydes*

3-phenylpropionaldehyde[1]

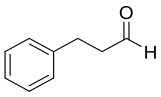

The reduction of 3-phenylpropionic acid **b15** (1,0 g, 6,7 mmol) was performed according to general procedure (Et_3SiH, 2.3 mL, 14.6 mmol, toluene 13 mL, hν 395 nm, 24 h). The reaction mixture was filtered through celite and evaporated. After hydrolysis of the crude mixture(1 N HCl, 50 mL, THF 50 mL, 4 h) and extraction with Et_2O (3*50 mL), 3-phenylpropionaldehyde was isolated by bulb to bulb distillation (450 mg, 61% yield). **^{1}H NMR** (400 MHz, $CDCl_3$) δ 9.82 (t, *J* = 1.4 Hz, 1H), 7.36 – 7.27 (m, 2H), 7.26 – 7.15 (m, 3H), 2.97 (t, *J* = 7.6 Hz, 2H), 2.83 – 2.75 (m, 2H); **^{13}C{^{1}H} NMR** (101 MHz, $CDCl_3$) δ 201.6, 140.4, 128.7, 128.5, 128.4, 126.4, 45.3, 28.2.

2,4,6-tri(2-phenylethyl)-1,3,5-trioxane[2]

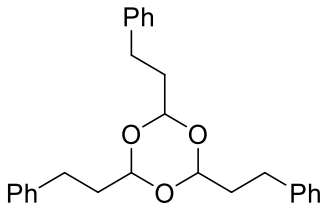

^{1}H NMR (300 MHz, $CDCl_3$) δ 7.38 – 7.11 (m, 15H), 4.83 (t, *J* = 5.3 Hz, 3H), 2.88 – 2.66 (m, 6H), 2.17 – 1.91 (m, 6H); **^{13}C{^{1}H} NMR** (101 MHz, $CDCl_3$) δ 141.4, 128.6, 128.5, 126.1, 100.7, 35.8, 29.7.

f1

The compound **f1** was prepared as described in the general procedure (17.2 mg) in 65% yield.[3] **^{1}H NMR** (400 MHz, $CDCl_3$) 10.02 (s, 1H), 7.90 – 7.87 (m, 2H), 7.66 – 7.61 (m, 1H), 7.55 – 7.51 (m, 2H); **^{13}C{^{1}H} NMR** (101 MHz, $CDCl_3$) δ 192.5, 136.6, 134.6, 129.9, 129.1.

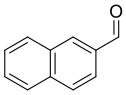

f2

The compound **f2** was prepared as described in the general procedure (32.0 mg) in 82% yield.[3] **^{1}H NMR** (400 MHz, $CDCl_3$) δ 10.14 (s, 1H), 8.31 (s, 1H), 7.98 (d, *J* = 8.1 Hz, 1H), 7.96 – 7.87 (m, 3H), 7.65 – 7.61 (m, 1H), 7.60 – 7.56 (m, 1H); **^{13}C{^{1}H} NMR** (101 MHz, $CDCl_3$) δ 192.3, 136.5, 134.6, 134.2, 132.7, 129.6, 129.18, 129.15, 128.1, 127.2, 122.8.

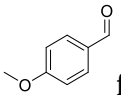

f3

The compound **f3** was prepared as described in the general procedure (26.9 mg) in 79% yield.[4] **^{1}H NMR** (400 MHz, $CDCl_3$) δ 9.88 (s, 1H), 7.83 (d, *J* = 8.8 Hz, 2H), 6.99 (d, *J* = 8.8 Hz, 2H), 3.88 (s, 3H); **^{13}C{^{1}H} NMR** (101 MHz, $CDCl_3$) δ 190.9, 164.7, 132.1, 130.1, 114.4, 55.7.

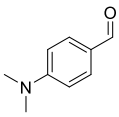

f4

The compound **f4** was prepared as described in the general procedure (23.5 mg) in 63% yield.[5] **^{1}H NMR** (400 MHz, $CDCl_3$) δ 9.74 (s, 1H), 7.73 (d, *J* = 8.9 Hz, 2H), 6.70 (d, *J* = 8.9 Hz, 2H), 3.08 (s, 6H); **^{13}C{^{1}H} NMR** (101 MHz, $CDCl_3$) δ 190.4, 154.5, 132.1, 125.3, 111.1, 40.2.

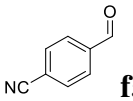

f5

The compound **f5** was prepared as described in the general procedure (8.8 mg) in 27% yield.[6] **^{1}H NMR** (400 MHz, $CDCl_3$) δ 10.09 (s, 1H), 7.99 (d, *J* = 8.4 Hz, 2H), 7.84 (d, *J* = 8.2 Hz, 2H); **^{13}C{^{1}H} NMR** (101 MHz, $CDCl_3$) δ 190.7, 138.9, 133.0, 130.0, 117.8, 117.7.

f6

The compound **f6** was prepared as described in the general procedure (13.9 mg) in 58% yield.[7] **^{1}H NMR** (400 MHz, $CDCl_3$) δ 9.65 (s, 1H), 7.68 – 7.68 (m, 1H), 7.24 (dd, *J* = 3.6, 0.8 Hz, 1H), 6.59 (dd, *J* = 3.6, 1.7 Hz, 1H); **^{13}C{^{1}H} NMR** (101 MHz, $CDCl_3$) δ 178.0, 153.1, 148.2, 121.1, 112.7.

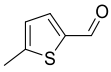

f7

The compound **f7** was prepared as described in the general procedure (17.3 mg) in 55% yield.[8] **^{1}H NMR** (400 MHz, $CDCl_3$) δ 9.80 (s, 1H), 7.59 (d, *J* = 3.7 Hz, 1H), 6.88 (dd, *J* = 3.7, 0.8 Hz, 1H), 2.57 (s, 3H); **^{13}C{^{1}H} NMR** (101 MHz, $CDCl_3$) δ 182.7, 151.8, 142.1, 137.4, 127.2, 16.4.

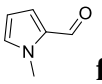

f8

The compound **f8** was prepared as described in the general procedure (6.3 mg) in 23% yield.[9] **^{1}H NMR** (400 MHz, $CDCl_3$) δ 9.55 (d, *J* = 0.8 Hz, 1H), 6.91 (dd, *J* = 4.0, 1.7 Hz, 1H), 6.88 – 6.87 (m, 1H), 6.21 (dd, *J* = 4.0, 2.4 Hz, 1H), 3.95 (s, 3H); **^{13}C{^{1}H} NMR** (101 MHz, $CDCl_3$) δ 179.7, 132.15, 132.12, 124.2, 109.6, 36.6.

f12

The compound **f12** was prepared as described in the general procedure for aliphatic α,β-unsaturated carboxylic acids (59 mg) in 82% yield. **^{1}H NMR** (400 MHz, $CDCl_3$) δ. 9.76 (t, *J* = 1.8 Hz, 1H)., 2.41 (td, *J* = 7.2, 1.8 Hz, 2H), 1.72 – 1.62 (m, 2H), 0.97 (t, *J* = 7.2 Hz, 3H); **^{13}C{^{1}H} NMR** (101 MHz, $CDCl_3$) δ. 203.0, 45.9, 15.8, 13.8.

f13

The compound **f13** was prepared as described in the general procedure for aliphatic α,β-unsaturated carboxylic acids (78 mg) in 91% yield. **^{1}H NMR** (400 MHz, $CDCl_3$) δ. 9.75 (t, *J* = 2.3 Hz, 1H), 2.30 (dd, *J* = 6.6, 2.3 Hz, 2H), 2.25 – 2.15 (m, 1H), 0.98 (d, *J* = 6.6 Hz, 6H); **^{13}C{^{1}H} NMR** (101 MHz, $CDCl_3$) δ. 203.0, 52.7, 23.6, 22.7.

7.3 Typical procedure for Mn2(CO)10 or Re2(CO)10 catalyzed hydrosilylation of esters

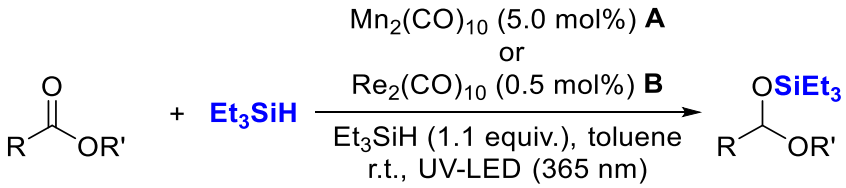

7.3.1 *Typical 0.5 mmol scale hydrosilylation reaction:*

$Mn_2(CO)_{10}$ (9.7 mg, 5.0 mol%) (method **A**) or $Re_2(CO)_{10}$ (1.6 mg, 0.5 mol%) (method **B**) was charged in a 20 ml Schlenk tube under argon atmosphere, followed by toluene (1 mL), carboxylic ester (0.5 mmol), Et_3SiH (88 µL, 0.55 mmol, 1.1 equiv.), then the Schlenk tube was stirred at room temperature under UV-LED irradiation (365 nm, 4*10 W) for 9 h. The crude solution was then diluted with ethyl acetate (2.0 mL) and filtered through a small pad of celite (2 cm in a Pasteur pipette). The celite was washed with ethyl acetate (2×2.0 mL). The filtrate was evaporated and the crude residue was purified by column chromatography (SiO_2, mixture of petroleum ether/ethyl acetate as eluent) to afford the desired product.

7.3.2 *Typical 1 mmol scale hydrosilylation reaction:*

$Mn_2(CO)_{10}$ (19.4 mg, 5.0 mol%) (method **A**) or $Re_2(CO)_{10}$ (3.2 mg, 0.5 mol%) (method **B**) was charged in a 20 ml Schlenk tube under argon atmosphere, followed by toluene (1 mL), carboxylic ester (1 mmol), Et_3SiH (176 µL, 1.1 mmol, 1.1 equiv.), then the Schlenk tube was stirred at room temperature under UV-LED irradiation (365 nm, 4*10 W) for 9 h. The crude solution was then diluted with ethyl acetate (2.0 mL) and filtered through a small pad of celite (2 cm in a Pasteur pipette). The celite was washed with ethyl acetate (2×2.0 mL). The filtrate was evaporated and the crude residue was purified by column chromatography (SiO_2, mixture of petroleum ether/ethyl acetate as eluent) to afford the desired product.

7.3.3 *Typical 1 mmol scale synthesis of aldehyde:*

After irradiation, the reaction mixture was filtered through celite and evaporated. After hydrolysis of the crude mixture (1N HCl, 10 mL, THF 10 mL, 4 h) and extraction with Et_2O (3*20 mL), the crude residue was purified by column chromatography (SiO_2, mixture of petroleum ether/ethyl acetate as eluent) to afford the desired product.

7.3.4 *"1 g scale" procedure:*

The reduction of ethyl 1-naphthaleneacetate (1,0 g, 4,67 mmol) was performed according to general procedure ($Re_2(CO)_{10}$, 15 mg, 0.5 mol%, Et_3SiH, 0.8 mL, 5.1 mmol, toluene 4 mL, *hv* 365 nm, 18 h). The reaction mixture was filtered through celite and evaporated. After hydrolysis of the crude mixture (1N HCl, 10 mL, THF 10 mL, 4 h) and extraction with Et_2O (3*20 mL), 1-naphthaleneacetaldehyde was isolated by bulb to bulb distillation (599 mg, 75% yield).

7.3.5 *Characterization data for the hydrosilylation products*

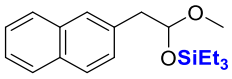

h1

The compound **h1** was prepared as described in the general procedure method **A** (129.8 mg) in 82% yield. **^{1}H NMR** (400 MHz, $CDCl_3$) δ 7.82 – 7.76 (m, 3H, CH_{Ar}), 7.67 (s, 1H, CH_{Ar}), 7.47 – 7.40 (m, 2H, CH_{Ar}), 7.38 (dd, J = 8.4, 1.6, 1H, CH_{Ar}), 4.94 (dd, J = 6.1, J = 4.7 Hz, 1H, CH), 3.34 (s, 3H, OCH_3), 3.11 (dd, J = 13.7, 6.1 Hz, 1H, CH_2), 3.00 (dd, J = 13.7, 4.7 Hz, 1H, CH_2), 0.94 (t, J = 8.0 Hz, 9H, CH_2CH_3), 0.60 (q, J = 8.2 Hz, 6H, CH_2CH_3); **^{13}C{^{1}H} NMR** (101 MHz, $CDCl_3$) δ 134.9 (C_{Ar}), 133.6 (C_{Ar}), 132.4 (C_{Ar}), 128.4 (CH_{Ar}), 128.3 (CH_{Ar}) 127.76 (CH_{Ar}), 127.72(CH_{Ar}), 127.68 (CH_{Ar}), 126.0 (CH_{Ar}), 125.4 (CH_{Ar}), 99.9 (CH), 54.1 (OCH_3), 44.4 (CH_2), 6.9 (CH_2CH_3), 5.1 (CH_2CH_3); **^{29}Si{^{1}H} NMR** (80 MHz, C_6D_6) δ 16.8; **HRMS** (ESI): m/z calcd for $C_{18}H_{25}OSi$ $[M - OMe]^+$ 285.1675, found 285.1679 (1 ppm); **LRMS** (DCI-NH_3): m/z calcd for $C_{19}H_{32}O_2SiN$ $[M + NH_4]^+$ 334.2, found 334.2.

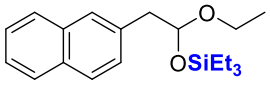

h2

The compound **h2** was prepared as described in the general procedure method **B** (155 mg) in 94% yield. **^{1}H NMR** (400 MHz, $CDCl_3$) δ 7.82 – 7.76 (m, 3H, CH_{Ar}), 7.68 (s, 1H, CH_{Ar}), 7.48 – 7.39 (m, 3H, CH_{Ar}), 5.00 (dd, J = 6.1, 4.7 Hz, 1H, CH), 3.74 (dq, J = 9.0, 7.0 Hz, 1H, OCH_2CH$_3$), 3.39 (dq, J = 9.1, 7.0 Hz, 1H, OCH_2CH$_3$), 3.13 (dd, J = 13.6, 6.1 Hz, 1H, CH_2),

3.00 (dd, J = 13.6, 4.7 Hz, 1H, CH_2), 1.16 (t, J = 7.0 Hz, 3H, OCH$_2$CH_3), 0.94 (t, J = 7.9 Hz, 9H, CH$_2$CH_3), 0.59 (q, J = 8.2 Hz, 6H, CH_2CH$_3$); **^{13}C{^{1}H} NMR** (101 MHz, $CDCl_3$) δ 135.1 (C_{Ar}), 133.6 (C_{Ar}), 132.4 (C_{Ar}), 128.6 (CH_{Ar}), 128.3 (CH_{Ar}), 127.71 (CH_{Ar}), 127.66 (CH_{Ar}), 127.64 (CH_{Ar}), 125.9 (CH_{Ar}), 125.4 (CH_{Ar}), 99.0 (*C*H), 62.3 (O*C*H$_2$CH$_3$), 44.8 (*C*H$_2$), 15.3 (OCH$_2$*C*H$_3$), 6.9 (CH$_2$*C*H$_3$), 5.1 (*C*H$_2$CH$_3$); **^{29}Si{^{1}H} NMR** (80 MHz, $CDCl_3$) δ 17.69; **HRMS** (ESI): m/z calcd for $C_{20}H_{30}O_2SiNa$ $[M + Na]^+$ 353.1913, found 353.1918 (1.4 ppm); **LRMS** (DCI-NH_3, POS): m/z calcd for $C_{20}H_{34}O_2SiN$ $[M + NH_4]^+$ 348.2, found 348.2.

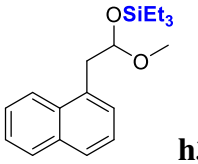

h3

The compound **h3** was prepared as described in the general procedure method **A** (125.3 mg) in 79% yield. **^{1}H NMR** (400 MHz, C_6D_6) δ 8.14 (d, J = 8.3 Hz, 1H, CH_{Ar}), 7.67 (d, J = 8.5 Hz, 1H, CH_{Ar}), 7.58 (d, J = 8.2 Hz, 1H, CH_{Ar}), 7.37 – 7.32 (m, 2H, CH_{Ar}), 7.29 – 7.24 (m, 2H, CH_{Ar}), 5.11 (t, J = 5.4 Hz, 1H, C*H*), 3.46 (dd, J = 13.8, 5.2 Hz, 1H, CH_2), 3.38 (dd, J = 13.8, 5.5 Hz, 1H, CH_2), 3.14 (s, 3H, OCH_3), 0.88 (t, J = 7.9 Hz, 9H,CH$_2$CH_3), 0.47 (q, J = 8.2 Hz, 6H, CH_2CH$_3$); **^{13}C{^{1}H} NMR** (101 MHz, C_6D_6) δ 134.5 (C_{Ar}), 134.2 (C_{Ar}), 133.2 (C_{Ar}), 129.1 (CH_{Ar}), 128.5 (CH_{Ar}), 127.6 (CH_{Ar}), 126.0 (CH_{Ar}), 125.72 (CH_{Ar}), 125.67 (CH_{Ar}), 124.6 (CH_{Ar}), 99.7 (*C*H), 53.3 (O*C*H$_3$), 41.3 (*C*H$_2$), 7.0 (s, CH$_2$*C*H$_3$)., 5.4 (s, *C*H$_2$CH$_3$); **^{29}Si{^{1}H} NMR** (80 MHz, C_6D_6) δ 16.90; **LRMS** (DCI-NH_3): m/z calcd for $C_{12}H_{14}NO$ [Aldehyde + $NH_4]^+$ 188.1, found 188.0.

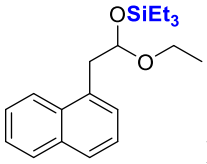

h4

The compound was **h4** prepared as described in the general procedure method **B** (158.3 mg) in 96% yield. **^{1}H NMR** (400 MHz, C_6D_6) δ 8.17 (d, J = 8.4 Hz, 1H, CH_{Ar}), 7.67 (d, J = 7.6 Hz, 1H, CH_{Ar}), 7.59 (d, J = 8.2 Hz, 1H, CH_{Ar}), 7.39 – 7.32 (m, 2H, CH_{Ar}), 7.29 – 7.25 (m, 2H, CH_{Ar}), 5.18 (t, J = 5.4 Hz, 1H, C*H*), 3.60 (dq, J = 8.9, 7.0 Hz, 1H, OCH_2CH$_3$), 3.49 (dd, J = 13.8, 5.3 Hz, 1H, CH_2), 3.40 (dd, J = 13.8, 5.5 Hz, 1H, CH_2), 3.22 (dq, J = 8.8, 7.0 Hz, 1H, OCH_2CH$_3$), 1.03 (t, J = 7.0 Hz, 3H, OCH$_2$CH_3), 0.90 (t, J = 7.9 Hz, 9H, CH$_2$CH_3), 0.49 (q, J = 8.1 Hz, 6H, CH_2CH$_3$); **^{13}C{^{1}H} NMR** (101 MHz, C_6D_6) δ 134.5 (C_{Ar}), 134.4 (C_{Ar}), 133.2 (C_{Ar}), 129.1 (CH_{Ar}), 128.5 (CH_{Ar}), 127.5 (CH_{Ar}), 125.9 (CH_{Ar}), 125.70 (CH_{Ar}), 125.67 (CH_{Ar}), 124.8

(CH_{Ar}), 98.9 (*C*H), 61.8 (O*C*$H_2$$CH_3$), 41.8 (*C*$H_2$), 15.5 (O$CH_2$*C*$H_3$), 7.0 ($CH_2$*C*$H_3$), 5.5 (*C*$H_2$$CH_3$); **^{29}Si{^{1}H} NMR** (80 MHz, C_6D_6) δ 16.44; **LRMS** (DCI-NH_3): m/z calcd for $C_{12}H_{14}NO$ [Aldehyde + NH_4]$^+$ 188.1, found 187.9.

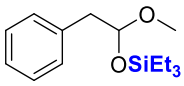

h5

The compound **h5** was prepared as described in the general procedure method **A** (94.3 mg) in 71% yield.[10] **^{1}H NMR** (400 MHz, C_6D_6) *δ* 7.23 – 7.20 (m, 2H, C*H*$_{Ar}$), 7.18 – 7.15 (m, 2H, C*H*$_{Ar}$), 7.10 – 7.06 (m, 1H, C*H*$_{Ar}$), 4.88 (t, *J* = 5.3, 1H, C*H*), 3.15 (s, 3H, OC*H*$_3$), 3.00 (dd, *J* = 13.5, 5.7 Hz, 1H, C*H*$_2$), 2.88 (dd, *J* = 13.5, 5.0 Hz, 1H, C*H*$_2$)., 0.96 (t, *J* = 8.0 Hz, 9H, CH_2C*H*$_3$), 0.56 (q, *J* = 8.0 Hz, 6H, C*H*$_2$$CH_3$); **^{13}C{^{1}H} NMR** (101 MHz, C_6D_6) *δ* 137.9 (*C*$_{Ar}$), 130.2 (*C*H_{Ar}) , 128.5 (*C*H_{Ar}), 126.6 (*C*H_{Ar}), 100.2 (*C*H), 53.3 (O*C*H_3), 44.4 (*C*H_2), 7.1 (CH_2*C*H_3), 5.4 (*C*$H_2$$CH_3$); **^{29}Si{^{1}H} NMR** (80 MHz, C_6D_6) *δ* 16.68.

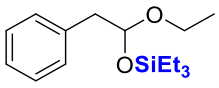

h6

The compound **h6** was prepared as described in the general procedure method **B** (132.7 mg) in 95% yield. [11] **^{1}H NMR** (400 MHz, C_6D_6) δ 7.24 – 7.22 (m, 2H, C*H*$_{Ar}$), 7.19 – 7.17 (m, 2H, C*H*$_{Ar}$) , 7.10 – 7.06 (m, 1H, C*H*$_{Ar}$), 4.95 (dd, *J* = 5.7, 5.0 Hz, 1H, C*H*), 3.61 (dq, *J* = 9.0, 7.0 Hz, 1H, OC*H*$_2$$CH_3$), 3.25 (dq, *J* = 9.0, 7.0 Hz, 1H, OC*H*$_2$$CH_3$), 3.02 (dd, *J* = 13.5, 5.8 Hz, 1H, C*H*$_2$), 2.90 (dd, *J* = 13.5, 4.9 Hz, 1H, C*H*$_2$), 1.07 (t, *J* = 7.0 Hz, 3H, OCH_2C*H*$_3$), 0.97 (t, *J* = 8.0 Hz, 9H, CH_2C*H*$_3$), 0.58 (q, *J* = 8.0 Hz, 6H, C*H*$_2$$CH_3$); **^{13}C{^{1}H} NMR** (101 MHz, C_6D_6) δ 138.0 (*C*$_{Ar}$), 130.2 (*C*H_{Ar}), 128.4 (*C*H_{Ar}), 126.6 (*C*H_{Ar}), 99.3 (*C*H), 61.8 (O*C*$H_2$$CH_3$), 44.9 (*C*$H_2$), 15.5 (O$CH_2$*C*$H_3$), 7.1 ($CH_2$*C*$H_3$), 5.5(*C*$H_2$$CH_3$); **^{29}Si{^{1}H} NMR** (80 MHz, C_6D_6) δ 16.79.

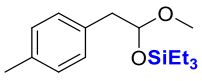

h7

The compound **h7** was prepared as described in the general procedure method **A** (112.2 mg) in 80% yield (95% purity according to ^{1}H NMR). **^{1}H NMR** (300 MHz, C_6D_6) *δ* 7.17 (d, *J* = 7.8 Hz, 2H, C*H*$_{Ar}$), 7.01 (d, *J* = 7.8 Hz, 2H, C*H*$_{Ar}$), 4.90 (dd, *J* = 5.8, 4.9 Hz, 1H, C*H*), 3.17 (s, 3H, OC*H*$_3$), 3.01 (dd, *J* = 13.6, 5.8 Hz, 1H, C*H*$_2$), 2.89 (dd, *J* = 13.6, 4.9 Hz, 1H, C*H*$_2$), 2.13 (s, 3H, C*H*$_3$), 0.97 (t, *J* = 7.9 Hz, 9H, CH_2C*H*$_3$), 0.58 (q, *J* = 8.2 Hz, 6H, C*H*$_2$$CH_3$); **^{13}C{^{1}H} NMR** (75 MHz, C_6D_6) *δ* 135.8 (*C*$_{Ar}$), 134.9 (*C*$_{Ar}$), 130.1 (*C*H_{Ar}), 129.2 (*C*H_{Ar}), 100.4 (*C*H), 53.4 (O*C*H_3), 44.1 (*C*H_2), 21.1 (*C*H_3), 7.1 (CH_2*C*H_3), 5.5 (*C*$H_2$$CH_3$); **^{29}Si{^{1}H} NMR** (80 MHz, C_6D_6) *δ* 16.54;

HRMS (ESI): m/z calcd for $C_{15}H_{25}OSi$ [M – OMe]$^+$ 249.1675, found 249.1679 (1.6 ppm); **LRMS** (DCI-NH_3, POS): m/z calcd for $C_{16}H_{32}O_2SiN$ [M + NH_4]$^+$ 298.2, found 298.2.

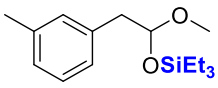

h8

The compound **h8** was prepared as described in the general procedure method **B** (95.4 mg) in 68% yield. **^{1}H NMR** (400 MHz, C_6D_6) δ 7.13 – 7.11 (m, 1H, CH_{Ar}), 7.08 – 7.06 (m, 2H, CH_{Ar}), 6.93 (d, *J* = 7.2 Hz, 1H, CH_{Ar}), 4.91 (t, *J* = 5.4 Hz, 1H, C*H*), 3.17 (s, 3H, OCH_3), 3.01 (dd, *J* = 13.5, 5.6 Hz, 1H, CH_2), 2.90 (dd, *J* = 13.5, 5.1 Hz, 1H, CH_2), 2.16 (s, 3H, CH_3), 0.97 (t, *J* = 7.9 Hz, 9H, CH_2CH_3), 0.58 (t, *J* = 8.0 Hz, 6H, CH_2CH_3); **^{13}C{^{1}H} NMR** (101 MHz, C_6D_6) *δ* 137.8 (*C*$_{Ar}$), 137.7 (*C*$_{Ar}$), 131.1 (*C*H$_{Ar}$), 128.4 (*C*H$_{Ar}$), 127.4 (*C*H$_{Ar}$), 127.3 (*C*H$_{Ar}$), 100.3 (*C*H), 53.3 (O*C*H$_3$), 44.4 (*C*H$_2$), 21.4 (*C*H$_3$), 7.1 (CH_2CH_3), 5.5 (CH_2CH_3); **^{29}Si{^{1}H} NMR** (80 MHz, C_6D_6) *δ* 16.55; **HRMS** (ESI): m/z calcd for $C_{15}H_{25}OSi$ [M – OMe]$^+$ 249.1675, found 249.1679 (1.6 ppm); **LRMS** (DCI-NH_3): m/z calcd for $C_9H_{14}NO$ [Aldehyde+NH4]$^+$ 152.1, found 152.1.

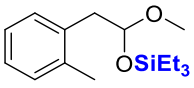

h9

The compound **h9** was prepared as described in the general procedure method **B** (105.2 mg) in 75% yield (> 95% purity according to ^{1}H NMR). **^{1}H NMR** (300 MHz, $CDCl_3$) *δ* 7.20 – 7.10 (m, 4H, CH_{Ar}), 4.87 (dd, *J* = 5.8, 5.2 Hz, 1H, C*H*), 3.33 (s, 3H, OCH_3), 2.97 (dd, *J* = 13.8, 5.8 Hz, 1H, CH_2), 2.87 (dd, *J* = 13.8, 5.2 Hz, 1H, CH_2), 2.35 (s, 3H, CH_3), 0.93 (t, *J* = 7.9 Hz, 9H, CH_2CH_3), 0.57 (q, *J* = 7.5 Hz, 6H, CH_2CH_3); **^{13}C{^{1}H} NMR** (75 MHz, $CDCl_3$) *δ* 136.9 (*C*$_{Ar}$), 135.8 (*C*$_{Ar}$), 130.6 (*C*H$_{Ar}$), 130.2 (*C*H$_{Ar}$), 126.6 (*C*H$_{Ar}$), 125.8 (*C*H$_{Ar}$), 99.5 (*C*H), 54.0 (O*C*H$_3$), 41.2 (*C*H$_2$), 20.0 (*C*H$_3$), 6.9 (CH_2CH_3), 5.1 (CH_2CH_3); **^{29}Si{^{1}H} NMR** (80 MHz, C_6D_6) *δ* 16.7; **HRMS** (ESI): m/z calcd for $C_{15}H_{25}OSi$ [M – OMe]$^+$ 249.1675, found 249.1680 (1 ppm); **LRMS** (DCI-NH3): m/z calcd for $C_{16}H_{32}O_2SiN$ [M + NH_4]$^+$ 298.2, found 298.2.

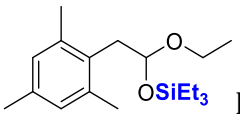

h10

The compound **h10** was prepared as described in the general procedure method **B** (156.3 mg) in 97% yield. **^{1}H NMR** (400 MHz, C_6D_6) δ 6.79 (s, 2H, CH_{Ar}), 5.02 (t, *J* = 5.7 Hz, 1H, C*H*), 3.61 (dq, *J* = 8.9, 7.0 Hz, 1H, OCH_2CH$_3$), 3.20 (dq, J = 8.9, 7.0 Hz, 1H, OCH_2CH$_3$), 3.09 (dd, *J* = 13.7, 6.0 Hz, 1H, CH_2), 3.02 (dd, *J* = 13.7, 5.3 Hz, 1H, CH_2), 2.36 (s, 6H, CH_3), 2.15 (s,

3H, CH_3), 1.03 (t, J = 7.0 Hz, 3H, OCH$_2$CH_3), 0.97 (t, J = 7.9 Hz, 9H, CH$_2$CH_3), 0.60 (q, J = 7.9 Hz, 6H, CH_2CH$_3$); **^{13}C{^{1}H} NMR** (101 MHz, C_6D_6) δ 137.3 (C_{Ar}), 135.5 (C_{Ar}), 131.8 (C_{Ar}), 129.3 (CH_{Ar}), 98.8 (*C*H), 62.3 (O*C*H$_2$CH$_3$), 38.1 (*C*H$_2$), 21.0 (*C*H$_3$), 20.8 (*C*H$_3$), 15.5 (OCH$_2$*C*H$_3$), 7.1 (CH$_2$*C*H$_3$), 5.6 (*C*H$_2$CH$_3$); **^{29}Si{^{1}H} NMR** (80 MHz, C_6D_6) δ 16.07; **HRMS** (ESI): m/z calcd for $C_{13}H_{19}O$ [M – OSiEt$_3$]$^+$ 191.1436, found 191.1437 (0.5 ppm): m/z calcd for $C_{11}H_{15}O$ [Aldehyde + H]$^+$ 163.1122, found 163.1124 (1.2 ppm); **LRMS** (DCI-NH$_3$, POS): m/z calcd for $C_{11}H_{18}NO$ [Aldehyde + NH$_4$]$^+$ 180.1, found 180.1.

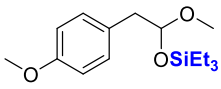

h11

The compound **h11** was prepared as described in the general procedure method **A** (129.0 mg) in 87% yield. **^{1}H NMR** (300 MHz, C_6D_6) *δ* 7.17 – 7.14 (m, 2H, CH_{Ar}), 6.83 – 6.79 (m, 2H, CH_{Ar}), 4.87 (dd, *J* = 5.7, 4.9 Hz, 1H, C*H*), 3.32 (s, 3H, OCH_3), 3.18 (s, 3H, OCH_3), 2.99 (dd, *J* = 13.7, 5.8 Hz, 1H, CH_2), 2.87 (dd, *J* = 13.7, 4.9 Hz, 1H, CH_2), 0.98 (t, *J* = 7.9 Hz, 9H, CH$_2$CH_3), 0.59 (q, *J* = 8.2 Hz, 6H, CH_2CH$_3$); **^{13}C{^{1}H} NMR** (75 MHz, C_6D_6) *δ* 159.0 (C_{Ar}), 131.1 (CH_{Ar}), 129.9 (C_{Ar}), 114.0 (CH_{Ar}), 100.4 (*C*H), 54.8 (O*C*H$_3$), 53.4 (O*C*H$_3$), 43.6 (*C*H$_2$), 7.1 (CH$_2$*C*H$_3$), 5.5 (*C*H$_2$CH$_3$); **^{29}Si{^{1}H} NMR** (80 MHz, C_6D_6) *δ* 16.54; **HRMS** (ESI): m/z calcd for $C_{15}H_{25}O_2Si$ [M – OMe]$^+$ 265.1624, found 265.1628 (1.5 ppm); **LRMS** (DCI-NH$_3$, POS): m/z calcd for $C_{16}H_{32}O_3SiN$ [M + NH$_4$]$^+$ 314.2, found 314.2.

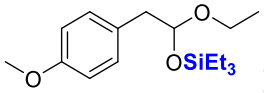

h12

The compound **h12** was prepared as described in the general procedure method **A** (150.4 mg) in 97% yield. **^{1}H NMR** (400 MHz, C_6D_6) δ 7.17 – 7.13 (m, 2H, CH_{Ar}), 6.81 – 6.77 (m, 2H, CH_{Ar}), 4.93 (dd, *J* = 5.8, 4.9 Hz, 1H, C*H*), 3.62 (dq, *J* = 8.9, 7.0 Hz, 1H, OCH_2CH$_3$), 3.32 (s, 3H, OCH_3), 3.26 (dq, *J* = 8.9, 7.0 Hz, 1H, OCH_2CH$_3$), 2.99 (dd, *J* = 13.6, 5.9 Hz, 1H, CH_2), 2.86 (dd, *J* = 13.6, 4.8 Hz, 1H, CH_2), 1.08 (t, *J* = 7.0 Hz, 3H, OCH$_2$CH_3), 0.98 (t, *J* = 7.9 Hz, 9H, CH$_2$CH_3), 0.59 (q, *J* = 7.8 Hz, 6H, CH_2CH$_3$); **^{13}C{^{1}H} NMR** (101 MHz, C_6D_6) δ 158.9 (C_{Ar}), 131.1 (CH_{Ar}), 130.0 (C_{Ar}), 114.0 (CH_{Ar}), 99.6 (*C*H), 61.9 (O*C*H$_2$CH$_3$), 54.8 (O*C*H$_3$), 44.0 (*C*H$_2$), 15.5 (OCH$_2$*C*H$_3$), 7.1 (CH$_2$*C*H$_3$), 5.6 (*C*H$_2$CH$_3$); **^{29}Si{^{1}H} NMR** (80 MHz, C_6D_6) δ 16.02; **HRMS** (ESI): m/z calcd for $C_9H_{11}O_2$ [Aldehyde + H]$^+$ 151.0759, found 151.0751(5.2 ppm); **LRMS** (DCI-NH$_3$): m/z calcd for $C_{17}H_{34}NO_3Si$ [M + NH$_4$]$^+$ 328.2, found 328.1.

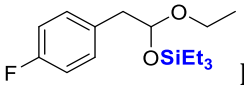

h13

The compound **h13** was prepared as described in the general procedure method **B** (145.4 mg) in 97% yield. **^{1}H NMR** (400 MHz, C_6D_6) δ 7.01 – 6.97 (m, 2H, CH_{Ar}), 6.84 – 6.78 (m, 2H, CH_{Ar}), 4.81 (dd, *J* = 5.8, 4.9 Hz, 1H, C*H*), 3.57 (dq, *J* = 9.0, 7.0 Hz, 1H, OCH_2CH$_3$), 3.21(dq, *J* = 9.0, 7.0 Hz, 1H, OCH_2CH$_3$), 2.85 (dd, *J* = 13.6, 5.7 Hz, 1H, CH_2), 2.74 (dd, *J* = 13.6, 4.8 Hz, 1H, CH_2), 1.04 (t, *J* = 7.0 Hz, 3H, OCH$_2$CH_3), 0.95 (t, J = 8.0 Hz, 9H, CH$_2$CH_3), 0.55 (q, J = 8.0 Hz, 6H, CH_2CH$_3$); **^{13}C{^{1}H} NMR** (101 MHz, C_6D_6) δ 162.2 (d, *J* = 243.7 Hz, C_{Ar}), 133.6 (d, *J* = 3.2 Hz, C_{Ar}), 131.7 (d, *J* = 7.7 Hz, *C*H$_{Ar}$), 115.1 (d, *J* = 21.0 Hz, *C*H$_{Ar}$), 99.0 (d, *J* = 1.1 Hz, *C*H), 61.9 (s, O*C*H$_2$CH$_3$), 43.9 (s, *C*H$_2$), 15.4 (s, OCH$_2$*C*H$_3$), 7.1 (s, CH$_2$*C*H$_3$), 5.5 (s, *C*H$_2$CH$_3$); **^{29}Si{^{1}H} NMR** (80 MHz, C_6D_6) δ 16.29; **^{19}F NMR** (377 MHz, C_6D_6) δ -117.03; **HRMS** (DCI-CH_4): m/z calcd for $C_{16}H_{26}FO_2Si$ $[M - H]^+$ 297.1686, found 297.1691 (1.7 ppm); **LRMS** (DCI-NH_3): m/z calcd for $C_{16}H_{31}FNO_2Si$ $[M + NH_4]^+$ 316.2, found 316.1.

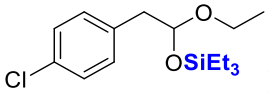

h14

The compound **h14** was prepared as described in the general procedure. However, the acetal **h14** decomposed into the corresponding aldehyde **j14** during its purification on silica gel. ^{1}H NMR of crude mixture was used for the description of **h14**. **^{1}H NMR** (300 MHz, C_6D_6) δ 7.14 – 7.11 (m, 2H, CH_{Ar}), 6.96 – 6.92 (m, 2H, CH_{Ar}), 4.81 (dd, *J* = 5.8, 4.8 Hz, 1H, C*H*), 3.56 (dq, *J* = 9.0, 7.0 Hz, 1H, OCH_2CH$_3$), 3.19 (dq, *J* = 9.0, 7.0 Hz, 1H, OCH_2CH$_3$), 2.83 (dd, *J* = 13.5, 5.8 Hz, 1H, CH_2), 2.71 (dd, *J* = 13.5, 4.8 Hz, 1H, CH_2), 1.04 (t, *J* = 7.0 Hz, 3H, OCH$_2$CH_3), 0.95 (t, *J* = 8.0 Hz, 9H, CH$_2$CH_3), 0.56 (q, *J* =8.0 Hz, 6H, CH_2CH$_3$); **HRMS** (ESI): m/z calcd for $C_{10}H_{12}ClO$ $[M - OSiEt_3]^+$ 183.0577, found 183.0576 (0.5 ppm).m/z calcd for C_8H_8ClO [Aldehyde + H]$^+$ 155.0264, found 155.0265 (0.6 ppm); **LRMS** (DCI-NH_3): m/z calcd for $C_{16}H_{31}ClNO_2Si$ $[M + NH_4]^+$ 332.2, found 332.1.

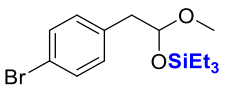

h15

The compound **h15** was prepared as described in the general procedure method **A** (101.9 mg) in 59% yield. **^{1}H NMR** (300 MHz, $CDCl_3$) *δ* 7.42 – 7.37 (m, 2H, CH_{Ar}), 7.12 – 7.08 (m, 2H, CH_{Ar}), 4.81 (dd, *J* = 5.9, 4.6 Hz, 1H, C*H*), 3.31 (s, 3H, OCH_3), 2.88 (dd, *J* = 13.7, 5.9 Hz, 1H, CH_2), 2.78 (dd, *J* = 13.7, 4.6 Hz, 1H, CH_2), 0.94 (t, *J* = 7.9 Hz, 9H, CH$_2$CH_3), 0.59 (q, *J* = 8.5,

8.0 Hz, 6H, CH_2CH$_3$). **^{13}C{^{1}H} NMR** (75 MHz, $CDCl_3$) δ 136.3 (C_{Ar}), 131.6 (CH_{Ar}), 131.3 (CH_{Ar}), 120.4 (C_{Ar}), 99.4 (*C*H), 54.0 (O*C*H$_3$), 43.5 (*C*H$_2$), 6.9 (CH$_2$*C*H$_3$), 5.1 (*C*H$_2$CH$_3$); **^{29}Si{^{1}H} NMR** (80 MHz, C_6D_6) δ 16.96; **HRMS** (ESI): m/z calcd for $C_9H_{10}BrO$ [M – OSiEt$_3$]$^+$ 212.9915, found 212.9915 (0 ppm); **LRMS** (DCI-NH$_3$): m/z calcd for $C_{15}H_{29}BrO_2SiN$ [M + NH$_4$]$^+$ 362.1, found 362.1.

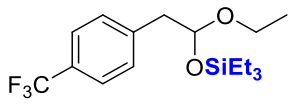

h16

The compound **h16** was prepared as described in the general procedure method **B** (131 mg) in 75% yield. **^{1}H NMR** (400 MHz, C_6D_6) δ 7.36 (d, *J* = 8.0 Hz, 2H, C*H*$_{Ar}$), 7.05 (d, *J* = 8.0 Hz, 2H, C*H*$_{Ar}$), 4.81 (dd, *J* = 5.8, 4.7 Hz, 1H, C*H*), 3.55 (dq, *J* = 9.0, 7.0 Hz, 1H, OC*H*$_2$CH$_3$), 3.18 (dq, *J* = 9.0, 7.0 Hz, 1H, OC*H*$_2$CH$_3$), 2.85 (dd, *J* = 13.5, 5.7 Hz, 1H, C*H*$_2$), 2.75 (dd, *J* = 13.5, 4.7 Hz, 1H, C*H*$_2$), 1.03 (t, *J* = 7.0 Hz, 3H, OCH$_2$C*H*$_3$), 0.94 (t, *J* = 8.0 Hz, 9H, CH$_2$C*H*$_3$)), 0.54 (q, *J* = 8.0 Hz, 6H, C*H*$_2$CH$_3$); **^{13}C{^{1}H} NMR** (101 MHz, $CDCl_3$) δ 141.6 (s, C_{Ar}), 130.3 (s, CH_{Ar}), 128.8 (q, *J* = 32.3 Hz, C_{Ar}), 125.1 (q, *J* = 3.8 Hz, CH_{Ar}), 124.5 (q, *J* = 271.8 Hz, *C*F$_3$), 98.3 (s, *C*H), 62.3 (s, O*C*H$_2$CH$_3$), 44.3 (s, *C*H$_2$), 15.2 (s, OCH$_2$*C*H$_3$), 6.8 (s, CH$_2$*C*H$_3$), 5.1 (s, *C*H$_2$CH$_3$); **^{29}Si{^{1}H} NMR** (80 MHz, C_6D_6) δ 18.04; **^{19}F NMR** (377 MHz, C_6D_6) δ -62.05; **HRMS** (ESI): m/z calcd for $C_9H_8F_3O$ [Aldehyde + H]$^+$ 189.0522, found 189.0520 (1.0 ppm).

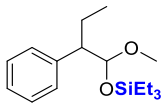

h17

The compound **h17** was prepared as described in the general procedure method **A** (100.1 mg) in 68% yield. The product is present a mixture of two diastereoisomers with a ratio 1 : 0.3 (M = major, m= minor). **^{1}H NMR** (400 MHz, C_6D_6) δ 7.28 – 7.06 (m, 5H, M+m, C*H*$_{Ar}$), 4.81 (d, *J* = 5.6 Hz, 1H, M, C*H*OCH$_3$), 4.77 (d, *J* = 5.1 Hz, m, C*H*OCH$_3$) 3.17 (s, 3H, m, OC*H*$_3$), 3.04 (s, 3H, M, OC*H*$_3$), 2.82 – 2.69 (m, 1H, M+m, C*H*), 2.22 – 2.01 (m, 1H, M+m, C*H*$_2$), 1.85 – 1.65 (m, 1H, M+m, C*H*$_2$), 1.00 (t, *J* = 7.9 Hz, 9H, M, CH$_2$C*H*$_3$), 0.93 (t, *J* = 7.9 Hz, 9H, m, CH$_2$C*H*$_3$), 0.83 (t, *J* = 7.4 Hz, 3H, m, C*H*$_3$), 0.82 (t, *J* = 7.4 Hz, 3H, M, C*H*$_3$), 0.63 (q, *J* = 8.0 Hz, 6H, M, C*H*$_2$CH$_3$), 0.54 (q, *J* = 8.1 Hz, 6H, m, C*H*$_2$CH$_3$); **^{13}C{^{1}H} NMR** (101 MHz, C_6D_6) δ 142.0 (m, C_{Ar}), 141.6 (M, C_{Ar}), 129.54 (m, CH_{Ar}), 129.51 (M, CH_{Ar}), 128.43 (m, CH_{Ar}), 128.35 (M, CH_{Ar}), 126.73 (m, CH_{Ar}), 126.62 (M, CH_{Ar}), 102.6 (M, *C*HOCH$_3$), 101.3 (m, *C*HOCH$_3$), 55.1 (m, C*H*), 54.3 (M,C*H*), 53.8 (M, OCH$_3$), 53.4 (m, OCH$_3$), 23.9 (M, C*H*$_2$), 23.0 (m, C*H*$_2$), 12.5 (m, *C*H$_3$), 12.3 (M, *C*H$_3$), 7.15 (M, CH$_2$*C*H$_3$), 7.07 (m, CH$_2$*C*H$_3$), 5.6 (M,

CH_2CH_3), 5.3 (m, CH_2CH_3); **^{29}Si{^{1}H} NMR** (80 MHz, C_6D_6) δ 16.77, 15.97; **HRMS** (ESI): m/z calcd for $C_{16}H_{27}OSi$ [M – OMe]$^+$ 263.1831, found 263.1829 (0.8 ppm); **LRMS** (DCI-NH_3): m/z calcd for $C_{17}H_{34}NO_2Si$ [M + NH_4]$^+$ 312.2, found 312.2.

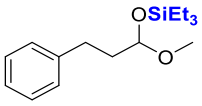

h18

The compound **h18** was prepared as described in the general procedure method **B** (102.4 mg) in 73% yield. **^{1}H NMR** (300 MHz, C_6D_6) δ 7.21 – 7.18 (m, 4H, CH_{Ar}), 7.11 – 7.05 (m, 1H, CH_{Ar}), 4.72 (dd, J = 5.8, 4.4 Hz, 1H, CH), 3.22 (s, 3H, OCH_3), 2.78 (m, 2H, CH_2), 2.10 – 1.89 (m, 2H, CH_2), 1.02 (t, J = 7.9 Hz, 9H, CH_2CH_3), 0.64 (q, J = 8.2 Hz, 6H, CH_2CH_3); **^{13}C{^{1}H} NMR** (101 MHz, C_6D_6) δ 142.0 (C_{Ar}), 128.4 (CH_{Ar}), 128.3 (CH_{Ar}), 125.7 (CH_{Ar}), 98.3 (CH), 52.9 (OCH_3), 38.9 (CH_2), 30.8 (CH_2), 6.7 (CH_2CH_3), 5.2 (CH_2CH_3); **^{29}Si{^{1}H} NMR** (80 MHz, C_6D_6) δ 16.15; **HRMS** (ESI): m/z calcd for $C_{15}H_{25}OSi$ [M – OMe]$^+$ 249.1675, found 249.1670 (2 ppm); **LRMS** (DCI-NH_3): m/z calcd for $C_{16}H_{32}NO_2Si$ [M + NH_4]$^+$ 298.2, found 298.2.

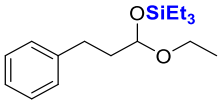

h19

The compound **h19** was prepared as described in the general procedure method **A** (135.5 mg) in 92% yield. [11] **^{1}H NMR** (300 MHz, C_6D_6) δ 7.21 – 7.18 (m, 4H, CH_{Ar}), 7.12 – 7.05 (m, 1H, CH_{Ar}), 4.81 (dd, J = 5.9, 4.3 Hz, 1H, CH), 3.72 – 3.62 (m, 1H, OCH_2CH$_3$), 3.36 – 3.22 (m, 1H, OCH_2CH$_3$), 2.83 – 2.77 (m, 2H, CH_2), 2.12 – 1.91 (m, 2H, CH_2), 1.16 (t, J = 7.0 Hz, 3H, OCH$_2$CH_3), 1.03 (t, J = 7.9 Hz, 9H, CH_2CH_3), 0.64 (q, J = 8.2 Hz, 6H, CH_2CH_3); **^{13}C{^{1}H} NMR** (75 MHz, C_6D_6) δ 142.5 (C_{Ar}), 128.8 (CH_{Ar}), 128.7 (CH_{Ar}), 126.1 (CH_{Ar}), 97.7 (CH), 61.8 (OCH_2CH$_3$), 39.8 (CH_2), 31.2 (CH_2), 15.6 (OCH$_2$CH_3), 7.2 (CH_2CH_3), 5.7 (CH_2CH_3); **^{29}Si{^{1}H} NMR** (80 MHz, C_6D_6) δ 15.66.

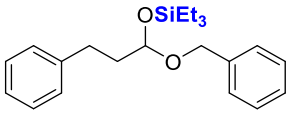

h20

The compound **h20** was prepared as described in the general procedure method **B** (165.8 mg) in 93% yield. **^{1}H NMR** (300 MHz, $CDCl_3$) δ 7.40 – 7.36 (m, 4H, CH_{Ar}), 7.35 – 7.26 (m, 3H, CH_{Ar}), 7.23 – 7.16 (m, 3H, CH_{Ar}), 4.93 (dd, J = 6.3, 4.0 Hz, 1H, CH), 4.77 (d, J = 11.8 Hz, 1H, OCH_2Ph), 4.49 (d, J = 11.8 Hz, 1H, OCH_2Ph), 2.86 – 2.65 (m, 2H, CH_2), 2.12 – 1.83 (m, 2H,

CH_2), 1.00 (t, J = 7.9 Hz, 9H, CH_2CH_3), 0.67 (q, J = 7.8 Hz, 6H, CH_2CH_3); **^{13}C{^{1}H} NMR** (75 MHz, $CDCl_3$) δ 142.1 (C_{Ar}), 138.6 (C_{Ar}), 128.5 (CH_{Ar}), 128.49 (CH_{Ar}), 128.47 (CH_{Ar}), 127.8 (CH_{Ar}), 127.6 (CH_{Ar}), 125.9 (CH_{Ar}), 97.1 (*C*H), 68.3 (O*C*H_2Ph), 39.5 (*C*H_2), 30.9 (*C*H_2), 7.0 (CH_2CH_3), 5.3 (CH_2CH_3); **^{29}Si{^{1}H} NMR** (80 MHz, C_6D_6) δ 17.1; **HRMS** (DCI-CH_4): m/z calcd for $C_{22}H_{31}O_2Si$ $[M - H]^+$ 355.2093, found 355.2103 (2.8 ppm).; m/z calcd for $C_{20}H_{27}O_2Si$ $[MH - C_2H_6]^+$ 327.1780, found 327.1788 (2.4 ppm).

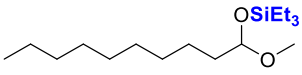

h21

The compound **h21** was prepared as described in the general procedure method **B** (140.7 mg) in 93% yield. **^{1}H NMR** (400 MHz, C_6D_6) δ 4.76 (dd, J = 5.8, 4.6 Hz, 1H, C*H*), 3.23 (s, 3H, OCH_3), 1.83 – 1.64 (m, 2H, CH_2), 1.54-1.47 (m, 2H, CH_2); 1.31 – 1.26 (m, 12H, CH_2), 1.04 (t, J = 7.9 Hz, 9H, CH_2CH_3), 0.90 (t, J = 6.8 Hz, 3H, CH_3), 0.67 (q, J = 7.9 Hz, 6H, CH_2CH_3); **^{13}C{^{1}H} NMR** (101 MHz, C_6D_6) δ 99.5 (*C*H), 53.1 (O*C*H_3), 37.6 (*C*H_2), 32.3 (*C*H_2), 30.2 (*C*H_2), 30.1 (*C*H_2), 30.0 (*C*H_2), 29.8 (*C*H_2), 25.0 (*C*H_2), 23.1 (*C*H_2), 14.4 (*C*H_3), 7.2 (CH_2CH_3), 5.7 (CH_2CH_3); **^{29}Si{^{1}H} NMR** (80 MHz, C_6D_6) δ 15.7; **HRMS** (ESI): m/z calcd for $C_{16}H_{35}OSi$ $[M - OMe]^+$ 271.2457, found 271.2469 (4.4 ppm); **LRMS** (DCI-NH_3): m/z calcd for $C_{17}H_{42}NO_2Si$ $[M + NH_4]^+$ 320.3, found 320.3.

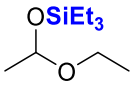

h22

The compound **h22** was prepared as described in the general procedure method **A** (91.0 mg) in 89% yield.[12] **^{1}H NMR** (400 MHz, C_6D_6) δ 4.91 (q, J = 5.1 Hz, 1H, C*H*), 3.71 – 3.64 (m, 1H, OCH_2CH$_3$), 3.32 – 3.24 (m, 1H, OCH_2CH$_3$), 1.33 (d, J = 4.8 Hz, 3H, CH_3), 1.14 (t, J = 7.0 Hz, 3H, OCH$_2$CH_3), 1.01 (t, J = 7.9 Hz, 9H, CH_2CH_3), 0.62 (q, J = 9.6, 8.7 Hz, 6H, CH_2CH_3); **^{13}C{^{1}H} NMR** (101 MHz, C_6D_6) δ 95.2 (*C*H), 61.6 (O*C*H_2CH$_3$), 24.4 (*C*H_3), 15.6 (OCH$_2$*C*H_3), 7.1 (CH_2CH_3), 5.6 (CH_2CH_3); **^{29}Si{^{1}H} NMR** (80 MHz, C_6D_6) δ 15.0.

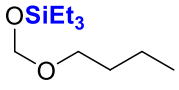

h23

The compound **h23** was prepared as described in the general procedure method **B** (99.4 mg) in 91% yield. **^{1}H NMR** (300 MHz, $CDCl_3$) δ 4.85 (s, 2H, OCH_2O), 3.55 (t, J = 6.6 Hz, 2H, OCH_2), 1.61 – 1.52 (m, 2H, CH_2), 1.44 – 1.32 (m, 2H, CH_2), 1.00-0.90 (m, 9H + 3H, CH_2CH_3 + CH_3), 0.64 (q, J = 8.3 Hz, 6H, CH_2CH_3); **^{13}C{^{1}H} NMR** (75 MHz, $CDCl_3$) δ 90.0 (O*C*H_2O), 67.9

(OCH_2), 32.0 (CH_2), 19.5 (CH_2), 14.1 (CH_3), 6.8 (CH_2CH_3), 4.8 (CH_2CH_3); **^{29}Si{^{1}H} NMR** (80 MHz, $CDCl_3$) δ 19.9; **LRMS** (DCI-NH_3): m/z calcd for $C_{11}H_{30}NO_2Si$ $[M + NH_4]^+$ 236.2, found 236,2.

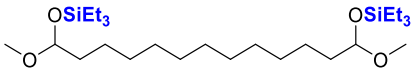

h24

The compound **h24** was prepared as described in the general procedure method **B** (231.9 mg) in 92% yield. **^{1}H NMR** (400 MHz, C_6D_6) δ 4.77 (dd, J = 5.8, 4.5 Hz, 2H, C*H*), 3.23 (s, 6H, OCH_3), 1.84 – 1.64 (m, 4H, CH_2), 1.55 – 1.48 (m, 4H, CH_2), 1.34 – 1.28 (m, 14H, CH_2), 1.04 (t, J = 7.9 Hz, 18H, CH_2CH_3), 0.67 (q, J = 7.9 Hz, 12H, CH_2CH_3); **^{13}C{^{1}H} NMR** (101 MHz, C_6D_6) δ 99.5 (*C*H), 53.1 (O*C*H_3), 37.6 (*C*H_2), 30.17 (*C*H_2), 30.08 (*C*H_2), 30.06 (*C*H_2), 25.0 (*C*H_2), 7.2 (CH_2CH_3), 5.7 (CH_2CH_3); **^{29}Si{^{1}H} NMR** (80 MHz, C_6D_6) δ 15.75; **LRMS** (DCI-NH_3): m/z calcd for $C_{26}H_{58}O_3Si_2$ $[M - OMe + H]^+$ 474.4, found 474.3.

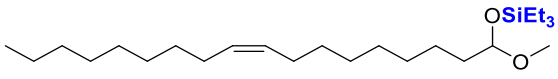

h25

The compound **h25** was prepared as described in the general procedure method **B** (152.7 mg) in 74% yield. **^{1}H NMR** (400 MHz, C_6D_6) δ 5.53 – 5.43 (m, 2H, C*H*=C*H*), 4.75 (dd, J = 5.7, 4.6 Hz, 1H, C*H*), 3.23 (s, 3H, OCH_3), 2.1 – 2.05 (m, 4H, CH_2), 1.80 – 1.62 (m, 2H, CH_2), 1.53 – 1.28 (m, 22H, CH_2), 1.04 (t, J = 7.9 Hz, 9H, CH_2CH_3), 0.91 (t, J = 6.8 Hz, 3H, CH_3), 0.66 (q, J = 7.9 Hz, 6H, CH_2CH_3); **^{13}C{^{1}H} NMR** (126 MHz, C_6D_6) δ 130.2 (*C*H=*C*H), 99.5 (*C*H), 53.1 (O*C*H_3), 37.6 (*C*H_2), 32.3 (*C*H_2), 32.33 (*C*H_2), 30.26 (*C*H_2), 30.23 (*C*H_2), 30.04 (*C*H_2), 30.02 (*C*H_2), 30.00 (*C*H_2), 29.8 (*C*H_2), 29.7 (*C*H_2), 27.7 (*C*H_2), 25.0 (*C*H_2), 23.1 (*C*H_2), 14.4 (*C*H_3), 7.2 (CH_2CH_3), 5.7 (CH_2CH_3); **^{29}Si{^{1}H} NMR** (79 MHz, C_6D_6) δ 15.70; **LRMS** (DCI-NH_3): m/z calcd for $C_{25}H_{56}O_2SiN$ $[M + NH_4]^+$ 430.4, found 430.3.

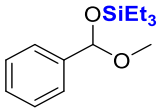

h26

The compound **h26** was prepared as described in the general procedure method **A** (135.5 mg) in 86% yield. [13] **^{1}H NMR** (400 MHz, C_6D_6) δ 7.57 – 7.55 (m, 2H, CH_{Ar}), 7.22 – 7.17 (m, 2H, CH_{Ar}), 7.13 – 7.09 (m, 1H, CH_{Ar}), 5.81 (s, 1H, C*H*), 3.15 (s, 3H, OCH_3), 0.98 (t, J = 7.9 Hz, 9H, CH_2CH_3), 0.63 (q, J = 8.0 Hz, 6H, CH_2CH_3); **^{13}C{^{1}H} NMR** (101 MHz, C_6D_6) δ 141.7 (*C*$_{Ar}$), 128.5 (*C*H$_{Ar}$), 128.4 (*C*H$_{Ar}$), 126.9 (*C*H$_{Ar}$), 98.0 (*C*H), 51.6 (O*C*H_3), 7.0 (CH_2CH_3), 5.4

(CH_2CH_3); **^{29}Si{^{1}H} NMR** (80 MHz, C_6D_6) δ 18.57; **LRMS** (DCI-NH_3): m/z calcd for $C_{13}H_{21}OSi$ $[M - OMe]^+$ 221.1, found 221.1.

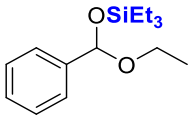

h27

The compound **h27** was prepared as described in the general procedure. However, the acetal **h27** decomposed into the corresponding aldehyde **j27** during its purification on silica gel. NMR of crude mixture was used for the description of **h27**. **^{1}H NMR** (300 MHz, C_6D_6) δ 7.59 – 7.56 (m, 2H, CH_{Ar}), 7.23 – 7.17 (m, 2H, CH_{Ar}), 7.14 – 7.10 (m, 1H, CH_{Ar}), 5.85 (s, 1H, C*H*), 3.52 (dq, *J* = 9.2, 7.1 Hz, 1H, OCH_2CH$_3$), 3.42 (dq, *J* = 9.2, 7.0 Hz, 1H, OCH_2CH$_3$), 1.11 (t, *J* = 7.0 Hz, 3H, OCH$_2$CH_3), 0.99 (t, *J* = 7.9 Hz, 9H, CH$_2$CH_3), 0.64 (q, *J* = 7.9 Hz, 6H, CH_2CH$_3$); **^{13}C{^{1}H} NMR** (101 MHz, C_6D_6) δ 142.3 (*C*$_{Ar}$), 128.4 (*C*H$_{Ar}$), 128.3 (*C*H$_{Ar}$), 126.8 (*C*H$_{Ar}$), 97.5 (*C*H), 60.3 (O*C*H$_2$CH$_3$), 15.5 (OCH$_2$*C*H$_3$), 7.1 (CH$_2$*C*H$_3$), 5.4 (*C*H$_2$CH$_3$).

h28

The compound **h28** was prepared as described in the general procedure method **A** (133.5 mg) in 90% yield. **^{1}H NMR** (400 MHz, C_6D_6) δ 7.48 (d, *J* = 8.6 Hz, 2H, CH_{Ar}), 6.80 (d, *J* = 8.7 Hz, 2H, CH_{Ar}), 5.84 (s, 1H, C*H*), 3.55 (dq, *J* = 9.0, 7.1 Hz, 1H, OCH_2CH$_3$), 3.43 (dq, *J* = 9.1, 7.0 Hz, 1H, OCH_2CH$_3$), 3.32 (s, 3H, OCH_3), 1.13 (t, *J* = 7.1 Hz, 3H, OCH$_2$CH_3), 1.00 (t, *J* = 7.9 Hz, 9H, CH$_2$CH_3), 0.65 (q, *J* = 7.9 Hz, 6H, CH_2CH$_3$); **^{13}C{^{1}H} NMR** (101 MHz, C_6D_6) δ 160.2 (*C*$_{Ar}$), 134.6 (*C*$_{Ar}$), 128.0 (*C*H$_{Ar}$), 113.8 (*C*H$_{Ar}$), 97.4 (*C*H), 60.3 (O*C*H$_3$), 54.8 (O*C*H$_2$CH$_3$), 15.5 (OCH$_2$*C*H$_3$), 7.1 (CH$_2$*C*H$_3$), 5.5 (*C*H$_2$CH$_3$); **^{29}Si{^{1}H} NMR** (80 MHz, C_6D_6) δ 17.65; **HRMS** (ESI): m/z calcd for $C_{14}H_{23}O_2Si$ $[M - OEt]^+$ 251.1467, found 251.1477 (4 ppm); LRMS (DCI-NH_3): m/z calcd for $C_{14}H_{23}O_2Si$ $[M - OEt]^+$251.1, found 251.1.

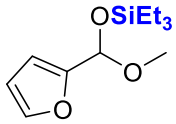

h30

The compound **h30** was prepared as described in the general procedure method **A** (94.5 mg) in 40% yield. **^{1}H NMR** (300 MHz, $CDCl_3$) δ 7.38 (s, 1H, CH_{Ar}), 6.38 (d, *J* = 3.3 Hz, 1H, CH_{Ar}), 6.36 – 6.31 (m, 1H, CH_{Ar}), 5.75 (s, 1H, C*H*), 3.32 (s, 3H, OCH_3), 0.96 (t, *J* = 7.9 Hz, 9H, CH$_2$CH_3), 0.65 (q, *J* = 7.8 Hz, 6H, CH_2CH$_3$); **^{13}C{^{1}H} NMR** (101 MHz, $CDCl_3$) δ 142.3 (*C*H$_{Ar}$),

110.1 (CH_{Ar}), 107.5 (CH_{Ar}), 92.4 (*C*H), 52.6 (OCH_3), 6.8 (CH_2CH_3), 4.9 (CH_2CH_3) (The signal of the quaternary carbon was not observed); **HRMS** (DCI-CH_4): m/z calcd for $C_{11}H_{19}O_2S$ [M – OMe]$^+$ 211.1154, found 211.1155 (0.5 ppm); **LRMS** (DCI-NH_3): m/z calcd for $C_{11}H_{19}O_2S$ ([M – OMe]$^+$) 211.1, found 211.1.

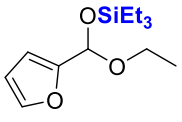

h31

The compound **h31** was prepared as described in the general procedure method **A** (94.5 mg) in 96% yield. **^{1}H NMR** (400 MHz, C_6D_6) δ 7.09 (s, 1H, C*H*$_{Ar}$), 6.38 (d, *J* = 3.0 Hz, 1H, C*H*$_{Ar}$), 6.09 – 6.08 (m, 1H, C*H*$_{Ar}$), 5.90 (s, 1H, C*H*), 3.60 – 3.48 (m, 2H, OCH_2CH_3), 1.11 (t, *J* = 7.0 Hz, 3H, OCH_2CH_3), 1.00 (t, *J* = 7.9 Hz, 9H, CH_2CH_3), 0.65 (q, *J* = 7.9 Hz, 6H, CH_2CH_3); **^{13}C{^{1}H} NMR**(101 MHz, C_6D_6) δ 155.0 (C_{Ar}), 142.0 (CH_{Ar}), 110.3 (CH_{Ar}), 107.5 (CH_{Ar}), 92.1 (*C*H), 60.6 (OCH_2CH_3), 15.4 (OCH_2CH_3), 7.0 (CH_2CH_3), 5.3 (CH_2CH_3); **^{29}Si{^{1}H} NMR** (79 MHz, C_6D_6) δ 19.10; **LRMS** (DCI-NH_3): m/z calcd for $C_{11}H_{19}O_2Si$ [M – OEt]$^+$ 211.1, found 211.1.

7.3.6 *Characterization data for the aldehyde products*

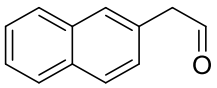

j1

The compound **j1** was prepared as described in the general procedure method **A** (79 mg) in 93% yield.[14] **^{1}H NMR** (400 MHz, $CDCl_3$) δ 9.83 (t, *J* = 2.4 Hz, 1H, C*H*=O), 7.87 – 7.81 (m, 3H, C*H*$_{Ar}$), 7.70 (br s, 1H, C*H*$_{Ar}$), 7.51 – 7.48 (m, 2H, C*H*$_{Ar}$), 7.33 (dd, *J* = 8.4, 1.8 Hz, 1H, C*H*$_{Ar}$), 3.86 (d, *J* = 2.4 Hz, 2H, C*H*$_2$); **^{13}C{^{1}H} NMR** (101 MHz, $CDCl_3$) δ 199.5 (*C*H=O), 133.8 (C_{Ar}), 132.7 (C_{Ar}), 129.4 (C_{Ar}), 128.9 (CH_{Ar}), 128.7 (CH_{Ar}), 127.9 (CH_{Ar}), 127.7 (CH_{Ar}), 127.6 (CH_{Ar}), 126.6 (CH_{Ar}), 126.2 (CH_{Ar}), 50.9 (CH_2).

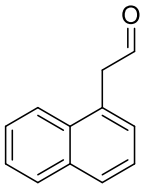

j4

The reduction of ethyl 1-naphthaleneacetate **g4** (1,0 g, 4,67 mmol) was performed according to general procedure ($Re_2(CO)_{10}$, 15 mg, 0.5 mol%, Et_3SiH, 0.8 mL, 5.1 mmol, toluene 4 mL, hν 365 nm, 18 h). The reaction mixture was filtered through celite and evaporated. After

hydrolysis of the crude mixture(1N HCl, 10 mL, THF 10 mL, 4 h) and extraction with Et_2O (3*20 mL), 1-naphthaleneacetaldehyde **j4** was isolated by bulb to bulb distillation (599 mg, 75% yield).[15] **^{1}H NMR** (400 MHz, $CDCl_3$) δ 9.64 (t, *J* = 2.4 Hz, 1H, C*H*=O), 7.78 – 7.74 (m, 2H, CH_{Ar}), 7.71 (d, *J* = 8.2 Hz, 1H, CH_{Ar}), 7.44 – 7.39 (m, 2H, CH_{Ar}), 7.36 – 7.32 (m, 1H, CH_{Ar}), 7.27 (d, *J* = 6.9 Hz, 1H, CH_{Ar}), 3.96 (d, *J* = 2.4 Hz, 2H, CH_2); **^{13}C{^{1}H} NMR** (101 MHz, $CDCl_3$) δ 199.7 (*C*H=O), 134.0 (C_{Ar}), 132.4 (C_{Ar}), 129.0 (*C*H_{Ar}), 128.6 (*C*H_{Ar}), 128.50 (*C*H_{Ar}), 128.47 (C_{Ar}), 126.8 (*C*H_{Ar}), 126.2 (*C*H_{Ar}), 125.7 (*C*H_{Ar}), 123.6 (*C*H_{Ar}), 48.4 (*C*H_2).

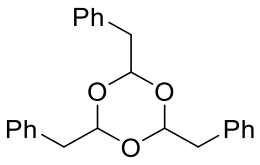

j5'

The compound **j5'** was prepared as described in the general procedure method **B** (1 mmol scale, 90 mg) in 75% yield.[16] **^{1}H NMR** (400 MHz, $CDCl_3$) δ 7.26 – 7.22 (m, 15H, CH_{Ar}), 4.95 (t, *J* = 5.4 Hz, 3H, C*H*), 3.02 (d, *J* = 5.4 Hz, 6H, CH_2); **^{13}C{^{1}H} NMR** (101 MHz, $CDCl_3$) δ 135.7 (C_{Ar}), 130.1 (*C*H_{Ar}), 128.3 (*C*H_{Ar}), 126.7 (*C*H_{Ar}), 101.9 (*C*H), 41.2 (*C*H_2).

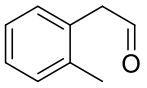

j9

The compound **j9** was prepared as described in the general procedure method **B** (1 mmol scale, 94.5 mg) in 70% yield.[17] **^{1}H NMR** (400 MHz, $CDCl_3$) δ 9.63 (t, *J* = 2.2 Hz, 1H, C*H*=O), 7.18 – 7.07 (m, 4H, CH_{Ar}), 3.63 (d, *J* = 2.2 Hz, 2H, CH_2), 2.20 (s, 3H, CH_3); **^{13}C{^{1}H} NMR** (101 MHz, $CDCl_3$) δ 199.4 (*C*H=O), 137.3 (C_{Ar}), 130.8 (*C*H_{Ar}), 130.7 (C_{Ar}), 130.6 (*C*H_{Ar}), 127.9 (*C*H_{Ar}), 126.6 (*C*H_{Ar}), 48.9 (*C*H_2), 19.8 (*C*H_3).

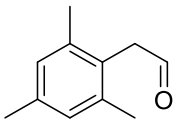

j10

The compound **j10** was prepared as described in the general procedure method **B** (75 mg) in 93% yield.[18] **^{1}H NMR** (400 MHz, $CDCl_3$) δ 9.57 (t, *J* = 2.1 Hz, 1H, C*H*=O), 6.83 (s, 2H, CH_{Ar}), 3.64 (d, *J* = 2.1 Hz, 2H, CH_2), 2.20 (s, 3H, CH_3), 2.17 (s, 6H, CH_3); **^{13}C{^{1}H} NMR** (101 MHz, $CDCl_3$) δ 199.2 (*C*H=O), 137.3 (C_{Ar}), 137.1 (C_{Ar}), 129.3 (*C*H_{Ar}), 126.3 (C_{Ar}), 44.9 (*C*H_2), 21.0 (*C*H_3), 20.5(*C*H_3).

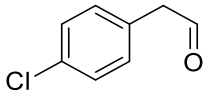

j14

The compound **j14** was prepared as described in the general procedure method **B** (1 mmol scale, 118 mg) in 76% yield.[14] **^{1}H NMR** (400 MHz, $CDCl_3$) δ 9.67 (t, *J* = 2.1 Hz, 1H, C*H*=O), 7.27 (d, *J* = 8.3 Hz, 2H, CH_{Ar}), 7.08 (d, *J* = 8.3 Hz, 2H, CH_{Ar}), 3.61 (d, *J* = 2.1 Hz, 2H, CH_2); **^{13}C{^{1}H} NMR** (101 MHz, $CDCl_3$) δ 198.8 (*C*H=O), 131.1 (*C*H_{Ar}), 130.4 (*C*$_{Ar}$), 129.3 (*C*H_{Ar}), 128.5 (*C*$_{Ar}$), 49.9 (*C*H_2).

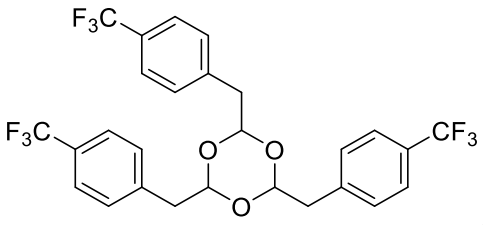

j16'

The compound **j16'** was prepared as described in the general procedure method **B** (1 mmol scale, 115 mg) in 61% yield. **^{1}H NMR** (400 MHz, $CDCl_3$) δ 7.42 (d, *J* = 8.0 Hz, 6H, CH_{Ar}), 7.20 (d, *J* = 8.6 Hz, 6H, CH_{Ar}), 4.89 (t, *J* = 5.2 Hz, 3H, C*H*), 2.96 (d, *J* = 5.2 Hz, 6H, CH_2); **^{13}C{^{1}H} NMR** (101 MHz, $CDCl_3$) δ 139.3 (s, *C*$_{Ar}$), 130.4 (s, *C*H_{Ar}), 129.3 (q, *J* = 32.5 Hz, *C*$_{Ar}$), 125.2 (q, *J* = 3.9 Hz, *C*H_{Ar}), 124.32 (q, *J* = 271.9 Hz, *C*F_3), 101.0 (s, *C*H), 40.7 (s, *C*H_2); **^{19}F NMR** (377 MHz, $CDCl_3$) δ -62.58; **HRMS** (DCI-CH_4): m/z calcd for $C_{27}H_{20}F_9O_3$ $[M - H]^+$ 563.1269, found 563.1289 (3.5 ppm); m/z calcd for $C_{27}H_{21}F_8O_3$ $[M - F]^+$ 545.1363, found 545.1366 (0.6 ppm); **LRMS** (DCI-NH_3, POS): m/z calcd for $C_{27}H_{25}F_9NO_3$ $[M + NH_4]^+$ 582.1, found 582.1.

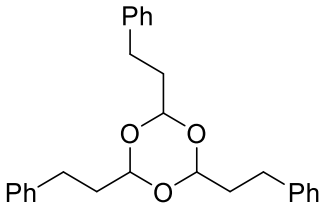

j19'

The compound **j19'** was prepared as described in the general procedure method **A** (1 mmol scale, 114.5 mg) in 85% yield.[19] **^{1}H NMR** (400 MHz, $CDCl_3$) δ 7.23 – 7.19 (m, 6H, CH_{Ar}), 7.13 – 7.10 (m, 9H, CH_{Ar}), 4.74 (t, *J* = 5.3 Hz, 3H, C*H*), 2.71-2.67 (m, 6H, CH_2), 1.98 – 1.93 (m, 6H, CH_2); **^{13}C{^{1}H} NMR** (101 MHz, $CDCl_3$) δ 141.5 (*C*$_{Ar}$), 128.6 (*C*H_{Ar}), 128.5 (*C*H_{Ar}), 126.1 (*C*H_{Ar}), 100.8 (*C*H), 35.8 (*C*H_2), 29.7 (*C*H_2).

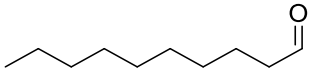

j21

The compound **j21** was prepared as described in the general procedure method **B** (65 mg) in 83% yield.[20] **^{1}H NMR** (300 MHz, $CDCl_3$) δ 9.76 (t, *J* = 1.9 Hz, 1H, C*H*=O), 2.41 (td, *J* = 7.3, 1.9 Hz, 2H, CH_2), 1.67 – 1.57 (m, 2H, CH_2), 1.35 – 1.23 (m, 12H, CH_2), 0.87 (d, *J* = 6.4 Hz, 3H, CH_3); **^{13}C{^{1}H} NMR** (101 MHz, $CDCl_3$) δ 203.1 (*C*H=O), 44.1 (*C*H_2), 31.9 (*C*H_2), 29.52 (*C*H_2), 29.49 (*C*H_2), 29.38 (*C*H_2), 29.30 (*C*H_2), 22.8 (*C*H_2), 22.2 (*C*H_2), 14.2 (*C*H_3).

7.4 References

[1] J. Zheng, S. Chevance, C. Darcel, J.-B. Sortais, *Chem. Commun.* **2013**, *49*, 10010–10012.

[2] A. Seifert, R. Mahrwald, *Tetrahedron Lett.* **2009**, *50*, 6466–6468.

[3] B. Guan, D. Xing, G. Cai, X. Wan, N. Yu, Z. Fang, L. Yang, Z. Shi, *J. Am. Chem. Soc.* **2005**, *127*, 18004–18005.

[4] N. Jiang, A. J. Ragauskas, *Org. Lett.* **2005**, *7*, 3689–3692.

[5] J. Dorie, J.-P. Gouesnard, M. L. Martin, *J. Chem. Soc. Perkin Trans. 2* **1981**, 912–917.

[6] B. R. Kim, H.-G. Lee, E. J. Kim, S.-G. Lee, Y.-J. Yoon, *J. Org. Chem.* **2010**, *75*, 484–486.

[7] M. Mascal, E. B. Nikitin, *ChemSusChem* **2009**, *2*, 423–426.

[8] D. L. Comins, M. O. Killpack, *J. Org. Chem.* **1987**, *52*, 104–109.

[9] M. L. Laurila, N. A. Magnus, M. A. Staszak, *Org. Process Res. Dev.* **2009**, *13*, 1199–1201.

[10] L. Schiavo, L. Lebedel, P. Massé, S. Choppin, G. Hanquet, *J. Org. Chem.* **2018**, *83*, 6247–6258.

[11] Y. Corre, V. Rysak, F. Capet, J.-P. Djukic, F. Agbossou-Niedercorn, C. Michon, *Chem. – Eur. J.* **2016**, *22*, 14036–14041.

[12] A. Y. Khalimon, W. E. Piers, J. M. Blackwell, D. J. Michalak, M. Parvez, *J. Am. Chem. Soc.* **2012**, *134*, 9601–9604.

[13] M. Igarashi, R. Mizuno, T. Fuchikami, *Tetrahedron Lett.* **2001**, *42*, 2149–2151.

[14] G.-Q. Chen, Z.-J. Xu, C.-Y. Zhou, C.-M. Che, *Chem. Commun.* **2011**, *47*, 10963–10965.

[15] H. Chikashita, Y. Morita, K. Itoh, *Synth. Commun.* **1987**, *17*, 677–683.

[16] J. Kagan, D. A. Agdeppa Jr, A. I. Chang, S.-A. Chen, M. A. Harmata, B. Melnick, G. Patel, C. Poorker, S. P. Singh, *J. Org. Chem.* **1981**, *46*, 2916–2920.

[17] S. A. Kavanagh, A. Piccinini, E. M. Fleming, S. J. Connon, *Org. Biomol. Chem.* **2008**, *6*, 1339–1343.

[18] R. Knorr, P. Löw, P. Hassel, *Synthesis* **1983**, *1983*, 785–786.

[19] D. Wei, R. Buhaibeh, Y. Canac, J.-B. Sortais, *Org. Lett.* **2019**, *21*, 7713–7716.

[20] P. Gogoi, D. Konwar, *Org. Biomol. Chem.* **2005**, *3*, 3473–3475.

General Conclusion

General Conclusion

The first part of this work was to develop new catalytic systems for hydrogenation reactions, based on manganese as an earth abundant metal and involving electron-rich NHC ligands.

-> To achieve this goal, a new family of bidentate NHC-phosphine Mn(I) complexes was readily obtained from their corresponding phosphine-imidazolium salts through the sequential addition of equimolar quantities of KHMDS and $[Mn(CO)_5Br]$. All these Mn(I) complexes were fully characterized and were shown to present moderate to excellent catalytic activity in the hydrogenation of ketones. This catalytic process highlights a new mode of metal-ligand cooperation involving the unsaturated 16-e mangana-substituted phosphonium ylide complex *fac*-$[Mn(CO)_3(\kappa^2P,\hat{C}\text{-}Ph_2P{=}CHNHC)]$ as key intermediate able to activate H_2 *via* a non-classical mode of metal-ligand cooperation implying a formal λ^5-P – λ^3-P phosphorus valence change, thus providing the first evidence of the involvement of λ^5-phosphorous species in metal-ligand cooperation.

-> Considering the great stability and reactivity of pincer complexes, the next challenge of our work was to prepare the tridentate version of NHC-phosphine Mn(I) complexes. By using a similar procedure as the one developed in the bidentate series, we succeeded in synthesizing two new families of cationic NHC Mn(I) pincer complexes involving PCN and PCP ligands. These complexes were fully characterized and their catalytic activity was investigated in the hydrogenation of acetophenone, showing a lower activity compared to their bidentate version, indicating that the development of more complex systems is not always a prerequisite to reach better performances in the field of catalysis.

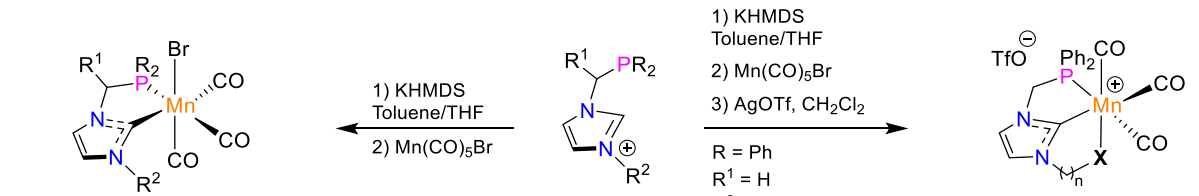

C1, R = Ph, R^1 = H, R^2 = Mes (86%)
C1.b, R = Ph, R^1 = Me, R^2 = Mes (40%)
C2, R = Ph, R^1 = H, R^2 = Me (82%)
C3, R = Ph, R^1 = H, R^2 = iPr (60%)
C4, R = iPr, R^1 = H, R^2 = Mes (78%)
C5, R = Ph, R^1 = Ph, R^2 = Mes (80%)

C6^t, n = 1, **X** = PPh_2 (88%)
C7^t, n = 0, **X** = Py (76%)
C8^t, n = 1, **X** = Py (96%)

The second part of this PhD was to develop a new catalytic system for the selective reduction of carboxylic acids and esters. With the commercially available $Mn_2(CO)_{10}$ (5 mol%) and $Re_2(CO)_{10}$ (0.5 mol%) pre-catalysts in the presence of a silane as reducing agent under irradiation at room temperature, a large variety of carboxylic acids and esters were thus reduced with high chemo-selectivity to their corresponding protected aldehydes.

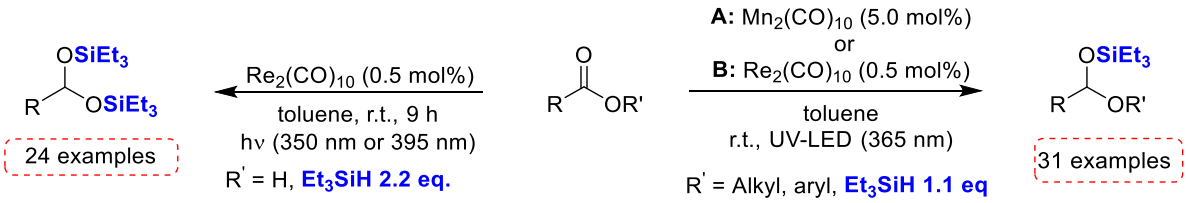

The perspectives of this work are numerous although they are mainly related to the first part of this Ph.D. Indeed, based on synthesized bi- and tridentate NHC core Mn(I) complexes, other catalytic transformations could be considered such as the hydrogenation of more challenging ester and amide substrates. Different metal centers belonging to the first row of the periodic classification (Fe, Co, Ni,…) could be also investigated using this new class of chelating NHC-based ligands. One relevant question will be to know if we can obtain the same type of cooperativity with other metal centers?

Résumé en Français

Résumé en français

Introduction générale

L'hydrogénation, avec le dihydrogène moléculaire, est l'une des méthodes les plus efficaces, les plus économiques et les plus propres de la chimie organique pour réduire les liaisons insaturées, et présente donc un grand intérêt aussi bien pour le monde académique qu'industriel.[1] Après les travaux de pionnier de Döbereiner[2], Sabatier a apporté en 1912 la première contribution significative dans ce domaine, en démontrant que l'hydrogène moléculaire pouvait être additionné à une liaison insaturée en présence de nickel comme catalyseur[3]. Cette percée a été suivie par de nombreuses autres, dans le domaine de la catalyse hétérogène, puis en catalyse homogène, à la suite de la préparation par Wilkinson du premier catalyseur au rhodium.[4] Ce travail pionnier a permis le développement de l'hydrogénation asymétrique par Knowles[5] et Noyori[6] en utilisant des ligands chiraux phosphorés, ce qui leur a permis d'obtenir le prix Nobel quelques années plus tard, comme Sabatier en son temps[7]. Les réactions d'hydrogénation en phase homogène sont généralement réalisées avec des catalyseurs à base de métaux de transition nobles tels que le ruthénium, le palladium et le rhodium[1]. La rareté et la toxicité de ces métaux sont des désavantages par rapport aux métaux de transition abondants comme ceux de la première ligne du tableau périodique. À cet égard, en tant que métaux de transition le plus abondant, et donc le moins cher, le fer a été le premier métal non-noble à démontrer des performances comparables à celles des métaux nobles dans le domaine de l'hydrogénation[8]. Le manganèse est le troisième métal de transition le plus abondant dans la croûte terrestre, derrière le fer et le titane, son abondance naturelle et sa biocompatibilité en font un élément très prometteur pour les applications en catalyse, notamment pour la production de composés pharmaceutiques.[9–18]

Avec cet objectif en tête, nous nous sommes donc intéressés au développement de complexes de manganèse bien définis supportés par des ligands à coeur NHC et à l'évaluation de leur réactivité pour l'activation de H_2, puis au développement de catalyseurs efficaces d'hydrogénation. Parallèlement, nous avons explorer l'utilisation de complexes carbonyles de manganèse et de rhénium commerciaux dans les réactions d'hydrosilylation.

Ce manuscrit de thèse est composé de trois parties. Le premier chapitre de cette thèse résume une sélection des avancées les plus significatives dans les réactions de (dé)-hydrogénation catalysées par des complexes de manganèse bien définis.

Le deuxième chapitre se concentre sur la synthèse de divers complexes de manganèse(I) supportés par des ligands NHC-phosphine bidentés facilement accessibles. Ces complexes ont

été utilisés pour l'hydrogénation des cétones. Ce processus catalytique a mis en évidence un nouveau mode de coopération métal-ligand non classique impliquant un ylure de phosphonium obtenu par déprotonation du bras du ligand NHC-phosphine chélatant dans la sphère de coordination du manganèse. Ce dernier peut facilement activer le dihydrogène H_2, fournissant ainsi la première preuve de l'implication d'espèces λ^5-phosphorées dans la coopération métal-ligand. En raison de la rigidité et de la robustesse supérieures des complexes pinces, des complexes tridentés de manganèse basés sur des ligands PCN et PCP, à cœur NHC, ont également été préparés et entièrement caractérisés. Toutefois, nous avons constaté que ces derniers étaient moins actifs dans l'hydrogénation des cétones que leurs analogues bidentés.

Le troisième chapitre est consacré à la réduction sélective d'acides carboxyliques et des esters en aldéhydes, via la formation d'alkylsilylacétals stables, en utilisant les pré-catalyseurs $Mn_2(CO)_{10}$ et $Re_2(CO)_{10}$ commerciaux en présence de silane, comme agent réducteur, sous irradiation lumineuse à température ambiante.

Chapitre 1 : Hydrogénation et réactions de transfert d'hydrogène catalysées par le manganèse

Les premières applications du manganèse dans les réactions de (dé)-hydrogénation ont été décrites en 2016 par les groupes de Beller et Milstein, respectivement, pour l'hydrogénation de nitriles, cétones et aldéhydes[19] et le couplage déshydrogénant d'alcools et d'amines pour former des imines[20]. Dans les deux cas, le centre Mn(I) a été stabilisé par un ligand pince bis(phosphine)-amine rigide et fortement chélatant, ce qui a permis dans le cas de l'hydrogénation de réduire une large gamme de substrats insaturés. Suite à ces résultats prometteurs, de nombreux autres systèmes à base de manganèse présentant une structure de type pince avec différentes extrémités donneuses à base d'azote et phosphore ont été élaborés pour l'hydrogénation de substrats organiques contenant des liaisons multiples polaires, tels que les aldéhydes, les cétones, les nitriles, les esters, les amides, les imines, les carbonates ou le CO_2[21–28]. Des systèmes bidentés combinant des extrémités donneuses à base de phosphore, d'azote mais aussi de carbone ont été développés plus récemment, ce qui a permis des avancées spectaculaires dans ce domaine. D'autres systèmes contenant du manganèse ont été plus ponctuellement envisagés comme des complexes moléculaires basés sur des ligands tétradentés et/ou des ligands avec différents atomes donneurs (O, Si), ainsi que des nanoclusters[29,30]. Comme alternative à l'hydrogène moléculaire, les alcools agissent également comme une

source précieuse d'hydrogène, rendant ainsi le transfert d'hydrogène un processus complémentaire à l'hydrogénation classique. Quel que soit le processus de réduction, l'efficacité catalytique des complexes métalliques a été largement rationalisée grâce au concept de coopération métal-ligand, qui consiste à tirer parti de la forte synergie créée entre le ligand et le métal pour favoriser le clivage de H_2 suivie du transfert d'atomes d'hydrogène sur des liaisons insaturées.[31–33] La plupart des systèmes catalytiques ont donc été développés sur la base de deux architectures bifonctionnelles, impliquant soit une interconversion amide/amine, ou bien un processus d'aromatisation/désaromatisation d'un noyau pyridine.

Dans ce chapitre introductif, une sélection des avancées récentes réalisées dans le domaine des réactions d'hydrogénation catalysées par des complexes de manganèse bien définis a été examinée. Ces complexes métalliques ont été classés en fonction de la structure du ligand, et en particulier, de la denticité et de la nature des extrémités donneuses.

Cet état de l'art montre qu'en très peu de temps, l'utilisation du manganèse en catalyse a considérablement augmenté en raison de sa disponibilité mais aussi de ses propriétés uniques. Les réactions de type hydrogénation représentent l'un des domaines les plus développés de la catalyse au manganèse, et les réalisations récentes confirment que le manganèse peut fournir une alternative viable aux métaux nobles. La conception d'une grande diversité de ligands chélatants, principalement dans les séries bi- et tridentés combinant différentes extrémités coordinantes avec des atomes donneurs N-, P- et C-, explique en grande partie ce développement exponentiel et rapide. Outre les propriétés électroniques (donneur contre accepteur) et stériques (rigidité contre flexibilité) intrinsèques à chaque ligand, la coopération métal-ligand a sans aucun doute joué un rôle déterminant dans le succès des applications des complexes de manganèse dans la catalyse d'hydrogénation. Le métal n'est ici pas le seul acteur mais c'est son rôle associé à celui du ligand qui est à l'origine de la transformation catalytique. Afin de maximiser le potentiel catalytique de ces complexes métalliques en termes d'activité et de sélectivité, une meilleure compréhension de la relation structure-activité serait toutefois nécessaire, et en particulier de la manière dont la réactivité du métal est influencée par la structure du ligand. Si l'accès à des systèmes catalytiques simples et bon marché est clairement d'un grand intérêt à des fins industrielles, l'amélioration de ces systèmes nécessitera le développement de ligands alternatifs. Il est très probable que les ligands à base de carbone deviendront bientôt très populaires dans ce domaine de la catalyse au manganèse.

Chapitre 2 : Synthèse et applications catalytiques de complexes de manganèse NHC-Phosphine bi- et tridentés

1. Introduction

1.1 Coopérativité métal-ligand

Au cours des 20 dernières années, les systèmes organométalliques dans lesquels le centre métallique est stabilisé par un ligand coopératif sont devenus des outils puissants pour la conception de catalyseurs organométalliques efficaces. Dans ces systèmes, le ligand et le métal sont tous deux impliqués dans la formation du produit sans changement de l'état d'oxydation du métal, contrairement aux mécanismes classiques d'addition oxydante/élimination réductrice (**Schéma 1**)[33].

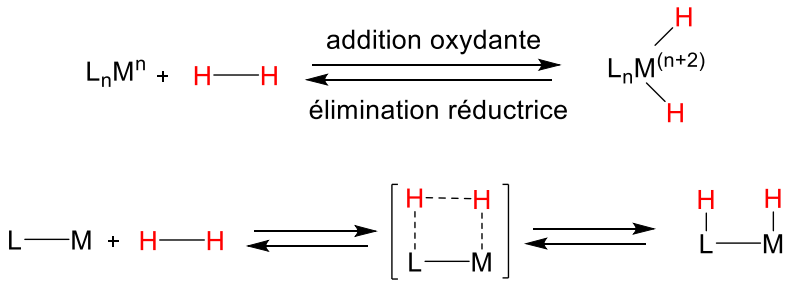

Schéma 1. Addition oxydante /élimination réductrice (*haut*) et activation coopérative métal-ligand (*bas*).

Après la découverte des catalyseurs de Shvo,[34,35] une grande variété de complexes de métaux de transition portant des ligands non innocents a été exploitée pour l'activation des liaisons E-H (E = H, C, S, Si, N, O, B), [33] récemment complétée par la réactivité des paires de Lewis frustrées[36] et des ambiphiles du groupe principal.[37,38] Parmi toutes ces transformations, l'activation du dihydrogène est de la plus haute importance en raison de son rôle essentiel dans les processus d'hydrogénation[1,39,40] et d'auto-transfert d'hydrogène[41,42] pertinents dans l'industrie de la chimie fine.

1.1.1 Coopération métal-ligand par le biais des liaisons M-L

De nombreux exemples d'activation de la liaison H_2 par des liaisons M-L impliquant divers atomes donneurs (N, O, P, S, B, C) ont été décrits au fil des ans.[33,43] Deux exemples pertinents

où l'atome donneur peut être l'azote et l'oxygène (le phosphore étant plus anecdotique) seront plus particulièrement examinés dans cette section (**Schéma 2**).

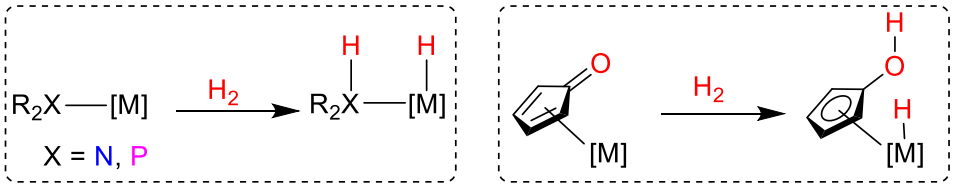

Schéma 2. Activation de H_2 par des ligands non innocents via une coopération métal-ligand.

➢ *Coopération Métal-NH*

L'un des systèmes le plus important et le plus largement utilisé pour activer H_2 est la coopération des fragments NH des ligands avec le centre métallique, une telle coopération conduisant en effet à des activités catalytiques et des sélectivités considérablement améliorées avec les catalyseurs organométalliques correspondants.[44] L'exemple le plus impressionnant de la coopération M-NH est le système Ru(phosphine)$_2$-diamine développé par Noyori et ses collaborateurs en 1995[45], qui présentait une très forte activité pour l'hydrogénation des cétones. Noyori a notamment découvert que l'ajout d'un additif aminé contenant au moins un groupe NH tel que l'éthylènediamine avait un effet spectaculaire sur la réactivité du catalyseur de Ru. Un TOF de 6700 h^{-1} a été en effet obtenu pour l'hydrogénation des cétones à l'aide du complexe [$RuCl_2(PPh_3)_3$] avec 1 équivalent d'éthylènediamine en présence de 20 équivalents de KOH dans du 2-propanol comme solvant et sous 3 atm de H_2. Par opposition, en réalisant la réaction dans les mêmes conditions mais sans l'additif diamine, la fréquence de cycle a été réduite à 5 h^{-1}. Dans des conditions identiques, les additifs amines sans fragments NH, tels que la N,N,N',N'-tétraméthyléthylènediamine (TMEDA) se sont avérés inefficaces, confirmant que la présence de fragments NH est nécessaire pour augmenter l'activité du catalyseur. La version asymétrique de ce système de Ru a également été largement étudiée,[44,46] montrant des activités élevées sans précédent (TOF > 200 000 h-1, TON > 2 × 106) et une excellente énantiosélectivité (ee > 98%) pour l'hydrogénation des cétones (**Schéma 3**).

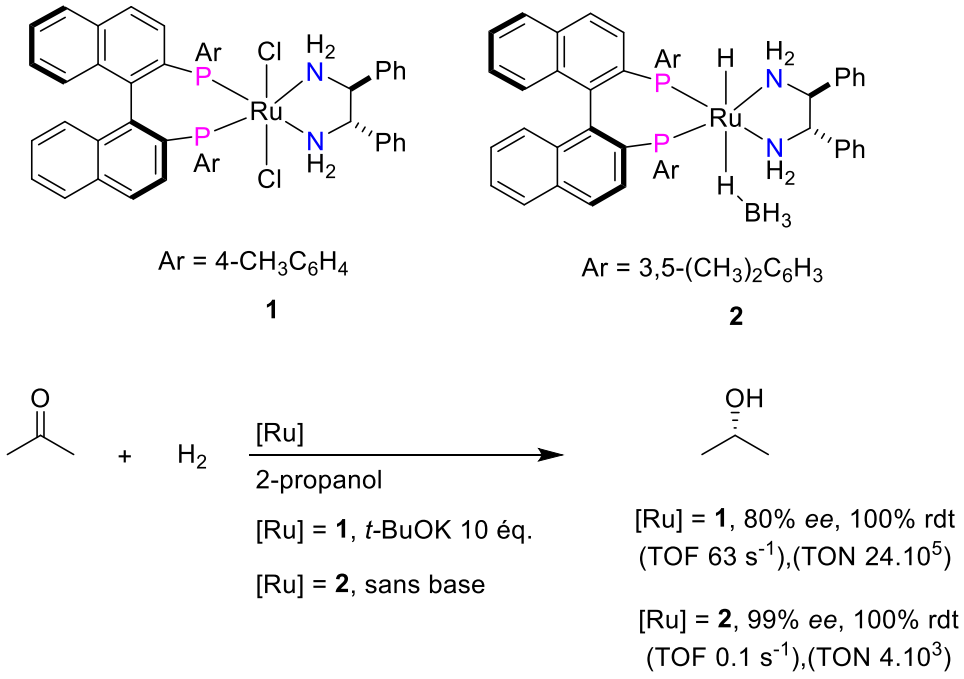

Schéma 3. Complexes de Ru-NH chiraux hautement actifs pour l'hydrogénation asymétrique des cétones. [44,46]

Des études mécanistiques ont été menées pour expliquer l'effet important du fragment NH sur l'activité du catalyseur. Un mécanisme de sphère externe a ainsi été proposé pour l'hydrogénation des cétones (**Schéma 4**).[47,48] Plus précisément, il a été postulé que la déprotonation du complexe [$RuCl_2$(phosphine)$_2$(1,2-diamine)] **3** sous atmosphère de H_2 conduisait à la formation de l'espèce active amido du complexe de Ru **4** à 16 e^-, suivie d'une étape de coordination de H_2 sur le site vacant du centre Ru via une liaison σ pour donner le complexe **5**, qui subit ensuite un clivage hétérolytique à travers la liaison Ru(II)-amido pour former un complexe Ru(II) amino-hydrure **6**. Dans ce dernier, le proton du ligand amine et l'hydrure du métal sont simultanément transférés au groupe C=O du substrat carbonyle par un état de transition à six chaînons (TS1) pour produire finalement l'alcool correspondant et régénérer le complexe amido Ru **4** à 16e^-.

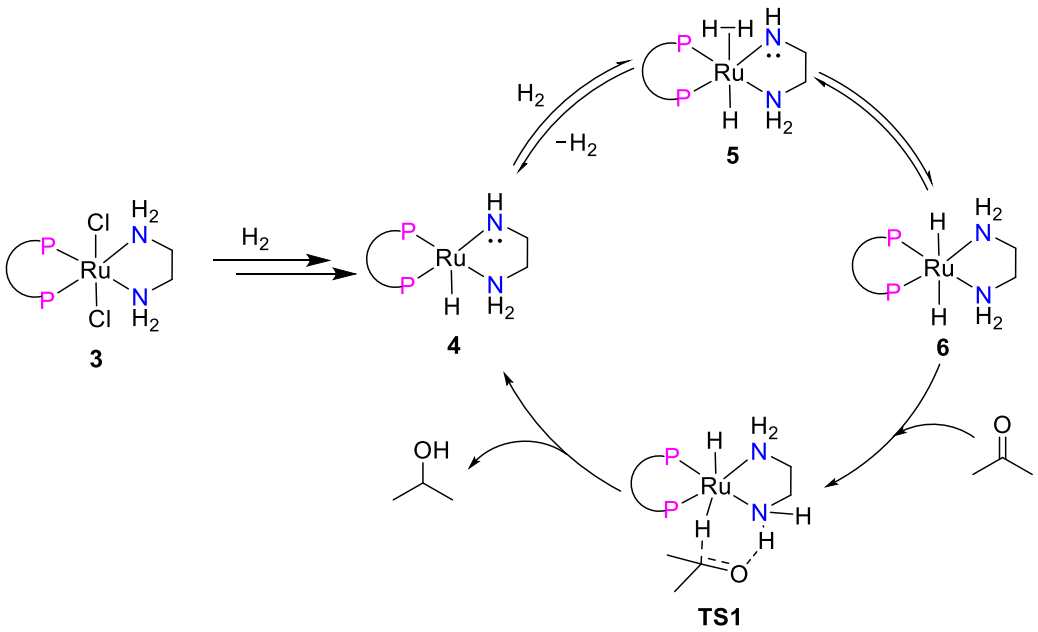

Schéma 4. Mécanisme proposé pour les complexes à base de Ru-NH dans l'hydrogénation catalysée des cétones.[47,48]

➢ *Coopération M-L-OH*

Par rapport aux complexes métalliques amides/amines, l'activation coopérative avec des catalyseurs métalliques alcoxydes/alcools est moins courante.[49–54] L'exemple le plus connu de ce type de coopération métal-ligand concerne le ligand hydroxy-cyclopentadiényle coordonné au ruthénium découvert par Shvo.[55] Le complexe dinucléaire de Ru **7** est en effet l'un des premiers complexes développés dans le domaine des catalyseurs bifonctionnels métal-ligand et il s'est avéré être un pré-catalyseur efficace pour de nombreuses transformations, notamment les réactions de type hydrogénation de divers substrats tels que les alcènes, les alcynes, les dérivés carbonylés et les imines.[56] Le rôle clé de sa forte activité catalytique est en fait lié à la dissociation possible du complexe dimère **7** au cours du processus catalytique en son monomère **8** et en l'espèce η^4-cyclopentadienone ruthénium **9** (**Schéma 5**).

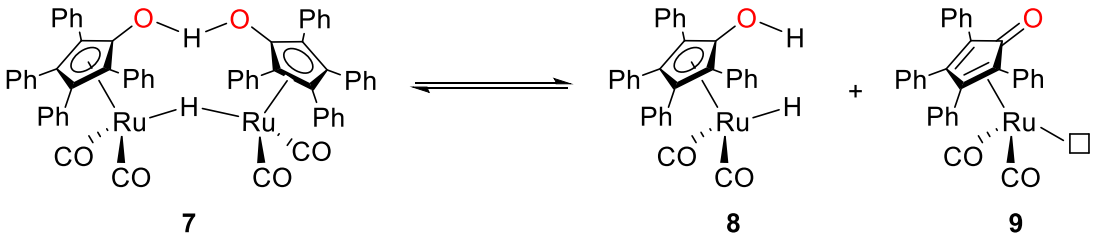

Schéma 5. Catalyseur de Shvo **7**en équilibre avec ses monomères actifs **8** et **9**.[56]

Des études expérimentales et théoriques[57–59] ont montré un mécanisme de sphère externe via un état de transition à six chaînons pour l'hydrogénation des dérivés carbonylés. Le complexe réducteur actif **8** transfère simultanément l'hydrure du centre de Ru(II) et le proton du groupe O-H du ligand au groupe carbonyle du substrat pour former le produit souhaité et générer le complexe de Ru **9** (**Schéma 6**).

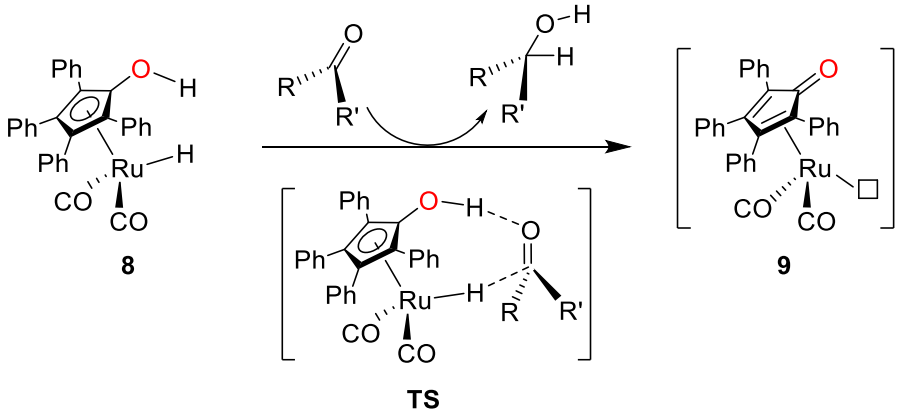

Schéma 6. Mécanisme proposé pour l'hydrogénation des dérivés carbonylés par le catalyseur de Shvo.[57]

1.1.2 Coopération métal-ligand par aromatisation/désaromatisation de la pyridine.

L'association de fragments donneurs à base d'N et de P pour les applications catalytiques a été plus développée, en particulier dans la série des pinces grâce aux travaux rapportés par Milstein et al. Dans ce cas précis, les espèces résultant de la déprotonation du pont méthylène dans les complexes phosphine-pyridine sont capables d'activer H_2 à travers le métal et le bras du ligand par un mécanisme dans lequel la réaromatisation du noyau pyridine joue un rôle clé (**Schéma 7**)[60,61]

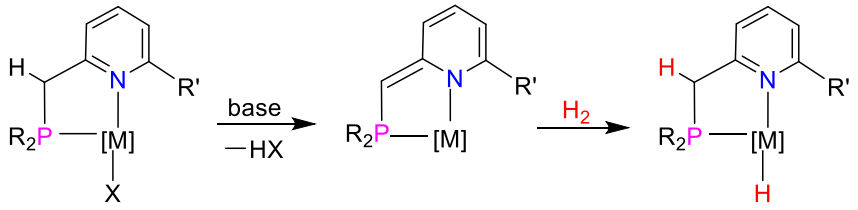

Schéma 7. Processus d'aromatisation/d'aromatisation dans les complexes de pinces de Milstein.

Le cycle catalytique proposé, pour le couplage déshydrogénant des amines et des alcools pour former des amides, implique la déshydrogénation de l'alcool primaire en aldéhyde correspondant à l'aide du complexe de Ru **14**. Dans un deuxième temps, la réaction entre l'aldéhyde et l'amine conduit à la formation d'un dérivé hémi-aminal qui réagit avec le complexe **14** pour donner l'intermédiaire aromatique **15**, suivi d'une étape d'élimination β-H pour former le produit amide souhaité et générer le complexe dihydrure de Ru **16**. L'élimination du dihydrogène du complexe dihydrure **16** régénère finalement le catalyseur **14**, complétant ainsi le cycle catalytique (**Schéma 8**).

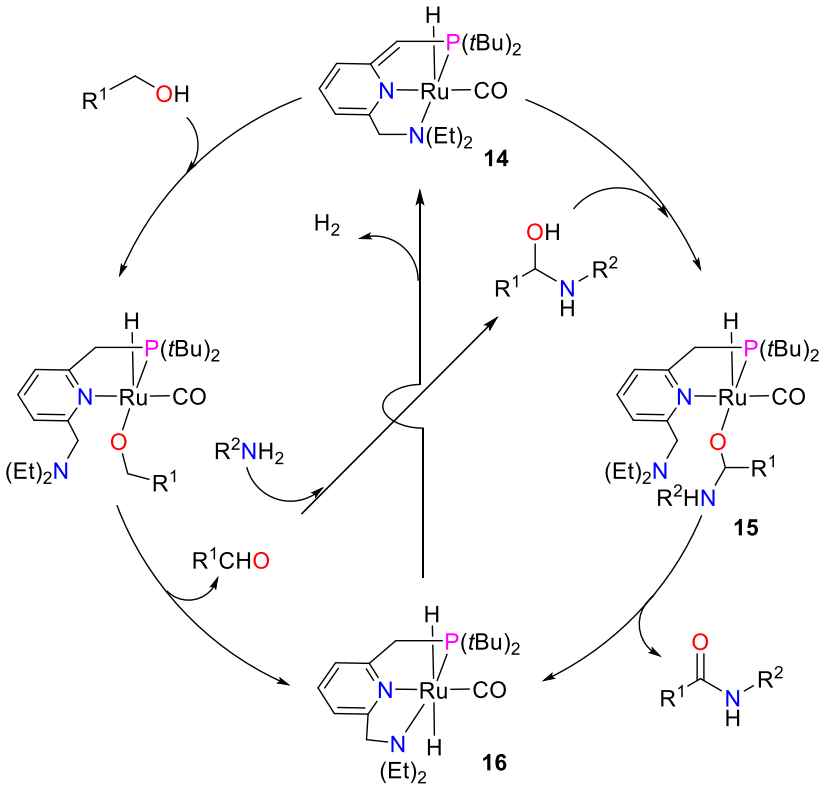

Schéma 8. Mécanisme proposé pour l'acylation déshydrogénante d'amines avec des alcools en utilisant le complexe pince PNN-Ru **14** comme catalyseur.[62]

Sur la base de ces différentes études et de l'expertise du groupe en chimie des carbènes et du phosphore, nous nous sommes intéressés au développement de nouveaux ligands NHC-phosphine caractérisés par des propriétés stériques et électroniques uniques. Après déprotonation, ces ligands chélatants pourraient éventuellement agir comme des ligands coopératifs grâce à l'implication d'atomes de carbone et/ou de phosphore et du centre métallique. L'objectif final était alors d'étudier leurs propriétés de coordination, principalement en ce qui concerne le manganèse(I) et de tester leur réactivité stoechiométrique et catalytique pour l'activation du dihydrogène avec des applications possibles dans le domaine de la catalyse d'hydrogénation (**Schéma 9**).

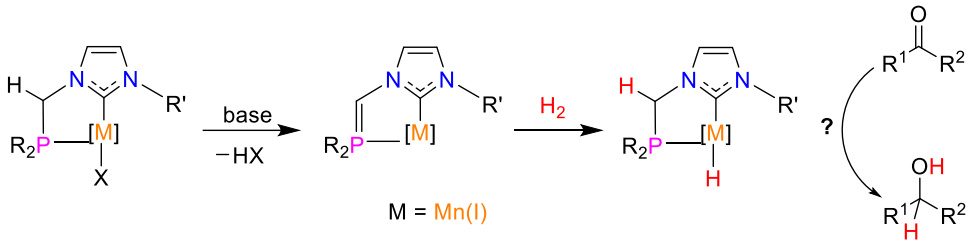

Schéma 9. Activation de H_2 par des ligands non-innocents de type NHC-phosphine par coopération métal-ligand.

2. Résultats et discussion

2.1 Synthèse des complexes NHC-Phosphine bidentés

2.1.1 Synthèse du complexe NHC-phosphine C1

Dans la continuité de nos récentes recherches sur l'application de complexes de manganèse supportés par des ligands bidentés dans les catalyses de (dé)-hydrogénation[63–67], nous avons porté notre attention sur l'utilisation de ligands associant des extrémités donneuses phosphine et NHC. Notre premier précurseur de type phosphine-imidazolium cible [Ph_2PCH_2Im]OTs (L1) a été obtenu par modification d'une procédure de la littérature précédemment utilisée pour la synthèse de [Ph_2PCH_2Im]Br.[68] La réaction du 1-mésityl-imidazole avec $Ph_2P(O)CH_2OTs$ à 130 °C pendant la nuit conduit au sel d'oxyde de phosphine-imidazolium N-substitué L1(O) avec un rendement de 86 %, qui a ensuite été réduit par un excès de $HSiCl_3$ (20 équivalents) à 80 °C dans du chlorobenzène pour donner le N-phosphino-imidazolium **L1** souhaité avec un rendement isolé de 93 % (**Schéma 10**).

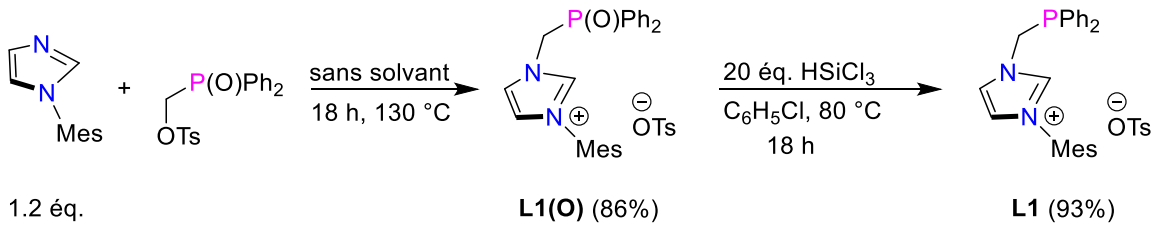

Schéma 10. Synthèse du sel de N-phosphino-imidazolium **L1** à partir du 1-mésityl-imidazole.

Nous avons ensuite étudié la complexation du pré-ligand **L1** sur le manganèse. L'addition séquentielle de KHMDS et du précurseur [$Mn(CO)_5Br$] à une solution de **L1** dans du toluène à température ambiante, suivie d'un chauffage du mélange à 60 °C pendant 30 minutes, a conduit à la formation sélective d'un complexe *fac*-[$MnBr(CO)_3(\kappa^2P,\hat{C}\text{-}Ph_2PCH_2NHC)$] (**C1**) avec un rendement de 86 % (**Schéma 11**).

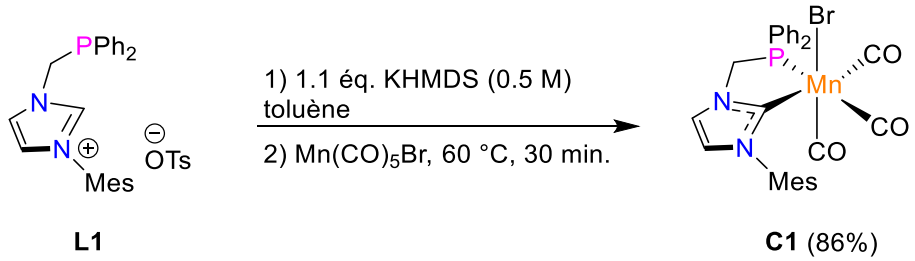

Schéma 11. Synthèse du complexe NHC-phosphine de Mn **C1** à partir du pré-ligand **L1**.

Une étude par diffraction des rayons X du complexe **C1** a été réalisée, indiquant la géométrie octaédrique du centre métallique et la disposition faciale des trois co-ligands carbonyles (**Figure 1**).

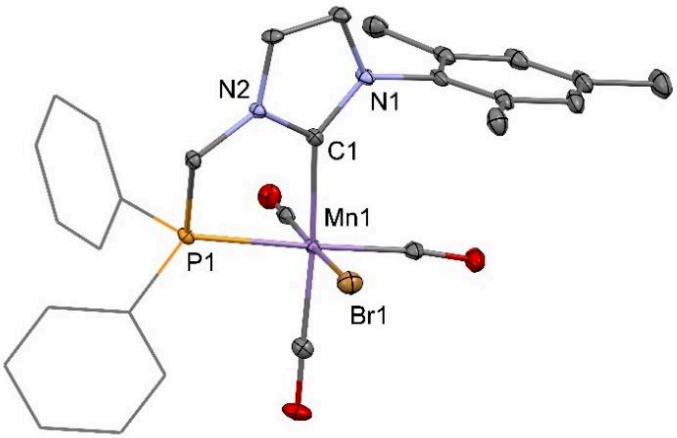

Figure 1. Structure moléculaire du complexe *fac*-**C1** (30% probability ellipsoids, aryl groups represented as a wireframe for clarity). Selected bond lengths (Å) and angles (°): Mn1–C1

2.032(2), Mn1–P1 2.3030(7), Mn1–Br1 2.4125(6), C1−Mn1−P1 80.11(7), C1−Mn1−Br1 83.78(6), P1−Mn1−Br1 89.18(2).

2.1.2 Réactivité du complexe NHC-phosphine C1

- *Vers l'activation de H_2*

Pour explorer le comportement chimique du complexe de Mn **C1** vis-à-vis du dihydrogène, ce dernier a été mis en présence de KHMDS dans du toluène à 0 °C sous 1 atm. de H_2. Dans ces conditions, **C1** a été converti en l'hydrure de manganèse correspondant **C1.a**, en quelques minutes à température ambiante (**Schéma 12**). Après lavage à l'eau dégazée, le complexe **C1.a** a finalement été isolé avec un rendement de 78 %, constituant le premier exemple de complexe d'hydrure de Mn portant un ligand NHC.

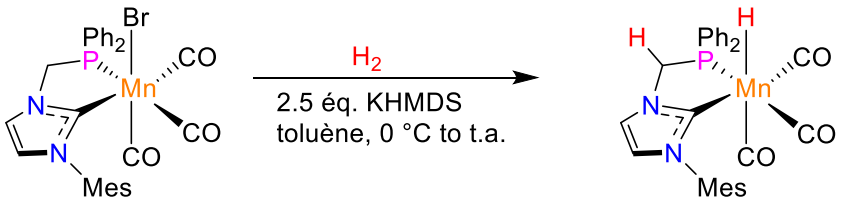

C1 **C1.a** (78%)

Schéma 12. Activation de H_2 par le complexe **C1** pour générer le complexe hydrure **C1.a**.

Comme observé dans le précurseur bromé **C1**, l'arrangement facial des trois co-ligands carbonyles du complexe **C1.a** a été confirmé de manière univoque par une étude de diffraction des rayons X (**Figure 3**).

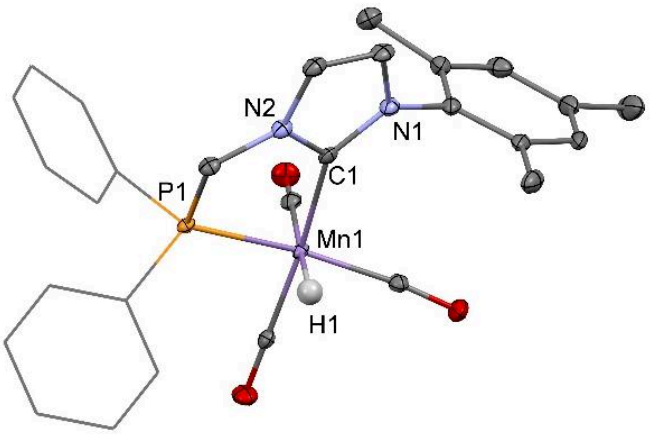

Figure 3. Structure moléculaire du complexe *fac*-**C1.a** (30% probability ellipsoids, aryl groups represented as a wireframe for clarity). Selected bond lengths (Å) and angles (°): Mn1–C1 2.034(3), Mn1–P1 2.2371(9), Mn1–H1 1.63(4), C1−Mn1−P1 79.95(9), C1−Mn1−H1 81.0(14), P1−Mn1−H1 78.5(14).

➢ *Réactivité avec des électrophiles tels que MeI et CO_2*

Afin de mieux caractériser le site acide dans le complexe **C1**, c'est-à-dire celui qui subit la réaction de déprotonation, différentes expériences de piégeage ont ensuite été réalisées. À cette fin, le complexe **C1** a d'abord été traité avec du KHMDS, puis un agent alkylant classique tel que MeI (5 équivalents). Le complexe **C1.b** correspondant montrant la méthylation de l'atome de carbone reliant les parties phosphine et NHC a été isolé avec un rendement modéré (environ 40 %) sous la forme d'un mélange de deux diastéréomères (rapport 6:1) différant par la position du groupe méthyle par rapport à l'atome d'iode coordonné (**Schéma 13**).

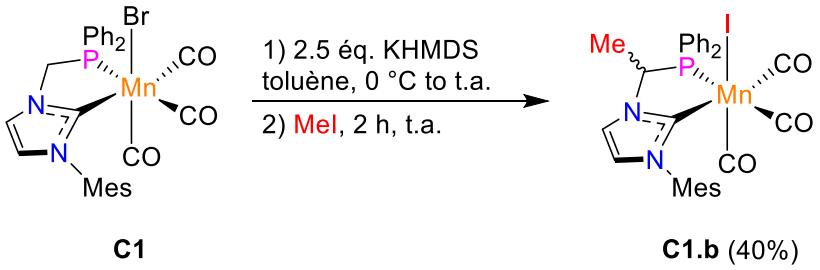

C1 **C1.b** (40%)

Schéma 13. Synthèse du complexe NHC-phosphine **C1.b** à partir du complexe **C1**.

2.1.3 Hydrogénation des cétones

Après avoir établi que le complexe **C1** pouvait effectivement activer H_2 dans des conditions en présence de base, nous avons ensuite porté notre attention sur l'hydrogénation des dérivés carbonylés comme réaction modèle.[63,69–72] Ayant optimisé les conditions de réduction, nous avons ensuite élargi la portée synthétique de cette transformation catalytique et constaté qu'une grande variété d'aryl(alkyl)cétones pouvait être facilement réduite (**Schéma 14**).

Schéma 14. Hydrogénation des cétones catalysée par le complexe **C1**[a].

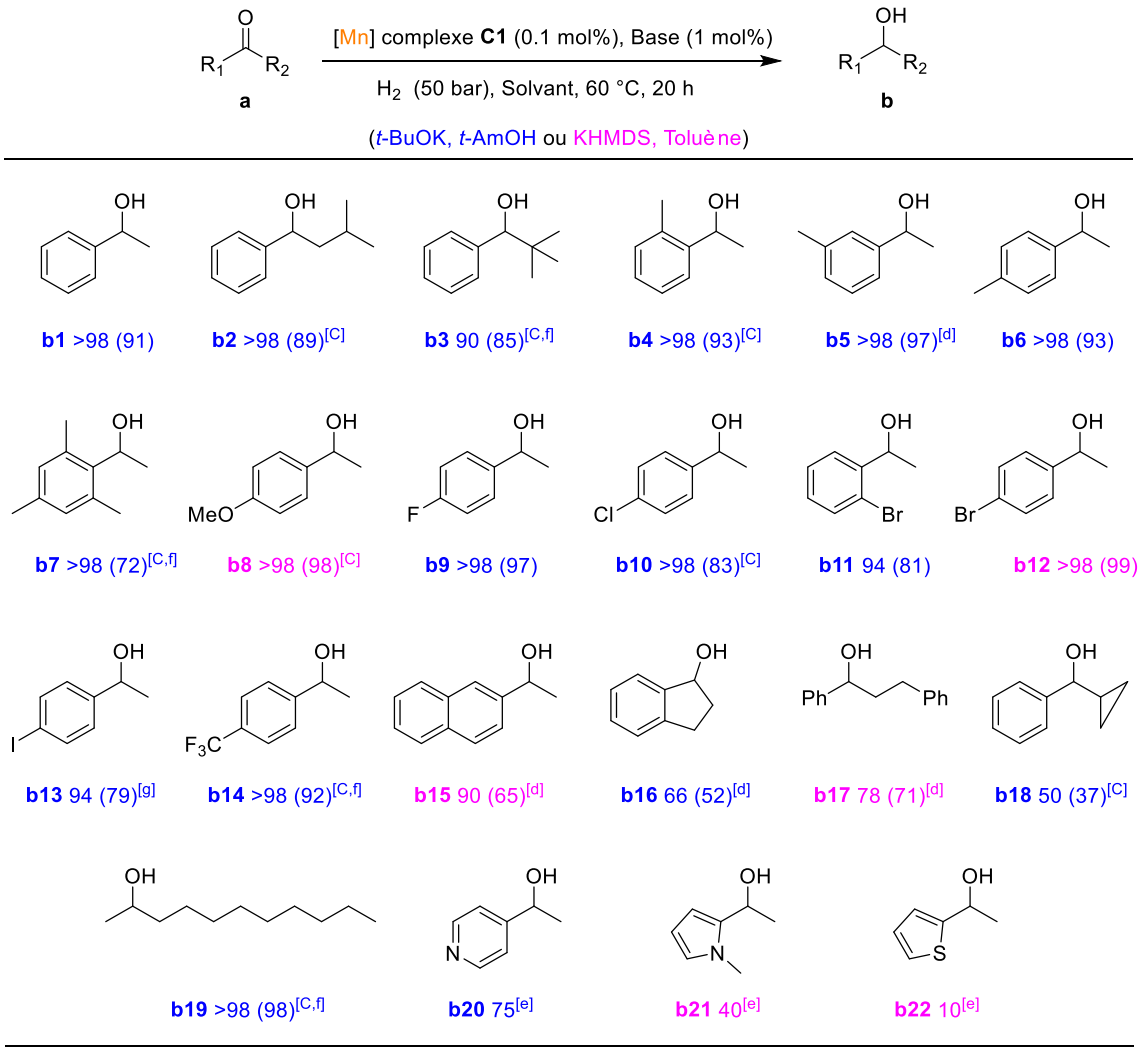

[a] Procédure générale : pré-catalyseur **C1** (0.1 mol%), cétone (2.0 mmol), base (1.0 mol%; **A**: *t*-BuOK, **B**: KHMDS), solvant (2 mL, **A**: *t*-AmOH, **B**: toluène), H_2 (50 bar), 60 °C, 20 h.

[b] Conversion déterminée par RMN ^{1}H, rendements isolés entre parenthèses.

[c] 2% de base, 0.5% de catalyseur

[d] 2% de base, 0.2% de catalyseur

[e] 1% de catalyseur, 5% de base, 100 °C, 72h

[f] 100 °C

[g] 5% de KOH

Suite à ces résultats encourageants, nous nous sommes intéressés à la modification des substituants au niveau des atomes d'N et de P et de la chaîne carbonée reliant les deux fragments coordinants dans les pré-ligands NHC-phosphine, afin d'étudier l'effet des substituants sur la

réactivité des complexes Mn(I) correspondants et surtout sur les propriétés catalytiques (**Schéma 15**).

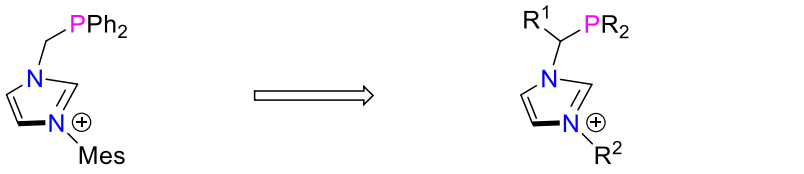

L1

L2, R = Ph, R^1 = H, R^2 = Me
L3, R = Ph, R^1 = H, R^2 = iPr
L4, R = iPr, R^1 = H, R^2 = Mes
L5, R = Ph, R^1 = Ph, R^2 = Mes

Schéma 15. Représentation du pré-ligand NHC-phosphine **L1** et des pré-ligands NHC-phosphine **L2-L5** ciblés correspondants en modifiant les substituants aux positions N, P et C.

2.1.4 Synthèse des complexes Mn(I) à base de ligands bidentés NHC-phosphine

L'étape de coordination des pré-ligands **L2-L5** a été réalisée en utilisant la même approche que celle développée dans le cas du complexe **C1** (**Schéma 11**). Ainsi, les complexes **C3-C5** ont été préparés en faisant réagir 1,1 équivalent de KHMDS avec les précurseurs correspondants **L3-L5** dans du toluène à température ambiante, tandis que la déprotonation du pré-ligand **L2** a été réalisée dans du THF à -40 °C. L'ajout d'un équivalent du précurseur [$Mn(CO)_5Br$] aux carbènes libres générés in situ, et le chauffage du mélange réactionnel à 50 °C, ont permis d'obtenir les complexes de Mn(I) **C2-C5** avec des rendements modérés à bons (60-82%) (**Schéma 16**).

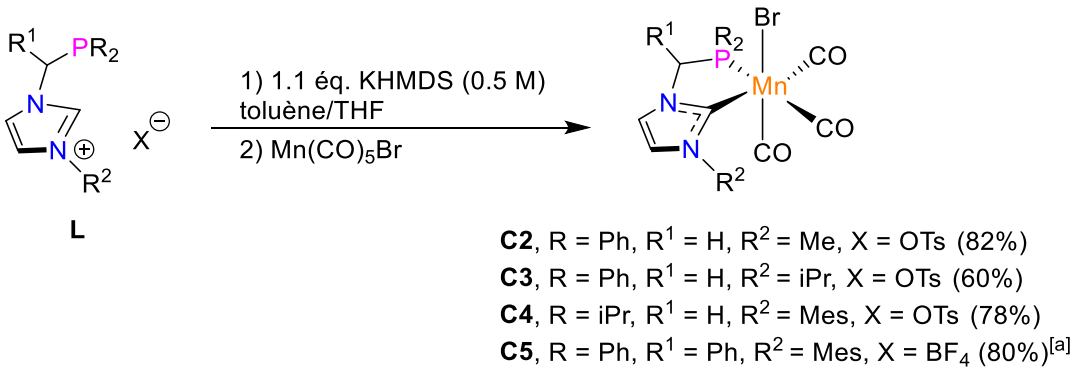

Schéma 16. Synthèse des complexes NHC-phosphine de Mn(I) **C2-C5** à partir des sels d'imidazolium correspondants **L2-L5**.

2.1.5 Conclusion

Divers complexes de manganèse(I) portant des ligands NHC-phosphine bidentés, facilement accessibles, ont été synthétisés à partir des sels d'imidazolium correspondants. En outre, nous avons également démontré dans le cas du complexe de Mn(I) **C1** que le ligand phosphine-NHC pouvait être déprotoné sélectivement au niveau de l'atome de carbone situé entre les deux parties donneuses pour donner un complexe à 18 électrons NHC-phosphinométhanide original. Ce dernier peut servir de réservoir à un complexe à 16 électrons NHC-ylure de phosphonium non conventionnel capable d'activer le dihydrogène par un mode de coopération métal-ligand. Il est intéressant de noter que la catalyse homogène peut tirer parti de ce nouveau mode d'activation du dihydrogène, comme le démontre le développement d'un des systèmes catalytiques à base de manganèse les plus efficaces pour l'hydrogénation des cétones. Il est à noter que le changement des substituants sur les atomes d'azote et de phosphore a un effet sensible sur l'activité des complexes. Le complexe **C2** avec un groupe méthyle sur l'atome d'azote s'est avéré être le moins actif dans ce processus. En revanche, l'introduction d'un groupe phényle sur le pont méthylène a augmenté de manière significative l'activité catalytique du complexe **C5**, qui s'est avéré être le pré-catalyseur le plus efficace dans cette transformation. Cette activité catalytique peut être liée à l'acidité du pont méthylène substitué qui relie les extrémités donneuses NHC et phosphine.

2.2 Synthèse des complexes NHC-Phosphine de Mn(I) tridentés

Sur la base de la structure générale des ligands NHC-phosphine bidentés de type **A**, nous nous sommes interrogés de l'impact possible sur l'activité catalytique du changement du substituant

N-R "spectateur" par un groupe donneur capable d'interagir avec le centre métallique. À cette fin, nous avons porté notre attention sur la préparation, les propriétés de coordination et l'activité catalytique des nouveaux ligands tridentés à coeur NHC de type **B** portant des bras donneurs phosphine et pyridine (**Schéma 17**). Dans un contexte plus large, cette étude comparative visait également à évaluer si l'amélioration des performances catalytiques impliquait nécessairement la conception d'architectures plus complexes, comme le sont les systèmes pinces.

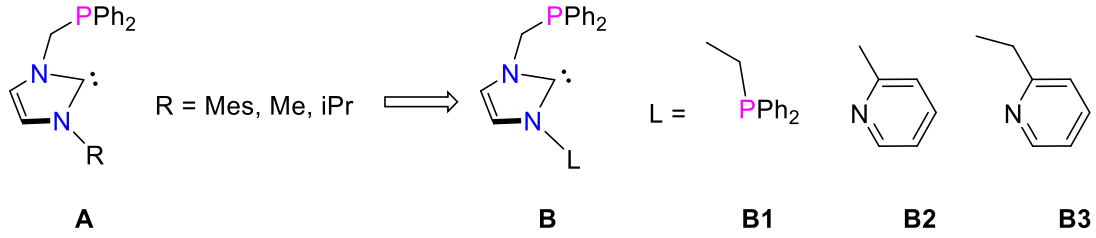

Schéma 17. Représentation des ligands phosphine-NHC bidentés **A** préalablement préparés, et des systèmes à coeur NHC tridentés ciblés de type **B** correspondants.

2.2.1 Synthèse et caractérisation spectroscopique des complexes tridentés de manganèse(I) à coeur NHC

Après avoir effectué la synthèse des pré-ligands **L6**, **L7** et **L8**, leur complexation a été envisagée en suivant une stratégie développée précédemment dans le cas des versions bidentées (voir **Schéma 16**). Les complexes **C6**, **C7**, **C7'** et **C8** ont donc été facilement obtenus à partir des précurseurs de sels d'imidazolium correspondants par l'addition séquentielle de quantités équimolaires de KHMDS et de $[Mn(CO)_5Br]$ avec des rendements isolés de 71, 80 et 60%, respectivement (**Schéma 18**). Alors que tous les complexes $[(L_x)Mn(CO)_3Br]$ neutres formés semblaient être de nature bidentée, une différence dans le mode de coordination a été observée entre les deux ligands portant une extrémité pyridine. A partir de **L7** où la pyridine est directement connectée au noyau imidazole, deux complexes isomères **C7** et **C7'**, dans un rapport de 1/3, ont été mis en évidence en raison de la formation possible de deux métallacycles à cinq chaînons favorisés thermodynamiquement lors de la coordination de la phosphine ou du bras pyridine. En revanche, dans le cas du ligand **L8**, seul le complexe bidenté **C8** résultant de la coordination concomitante des extrémités NHC et diphénylphosphine a été observée, la coordination de la pyridine aurait en effet conduit à un métallacycle à six chaînons moins stable.

Tous les complexes neutres bromés de Mn(I) ont ensuite été facilement convertis en présence d'AgOTf dans CH_2Cl_2 en leurs complexes tridentés cationiques correspondants, stables à l'air, **C6t**, **C7t** et **C8t**, isolés en tant qu'isomères uniques, avec des rendements respectifs de 88, 76 et 96 %.

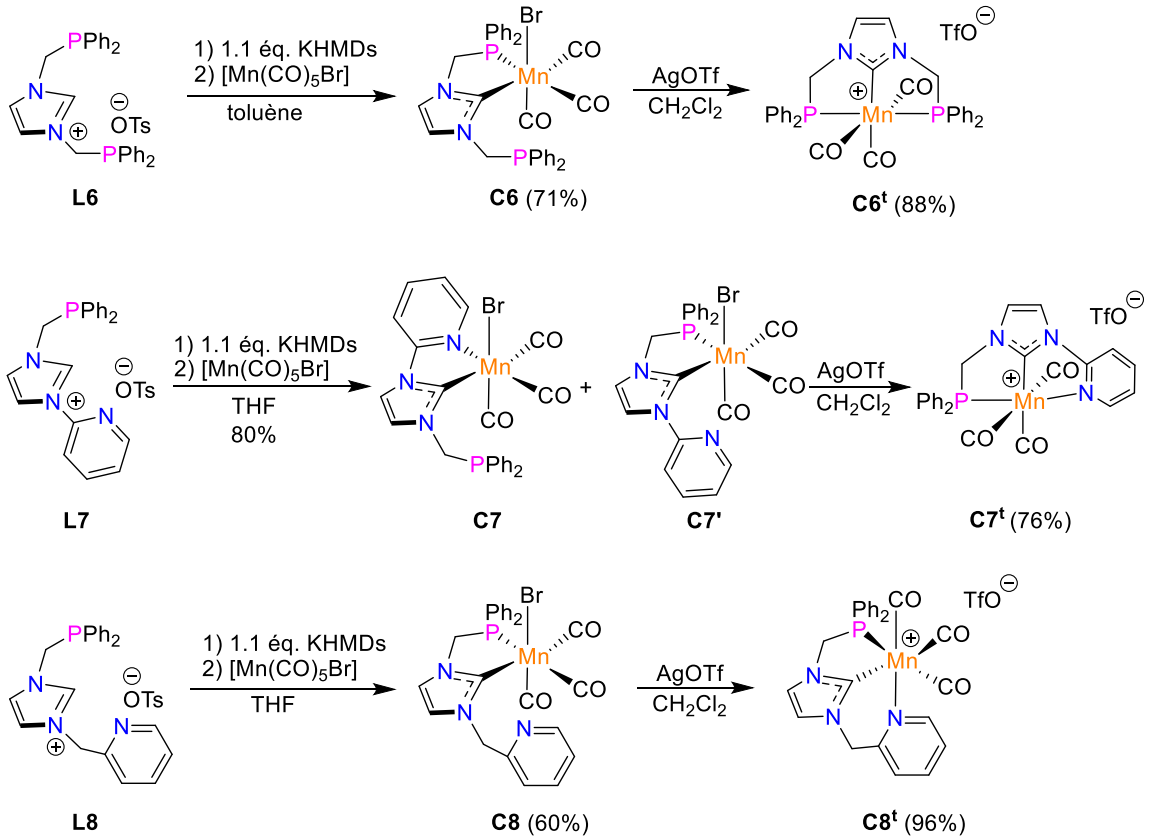

Schéma 18. Synthèses des complexes de Mn(I) cationiques tridentés à coeur NHC **C6t**, **C7t** et **C8t** à partir des précurseurs correspondants **L6**, **L7** et **L8**.

2.2.2 Conclusion

Une famille de complexes de manganèse(I) de type pince à motif NHC-phosphine, dont la troisième extrémité donneuse peut être modifiée, a été décrite à partir du 1*H*-imidazole selon une procédure en cinq étapes. Des complexes cationiques symétriques *mer*-[$Mn(CO)_3(\kappa^3P,C,P)(OTf)$] **C6t**, et non symétriques *mer*-[$Mn(CO)_3(\kappa^3P,C,N)(OTf)$] **C7t**, *fac*-[$Mn(CO)_3(\kappa^3P,C,N)(OTf)$] **C8t** ont ainsi été préparés sélectivement, entièrement caractérisés, y compris par diffraction des rayons X, et évalués dans l'hydrogénation catalytique de l'acétophénone. Le pré-catalyseur **C6t** *fac*-[$Mn(CO)_3(\kappa^3P,C,N)(OTf)$] s'est avéré être le système le plus actif dans l'hydrogénation des cétones, dont l'efficacité a été attribuée à la présence d'une

architecture métallacyclique à 5,6 chaînons fusionnés favorisant la dissociation du bras pyridine et libérant ainsi un site de coordination vacant bénéfique au processus catalytique. Les études futures viseront à engager ces complexes de manganèse(I) dans différents processus catalytiques, mais aussi à implanter cette nouvelle classe de ligands de type pince à noyau NHC sur d'autres centres métalliques.

Chapitre 3 : Hydrosilylation d'acides carboxyliques et d'esters en aldéhydes catalysée par les complexes $Mn_2(CO)_{10}$ et $Re_2(CO)_{10}$

La deuxième partie de ce travail de thèse consistait à développer un nouveau système catalytique pour la réduction sélective des acides carboxyliques et des esters en aldéhydes.

Sur la base d'études antérieures sur l'hydrosilylation des dérivés d'acides carboxyliques avec le fer, développées dans notre groupe,[73] l'hydrosilylation sélective des acides carboxyliques et des esters catalysée par le manganèse et le rhénium a été ciblée.

Le complexe $Re_2(CO)_{10}$, disponible commercialement, s'est révélé être un catalyseur efficace pour la réduction directe de divers acides carboxyliques dans des conditions douces (température ambiante, sous irradiation à 350 ou 395 nm). Tandis que les acides carboxyliques aliphatiques ont été facilement convertis en disilylacétals correspondants avec une faible charge de catalyseur (0,5 mol%) en présence d'Et_3SiH (2,2 équivalents), leurs analogues aromatiques ont nécessité des conditions plus drastiques ($Re_2(CO)_{10}$ 5 mol%, Ph_2MeSiH 4,0 équivalents) pour obtenir les aldéhydes correspondants après traitement acide (**Schéma 19**).

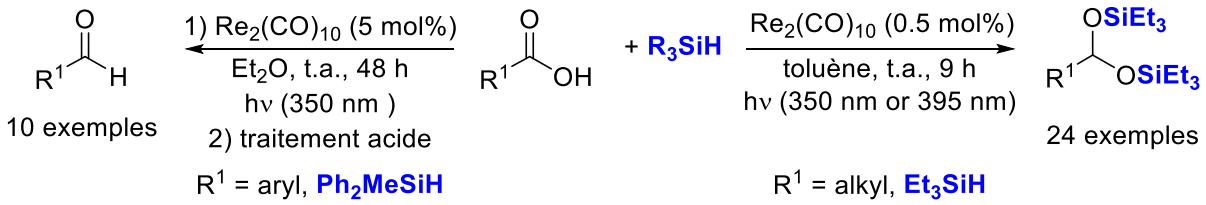

Schéma 19. Hydrosilylation des acides carboxyliques catalysée par le rhénium.

Dans des conditions similaires, nous avons effectué l'hydrosilylation d'esters carboxyliques en utilisant les complexes $Mn_2(CO)_{10}$ (5,0 mol%) et $Re_2(CO)_{10}$ (0,5 mol) comme catalyseurs, en présence d'une quantité stoechiométrique d'Et_3SiH (1,1 équivalent) comme source de silane peu coûteuse. Avec les deux catalyseurs, à température ambiante sous irradiation à 365 nm (LED, 4*10W), une grande variété d'esters carboxyliques a ainsi été réduite avec des rendements

modérés à bons en aldéhydes protégés correspondants sans formation notable de silyléthers résultant d'une sur-réduction. Après hydrolyse, les aldéhydes aromatiques et aliphatiques, y compris les di-aldéhydes, ont été facilement formés et isolés avec de bons rendements (**Schéma 20**).

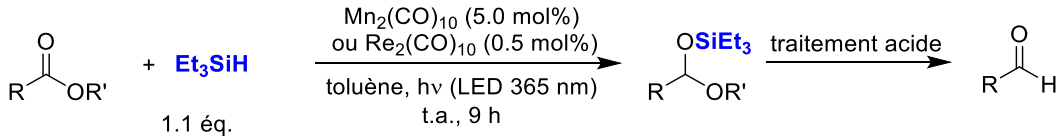

Schéma 20. Hydrosilylation sélective des esters en aldéhydes, catalysée par le manganèse et le rhénium.

Pour les développements futurs dans ce domaine concurrentiel, les deux systèmes métalliques développés ici devront être envisagés de manière complémentaire, la charge catalytique 10 fois moindre utilisée avec le rhénium devant être opposée au prix plus faible du manganèse.

Conclusion générale

La première partie de ce travail consistait à développer de nouveaux systèmes catalytiques pour les réactions d'hydrogénation, basés sur le manganèse, métal abondant, et impliquant des ligands NHC riches en électrons :

-> Pour atteindre cet objectif, une nouvelle famille de complexes NHC-phosphine de Mn(I) bidentés a été obtenue à partir de leurs sels d'imidazolium correspondants via l'addition séquentielle de quantités équimolaires de KHMDS et du précurseur $[Mn(CO)_5Br]$. Tous ces complexes de manganèse(I) ont été entièrement caractérisés et se sont révélés présenter une activité catalytique modérée à excellente dans l'hydrogénation des cétones. Ce processus catalytique a mis en évidence un nouveau mode de coopération métal-ligand impliquant un complexe de manganèse insaturé à 16 électrons de type ylure de phosphonium *fac*-$[Mn(CO)_3(\kappa^2P,\hat{C}\text{-}Ph_2P{=}CHNHC)]$ comme intermédiaire clé capable d'activer H_2 via un mode non-classique de coopération métal-ligand et un changement formel de valence de l'atome de phosphore (λ^5-P à λ^3-P), fournissant ainsi la première preuve de l'implication d'espèces λ^5-phosphorées dans la coopération métal-ligand.

-> Compte tenu de la grande stabilité et de la réactivité des complexes pinces, le prochain défi de notre travail était de préparer une version tridentée des complexes NHC-phosphine de manganèse(I). En utilisant une procédure similaire à celle développée dans la série des ligands bidentés, nous avons réussi à synthétiser deux nouvelles familles de complexes pinces cationiques NHC de Mn(I) impliquant des ligands PCN et PCP. Ces complexes ont été entièrement caractérisés et leur activité catalytique a été étudiée dans l'hydrogénation de l'acétophénone, montrant une activité inférieure par rapport à leur version bidentée. Ceci indique que le développement de systèmes plus complexes n'est pas toujours une condition préalable pour atteindre de meilleures performances dans le domaine de la catalyse.

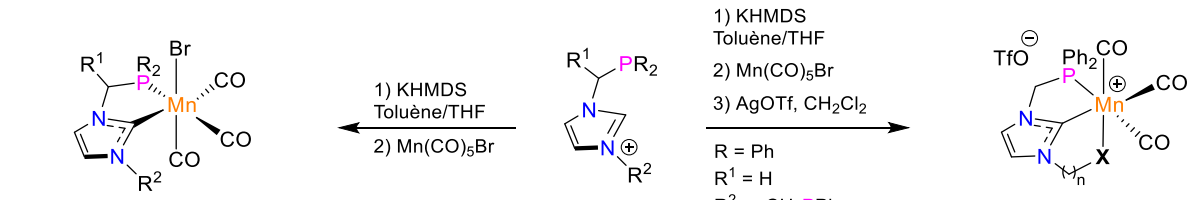

C1, R = Ph, R^1 = H, R^2 = Mes (86%)
C1.b, R = Ph, R^1 = Me, R^2 = Mes (40%)
C2, R = Ph, R^1 = H, R^2 = Me (82%)
C3, R = Ph, R^1 = H, R^2 = iPr (60%)
C4, R = iPr, R^1 = H, R^2 = Mes (78%)
C5, R = Ph, R^1 = Ph, R^2 = Mes (80%)

C6^t, n = 1, **X** = PPh_2 (88%)
C7^t, n = 0, **X** = Pyr (76%)
C8^t, n = 1, **X** = Pyr (96%)

La deuxième partie de cette thèse consistait à développer un nouveau système catalytique pour la réduction sélective des acides carboxyliques et des esters. Avec les pré-catalyseurs $Mn_2(CO)_{10}$ (5 mol%) et $Re_2(CO)_{10}$ (0,5 mol%) disponibles dans le commerce, en présence d'un silane comme agent réducteur, sous irradiation lumineuse et à température ambiante, une grande variété d'acides carboxyliques et d'esters ont ainsi été réduits en leurs aldéhydes protégés correspondants avec une chimio-sélectivité élevée.

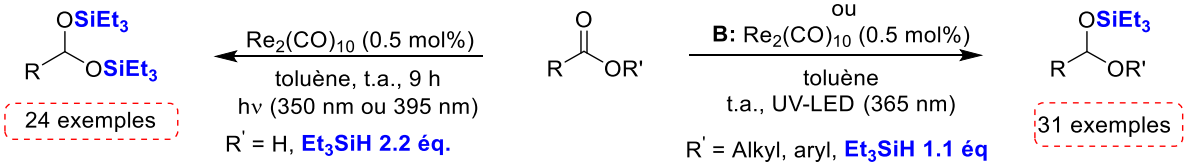

Les perspectives de ce travail sont nombreuses, bien qu'elles soient principalement liées à la première partie de ce travail. En effet, sur la base des complexes de manganèse(I) synthétisés à partir de ligands NHC bi- et tridentés, d'autres transformations catalytiques pourront être envisagées comme l'hydrogénation d'esters et d'amides plus difficiles à réduire. Différents centres métalliques appartenant à la première ligne de la classification périodique (Ni, Fe, Co...) pourront également être étudiés en utilisant cette nouvelle classe de ligands chélatants à base de NHC. Une question pertinente sera de savoir si nous pourrons observer ce même type de coopération métal-ligand avec d'autres centres métalliques ?

Références

[1] L. Stahl, *J. Am. Chem. Soc.* **2007**, *129*, 10297–10298.

[2] G. B. Kauffman, *Platin. Met. Rev.* **1999**, *43*, 122–128.

[3] H. Grünewald, *Angew. Chem.* **1968**, *80*, 52–52.

[4] J. A. Osborn, F. H. Jardine, J. F. Young, G. Wilkinson, *J. Chem. Soc. Inorg. Phys. Theor.* **1966**, 1711–1732.

[5] W. S. Knowles, *Angew. Chem. Int. Ed.* **2002**, *41*, 1998–2007.

[6] R. Noyori, *Angew. Chem. Int. Ed.* **2002**, *41*, 2008–2022.

[7] D. M. Sedgwick, G. B. Hammond, *J. Fluor. Chem.* **2018**, *207*, 45–58.

[8] D. Wei, C. Darcel, *Chem. Rev.* **2019**, *119*, 2550–2610.

[9] R. I. Khusnutdinov, A. R. Bayguzina, U. M. Dzhemilev, *Russ. J. Org. Chem.* **2012**, *48*, 309–348.

[10] D. A. Valyaev, G. Lavigne, N. Lugan, *Coord. Chem. Rev.* **2016**, *308*, 191–235.

[11] R. J. Trovitch, *Acc. Chem. Res.* **2017**, *50*, 2842–2852.

[12] F. Kallmeier, R. Kempe, *Angew. Chem. Int. Ed.* **2018**, *57*, 46–60.

[13] G. A. Filonenko, R. van Putten, E. J. M. Hensen, E. A. Pidko, *Chem. Soc. Rev.* **2018**, *47*, 1459–1483.

[14] N. Gorgas, K. Kirchner, *Acc. Chem. Res.* **2018**, *51*, 1558–1569.

[15] A. Mukherjee, D. Milstein, *ACS Catal.* **2018**, *8*, 11435–11469.

[16] L. Alig, M. Fritz, S. Schneider, *Chem. Rev.* **2019**, *119*, 2681–2751.

[17] K. D. Vogiatzis, M. V. Polynski, J. K. Kirkland, J. Townsend, A. Hashemi, C. Liu, E. A. Pidko, *Chem. Rev.* **2019**, *119*, 2453–2523.

[18] T. Zell, R. Langer, *ChemCatChem* **2018**, *10*, 1930–1940.

[19] S. Elangovan, C. Topf, S. Fischer, H. Jiao, A. Spannenberg, W. Baumann, R. Ludwig, K. Junge, M. Beller, *J. Am. Chem. Soc.* **2016**, *138*, 8809–8814.

[20] A. Mukherjee, A. Nerush, G. Leitus, L. J. W. Shimon, Y. Ben David, N. A. Espinosa Jalapa, D. Milstein, *J. Am. Chem. Soc.* **2016**, *138*, 4298–4301.

[21] M. Garbe, K. Junge, M. Beller, *Eur. J. Org. Chem.* **2017**, *2017*, 4344–4362.

[22] B. Maji, M. K. Barman, *Synthesis* **2017**, *49*, 3377–3393.

[23] L. Maser, L. Vondung, R. Langer, *Polyhedron* **2018**, *143*, 28–42.

[24] N. Gorgas, K. Kirchner, in *Pincer Compd.* (Ed.: D. Morales-Morales), Elsevier, **2018**, pp. 19–45.

[25] N. V. Kulkarni, W. D. Jones, in *Pincer Compd.* (Ed.: D. Morales-Morales), Elsevier, **2018**, pp. 491–518.

[26] J. I. van der Vlugt, in *Pincer Compd.* (Ed.: D. Morales-Morales), Elsevier, **2018**, pp. 599–621.

[27] Z. Wei, H. Jiao, in *Adv. Inorg. Chem.* (Eds.: R. van Eldik, R. Puchta), Academic Press, **2019**, pp. 323–384.

[28] H. Valdés, M. A. García-Eleno, D. Canseco-Gonzalez, D. Morales-Morales, *ChemCatChem* **2018**, *10*, 3136–3172.

[29] U. Chakraborty, E. Reyes-Rodriguez, S. Demeshko, F. Meyer, A. Jacobi von Wangelin, *Angew. Chem. Int. Ed.* **2018**, *57*, 4970–4975.

[30] U. Chakraborty, S. Demeshko, F. Meyer, A. Jacobi von Wangelin, *Angew. Chem. Int. Ed.* **2019**, *58*, 3466–3470.

[31] H. Grützmacher, *Angew. Chem. Int. Ed.* **2008**, *47*, 1814–1818.

[32] J. I. van der Vlugt, *Eur. J. Inorg. Chem.* **2012**, *2012*, 363–375.

[33] J. R. Khusnutdinova, D. Milstein, *Angew. Chem. Int. Ed.* **2015**, *54*, 12236–12273.

[34] B. L. Conley, M. K. Pennington-Boggio, E. Boz, T. J. Williams, *Chem. Rev.* **2010**, *110*, 2294–2312.

[35] A. Quintard, J. Rodriguez, *Angew. Chem. Int. Ed.* **2014**, *53*, 4044–4055.

[36] D. W. Stephan, G. Erker, *Angew. Chem. Int. Ed.* **2015**, *54*, 6400–6441.

[37] E. von Grotthuss, M. Diefenbach, M. Bolte, H.-W. Lerner, M. C. Holthausen, M. Wagner, *Angew. Chem. Int. Ed.* **2016**, *55*, 14067–14071.

[38] J. W. Taylor, A. McSkimming, C. F. Guzman, W. H. Harman, *J. Am. Chem. Soc.* **2017**, *139*, 11032–11035.

[39] D. Wang, D. Astruc, *Chem. Rev.* **2015**, *115*, 6621–6686.

[40] C. Gunanathan, D. Milstein, *Chem. Rev.* **2014**, *114*, 12024–12087.

[41] A. Corma, J. Navas, M. J. Sabater, *Chem. Rev.* **2018**, *118*, 1410–1459.

[42] T. Irrgang, R. Kempe, *Chem. Rev.* **2019**, *119*, 2524–2549.

[43] M. Trincado, H. Grützmacher, in *Coop. Catal.*, John Wiley & Sons, Ltd, **2015**, pp. 67–110.

[44] B. Zhao, Z. Han, K. Ding, *Angew. Chem. Int. Ed.* **2013**, *52*, 4744–4788.

[45] T. Ohkuma, H. Ooka, S. Hashiguchi, T. Ikariya, R. Noyori, *J. Am. Chem. Soc.* **1995**, *117*, 2675–2676.

[46] R. Noyori, T. Ohkuma, *Angew. Chem. Int. Ed.* **2001**, *40*, 40–73.

[47] C. A. Sandoval, T. Ohkuma, K. Muñiz, R. Noyori, *J. Am. Chem. Soc.* **2003**, *125*, 13490–13503.

[48] M. Zimmer-De Iuliis, R. H. Morris, *J. Am. Chem. Soc.* **2009**, *131*, 11263–11269.

[49] S. Musa, I. Shaposhnikov, S. Cohen, D. Gelman, *Angew. Chem. Int. Ed.* **2011**, *50*, 3533–3537.

[50] G. A. Silantyev, O. A. Filippov, S. Musa, D. Gelman, N. V. Belkova, K. Weisz, L. M. Epstein, E. S. Shubina, *Organometallics* **2014**, *33*, 5964–5973.

[51] S. Musa, S. Fronton, L. Vaccaro, D. Gelman, *Organometallics* **2013**, *32*, 3069–3073.

[52] B. Saha, S. M. Wahidur Rahaman, P. Daw, G. Sengupta, J. K. Bera, *Chem. – Eur. J.* **2014**, *20*, 6542–6551.

[53] A. Bartoszewicz, R. Marcos, S. Sahoo, A. K. Inge, X. Zou, B. Martín-Matute, *Chem. – Eur. J.* **2012**, *18*, 14510–14519.

[54] W.-Y. Chu, X. Zhou, T. B. Rauchfuss, *Organometallics* **2015**, *34*, 1619–1626.

[55] Y. Blum, D. Czarkie, Y. Rahamim, Y. Shvo, *Organometallics* **1985**, *4*, 1459–1461.

[56] R. Karvembu, R. Prabhakaran, K. Natarajan, *Coord. Chem. Rev.* **2005**, *249*, 911–918.

[57] A. Comas-Vives, G. Ujaque, A. Lledós, *Organometallics* **2007**, *26*, 4135–4144.

[58] C. P. Casey, J. B. Johnson, *J. Org. Chem.* **2003**, *68*, 1998–2001.

[59] C. P. Casey, S. W. Singer, D. R. Powell, R. K. Hayashi, M. Kavana, *J. Am. Chem. Soc.* **2001**, *123*, 1090–1100.

[60] C. Gunanathan, D. Milstein, *Acc. Chem. Res.* **2011**, *44*, 588–602.

[61] L. Alig, M. Fritz, S. Schneider, *Chem. Rev.* **2019**, *119*, 2681–2751.

[62] C. Gunanathan, Y. Ben-David, D. Milstein, *Science* **2007**, *317*, 790–792.

[63] A. Bruneau-Voisine, D. Wang, T. Roisnel, C. Darcel, J.-B. Sortais, *Catal. Commun.* **2017**, *92*, 1–4.

[64] A. Bruneau-Voisine, D. Wang, V. Dorcet, T. Roisnel, C. Darcel, J.-B. Sortais, *Org. Lett.* **2017**, *19*, 3656–3659.

[65] D. Wang, A. Bruneau-Voisine, J.-B. Sortais, *Catal. Commun.* **2018**, *105*, 31–36.

[66] D. Wei, A. Bruneau-Voisine, T. Chauvin, V. Dorcet, T. Roisnel, D. A. Valyaev, N. Lugan, J.-B. Sortais, *Adv. Synth. Catal.* **2018**, *360*, 676–681.

[67] D. Wei, A. Bruneau-Voisine, D. A. Valyaev, N. Lugan, J.-B. Sortais, *Chem. Commun.* **2018**, *54*, 4302–4305.

[68] M. J. Bitzer, A. Pöthig, C. Jandl, F. E. Kühn, W. Baratta, *Dalton Trans.* **2015**, *44*, 11686–11689.

[69] S. Elangovan, C. Topf, S. Fischer, H. Jiao, A. Spannenberg, W. Baumann, R. Ludwig, K. Junge, M. Beller, *J. Am. Chem. Soc.* **2016**, *138*, 8809–8814.

[70] F. Kallmeier, T. Irrgang, T. Dietel, R. Kempe, *Angew. Chem. Int. Ed.* **2016**, *55*, 11806–11809.

[71] M. B. Widegren, G. J. Harkness, A. M. Z. Slawin, D. B. Cordes, M. L. Clarke, *Angew. Chem. Int. Ed.* **2017**, *56*, 5825–5828.

[72] S. Weber, B. Stöger, K. Kirchner, *Org. Lett.* **2018**, *20*, 7212–7215.

[73] H. Li, L. C. Misal Castro, J. Zheng, T. Roisnel, V. Dorcet, J.-B. Sortais, C. Darcel, *Angew. Chem. Int. Ed.* **2013**, *52*, 8045–8049.

List of Publications

Chapter 1: Manganese-Catalyzed Hydrogenation and Hydrogen Transfer Reactions

1. Manganese-catalyzed Hydrogenation and Hydrogen Transfer Reactions.

Jean-Baptiste Sortais, **Ruqaya Buhaibeh**, Yves Canac, Manganese catalysis in organic synthesis, J.-B. Sortais Ed., Wiley-VCH, in press.

Chapter 2: Synthesis and Catalytic Applications of Bi- and Tridentate NHC-Phosphine Manganese Complexes

2. Phosphine-NHC Manganese Hydrogenation Catalyst Exhibiting a Non-Classical Metal-Ligand Cooperative H_2 Activation Mode.

R. Buhaibeh, O. A. Filippov, A. Bruneau-Voisine, J. Willot, C. Duhayon, D. Valyaev, N. Lugan, Y. Canac, J. B. Sortais, *Angew. Chem. Int. Ed.* **2019**, *58*, 6727-6731.

3. Cationic PCP and PCN NHC Core Pincer-Type Mn(I) Complexes: From Synthesis to Catalysis.

R. Buhaibeh, C. Duhayon, D. A. Valyaev, J.-B. Sortais, Y. Canac, *Organometallics* **2021**, DOI 10.1021/acs.organomet.0c00717.

Chapter 3: Hydrosilylation of Carboxylic Acids and Esters to Aldehydes Catalyzed by $Mn_2(CO)_{10}$ and $Re_2(CO)_{10}$

4. Rhenium-Catalyzed Reduction of Carboxylic Acids with Hydrosilanes

D. Wei, **R. Buhaibeh**, Y. Canac, J.-B. Sortais, *Org. Lett.* **2019**, *21*, 7713-7716.

5. Manganese and Rhenium-catalyzed Selective Hydrosilylation of Esters to Aldehydes.

D. Wei, **R. Buhaibeh**, Y. Canac, J.-B. Sortais, *Chem. Commun.* **2020**, *56*, 11617-11620.

Résumé

Des avancées spectaculaires ont récemment été réalisées dans les réactions d'hydrogénation et de transfert d'hydrogène de liaisons insaturées catalysées par des complexes bien définis de manganèse(I). Une sélection des avancées récentes dans ce domaine est résumée dans le chapitre 1. Le deuxième chapitre est consacré à la préparation de différents complexes de manganèse(I) construits à partir de ligands bidentés phosphine-NHC facilement accessibles. Ces complexes ont conduit à des résultats catalytiques prometteurs en réaction d'hydrogénation de cétones, mettant en évidence un nouveau mode de coopération métal-ligand et impliquant un ylure de phosphore métallé non classique obtenu par déprotonation du lien CH_2 du ligand phosphine-NHC dans la sphère de coordination du manganèse. Ce dernier peut facilement activer le dihydrogène, fournissant ainsi la première évidence de l'implication d'espèces λ^5-phosphorées dans des processus de coopérativité métal-ligand. Suite à la version bidentée, afin d'obtenir des systèmes catalytiques plus actifs en raison d'une rigidité et d'une robustesse accrues, des complexes pinces cationiques de manganèse(I) à coeur NHC basés sur une architecture PCN et PCP ont été préparés et entièrement caractérisés. Ces complexes pinces se sont avérés cependant moins actifs dans l'hydrogénation de cétones que leurs analogues bidentés. Le troisième chapitre est relatif à la réduction chimio-sélective d'acide carboxyliques et d'esters en acétals silylés facilement transformés en aldéhydes par traitement acide. Ces transformations qui ne nécessitent pas la présence de ligands bien définis, ont été réalisées en utilisant les pré-catalyseurs commercialement disponibles $Mn_2(CO)_{10}$ et $Re_2(CO)_{10}$, en présence de triéthylsilane comme agent réducteur et sous irradiation à température ambiante.

Abstract

Spectacular advances have recently been achieved in hydrogenation and hydrogen transfer reactions of unsaturated bonds catalyzed by well-defined Mn(I) complexes. A selection of recent advances in this field is summarized in Chapter 1. The second Chapter is devoted to the preparation of various Mn(I) complexes of easily accessible bidentate NHC-phosphine ligands, these complexes afforded valuable catalytic results in the hydrogenation of ketones. This catalytic process highlights a new mode of metal-ligand cooperation involving a non-classical metalla-substituted phosphonium ylide obtained upon C-H deprotonation of a chelating NHC-phosphine ligand in the Mn coordination sphere. The latter can easily activate H_2, thus providing the first evidence of the involvement of λ^5-phosphorous species in metal-ligand cooperation. In order to reach more active catalytic systems because of higher rigidity and robustness, next to the bidentate series, cationic NHC core Mn(I) pincer complexes based on a PCN and PCP ligands were also prepared and fully characterized. They were found to be less active in the hydrogenation of ketones compared to their bidentate analogues. The third Chapter involved the reduction of carboxylic acid and esters with high chemo-selectivity to afford corresponding silyl acetals, which can then be easily converted into aldehydes by acid treatment. These transformations which do not require the presence of well-defined ligands were carried out using the commercially available $Mn_2(CO)_{10}$ and $Re_2(CO)_{10}$ pre-catalysts in the presence of triethylsilane as reducing agent under irradiation at room temperature.